ATMOSPHERIC PHOTOOXIDATION OF ORGANOSULFUR COMPOUNDS

Thesis by

Fangdong Yin

In Partial Fulfillment of the Requirements

for the Degree of

Doctor of Philosophy

California Institute of Technology

Pasadena, California

1990

(Submitted April 19, 1990)

To Xiaoming

ACKNOWLEDGEMENTS

I wish to express my deepest gratitude to my advisor, Prof. John H. Seinfeld, for his guidance, support and understanding during my graduate studies. His dedication to research and education combined with his kindness and patience are always appreciated. I would also like to express my special thanks to my co-advisors, Dr. Daniel Grosjean and Prof. Richard C. Flagan, for their encouragement, enthusiasm and numerous ideas on reaction mechanisms as well as on experimental techniques.

I would also like to express my appreciation to Prof. Michael Hoffmann and Prof. Glen Cass for their hospitality of allowing me to use various instruments in their laboratories, and to the students in their groups for the technical help on the instrumentations, including Bill, Bruce, Monica and Lynn.

Special thanks go to Shih-chen, Suzanne, George, Wolfgang, and Rudi for their direct help and participation in outdoor smog chamber experiments. I would like to thank Dale, Sonia, Ken, Toby, Carol, Pratim, Brian, Jennifer, Jin Jwang, Rueen Fang, Liyuan, Hung, David and Guojun for their help in computer facility, experimental techniques and solving numerous laboratory problems, and also for their friendship in introducing me to the American culture and society.

I wish also to express my appreciation to Joe, Rich, Chic, and Hai Vu for their technical help in building the experimental apparatus; Rayma and Gunilla for their excellent library assistance; and Christina, Helen, Evelina, Pat, and Benjamin for their administrative help.

The support from the National Science Foundation, Chinese Education Foundation, and California Institute of Technology during my graduate years are deeply appreciated.

Finally, I want to thank my wife, Xiaoming, who has participated in my experiments and helped me through the difficult times, and has always supported me with her love, patience and understanding.

ABSTRACT

The atmospheric chemistry of organosulfur compounds is of fundamental importance to understanding the biogeochemical sulfur cycle as well as environmental issues such as acid precipitation and sulfur aerosol formation in the atmosphere. The research goal of the present work is to elucidate the atmospheric reaction mechanisms of conversion of organosulfur compounds to sulfur-containing aerosols.

Based on the fundamental chemistry and the available kinetic and mechanistic information from experimental studies, detailed chemical reaction mechanisms have been developed for the atmospheric photooxidation of dimethyl sulfide, CH_3SCH_3, dimethyl disulfide, CH_3SSCH_3, methanethiol, CH_3SH, and diethyl sulfide, $C_2H_5SC_2H_5$. Predictions of the developed mechanisms by computer simulation are compared with available data on laboratory photooxidation of organosulfur compounds to identify critical uncertainties in chemical pathways and reaction rate constants. Further experimental studies have been designed based on the findings from computer modeling work. Using the outdoor smog chamber reactor, the dynamic behavior of various chemical species and particle nucleation and growth have been investigated in detail under well-defined atmospheric conditions for systems CH_3SCH_3–NO_x–air–$h\nu$ and CH_3SSCH_3–NO_x–air–$h\nu$. Through analysis of the experimental data from outdoor smog chamber experiments by computer simulation, the mechanisms developed for photooxidation of CH_3SCH_3 and CH_3SSCH_3 have been evaluated and reformulated. The key problems regarding the initial reactions, secondary reactions of RSO_x radicals and $RS(O)_xOO$ radicals, and the major chemical pathways for the formation of SO_2 and RSO_3H compounds have been elucidated and the discrepancies of the experimental results between different investigators have been resolved. Critical uncertatinties regarding chemical path-

ways and reaction rate constants have been identified and further detailed kinetic experimental studies have been recommended.

TABLE OF CONTENTS

V Recommendations for Future Research

APPENDICES

LIST OF TABLES

LIST OF FIGURES

II Analysis of Atmospheric Photooxidation Mechanism for Organosulfur Compounds

CHAPTER I

INTRODUCTION

INTRODUCTION

The atmosphere is a dynamic system into which enormous quantities of species are emitted from natural processes and from human activities, and where chemical reactions, physical transformations, and various types of transport take place. Sulfur compounds, an important class of such species, have both natural and anthropogenic emission sources. In contrast to anthropogenic emissions, which are locally concentrated and mostly in the oxidized state of SO_2, the natural emissions are much more uniformly distributed and are predominantly in the form of reduced sulfur compounds. Moreover, on a global scale the magnitude of the natural emissions is significant compared to those of anthropogenic emissions. Their emission rates are highly variable in both space and time, and strongly depend on a wide variety of parameters (e.g., temperature, sunlight, and biological activities). Biogenic sulfur sources, the most important natural source, have an estimated total sulfur flux of about 50–100 Tg S y^{-1} [Möller, 1984]. Although several reduced sulfur compounds, including carbonyl sulfide (COS), carbon disulfide (CS_2), hydrogen sulfide (H_2S), methanethiol (CH_3SH), dimethyl sulfide (CH_3SCH_3) and dimethyl disulfide (CH_3SSCH_3), have been identified from various biogenic sources, dimethyl sulfide is of the most importance in the atmospheric sulfur chemistry, with an estimated flux of about 40 Tg S y^{-1} from the ocean surface [Andreae and Raemdonck, 1983; Andreae et al., 1985] and about 13 Tg S y^{-1} from land sources [Adams et al., 1981]. Therefore, a fundamental understanding of atmospheric chemistry of dimethyl sulfide, which is the major research objective of this work, is very important not only to the chemistry of the natural troposphere, but also to the chemistry of the polluted atmosphere since the impact assessment of human activities on the environment must be based on the knowledges of the clean natural atmosphere.

In contrast to the atmospheric chemistry of hydrocarbons, the knowledge of the chemistry of reduced sulfur compounds in the atmosphere is quite limited, especially about four years ago (1985) when this project started. At that time, the only known fact was that photooxidation of dimethyl sulfide in the atmosphere leads to the formation of SO_2, H_2SO_4 and CH_3SO_3H. However, the information obtained from both kinetic and product studies was either not well-defined (e.g., rate constants of OH + CH_3SCH_3 and NO_3 + CH_3SCH_3) or puzzling and even conflicting (e.g., regeneration of CH_3SSCH_3, yield distribution of SO_2 and CH_3SO_3H, and the fate of CH_3S radical). Based on the limited available information, detailed chemical reaction mechanisms have been formulated for the atmospheric photooxidation of the organosulfur compounds, including CH_3SCH_3, CH_3SH, and $C_2H_5SC_2H_5$. Predictions of the mechanisms by computer simulation are compared with available data on laboratory photooxidation of organosulfur species in order to identify the major reaction pathways and critical uncertainties in the mechanisms. The formulation and simulation of the new organosulfur photooxidation mechanisms are described in Chapter 2.

Based on the findings from computer modeling of the developed mechanisms, further detailed experimental studies have been designed to elucidate the major reaction pathways of conversion of CH_3SCH_3 to SO_2 and CH_3SO_3H, and to determine the product yield distribution. Using the Caltech outdoor smog chamber reactor, the dynamic behavior of various chemical species and particle nucleation and growth has been investigated for CH_3SCH_3 and CH_3SSCH_3 photooxidation under well-defined conditions. From the available new experimental information of this work and that of other investigators (especially regarding the CH_3S radical), the proposed mechanism of CH_3SCH_3 photooxidation has been reformulated and updated, and a new reaction mechanism for atmospheric photooxidation of CH_3SSCH_3

has been developed. Furthermore, in order to develop qualitatively correct reaction mechanisms consistent with all available kinetic and mechanistic information, a large effort on fundamental chemistry has been made to ensure that in the developed mechanisms each reaction is chemically correct and all the important reaction pathways are included. The key problems regarding the initial reactions, secondary reactions of CH_3SO_x and $CH_3S(O)_xOO$ radicals, the pathways for the formation of SO_2 and CH_3SO_3H, and other puzzling facts such as regenation of CH_3SSCH_3 have been elucidated from the developed mechanisms. This is presented in Chapter 3. Through analysis of the experimental data from smog chamber experiments by computer simulation, the mechanisms developed have been carefully evaluated, and the discrepancies of the product yield distributions between different investigators have been resolved based on concentration effects both experimentally and theoretically (by computer modeling), which is described in Chapter 4.

In Chapter 5, the limitations of smog chamber experimental studies and computer simulation on elucidating the reaction mechanisms is discussed, and recommendations for future research studies are outlined.

REFERENCES

Adams, D. F., S. O. Farwell, E. Robinson, M. R. Pack, and W. L. Bamesberger, Biogenic sulfur source strengths, *Environ. Sci. Technol., 15*, 1493–1498, 1981.

Andreae, M. O., and H. Raemdonck, Dimethyl sulfide in the surface ocean and the marine atmosphere: A global view, *Science, 221*, 744–747, 1983.

Andreae, M. O., R. J. Ferek, F. Bermond, K. P. Byrd, R. T. Engstrom, S. Hardin, P. D. Houmira, F. Le Marrec, H. Raemdonck, and R. B. Chatfield, Dimethyl sulfide in the marine atmosphere, *J. Geophys. Res., 90*, 12891–12901, 1985.

Möller, D., On the global natural sulfur emission, *Atmos. Environ., 18*, 29–39, 1984.

CHAPTER II

ANALYSIS OF ATMOSPHERIC PHOTOOXIDATION MECHANISMS FOR ORGANOSULFUR COMPOUNDS

Published in the

Journal of Geophysical Research, 91, 14,417–14,438, 1986

ANALYSIS OF ATMOSPHERIC PHOTOOXIDATION MECHANISMS FOR ORGANO-SULFUR COMPOUNDS

ABSTRACT

Reaction mechanisms are formulated for the atmospheric photooxidation of the organo-sulfur compounds, dimethyl sulfide, CH_3SCH_3, methanethiol, CH_3SH, and diethyl sulfide, $C_2H_5SC_2H_5$. Predictions of the mechanisms are compared with available data on laboratory photooxidations of these three species to identify critical uncertainties in chemical pathways and reaction rate constants. The sensitivity of product yields to these uncertainties is investigated.

1. Introduction

The atmospheric chemistry of organo-sulfur compounds is directly relevant to a number of issues including global atmospheric sulfur budgets [e.g., Nguyen et al., 1983; Möller, 1984; Chatfield and Crutzen, 1984], formation of sulfur aerosol in marine air [e.g., Andreae and Raemdonck, 1983, Andreae and Barnard, 1984; Harvey and Lang, 1986], atmospheric fate of biogenic organo-sulfur emissions [e.g., Maroulis and Bandy, 1977; Adams et al., 1979; Aneja et al., 1982], and the acidity of precipitation in remote areas [e.g., Herron, 1982; Galloway et al., 1982, Haines et al., 1983]. In addition, organo-sulfur compounds have received attention in the context of potential development of energy technologies such as shale oil and synfuels [e.g., Daum et al., 1982; Sklarew et al., 1984; Wong et al., 1984].

Until recently, it had been assumed that oxidation to SO_2 and subsequently to sulfate aerosol was the sole atmospheric fate of organo-sulfur compounds [e.g., Graedel, 1979; Logan et al., 1979; Sze and Ko, 1980]. However, this assumption

must be revised on the basis of recent laboratory studies in which measured SO_2 yields (about 20% to 40%) were substantially lower than previously assumed, and alkane sulfonic acids (RSO_2OH) were identified as major reaction products [Grosjean and Lewis, 1982; Hatakeyama et al., 1982; Hatakeyama and Akimoto, 1983; Grosjean, 1984a; Hatakeyama et al., 1985].

A detailed examination of available organo-sulfur photooxidation product studies reveals the following features:

a. The products identified usually do not account for all of the reacted organo-sulfur compounds and reacted NO_x, which indicates some unidentified S- and N-containing compounds exist.

b. While SO_2 yields are substantially lower than 100% in all studies, reported product yields vary substantially from one study to the next, especially for the condensible products.

c. High photochemical reactivity, e.g., rapid conversion of NO to NO_2 and formation of substantial amounts of ozone.

d. Formation of aldehydes (RCHO) which serve as a source of free radicals.

e. Significant differences in experimental conditions including source of OH radicals, light source, irradiation time (from 2 mins to 2 days), concentration (0.2 ppm-800 ppm), and reactor vessel material and volume (from 11 liter quartz to 80,000 liter teflon) may have a significant effect on aerosol formation and loss.

The detailed atmospheric chemistry of organo-sulfur compounds is incompletely understood. Although as we have indicated some studies have been carried out to elucidate the chemical paths of conversion of organo-sulfur compounds to SO_2 and sulfur-containing aerosols, the mechanisms of the initial attack and subsequent reactions are still open to question.

Based on prior experimental studies, the present work includes a comprehen-

sive investigation of the atmospheric chemistry of organo-sulfur compounds with emphasis on following objectives:

a. To elucidate the chemical paths of conversion of organo-sulfur compounds to SO_2 and sulfur-containing aerosol and to study the dynamics of RSR' – NO_x–air systems on the basis of available information.

b. To attempt to explain the experimental data of Hatakeyama et al. [1982, 1983 and 1985], Grosjean and Lewis [1982] and Grosjean [1984a].

2. Atmospheric Photooxidation Mechanisms for Organosulfur Compounds

In this section, we present the detailed reaction mechanisms for the atmospheric photooxidation of dimethyl sulfide, CH_3SCH_3, methanethiol, CH_3SH, and diethyl sulfide, $C_2H_5SC_2H_5$, including inorganic reactions, aldehyde and PAN formation, RSR' initial reactions, reactions of the radicals: RS, RSO, RSO_2, RSO_3 and RSO_4, SO_2 formation and possible smog chamber wall effects. Following the presentation of the mechanisms in this section, a comprehensive analysis of them will be carried out based on the available experimental data. The mechanism of the system CH_3SCH_3–NO_x–air is given in Tables 1, 2 and 5 and depicted in Figure 1. For the systems of CH_3SH – NO_x–air and $C_2H_5SC_2H_5$ – NO_x–air, the mechanisms are given in Tables 3 and 4, and Figures 2 and 3, respectively.

2.1. Initial Reactions

Organo-sulfur compounds may react with OH, $O(^3P)$ and NO_3. From consideration of tropospheric concentrations of these species, reaction with NO_3 appears negligible during daytime, but may be of importance at night. Reaction with $O(^3P)$ is estimated to be of minor importance.

In the following sections, initial reaction pathways are discussed in terms of addition and abstraction mechanisms, keeping in mind that "abstraction" mechanisms may involve an initial addition step followed by rapid unimolecular decomposition of the adduct.

2.1.1. Reaction with $O(^3P)$

The mechanism of reaction of $O(^3P)$ with RSR′ has been suggested as electrophilic addition of the $O(^3P)$ atom to the sulfur atom contained in the thiol or sulfide to form an energy-rich complex that may either be collisionally stabilized or unimolecularly decompose by S-R bond cleavage [Slagle et al., 1976; Lee et al., 1976; Nip et al., 1981]. The hydrogen abstraction route has been estimated to be of minor importance. The possible paths are:

$$
\begin{aligned}
O(^3P) + R-S-R' \;&\rightarrow\; RS + OH \quad (R' = H) \\
&\rightarrow\; [R-\overset{\overset{O}{\|}}{S}-R']^* \;\rightarrow\; R + R'SO \\
&\qquad\qquad \rightarrow\; R' + RSO \\
&\qquad\qquad \rightarrow\; R-\overset{\overset{O}{\|}}{S}-R'
\end{aligned}
$$

The adduct, $[R-SO-R']^*$, is formed with 85-88 kcal/mole of excess internal energy which is about 23 kcal/mole more than is needed for unimolecular decomposition by $S-CH_3$ or $S-C_2H_5$ bond cleavage and about 4 kcal/mole above that necessary to break an S-H bond in the adduct. Thus where these two decomposition routes compete, decomposition by release of an alkyl radical is expected to predominate.

Cvetanović et al. [1981] studied the reactions of $O(^3P)$ with CH_3SH, C_2H_5SH, CH_3SCH_3 and CH_3SSCH_3. The results indicate that for the $CH_3SH - O(^3P)$ and $C_2H_5SH - O(^3P)$ reactions, abstraction may contribute as much as 10% to the total

rate, and for $CH_3SCH_3 - O(^3P)$ and $CH_3SSCH_3 - O(^3P)$ reactions at high pressures, the reactions proceed almost entirely by addition followed by rapid fragmentation to $CH_3 + CH_3SO$ and $CH_3S + CH_3SO$.

2.1.2. Reaction with OH

The RSR′ – OH reaction may proceed by OH addition to the sulfur atom or abstraction of an H atom from either the R or R′ groups, as shown in Figures 1–3.

2.1.2.1. Reaction of RSR with OH

Based on the decrease in the room temperature OH rate constants from CH_3SH to CH_3SCH_3, Atkinson et al. [1978] concluded that the reaction of RSR with OH proceeds via H atom abstraction. The negative Arrhenius activation energies were explained by zero or near zero activation energies combined with a temperature dependent preexponential factor. Kurylo [1978] also reported a negative temperature dependence, but suggested addition as the reaction mechanism, attributing the decrease of the rate constant going from CH_3SH to CH_3SCH_3 to steric effects.

By comparison of the magnitude and temperature dependence of $k_{CH_3SCH_3-OH}$ and $k_{CH_3OCH_3-OH}$, Wine et al. [1981] suggested that the dominant reaction path was H atom abstraction while noting a small but significant addition channel cannot be ruled out.

Niki et al. [1983b] studied the reaction of OH, generated from the photolysis of C_2H_5ONO in air, with CH_3SCH_3. They found CH_3SNO, arising from the reaction $CH_3S + NO$, as an intermediate product. The H atom abstraction reaction, followed by reaction with O_2 and NO and then decomposition (see Figure 1), was suggested by Niki et al. [1983b] as the primary step to account for the formation of CH_3S. However, Hatakeyama and Akimoto [1983] argued that if the final sulfur-containing

products were produced solely through CH_3S, the yields of SO_2 and CH_3SO_3H should be the same as in the case of CH_3SH. The yields of SO_2 and CH_3SO_3H were 0.21 and 0.50 for CH_3SCH_3 as compared to 0.29 and 0.40 for CH_3SH. The higher yield of CH_3SO_3H from CH_3SCH_3 than that from CH_3SH was attributed to the OH addition pathway [Hatakeyama and Akimoto, 1983] (see Figure 1).

Experimental identification of $CH_3S\dot{C}H_2$ and $CH_3S(OH)CH_3$ constitutes the most direct evidence of OH abstraction and addition pathways, respectively. Martin et al. [1985] found that the $CH_3S\dot{C}H_2$ radical represented 30% of the reacted CH_3SCH_3 and was in fact a lower limit since some $CH_3S\dot{C}H_2$ was lost by decomposition and by secondary reactions under the conditions of their study. For the reaction of $C_2H_5SC_2H_5$ with OH, the radical $C_2H_5S\dot{C}_2H_4$ was identified, but the adduct $C_2H_5S(OH)C_2H_5$ was not found, indicating abstraction is the major pathway for that reaction. Similar findings were reported for another sulfide, tetrahydrothiophene [Martin et al., 1985].

From the above cited experimental results, it appears that for the RSR-OH reactions, abstraction is the dominant pathway, but addition cannot be ruled out.

2.1.2.2. Reaction of RSH with OH

Reactions of OH with RSH, having negative activation energies [Atkinson et al., 1977; Wine et al., 1984], may indicate that the mechanism involves addition rather than abstraction. Wine et al. [1982, 1984] studied the kinetics of OH reactions with $C_1 - C_4$ carbon aliphatic thiols over the temperature range 250–430 K and found that all n-alkyl thiols react with OH at the same rate, nearly independent of the nature of the hydrocarbon chain, and that branched-chain thiols react with OH about 20% more slowly than do n-alkyl thiols. If H atom abstraction from the S-H bond is an important route, one would expect to observe kinetic isotope effects when

comparing the reactions of OH with CH_3SH and CH_3SD. In fact, Wine et al. [1984] found no such isotopic effect. These observations appear to rule out H abstraction from either S-H or C-H bonds, leaving addition as the dominant reaction pathway.

An addition step was suggested to explain CH_3SNO formation in the presence of initial RONO (see Figure 2) [Hatakeyama and Akimoto, 1983]. Although Mac Leod et al. [1984] did not detect the adduct $CH_3S(OH)H$ in their study of the $CH_3SH - OH$ reaction, Hatakeyama and Akimoto [1983] suggested that this adduct decomposes into CH_3S and H_2O in the absence of competing reactants such as RCH_2ONO, the net result of which is equivalent to the abstraction pathway. The above results indicate that the major initial step in the RSH-OH reaction is most likely addition.

It should be mentioned that the oxygen-dependent "apparent" rate constant observed by Cox and Sheppard [1980] may be attributed to the reaction between the adduct RS(OH)H and O_2 [Wine et al., 1984], which is analogous to the mechanism proposed by Kerr and Calvert [1984].

2.1.3. Reaction with NO_3

There are no studies of reaction products for the $NO_3 - RSR'$ reactions, and mechanisms are inferred from limited kinetic data. Atkinson et al. [1984a] compared the rate constant of $CH_3SCH_3 - NO_3$ with those of HCHO and CH_3CHO, which are 2–3 orders of magnitude lower, indicating that the $NO_3 - RSR'$ reaction would not be expected to proceed via H atom abstration, but by formation of an adduct, with subsequent O atom transfer to yield NO_2 and dimethyl sulfoxide molecule,

$$CH_3SCH_3 + NO_3 \rightarrow [CH_3S(ONO_2)CH_3] \rightarrow CH_3\overset{\overset{O}{\|}}{S}CH_3 + NO_2$$

Grosjean [1984a] suggested that reaction of $CH_3SCH_3 + NO_3$ may proceed by abstraction,

$$CH_3SCH_3 + NO_3 \rightarrow CH_3S\dot{C}H_2 + HNO_3$$

Since $CH_3S(O)CH_3$ was not identified as a product in the work of Grosjean and Lewis [1982], Grosjean [1984a] and Hatakeyama et al. [1982, 1983 and 1985], we have tentatively selected abstraction as the $RSR'-NO_3$ pathway in our mechanisms.

2.2. Formation of RS Radical

2.2.1. Formation of RS Radical from RSR

As the key S-containing radical responsible for the formation of SO_2 and CH_3SO_3H, the CH_3S radical has been postulated to form from $CH_3S\dot{C}H_2$ followed by reaction with O_2 and NO and then decomposition [Grosjean and Lewis, 1982; Niki et al., 1983b] (see Figure 1). Although CH_3S has not been directly detected in the CH_3SCH_3 – OH reaction, indirect evidence suggests its role as a major intermediate in the OH abstraction pathway. CH_3SNO, which is formed solely by the reaction of $CH_3S + NO$, was observed as a product in the $CH_3SCH_3 - OH - NO_x$ reaction [Niki et al., 1983b]. Furthermore the yields of the major S-containing products, SO_2 and CH_3SO_3H, coincided with those obtained from CH_3S radicals generated directly by photolysis of CH_3SNO [Niki et al., 1983a and 1983b]. Also CH_3SNO and CH_3SNO_2 were postulated as a source of missing nitrogen (not accounted for as $NO + NO_2 + HNO_3 + CH_3ONO_2$) and missing sulfur (not accounted for as $SO_2 + CH_3SO_3H + H_2SO_4$) by Grosjean [1984a]. Note that the indirect evidence of the existence of CH_3S radical is a strong indication for the abstraction pathway since this appears to be the only route that could generate that radical

[Niki et al., 1983b; Kerr and Calvert, 1984].

2.2.2. Formation of RS Radical from RSH

Although no direct identification of the RS radical has been reported in the RSH-OH reaction, it can be seen from Figure 2 that the CH_3S radical is formed from both abstraction and addition pathways in the $CH_3SH - OH$ reaction. Hatakeyama and Akimoto [1983] studied the reaction between CH_3SH and OH and indicated that the CH_3S radical was generated by photolysis of CH_3SNO produced from reaction of the adduct $CH_3S(OH)H$ with CH_3ONO (see Figure 2). Considering very low concentration of RONO under atmospheric conditions, they also studied the photooxidation of CH_3SH–2-methyl-2-butene–NO–air system and found the yield of SO_2 was in good agreement with that of the $CH_3SH - CH_3ONO - NO$–air system, indicating the existence of a common intermediate, CH_3S. In the presence of NO, CH_3SNO and C_2H_5SNO were directly detected in the reactions of RSH with OH [Mac Leod et al., 1984].

2.2.3. Summary

In all the experimental studies of the photooxidation of organo-sulfur compounds, the RS radical has been postulated as the major S-containing radical and as the precursor of the major sulfur products: $RSNO_x$, SO_2, H_2SO_4 and RSO_3H. Although indirect evidence of the RS radical has been discussed by several investigators [Niki et al., 1983b; Hatakeyama and Akimoto, 1983; Mac Leod et al., 1984], the conditions in their experimental studies were different from those existing in the atmosphere. Comparing the mechanisms of $CH_3SCH_3 - OH$, $CH_3SH - OH$ and $C_2H_5SC_2H_5 - OH$ (see Figures 1–3), it can be seen that the subsequent reactions of CH_3S are identical in the $CH_3SH - OH$ and $CH_3SCH_3 - OH$ mechanisms, and

that the reactions involving CH_3S and C_2H_5S are analogous.

2.3. Competition between $RS + O_2$ and $RS + NO_x$

The fate of the RS radical is a key element in the photooxidation mechanisms of organo-sulfur species. The CH_3S radical may react under ambient conditions with O_2, OH, NO, and NO_2:

$$CH_3S + O_2 \rightarrow CH_3SO_2 \quad (1)$$

$$+OH \rightarrow CH_3SOH \quad (2)$$

$$+NO \rightarrow CH_3SNO \quad (3)$$

$$+NO_2 \rightarrow CH_3SNO_2 \quad (4)$$

$$\rightarrow CH_3SO + NO \quad (5)$$

2.3.1. Formation of $RSNO_x$

RSNO ($R = CH_3, C_2H_5$) was directly observed by several investigators [Niki et al., 1983b; Hatakeyama and Akimoto, 1983; Mac Leod et al., 1984] in the systems of $RSR' - OH$. Niki et al. [1983b] observed the steady-state yield of CH_3SNO in the system of $CH_3SCH_3 - C_2H_5ONO - NO$–air as high as 30% of the CH_3SCH_3 consumed. The yield of CH_3SNO was found to increase with increasing concentration of NO in the system of $CH_3SSCH_3 - RONO - NO$–air [Hatakeyama and Akimoto, 1983]. Grosjean [1984a] also observed the missing nitrogen and missing sulfur increased as NO_x was increased.

Similar to CH_3ONO, CH_3SNO was found to photodissociate readily in the near-uv region,

$$CH_3SNO + h\nu\ (300 - 400\ \text{nm}) \rightarrow CH_3S + NO$$

and uv and ir absorption cross sections were measured for CH_3SNO at 298 K [Niki et al., 1983b]. From indirect evidence on the formation and subsequent decay of both CH_3SNO and C_2H_5SNO, the photolysis rate constants were estimated by Grosjean [1984a] as 0.07 min^{-1} for CH_3SNO and 0.12 min^{-1} for C_2H_5SNO. However, analysis of the data of Hatakeyama and Akimoto [1983] reveals that CH_3SNO decayed about 10 times faster than estimated by Grosjean.

No direct identification has been made for CH_3SNO_2, which was postulated as a source of missing nitrogen and missing sulfur by Niki et al. [1983b] and Grosjean [1984a]. However Balla and Heicklen [1984] did not find CH_3SNO_2 by mass spectrometry in their studies of the thermal reactions of NO_2 with organo-sulfur compounds although it is not clear that RS radical were present in their system. By analogy with $RONO_2$, $RSNO_2$ has been assumed to have negligible photodissociation rates and react slowly with OH [Grosjean, 1984a].

2.3.2. Competiton between $RS + O_2$ and $RS + NO_x$

Three possible paths exist for the $CH_3S + O_2$ reaction,

$$CH_3S + O_2 \rightarrow CH_2 = S + HO_2 \quad (1a)$$

$$\rightarrow CH_3 + SO_2 \quad (1b)$$

$$\rightarrow CH_3SO_2 \quad (1c)$$

H atom abstraction by O_2, pathway (1a), is the least favored on an energetic basis, and is deemed negligible since no $CH_2 = S$ has been observed [Hatakeyama and Akimoto, 1983; Grosjean, 1984a]. The relative importance of paths (1b) and (1c) will be discussed later since it has implications to the formation of SO_2.

In the presence of NO_x, the RS radical will react with NO_x to form $RSNO_x$, competing with the reaction $RS + O_2$. Grosjean [1984a] estimated that the ratio of

k_{RS+NO}/k_{RS+NO_2} is 2.3 for R = CH_3 and 6 for R = C_2H_5, which were similar to that of 2 for the alkoxy homologue, $RO+NO_x$. By use of CH_3SH as a souce of CH_3S, irradiations involving mixtures of $CH_3SH - NO$, $CH_3SH - Cl_2$ and $CH_3SH - Cl_2 - NO_2$ in air were carried out to investigate the competition between CH_3S+NO_2 and $CH_3S + O_2$, and Grosjean [1984a] estimated that $k_{CH_3S+NO_2}/k_{CH_3S+O_2} = 2 \times 10^6$. Therefore the resulting ratio of $k_{CH_3S+NO}/k_{CH_3S+O_2}$ as estimated by Grosjean is 4.6×10^6, substantially higher than that of 2×10^3 estimated from the yield ratio of CH_3SNO and SO_2 by Hatakeyama and Akimoto [1983].

Kerr and Calvert [1984] also estimated the following rate constants:

$$CH_3S + NO\ (+M) \rightarrow CH_3SNO\ (+M) \qquad 6 \times 10^{-11}\ cm^3\ molecule^{-1}\ sec{-}1$$

$$CH_3S + NO_2\ (+M) \rightarrow CH_3SNO_2\ (+M) \qquad 3 \times 10^{-11}\ cm^3\ molecule^{-1}\ sec{-}1$$

$$CH_3S + O_2\ (+M) \rightarrow CH_3SOO\ (+M) \qquad < 1 \times 10^{-17} cm^3\ molecule^{-1}\ sec^{-1}$$

which are consistent with Grosjean's estimates.

In the simulation results to be presented later, we have used as a starting point,

$$k_{CH_3S+O_2} : k_{CH_3S+NO} : k_{CH_3S+NO_2} = 10^{-2} : 2 \times 10^4 : 10^4$$

which is consistent with the estimates of Grosjean [1984a] and Kerr and Calvert [1984]. We will see, however, that the corresponding computer kinetic models are very sensitive to this ratio.

2.4. Formation of SO_2 and CH_3SO_3H

2.4.1. Fate of RS Radical

Niki et al. [1983a] studied the photolysis of CH_3SNO in air at wavelengths of 300-400 nm. After two minutes, the yields of SO_2, HCHO and NO were 20%, 20%

and nearly 100%, respectively, of the CH_3SNO consumed. Gaseous CH_3SO_3H was identified as a major product. Reaction (1b), corresponding to pathway (6) in Figure 1, could account for the formation of observed equimolar yields of SO_2 and HCHO. However, the mechanism leading to CH_3SO_3H from CH_3SO_2 was not specified. Also no conversion of NO to NO_2 occurred, as would be expected in path (6).

Similarly, Hatakeyama and Akimoto [1983] studied the photolysis of CH_3SNO above 500 nm and identified HCHO, NO, NO_2, CH_3SSCH_3, CH_3SO_3H and SO_2 with a yield of 26%. Based on the absence of CH_3ONO and CH_3ONO_2, they argued that pathway (6) is not the main route of SO_2 formation since following NO to NO_2 conversion by

$$CH_3O_2 + NO \rightarrow CH_3O + NO_2$$

some CH_3ONO might be expected to form by

$$CH_3O + NO\ (+M) \rightarrow CH_3ONO\ (+M)$$

The fact that photolysis of CH_3SSCH_3 in air gave SO_2 and HCHO in more than 90% yield but formed little CH_3OH was used by Hatakeyama and Akimoto [1983] to argue that the CH_3 radical is not the precursor of HCHO since the following mechanism,

$$CH_3SSCH_3 + h\nu \rightarrow 2\ CH_3S$$

$$CH_3S + O_2 \rightarrow CH_3SO_2$$

$$CH_3SO_2\ (+M) \xrightarrow{O_2} CH_3O_2 + SO_2\ (+M) \qquad (6)$$

$$2\ CH_3O_2 \rightarrow 2\ CH_3O + O_2 \qquad (7)$$

$$2\ CH_3O_2 \rightarrow HCHO + CH_3OH + O_2 \quad (8)$$

$$CH_3O + O_2 \rightarrow HCHO + HO_2 \quad (9)$$

predicts the yield of CH_3OH to be 46% of that of HCHO from available rate constant ratios of 1 : 1.7 between reactions (7) and (8) [Hatakeyama and Akimoto, 1983]. Therefore their results suggest pathway other than (6) in Figure 1 to form SO_2.

The above experimental observations of Hatakeyama and Akimoto, and Niki et al., are consistent with pathway (7) in Figure 1, as also noted by Balla and Heicklen [1985]. From pathway (7), SO_2 and HCHO are produced in equal yields, but no CH_3 radicals are generated.

Considering the relatively low enthalpy changes involved in the decomposition reactions of the CH_3SO_2 and CH_3SO_3 radicals, 17 kcal $mole^{-1}$ and 22 kcal $mole^{-1}$, respectively [Kerr and Calvert, 1984], the decomposition reactions are expected to be fast, so the competitive reactions of these radicals, which are necessary to lead to CH_3SO_3H, i.e., by pathways (5), (8) and (9) in Figure 1, have to be very rapid if they are important.

From the above studies of the reactions of the CH_3S radical, the fate of CH_3S and the nature of SO_2 and CH_3SO_3H formation pathways remain unclear.

2.4.2. Product Studies of RSR′–OH Reactions

The differences in the yields of SO_2 and CH_3SO_3H among investigators (see Table 6) have important implications for the overall photochemical reactivity of the organo-sulfur-NO_x systems as reflected in the number of NO to NO_2 conversions occurring on each path.

2.4.2.1. Formation of SO_2 and CH_3SO_3H from RSR

SO_2 and CH_3SO_3H are produced in both the addition and abstraction pathways

of the CH_3SCH_3 – OH reaction, as shown in Figure 1. Considering the addition pathway alone as a source of SO_2 and CH_3SO_3H [pathways (1)-(3)], SO_2 formation through path (1) leads to much higher reactivity for the system than that observed since 6 NO to NO_2 conversions can be expected to result along this path. The ratio of the yields of SO_2 to CH_3SO_3H should be a sensitive function of the initial NO concentration if paths (1) and (2) are important. Because no such sensitivity has been reported, pathways (1) and (2) can be neglected.

Rapid conversion of NO to NO_2 is one of the commonly observed features in the photooxidation of RSR′ – NO–air systems. Niki et al. [1983b] studied the system of CH_3SCH_3 – C_2H_5ONO – NO–air and observed that the reactants, CH_3SCH_3, C_2H_5ONO and NO were consumed approximately in the ratio of 1 : 1 : 2 and the yields of the products SO_2, HCHO and NO_2 per molecule of CH_3SCH_3 consumed were 0.22, 1.1 and 2.3, respectively. These results indicate that the OH initiated oxidation of CH_3SCH_3 converts approximately two molecules of NO to NO_2 and yields SO_2 (22%) and HCHO (100%). They also found CH_3ONO and CH_3ONO_2 as products, and the significant yield (25%) of CH_3ONO could be taken as a lower limit of the formation of CH_3 radicals in the CH_3SCH_3 – OH reaction. This result would be consistent with reaction pathways (5), (8) and (6) in Figure 1.

From the results of the CH_3SCH_3–OH system in Hatakeyama et al. [1982, 1983 and 1985], one finds rapid conversion of NO to NO_2 and yields of HCHO that were always 2–3 times higher than those of SO_2. CH_3ONO and CH_3ONO_2 were identified as major products, indicating clearly the existence of CH_3 radical [pathway (6)]. Also the observed high photochemical reactivity (e.g., rapid conversion of NO to NO_2 and formation of substantial amounts of O_3), formation of HCHO and CH_3ONO in the CH_3SCH_3 – NO_x–air system [Grosjean and Lewis, 1982; Grosjean, 1984a] do not support a major role for pathway (7) as a source of SO_2. The above

product studies of RSR – NO_x–air systems strongly support pathways (5), (8) and (6).

2.4.2.2. Formation of SO_2 and CH_3SO_3H from RSH

Grosjean [1984a] studied the system of CH_3SH – NO–air and CH_3SH – NO – Cl_2–air and observed a 100% yield of SO_2, in agreement with pathway (6).

The photooxidation of CH_3SH – RCH_2ONO – (NO)–air [Hatakeyama and Akimoto, 1983] yielded SO_2, NO, NO_2, HCHO, RCHO, RCH_2OH and CH_3SO_3H. Little conversion of NO to NO_2 occurred, indicating the absence of CH_3 radicals in the system. This result seems consistent with reaction pathway (7) for the formation of SO_2 in Figure 2. However no routes exist for the formation of CH_3SO_3H since paths (5) and (8) involve the conversion of NO to NO_2 and paths (9) and (10) will be shown to be negligible. Therefore the paths of SO_2 and CH_3SO_3H formation in the system of RSH-OH remain unclear.

2.4.3. Effect of NO_x on the Yields of SO_2 and CH_3SO_3H

For the three pathways, (4), (6) and (7), of formation of SO_2 following OH abstraction in Figure 1, the yield of SO_2, i.e.,

$$\text{Yield of } SO_2 = \frac{\Delta[SO_2]}{\Delta[RSR']}$$

will decrease with increasing NO_x concentrations, either due to the competition between RS + O_2 and RS + NO_x or due to the competition between SO_2 and CH_3SO_3H formation.

For the formation of CH_3SO_3H, there exist four possible routes, paths (5), (8), (9) and (10) in Figure 1. The relative rates of the reactions between $CH_3S + O_2$ and CH_3S + OH are,

$$\frac{R(CH_3S + OH)}{R(CH_3S + O_2)} = \frac{k_{CH_3S+OH}\,[OH]}{k_{CH_3S+O_2}\,[O_2]}$$

Typically, $[OH]/[O_2] \approx 10^{-12}$ in the atmosphere, and with k_{CH_3S+OH} unknown but $\leq 2 \times 10^{-10}$ cm^3 molecule^{-1} s^{-1} (the collision limit), and $k_{CH_3S+O_2} \approx 1 \times 10^{-17}$ cm^3 molecule^{-1} s^{-1}, the above ratio is $\leq 2 \times 10^{-5}$. Thus pathway (10) in Figure 1 will not be an important route to produce CH_3SO_3H.

Path (9) involves a competition for CH_3SO_2 radicals between reaction with O_2 and unimolecular decomposition. By similar analysis as above, we conclude that if path (9) is to be competitive with path (6) it is necessary that $k_{CH_3SO_2+OH} \approx 10^{-9}$cm^3 molecule^{-1} sec^{-1}, a value which exceeds the collision rate. Thus path (9) can also be ruled out as a source of CH_3SO_3H.

In addition to the remaining paths (5) and (8) we can postulate a route for CH_3SO_3H formation involving direct reaction of CH_3S and NO_2 to produce CH_3SO:

$$CH_3S + NO_2 \rightarrow CH_3SO + NO$$

which is similar to the reaction between HS and NO_2 [Black, 1984; Friedl et al, 1985].

Hatakeyama et al. [1982] found the yield of CH_3SO_3H decreased as the ratio of $[NO_x]/[CH_3SCH_3]$ increased for the $CH_3SCH_3 - NO_x - CH_3ONO$–air system, indicating the competition between $RS+O_2$ and $RS+NO_x$ has a major effect on the formation of CH_3SO_3H. However no effect of NO_x on the yield of CH_3SO_3H was observed for the $CH_3SH - CH_3ONO - NO$–air system [Hatakeyama and Akimoto, 1983]. No clear trends were observed from the data of Grosjean and Lewis [1982] and Grosjean [1984a], who measured only particulate phase (not gas phase) CH_3SO_3H.

From the analysis of the mechanism of SO_2 and CH_3SO_3H formation shown in

Figures 1, 2 and 3, it can be seen that the major pathways of the formation of products from RSR-OH system are (4), (6) and (7) for SO_2 formation and (5) and (8) for CH_3SO_3H formation, although the relative importance of these pathways is incompletely understood. For the RSH-OH reaction, the mechanism of formation of SO_2 and CH_3SO_3H is not clear. Assuming SO_2 and CH_3SO_3H are formed mainly from the CH_3S radical, the mechanism of SO_2 and CH_3SO_3H should be the same in the $CH_3SH - OH$ and $CH_3SCH_3 - OH$ systems. However, considering the experimental results of Hatakeyama and Akimoto for the $CH_3SH - CH_3ONO - NO -$ air system the relative importance between paths (6) and (7) for SO_2 formation is unknown.

2.5. Summary of the Reaction Mechanisms

Atmospheric photooxidation mechanisms for organo-sulfur compounds have been formulated in this section. We have analyzed the proposed mechanisms based on prior experimental work. Critical uncertainties regarding the chemical pathways, kinetic data and the yield distribution of the products exist in these mechanisms.

3. Comparison of Mechanism Predictions with Smog Chamber Data

In this section, we will present the results of simulations of the experiments of Grosjean and Lewis [1982], Grosjean [1984a] and Hatakeyama et al. [1982, 1983 and 1985]. The study will focus on identifying the critical uncertainties regarding chemical pathways, kinetic data and product yields.

The atmospheric photooxidation mechanisms for CH_3SCH_3, $C_2H_5SC_2H_5$ and CH_3SH are given in Tables 1–5. In performing the numerical simulations, necessary inputs for the chemical mechanisms are the irradiation time, the temperature, the NO_2 photolysis rate profile k_{NO_2} and the initial concentrations of the reactants, which are listed in Tables 7 and 8. The NO_2 photolysis rates we employed for the

experiments of Hatakeyama et al. [1982, 1983 and 1985] were those reported by the authors; the rates used for the experiments of Grosjean and Lewis [1982] and Grosjean [1984a] are calculated theoretically assuming clear sky conditions, as a function of date, time of day and latitude [Demerjian, 1980].

Reaction rate constants for inorganic species and aldehydes are taken from Baulch et al. [1982, 1984], Atkinson and Lloyd [1984b], Kerr and Calvert [1984] and Leone et al. [1985]. Many rate constants for organo-sulfur compounds have not been measured and have been estimated by Kerr and Calvert [1984] and Grosjean [1984a and 1984b]. Others are estimated in the present work.

3.1. Simulations of CH_3SCH_3 Photooxidation Experiments

Simulations of the CH_3SCH_3 photooxidations are summarized in Table 9 and Figures 4 and 5. Table 9 indicates that the yields of SO_2, H_2SO_4 and CH_3SO_3H are predicted reasonably well (to be discussed later). The agreement between the predicted and observed concentration-time profiles of reactants and major products was good. The mechanism predicted NO and NO_2 behavior quite well for Grosjean's experiments. The decay of CH_3SCH_3 and the production of SO_2 and HCHO were well predicted, especially the trends. Ozone formation was consistently overpredicted, but the time of the ozone appearance and trends were predicted accurately. One explanation for overpredicted O_3 formation is that O_3 may have been lost on the walls of the chambers.

3.1.1. Competition between $CH_3S + NO_x$ and $CH_3S + O_2$

Based on the estimates of Grosjean [1984a] and Kerr and Calvert [1984], the rate constants for reactions between $CH_3S + NO_x$ and $CH_3S + O_2$ could be selected as

		k(cm^3 $molecule^{-1}sec^{-1}$)	
$CH_3S + NO$	$\rightarrow$ CH_3SNO	6×10^{-11}	(113)
$CH_3S + NO_2$	$\rightarrow$ CH_3SNO_2	3×10^{-11}	(114)
$CH_3S + O_2$	$\rightarrow$ CH_3SO_2	1×10^{-17}	(115)

However, using these values simulation of the experiments of both groups resulted in very low reactivity for the system. By varying the ratios of k_{113}/k_{115} and k_{114}/k_{115}, the reactivity of the system was found to change substantially (see Figure 6).

Figure 6 indicates that as the ratios of k_{113}/k_{115} and k_{114}/k_{115} decrease, the system reactivity as reflected by the formation of SO_2, HCHO and O_3 and the decay of CH_3SCH_3 increases substantially. Fixing the ratio of k_{114}/k_{115}, the NO decay rates increase rapidly as the ratio k_{113}/k_{115} is decreased. The competition between $CH_3S + NO_2$ and $CH_3S + O_2$ will only affect the decay rate of NO in the latter part of the irradiation when NO_2 has reached substantial level. For the prediction of NO_2, both ratios are important and as the ratios are decreased, the NO_2 peaks are reached earlier because the system is more reactive.

The above conclusions are consistent with the role of CH_3SNO as a reservoir of both NO and CH_3S. As k_{113}/k_{115} is decreased, more CH_3S radical are available to react with O_2. However when k_{114}/k_{115} is decreased, the net amounts of CH_3S and NO_2 increase, leading to an increase in CH_3O_2 radicals along paths (4) and (6) and therefore increasing system reactivity.

We should point out that the reactivity of the system is also sensitive to the ratio k_{109}/k_{112} because even though both paths give CH_3S, the route involving reaction (109) produces two more HO_2 radicals.

3.1.2. Competition between RSO_x Decomposition and $RSO_x + O_2$

The competition between decomposition and reaction with O_2 controls the CH_3SO_x radicals:

$$CH_3SO\ (+M) \rightarrow CH_3 + SO\ (+M) \quad (130)$$

$$CH_3SO + O_2 \rightarrow CH_3SO_3 \quad (128)$$

$$CH_3SO_2\ (+M) \rightarrow CH_3 + SO_2\ (+M) \quad (137)$$

$$CH_3SO_2 + O_2 \rightarrow CH_3SO_4 \quad (138)$$

Of these reactions, rate constant estimates are available only for reaction (137). Thus the ratios, k_{130}/k_{128} and k_{137}/k_{138}, were varied to test the sensitivity of the system.

Figure 7 shows clearly that the system reactivity increases rapidly as the ratios k_{130}/k_{128} and k_{137}/k_{138} increase because of the production of CH_3O_2 radicals. The yield distribution of SO_2 and CH_3SO_3H depends significantly on these two ratios because reactions (128) and (138) lead largely to CH_3SO_3H whereas reactions (130) and (137) lead to SO_2.

3.1.3. Initial OH Reaction: addition vs. abstraction pathways

The effect on the performance of the mechanism of abstraction and addition for the initial OH reaction was evaluated by varying the ratio k_{84}/k_{83}. It was found on the basis of product yields that the addition pathway should be less than 25% of the overall reaction, $k_{84}/k_{83} = 0.15$ produced good fit to the experimental data, indicating that the major pathway of initial attack is abstraction, but addition is not insignificant. This is consistent with the recent observation of Martin et al. [1985].

Figure 8 shows the effect of the ratio k_{84}/k_{83} on SO_2 concentration. SO_2 formation through the addition path was not included as discussed earlier since

this route leads to much higher reactivity for the system. It can be seen that the system reactivity is relatively insensitive to the k_{84}/k_{83} ratio because we assume one CH_3O_2 is produced for each CH_3SO_3H formed on path (3) and SO_2 formed on paths (4) and (6), and the reactivity strongly depends on the formation of CH_3O_2 radicals. The yield distribution of SO_2 and CH_3SO_3H, however, changes greatly as the ratio varies because CH_3SO_3H is only produced on path (3).

3.1.4. Yield Distribution of SO_2 and CH_3SO_3H

From Table 9, we can see that the yields of CH_3SO_3H were consistently overpredicted for the experiments of Grosjean and Lewis [1982] and Grosjean [1984a], but underpredicted for the data of Hatakeyama et al. [1982, 1983 and 1985]. There are several possible reasons for these yield differences.

The experiments of Hatakeyama et al. were carried out using high NO_x concentrations, therefore the following reactions may be important,

$$\begin{aligned} CH_3S &\xrightarrow{NO_2} CH_3SO \rightarrow CH_3SO_3H \\ CH_3SO_2 &\xrightarrow{NO} CH_3SO \rightarrow CH_3SO_3H \\ CH_3SO_4 &\xrightarrow{NO} CH_3SO_3 \rightarrow CH_3SO_3H \end{aligned}$$

leading to a higher yield of CH_3SO_3H.

The large difference of the concentrations of CH_3SCH_3 and OH between the work of Grosjean and Lewis (CH_3SCH_3: 0.3-1.5 ppm, no additional OH source) and the work of Hatakeyama et al. (CH_3SCH_3 : 10 – 830 ppm, CH_3ONO : $\approx$ 45 ppm) is probably another reason since in relatively short irradiation periods (few mins), the rapid OH reaction provides large amounts of CH_3S, which may recombine to form dimethyl disulfide,

$$CH_3S + CH_3S \rightarrow CH_3SSCH_3$$

and the subsequent reaction of OH with CH_3SSCH_3 will increase the yields of CH_3SO_3H significantly through

$$CH_3SSCH_3 + OH \rightarrow CH_3S + CH_3SOH$$
$$CH_3SOH + O_2 \rightarrow CH_3SO_3H$$

It does not seem possible that the low yields of CH_3SO_3H observed by Grosjean and Lewis [1982] and Grosjean [1984a] are due to the reaction of CH_3SO_3H with OH since CH_3SO_3H was identified in ambient aerosol samples [Panter and Penzhorn, 1980; Saltzman et al., 1983]. However, Grosjean and Lewis measured only particulate phase alkanesulfonic acid in their experimental studies. Since alkanesulfonic acid may exist in both aerosol and gas phases and also could be lost on the walls, their data represent lower limits for actual CH_3SO_3H in their experiments, which is consistent with the simulations.

3.2. Simulations of $C_2H_5SC_2H_5$ Photooxidation Experiments

Simulations of $C_2H_5SC_2H_5$ – NO_x–air photooxidations of Grosjean [1984a] are shown in Figure 9 and Table 9. The temporal profiles of NO, $C_2H_5SC_2H_5$ and SO_2 were predicted very well, but O_3 was overpredicted consistently. One difference between $C_2H_5SC_2H_5$ and CH_3SCH_3 is the formation of peroxyacetyl nitrate (PAN). Uncertainties concerning the mechanism and kinetic data are large since only two experiments were reported [Grosjean, 1984a].

3.3. Simulation of CH_3SH Photooxidation Experiments

Only two concentration-time profiles for the CH_3SH – NO_x–air system were

reported [Hatakeyama and Akimoto, 1983; Grosjean, 1984a]. Concentrations of CH_3SNO, CH_3OH, CH_3ONO and CH_3SH from Hatakeyama and Akimoto are predicted very accurately as shown in Figure 10. Simulation of Grosjean's experiment was not successful and in order to predict his data the rate constants k_{113} and k_{114} need to be decreased from the values used for the CH_3SCH_3 system. Note that in the CH_3SH system NO is predicted to decrease, which conflicts with the experimental observations of Hatakeyama and Akimoto [1983].

Hydroxyl radicals were generated by Hatakeyama and Akimoto [1983] by the photolysis of RCH_2ONO in air as follows:

$$RCH_2ONO + h\nu \rightarrow RCH_2O + NO \quad \text{(a)}$$

$$RCH_2O + O_2 \rightarrow RCHO + HO_2 \quad \text{(b)}$$

$$HO_2 + NO \rightarrow OH + NO_2 \quad \text{(c)}$$

$$CH_3SH + OH \rightarrow CH_3S(OH)H \quad \text{(d)}$$

$$RCH_2ONO + CH_3S(OH)H \rightarrow CH_3SNO + RCH_2OH + OH \quad \text{(e)}$$

Under the experimental condition of high initial concentration of NO (10.9 ppm), NO was converted to NO_2 rapidly according to reactions (a)-(c) as long as RCH_2ONO photolysis occurred. In the presence of CH_3SH, although RCH_2ONO was mainly consumed by reaction (e), and NO was produced from photolysis of RCH_2ONO, NO was not predicted to accumulate as was observed [Hatakeyama and Akimoto, 1983] even assuming path (7) is the sole route to form SO_2, i.e., no CH_3 radicals are generated. By comparing the overall balance of total NO (NO, RCH_2ONO, CH_3SNO) between the beginning and end in the $CH_3SSCH_3 - C_2H_5ONO - NO$-air system [Hatakeyama and Akimoto, 1983], it can be seen that

no NO was consumed. Considering the fact that NO was converted to NO_2 in all the studies of $CH_3SCH_3 - NO_x$, we conclude that there exist some routes that are capable of converting NO_2 to NO in the system of $CH_3SH - RCH_2ONO - NO - air$. It is not clear whether these routes occur only because of the presence of RCH_2ONO in which case they would be of marginal relevance to the atmosphere.

4. Conclusions

There are limited experimental data that allow an adequate test of detailed gas-phase photooxidation mechanisms of organo-sulfur compounds. In the few available experiments, analysis of sulfuric acid, nitric acid and alkane sulfonic acid were usually not carried out. New experimental tests of the rates of generation of the important species including OH, NO_3, NO_x, HNO_3, RONO, $RONO_2$, PAN, RCHO, O_3, RSNO, $RSNO_2$, SO_2, H_2SO_4 and RSO_3H at low concentrations of organo-sulfur compounds and NO_x in air should be carried out in order to evaluate proposed chemical mechanisms.

Based on the available experimental data, simulations of current mechanisms have been carried out and focused on identifying the critical uncertainties regarding chemical pathways, kinetic data and product yields. The critical uncertainties for the proposed mechanisms include the nature of the initial OH reaction, the competition between $RS + NO_x$ and $RS + O_2$, the competition between $RSO_x + O_2$ and RSO_x unimolecular decomposition, the effects of NO_x in these pathways, and the formation of SO_2 and CH_3SO_3H. Critical differences in SO_2 and CH_3SO_3H yields among several systems have been addressed, but still remain to be elucidated.

ACKNOWLEDGMENT

This work was supported by National Science Foundation grant ATM–8503103.

Table 1. Inorganic and Aldehyde Chemistry Common to Mechanisms of Organosulfur Species

	REACTION	RATE CONSTANT[a]	ACTIVATION ENERGY(K)	REF.	NOTE
Inorganic Reactions					
1.	$NO_2 + h\nu \rightarrow NO + O(^3P)$	*			(1)
2.	$O(^3P) + O_2 \rightarrow O_3$	1.5×10^{-14}	-5.60×10^2	2,17	
3.	$O_3 + NO \rightarrow NO_2 + O_2$	1.8×10^{-14}	1.43×10^3	2	
4.	$O(^3P) + NO_2 \rightarrow NO + O_2$	9.3×10^{-12}	0.0	2,6	
5.	$O_3 + NO_2 \rightarrow NO_3 + O_2$	3.2×10^{-17}	2.45×10^3	2	
6.	$NO_3 + NO \rightarrow 2\ NO_2$	2.0×10^{-11}		6	
7.	$HO_2 + NO_2 \rightarrow HO_2NO_2$	1.4×10^{-12}		2	
8.	$NO_2 + OH \rightarrow HNO_3$	1.1×10^{-11}		2	
9.	$O_3 + OH \rightarrow HO_2 + O_2$	6.8×10^{-14}	9.4×10^2	2	
10.	$O_3 + HO_2 \rightarrow OH + 2\ O_2$	2.0×10^{-15}	5.8×10^2	2	
11.	$HO_2NO_2 \rightarrow HO_2 + NO_2$	8.5×10^{-2}	1.042×10^4	2	
12.	$HO_2 + NO \rightarrow NO_2 + OH$	8.3×10^{-12}	-2.4×10^2	2	
13.	$HO_2 + HO_2 \rightarrow H_2O_2 + O_2$	1.8×10^{-12}	-6.2×10^2	2	(2)
14.	$HO_2 + HO_2 \rightarrow H_2O_2 + O_2$	1.3×10^{-12}	-9.8×10^2	2	(2)
15.	$HO_2 + HO_2 + H_2O \rightarrow H_2O_2 + O_2 + H_2O$	4.0×10^{-30}	-2.8×10^3	2	(2)
16.	$HO_2 + HO_2 + H_2O \rightarrow H_2O_2 + O_2 + H_2O$	2.8×10^{-30}	-3.2×10^3	2	(2)
17.	$O_3 + h\nu \rightarrow O(^3P) + O_2$	$4.0 \times 10^{-2} k_{NO_2}$		1,19	
18.	$O_3 + H_2O + h\nu \rightarrow 2\ OH + O_2$	$9.34 \times 10^{-22} k_{NO_2}$		1,9	(3)
19.	$NO + OH \rightarrow HONO$	6.6×10^{-12}		2	
20.	$HONO + h\nu \rightarrow NO + OH$	$1.7 \times 10^{-1} k_{NO_2}$		1	
21.	$NO + NO + O_2 \rightarrow 2\ NO_2$	2.0×10^{-38}	-5.3×10^2	2	
22.	$NO_3 + NO_2 \rightarrow NO + NO_2 + O_2$	4.0×10^{-16}	1.23×10^3	2	
23.	$NO_3 + NO_2 \rightarrow N_2O_5$	1.2×10^{-12}	6.0×10^1	2,17	
24.	$N_2O_5 \rightarrow NO_2 + NO_3$	5.2×10^{-2}	1.084×10^4	5,17	
25.	$N_2O_5 + H_2O \rightarrow 2\ HNO_3$	3.0×10^{-21}		E1[b]	
26.	$H_2O_2 + OH \rightarrow HO_2 + H_2O$	1.7×10^{-12}	1.87×10^2	2	
27.	$H_2O_2 + h\nu \rightarrow 2\ OH$	$7.1 \times 10^{-4} k_{NO_2}$		1	
28.	$CO + OH \xrightarrow{O_2} HO_2 + CO_2$	2.2×10^{-13}		2	
29.	$NO_3 + h\nu \rightarrow 0.3\ NO + 0.7\ NO_2 + 0.7\ O(^3P)$	$1.55 \times 10^1 k_{NO_2}$		18	
30.	$NO_2 + O_3 \rightarrow NO + 2\ O_2$	9.7×10^{-19}	2.45×10^3	17	
31.	$NO_3\ (+M) \rightarrow NO + O_2\ (+M)$	3.0×10^{-3}	6.84×10^3	17	
32.	$NO_3 + HO_2 \rightarrow HNO_3 + O_2$	2.5×10^{-12}		17	
33.	$OH + HONO \rightarrow H_2O + NO_2$	6.6×10^{-12}	0.00	2,17	
34.	$OH + HNO_3 \rightarrow H_2O + NO_3$	1.3×10^{-13}	-7.78×10^2	2,6	
35.	$OH + HO_2NO_2 \rightarrow H_2O + O_2 + NO_2$	4.6×10^{-12}	-3.8×10^2	6,17	
36.	$O(^3P) + NO_2\ (+M) \rightarrow NO_3\ (+M)$	1.8×10^{-12}	-4.2×10^2	6,17	
37.	$HNO + O_2 \rightarrow HO_2 + NO$	2.1×10^{-20}	5.0×10^3	17	
38.	$OH + H_2 \xrightarrow{O_2} HO_2 + H_2O$	6.7×10^{-15}	2.10×10^3	6	

(continued)

	REACTION	RATE CONSTANT[a]	ACTIVATION ENERGY(K)	REF.	NOTE
	Aldehyde and PAN Formation				
39.	$HCHO + h\nu \rightarrow H_2 + CO$	$3.3 \times 10^{-3} k_{NO_2}$		19	
40.	$HCHO + h\nu \xrightarrow{2O_2} 2\ HO_2 + CO$	$2.3 \times 10^{-3} k_{NO_2}$		19	
41.	$HCHO + OH \xrightarrow{O_2} HO_2 + CO + H_2O$	1.0×10^{-11}		2,6	
42.	$HCHO + NO_3 \xrightarrow{O_2} CO + HNO_3 + HO_2$	6.3×10^{-16}		17	
43.	$HCHO + O(^3P) \xrightarrow{O_2} OH + HO_2 + CO$	1.6×10^{-13}	1.550×10^{3}	2	
44.	$HCHO + HO_2 \rightarrow O_2CH_2OH$	1.7×10^{-14}		17	
45.	$O_2CH_2OH \rightarrow HCHO + HO_2$	1.5×10^{0}		17	
46.	$O_2CH_2OH + NO \xrightarrow{O_2} HCOOH + NO_2 + HO_2$	7.6×10^{-12}	-1.8×10^{2}	17	
47.	$O_2CH_2OH + HO_2 \rightarrow HO_2CH_2OH + O_2$	1.5×10^{-12}	0.0	17	
48.	$HCOOH + OH \xrightarrow{O_2} H_2O + HO_2 + CO_2$	3.6×10^{-13}	7.7×10^{1}	17	
49.	$CH_3CHO + h\nu \xrightarrow{2O_2} CH_3O_2 + HO_2 + CO$	$2.6 \times 10^{-4} k_{NO_2}$		19	(4)
50.	$CH_3CHO + OH \xrightarrow{O_2} CH_3C(O)O_2 + H_2O$	1.2×10^{-11}	-1.65×10^{2}	22	(4)
51.	$CH_3CHO + NO_3 \xrightarrow{O_2} CH_3C(O)O_2 + HNO_3$	1.3×10^{-15}		3	(4)
52.	$CH_3CHO + O(^3P) \xrightarrow{O_2} CH_3C(O)O_2 + OH$	4.3×10^{-13}	9.86×10^{2}	2	(4)
53.	$CH_3C(O)O_2 + NO \xrightarrow{O_2} NO_2 + CH_3O_2 + CO_2$	7.6×10^{-12}	-1.80×10^{2}	2	(4)
54.	$CH_3C(O)O_2 + NO_2 \rightarrow PAN$	4.7×10^{-12}		2	(4)
55.	$CH_3C(O)O_2 + HO_2 \rightarrow CH_3C(O)O_2H + O_2$	3.0×10^{-12}		19	(4)
56.	$PAN \rightarrow CH_3C(O)O_2 + NO_2$	3.6×10^{-4}	1.354×10^{4}	2	(4)
57.	$CH_3 + O_2 \rightarrow CH_3O_2$	1.0×10^{-12}		2	
58.	$CH_3 + O_2 \rightarrow HCHO + OH$	5.0×10^{-17}		6	
59.	$C_2H_5 + O_2 \rightarrow C_2H_5O_2$	1.0×10^{-12}		2	(4)
60.	$CH_3O_2 + NO \rightarrow NO_2 + CH_3O$	7.6×10^{-12}	-1.80×10^{2}	6	
61.	$CH_3O_2 + HO_2 \rightarrow CH_3OOH + O_2$	6.5×10^{-12}	-1.3×10^{3}	6	
62.	$CH_3O_2H + OH \rightarrow 0.5\ CH_3O_2 + H_2O + 0.5\ HCHO + 0.5\ OH$	1.0×10^{-11}		17	
63.	$CH_3O_2 + CH_3O_2 \rightarrow 0.8\ CH_3O + 0.6\ HCHO + 0.6\ CH_3OH$	3.1×10^{-13}	2.2×10^{2}	19	
64.	$CH_3O + O_2 \rightarrow HCHO + HO_2$	1.3×10^{-15}	1.31×10^{3}	2,6	
65.	$CH_3O + NO_2 \rightarrow CH_3ONO_2$	1.5×10^{-11}	0.0	2	
66.	$CH_3O + NO \rightarrow HCHO + HNO$	1.3×10^{-12}		2	
67.	$CH_3O + NO \rightarrow CH_3ONO$	3.0×10^{-11}		2	
68.	$CH_3ONO + h\nu \rightarrow CH_3O + NO$	$0.17 k_{NO_2}$		E	(5)
69.	$C_2H_5O_2 + NO \rightarrow C_2H_5ONO_2$	1.1×10^{-13}	-1.80×10^{2}	2	(4)
70.	$C_2H_5O_2 + NO \rightarrow C_2H_5O + NO_2$	7.6×10^{-12}	-1.80×10^{2}	2	(4)
71.	$C_2H_5O_2 + HO_2 \rightarrow C_2H_5O_2H + O_2$	1.5×10^{-12}		17	(4)
72.	$C_2H_5O_2H + OH \rightarrow H_2O + 0.5\ C_2H_5O_2 + 0.5\ CH_3CHO + 0.5\ OH$	1.0×10^{-11}		17	(4)

(continued)

	REACTION	RATE CONSTANT[a]	ACTIVATION ENERGY(K)	REF.	NOTE
73.	$C_2H_5O + NO \rightarrow C_2H_5ONO$	3.0×10^{-11}		2	(4)
74.	$C_2H_5ONO + h\nu \rightarrow C_2H_5O + NO$	$0.17k_{NO_2}$		E	(4,5)
75.	$C_2H_5O + NO \rightarrow CH_3CHO + HNO$	6.6×10^{-12}		2	(4)
76.	$C_2H_5O + NO_2 \rightarrow C_2H_5ONO_2$	1.2×10^{-11}		2	(4)
77.	$C_2H_5O + NO_2 \rightarrow CH_3CHO + HONO$	5.5×10^{-12}		2	(4)
78.	$C_2H_5O + O_2 \rightarrow CH_3CHO + HO_2$	8.0×10^{-15}		6	(4)
79.	$2\ C_2H_5O_2 \rightarrow 1.58\ CH_3CHO + 0.44\ C_2H_5OH + O_2$	5.2×10^{-14}	5.0×10^{2}	E17	(4)
80.	$CH_3O_2 + C_2H_5O_2 \rightarrow 0.7\ HCHO + 0.22\ C_2H_5OH + 0.4\ HO_2 + 0.79\ CH_3CHO + 0.3\ CH_3OH$	1.8×10^{-13}	3.60×10^{2}	E17	(4)
81.	$CH_3OH + OH \xrightarrow{O_2} HCHO + HO_2 + H_2O$	1.0×10^{-12}	-3.3×10^{2}	5,17	
82.	$C_2H_5OH + OH \xrightarrow{O_2} CH_3CHO + HO_2 + H_2O$	3.5×10^{-12}	-3.1×10^{2}	17	(4)

* References and notes are listed at the bottom of Table 5.

Table 2. Atmospheric Photooxidation Mechanism

For Dimethyl Sulfide

	REACTION	RATE CONSTANT[a]	ACTIVATION ENERGY(K)	REF.	NOTE
Initial Reactions					
83.	$CH_3SCH_3+OH \rightarrow CH_3SCH_2+H_2O$	6.8×10^{-12}	-4.09×10^2	6,17	(6)
84.	$CH_3SCH_3+OH \rightarrow CH_3S(OH)CH_3$	1.0×10^{-12}	-4.09×10^2	6,17	(6)
85.	$CH_3SCH_3+O(^3P) \rightarrow CH_3SO+CH_3$	5.0×10^{-11}	-4.09×10^2	6	(6)
86.	$CH_3SCH_3+O(^3P) \rightarrow CH_3S+CH_3O$	0.0		E[b]	(6)
87.	$CH_3SCH_3+NO_3 \rightarrow CH_3SCH_2+HNO_3$	9.9×10^{-13}	6.00×10^1	17	(6)
88.	$CH_3SCH_3+NO_3 \rightarrow CH_3S(O)CH_3+NO_2$	0.0		E	(6)
89.	$CH_3SCH_3+O_3 \rightarrow P$	0.0		E	(7)
90.	$CH_3SCH_3+NO_2 \rightarrow CH_3S(O)CH_3+ NO$	9.0×10^{-21}		4	
91.	$CH_3SCH_3+h\nu \rightarrow P$	0.0		E	(7)
Radical Reactions					
92.	$CH_3S(OH)CH_3 +O_2 \rightarrow CH_3S(OH)O_2CH_3$	0.0		E	(6)
93.	$CH_3S(OH)CH_3+O_2 \rightarrow CH_3S(O)CH_3+HO_2$	0.0		E	(7)
94.	$CH_3S(OH)O_2CH_3 \xrightarrow{O_2} CH_3SO_3H+CH_3O_2$	2.5×10^1		E	(8)
95.	$CH_3S(OH)O_2CH_3+ NO \rightarrow CH_3S(OH)OCH_3 +NO_2$	7.6×10^{-12}		E17	
96.	$CH_3S(OH)OCH_3 \xrightarrow{O_2} CH_3S(OH)O+CH_3O_2$	2.5×10^{-1}		E	(8)
97.	$CH_3S(OH)O \xrightarrow{O_2} CH_3O_2 + SO_2H$	2.5×10^{-1}		E	(8)
98.	$SO_2H+O_2 \rightarrow HO_2 +SO_2$	1.0×10^{-14}		E	(10)
99.	$CH_3S(OH)CH_3 \rightarrow CH_3SOH +CH_3$	2.5×10^1		E	(8)
100.	$CH_3SOH+O_2 \rightarrow CH_3SO_3H$	1.0×10^{-14}		E	(11)
101.	$CH_3SO_3H+OH \rightarrow H_2O + CH_2SO_3H$	3.0×10^{-12}		E15	
102.	$CH_2SO_3H+O_2 \rightarrow O_2CH_2SO_3H$	2.0×10^{-12}		E	(12)
103.	$O_2CH_2SO_3H+ NO \rightarrow OCH_2SO_3H+NO_2$	5.0×10^{-12}		E	(13)
104.	$OCH_2SO_3H \rightarrow HCHO +HSO_3$	2.0×10^2		E	(8)
105.	$CH_3S(O)CH_3+NO_2 \rightarrow P$	0.0		E	(7)
106.	$CH_3S(O)CH_3 \rightarrow CH_3SO+CH_3$	0.0		E	(7)
107.	$CH_3SCH_2+O_2(+M) \rightarrow CH_3SCH_2O_2 (+M)$	5.0×10^{-13}		E	(12)
108.	$CH_3SCH_2O_2+ NO \rightarrow CH_3SCH_2O+NO_2$	7.6×10^{-12}	-1.8×10^2	E17	
109.	$CH_3SCH_2O+O_2 \rightarrow CH_3SCHO+HO_2$	1.2×10^{-16}	7.50×10^2	E	(6,10)
110.	$CH_3SCHO +h\nu \xrightarrow{2O_2} CH_3SO_2 +HO_2 +CO$	$2.6 \times 10^{-4} k_{NO_2}$		E	(14)
111.	$CH_3SCHO+ OH \rightarrow H_2O +CH_3+COS$	1.0×10^{-13}		E	(15)
112.	$CH_3SCH_2O \rightarrow CH_3S+HCHO$	2.0×10^4		E	(6,9)
113.	$CH_3S+NO \rightarrow CH_3SNO$	2.7×10^{-12}		E	(6)
114.	$CH_3S+NO_2 \rightarrow CH_3SNO_2$	5.1×10^{-12}		E	(6)
115.	$CH_3S+O_2 \rightarrow CH_3SO_2$	1.4×10^{-17}		E	(6)

(continued)

	REACTION	RATE CONSTANT[a]	ACTIVATION ENERGY(K)	REF.	NOTE
116.	$CH_3S+O_3 \rightarrow CH_3SO+O_2$	3.0×10^{-12}		E17	
117.	$CH_3S+ OH \rightarrow CH_3SOH$	6.8×10^{-11}		E	(15)
118.	$CH_3S+NO_2 \rightarrow CH_3SO+NO$	6.8×10^{-12}		E	(16)
119.	$CH_3S+CH_3S \rightarrow CH_3SH + CH_2S$	0.0		E	(7)
120.	$CH_3S+CH_3S \rightarrow (CH_3S)_2$	4.1×10^{-14}		11	
121.	$CH_3S+CH_3SNO \rightarrow (CH_3S)_2 + NO$	0.0		E	(7)
122.	$CH_3S+CH_3SNO_2 \rightarrow (CH_3S)_2+NO_2$	0.0		E	(7)
123.	$CH_3SNO +h\nu \rightarrow CH_3S+NO$	$0.1k_{NO_2}$		E14	
124.	$CH_3SNO_2 +h\nu \rightarrow CH_3S+NO_2$	0.0		E	(7)
125.	$CH_3SNO+NO_2 \rightarrow CH_3S(O)NO +NO$	0.0		E	(7)
126.	$CH_3S(O)NO \rightarrow CH_3SO+ NO$	0.0		E	(7)
127.	$CH_3SO+O_3 \rightarrow CH_3SO_2 +O_2$	1.0×10^{-14}		E	(17)
128.	$CH_3SO+O_2 \rightarrow CH_3SO_3$	1.0×10^{-17}		E	(6,18)
129.	$CH_3SO+O_2 \rightarrow CH_3O+SO_2$	0.0		E	(7)
130.	$CH_3SO \rightarrow CH_3+ SO$	3.6×10^{1}		E	(6,9)
131.	$CH_3SO+CH_3SNO \rightarrow (CH_3S)_2 +NO_2$	0.0		E	(7)
132.	$CH_3SO+CH_3SNO \rightarrow (CH_3S)_2O +NO$	0.0		E	(7)
133.	$CH_3SO+CH_3SO \rightarrow (CH_3SO)_2$	1.0×10^{-12}		E	(15)
134.	$CH_3SO+NO_2 \rightarrow CH_3SONO_2$	0.0		E	(7)
135.	$CH_3SO_2 +OH \rightarrow CH_3SO_3H$	1.0×10^{-11}		E	(15)
136.	$CH_3SO_2 +NO \rightarrow CH_3SO+NO_2$	2.0×10^{-13}		E	(13)
137.	$CH_3SO_2 (+M) \xrightarrow{O_2} CH_3O_2 +SO_2 (+M)$	8.7×10^{0}	1.0×10^{4}	E	(6,9)
138.	$CH_3SO_2 +O_2 \rightarrow CH_3SO_4$	4.9×10^{-19}		E	(6,18)
139.	$CH_3SO_2 +O_3 \rightarrow CH_3SO_3 +O_2$	6.8×10^{-14}		E	(17)
140.	$CH_3SO_2 +CH_3SH \rightarrow C_2H_7S_2O_2$	0.0		E	(7)
141.	$CH_3SO_3 +H_2O \rightarrow CH_3SO_3H+OH$	5.0×10^{-13}		E	(15)
142.	$CH_3SO_3 + HCHO \xrightarrow{O_2} HO_2 +CO+CH_3SO_3H$	6.0×10^{-16}		E17	
143.	$CH_3SO_3 +CH_3CHO \xrightarrow{O_2} CH_3C(O)O_2+CH_3SO_3H$	2.0×10^{-15}		E17	
144.	$CH_3SO_3 +CH_3SCH_3 \rightarrow CH_3SO_3H+CH_3SCH_2$	6.8×10^{-14}		E	(15)
145.	$CH_3SO_3 +NO \rightarrow CH_3SO_2 +NO_2$	0.0		E	(7)
146.	$CH_3SO_3 (+M) \xrightarrow{O_2} CH_3O_2 +SO_3$	1.0×10^{-4}	1.2×10^{4}	E17	
147.	$CH_3SO_3 +NO_2 \rightarrow CH_3SO_3NO_2$	0.0		E	(7)
148.	$CH_3SO_3 +NO \rightarrow CH_3SO_3NO$	0.0		E	(7)
149.	$CH_3SO_4 \rightarrow HCHO +OH +SO_2$	2.5×10^{0}		E	(6,9)
150.	$CH_3SO_4 + NO \rightarrow CH_3SO_3 +NO_2$	6.8×10^{-15}		E	(13)
151.	$CH_3SO_4 +CH_3SH \rightarrow C_2H_7S_2O_4$	0.0		E	(7)
152.	$CH_3SO_4 +(CH_3S)_2 \rightarrow P$	0.0		E	(7)
153.	$CH_3SO_4 +CH_3SO_4 \rightarrow 2\ CH_3SO_3 +O_2$	6.8×10^{-12}		E	(15)

Table 3. Atmospheric Photooxidation Mechanism

For Methanethiol

REACTION	RATE CONSTANT[a]	ACTIVATION ENERGY(K)	REF.	NOTE
Initial Reactions				
154. $CH_3SH + OH \rightarrow CH_3S + H_2O$	3.4×10^{-12}	-3.38×10^2	23	(6)
155. $CH_3SH + OH \rightarrow CH_3S(OH)H$	3.1×10^{-11}	-3.38×10^2	23	(6)
156. $CH_3SH + O(^3P) \rightarrow CH_3 + HSO$	1.1×10^{-12}	1.673×10^3	8,21	(19)
157. $CH_3SH + O(^3P) \xrightarrow{O_2} CH_3SO + HO_2$	5.2×10^{-13}	1.673×10^3	8,21	(19)
158. $CH_3SH + O(^3P) \rightarrow CH_3S + OH$	1.8×10^{-13}	1.673×10^3	8,21	(19)
159. $CH_3SH + NO_3 \rightarrow CH_3S + HNO_3$	1.2×10^{-12}		E[b]	(6)
160. $CH_3SH + NO_3 \rightarrow CH_3SOH + NO_2$	0.0		E	(6)
161. $CH_3SH + h\nu \xrightarrow{O_2} CH_3S + HO_2$	0.0		E	(7)
162. $CH_3SH + NO_2 \rightarrow CH_3SNO + OH$	0.0		E	(7)
163. $CH_3SH + NO_2 \rightarrow CH_3S + HONO$	0.0		E	(7)
164. $CH_3SH + NO_2 \rightarrow CH_3SOH + NO$	0.0		E	(7)
165. $CH_3SH + O_3 \rightarrow P$	0.0		E	(7)
166. $CH_3SH + CH_3SO \rightarrow CH_3SOH + CH_3S$	0.0		E	(7)
Radical Reactions				
167. $CH_3S(OH)H + CH_3ONO \rightarrow CH_3SNO + CH_3OH + OH$	5.9×10^{-13}		E	(20)
168. $CH_3S(OH)H \rightarrow CH_3S + H_2O$	2.5×10^1		E	(8)
169. $CH_3S(OH)H + O_2 \rightarrow CH_3S(OH)O_2H$	0.0		E	(6)
170. $CH_3S(OH)H + O_2 \rightarrow CH_3S(O)H + HO_2$	0.0		E	(21)
171. $CH_3S(OH)O_2H \xrightarrow{O_2} CH_3SO_3H + HO_2$	2.5×10^1		E	(21)
172. $CH_3S(OH)O_2H + NO \rightarrow CH_3S(OH)(O)H + NO_2$	7.6×10^{-12}		E	(21)
173. $CH_3S(OH)(O)H \xrightarrow{O_2} CH_3S(OH)O + HO_2$	2.5×10^{-1}		E	(21)
174. $CH_3S(OH)O \xrightarrow{O_2} CH_3O_2 + SO_2H$	2.5×10^{-1}		E	(8)
175. $SO_2H + O_2 \rightarrow HO_2 + SO_2$	1.0×10^{-14}		E	(10)
176. $CH_3S(OH)H \xrightarrow{O_2} CH_3SOH + HO_2$	2.5×10^0		E	(8)
177. $CH_3SOH + O_2 \rightarrow CH_3SO_3H$	1.0×10^{-14}		E	(11)
178. $CH_3SO_3H + OH \rightarrow H_2O + CH_2SO_3H$	3.0×10^{-12}		E15	
179. $CH_2SO_3H + O_2 \rightarrow O_2CH_2SO_3H$	2.0×10^{-12}		E	(12)
180. $O_2CH_2SO_3H + NO \rightarrow OCH_2SO_3H + NO_2$	5.0×10^{-12}		E	(13)
181. $OCH_2SO_3H \rightarrow HCHO + HSO_3$	2.0×10^2		E	(8)
182. $CH_3S + NO \rightarrow CH_3SNO$	2.7×10^{-12}		E	(6)
183. $CH_3S + NO_2 \rightarrow CH_3SNO_2$	5.1×10^{-12}		E	(6)
184. $CH_3S + O_2 \rightarrow CH_3SO_2$	1.4×10^{-17}		E	(6)
185. $CH_3S + O_3 \rightarrow CH_3SO + O_2$	3.0×10^{-12}		E17	
186. $CH_3S + OH \rightarrow CH_3SOH$	6.8×10^{-11}		E	(15)

(continued)

	REACTION	RATE CONSTANT[a]	ACTIVATION ENERGY(K)	REF.	NOTE
187.	$CH_3S+NO_2 \rightarrow CH_3SO+NO$	6.8×10^{-12}		E	(16)
188.	$CH_3S+CH_3S \rightarrow CH_3SH + CH_2S$	0.0		E	(7)
189.	$CH_3S+CH_3S \rightarrow (CH_3S)_2$	4.1×10^{-14}		11	
190.	$CH_3S+CH_3SNO \rightarrow (CH_3S)_2 + NO$	0.0		E	(7)
191.	$CH_3S+CH_3SNO_2 \rightarrow (CH_3S)_2+NO_2$	0.0		E	(7)
192.	$CH_3SNO + h\nu \rightarrow CH_3S+NO$	$5.0k_{NO_2}$		E	(22)
193.	$CH_3SNO_2 + h\nu \rightarrow CH_3S+NO_2$	0.0		E	(7)
194.	$CH_3SNO+NO_2 \rightarrow CH_3S(O)NO + NO$	0.0		E	(7)
195.	$CH_3S(O)NO \rightarrow CH_3SO + NO$	0.0		E	(7)
196.	$CH_3SO+O_3 \rightarrow CH_3SO_2 + O_2$	1.0×10^{-14}		E	(17)
197.	$CH_3SO+O_2 \rightarrow CH_3SO_3$	1.0×10^{-17}		E	(6,18)
198.	$CH_3SO+O_2 \rightarrow CH_3O+SO_2$	0.0		E	(7)
199.	$CH_3SO \rightarrow CH_3 + SO$	3.6×10^{1}		E	(6,9)
200.	$CH_3SO+CH_3SNO \rightarrow (CH_3S)_2 + NO_2$	0.0		E	(7)
201.	$CH_3SO+CH_3SNO \rightarrow (CH_3S)_2O + NO$	0.0		E	(7)
202.	$CH_3SO+CH_3SO \rightarrow (CH_3SO)_2$	1.0×10^{-12}		E	(15)
203.	$CH_3SO+NO_2 \rightarrow CH_3SONO_2$	0.0		E	(7)
204.	$CH_3SO_2 + OH \rightarrow CH_3SO_3H$	1.0×10^{-11}		E	(15)
205.	$CH_3SO_2 + NO \rightarrow CH_3SO+NO_2$	2.0×10^{-13}		E	(13)
206.	CH_3SO_2 (+M) $\xrightarrow{O_2}$ $CH_3O_2 + SO_2$ (+M)	8.7×10^{0}	1.0×10^{4}	E	(6,9)
207.	$CH_3SO_2 + O_2 \rightarrow CH_3SO_4$	4.9×10^{-19}		E	(6,18)
208.	$CH_3SO_2 + O_3 \rightarrow CH_3SO_3 + O_2$	6.8×10^{-14}		E	(17)
209.	$CH_3SO_2 + CH_3SH \rightarrow C_2H_7S_2O_2$	0.0		E	(7)
210.	$CH_3SO_3 + H_2O \rightarrow CH_3SO_3H+OH$	5.0×10^{-13}		E	(15)
211.	CH_3SO_3 + HCHO $\xrightarrow{O_2}$ $HO_2 + CO + CH_3SO_3H$	6.0×10^{-16}		E17	
212.	$CH_3SO_3 + CH_3CHO \xrightarrow{O_2} CH_3C(O)O_2 + CH_3SO_3H$	2.0×10^{-15}		E17	
213.	$CH_3SO_3 + CH_3SH \rightarrow CH_3SO_3H + CH_3S$	6.8×10^{-14}		E	(15)
214.	$CH_3SO_3 + NO \rightarrow CH_3SO_2 + NO_2$	0.0		E	(7)
215.	CH_3SO_3 (+M) $\xrightarrow{O_2}$ $CH_3O_2 + SO_3$	1.0×10^{-4}	1.2×10^{4}	E17	
216.	$CH_3SO_3 + NO_2 \rightarrow CH_3SO_3NO_2$	0.0		E	(7)
217.	$CH_3SO_3 + NO \rightarrow CH_3SO_3NO$	0.0		E	(7)
218.	$CH_3SO_4 \rightarrow HCHO + OH + SO_2$	2.5×10^{0}		E	(6,9)
219.	$CH_3SO_4 + NO \rightarrow CH_3SO_3 + NO_2$	6.8×10^{-15}		E	(13)
220.	$CH_3SO_4 + CH_3SH \rightarrow C_2H_7S_2O_4$	0.0		E	(7)
221.	$CH_3SO_4 + (CH_3S)_2 \rightarrow P$	0.0		E	(7)
222.	$CH_3SO_4 + CH_3SO_4 \rightarrow 2\ CH_3SO_3 + O_2$	6.8×10^{-12}		E	(15)
223.	$HSO + O_3 \rightarrow HS + 2\ O_2$	1.0×10^{-13}		10	
224.	$HS + NO_2 \rightarrow HSO + NO$	3.0×10^{-11}		10	
225.	$HS + O_3 \rightarrow HSO + O_2$	3.2×10^{-12}		10	
226.	$HS + O_2 \rightarrow SO + OH$	1.0×10^{-17}		10	
227.	$HS + O_2 \rightarrow HSO2$	0.0		E	(7)
228.	$HSO_2 + O_2 \rightarrow HO_2 + SO_2$	1.0×10^{-14}		E	(10)

Table 4. Atmospheric Photooxidation Mechanism

For Diethyl Sulfide

	REACTION	RATE CONSTANT[a]	ACTIVATION ENERGY(K)	REF.	NOTE
Initial Reactions					
229.	$C_2H_5SC_2H_5+OH \rightarrow C_2H_5SCHCH_3+H_2O$	1.1×10^{-11}		20	(6)
230.	$C_2H_5SC_2H_5+OH \rightarrow C_2H_5S(OH)C_2H_5$	1.2×10^{-12}		20	(6)
231.	$C_2H_5SC_2H_5+O(^3P) \rightarrow C_2H_5SO+C_2H_5$	5.0×10^{-11}	-4.09×10^2	E[b]	(21)
232.	$C_2H_5SC_2H_5+O(^3P) \rightarrow C_2H_5S+C_2H_5O$	0.0		E	(21)
233.	$C_2H_5SC_2H_5+NO_3 \rightarrow C_2H_5SCHCH_3+HNO_3$	1.0×10^{-12}	6.00×10^1	E	(21)
234.	$C_2H_5SC_2H_5+NO_3 \rightarrow C_2H_5S(O)C_2H_5+NO_2$	0.0		E	(21)
235.	$C_2H_5SC_2H_5+O_3 \rightarrow P$	0.0		E	(7)
236.	$C_2H_5SC_2H_5+NO_2 \rightarrow C_2H_5S(O)C_2H_5+NO$	0.0		E	(7)
237.	$C_2H_5SC_2H_5+h\nu \rightarrow P$	0.0		E	(7)
Radical Reactions					
238.	$C_2H_5S(OH)C_2H_5+O_2 \rightarrow C_2H_5S(OH)O_2C_2H_5$	0.0		E	(6)
239.	$C_2H_5S(OH)C_2H_5+O_2 \rightarrow C_2H_5S(O)C_2H_5+HO_2$	0.0		E	(21)
240.	$C_2H_5S(OH)O_2C_2H_5 \xrightarrow{O_2} C_2H_5SO_3H+C_2H_5O_2$	2.5×10^1		E	(21)
241.	$C_2H_5S(OH)O_2C_2H_5+NO \rightarrow C_2H_5S(OH)OC_2H_5+NO_2$	7.6×10^{-12}		E	(21)
242.	$C_2H_5S(OH)OC_2H_5 \xrightarrow{O_2} C_2H_5S(OH)O+C_2H_5O_2$	2.5×10^{-1}		E	(21)
243.	$C_2H_5S(OH)O \xrightarrow{O_2} C_2H_5O_2+SO_2H$	2.5×10^{-1}		E	(21)
244.	$SO_2H+O_2 \rightarrow HO_2+SO_2$	1.0×10^{-14}		E	(21)
245.	$C_2H_5S(OH)C_2H_5 \rightarrow C_2H_5SOH+C_2H_5$	2.5×10^1		E	(21)
246.	$C_2H_5SOH+O_2 \rightarrow C_2H_5SO_3H$	1.0×10^{-14}		E	(21)
247.	$C_2H_5SO_3H+OH \rightarrow H_2O+CH_3CHSO_3H$	3.0×10^{-12}		E	(21)
248.	$CH_3CHSO_3H+O_2 \rightarrow CH_3CH(O_2)SO_3H$	2.0×10^{-12}		E	(21)
249.	$CH_3CH(O_2)SO_3H+NO \rightarrow CH_3CH(O)SO_3H+NO_2$	5.0×10^{-12}		E	(21)
250.	$CH_3CH(O)SO_3H \rightarrow CH_3CHO+HSO_3$	2.0×10^2		E	(21)
251.	$C_2H_5S(O)C_2H_5+NO_2 \rightarrow P$	0.0		E	(21)
252.	$C_2H_5S(O)C_2H_5 \rightarrow C_2H_5SO+C_2H_5$	0.0		E	(21)
253.	$C_2H_5SCHCH_3+O_2 (+M) \rightarrow C_2H_5SCH(O_2)CH_3 (+M)$	5.0×10^{-13}		E	(21)
254.	$C_2H_5SCH(O_2)CH_3+NO \rightarrow C_2H_5SCH(O)CH_3+NO_2$	7.6×10^{-12}	-1.80×10^2	E	(21)
255.	$C_2H_5SCH(O)CH_3+O_2 \rightarrow C_2H_5SCOCH_3+HO_2$	1.2×10^{-16}	7.50×10^2	E	(21)
256.	$C_2H_5SCOCH_3+h\nu \xrightarrow{2O_2} C_2H_5SO_2+CH_3CO_3$	$2.6 \times 10^{-4} k_{NO_2}$		E	(21)
257.	$C_2H_5SCOCH_3+OH \rightarrow P$	1.0×10^{-13}		E	(21)
258.	$C_2H_5SCH(O)CH_3 \rightarrow C_2H_5S+CH_3CHO$	2.0×10^4		E	(21)
259.	$C_2H_5S+NO \rightarrow C_2H_5SNO$	2.7×10^{-12}		E	(21)

(continued)

	REACTION	RATE CONSTANT[a]	ACTIVATION ENERGY(K)	REF.	NOTE
260.	$C_2H_5S+NO_2 \rightarrow C_2H_5SNO_2$	5.1×10^{-12}		E	(21)
261.	$C_2H_5S+O_2 \rightarrow C_2H_5SO_2$	1.4×10^{-17}		E	(21)
262.	$C_2H_5S+O_3 \rightarrow C_2H_5SO+O_2$	3.0×10^{-12}		E	(21)
263.	$C_2H_5S+OH \rightarrow C_2H_5SOH$	6.8×10^{-11}		E	(21)
264.	$C_2H_5S+NO_2 \rightarrow C_2H_5SO+ NO$	6.8×10^{-12}		E	(21)
265.	$C_2H_5S+C_2H_5S \rightarrow C_2H_5SH + CH_3CHS$	0.0		E	(21)
266.	$C_2H_5S+C_2H_5S \rightarrow (C_2H_5S)_2$	4.1×10^{-14}		E	(21)
267.	$C_2H_5S+C_2H_5SNO \rightarrow (C_2H_5S)_2 +NO$	0.0		E	(21)
268.	$C_2H_5S+C_2H_5SNO_2 \rightarrow (C_2H_5S)_2+NO_2$	0.0		E	(21)
269.	$C_2H_5SNO+h\nu \rightarrow C_2H_5S+NO$	$0.3k_{NO_2}$		E14	
270.	$C_2H_5SNO_2+h\nu \rightarrow C_2H_5S+NO_2$	0.0		E	(21)
271.	$C_2H_5SNO +NO_2 \rightarrow C_2H_5S(O)NO + NO$	0.0		E	(21)
272.	$C_2H_5S(O)NO \rightarrow C_2H_5SO+ NO$	0.0		E	(21)
273.	$C_2H_5SO+O_3 \rightarrow C_2H_5SO_2 +O_2$	1.0×10^{-14}		E	(21)
274.	$C_2H_5SO+O_2 \rightarrow C_2H_5SO_3$	1.0×10^{-17}		E	(21)
275.	$C_2H_5SO+O_2 \rightarrow C_2H_5O+SO_2$	0.0		E	(21)
276.	$C_2H_5SO \rightarrow C_2H_5 + SO$	8.6×10^{1}		E	(23)
277.	$C_2H_5SO+C_2H_5SNO \rightarrow (C_2H_5S)_2 +NO_2$	0.0		E	(21)
278.	$C_2H_5SO+C_2H_5SNO \rightarrow (C_2H_5S)_2O + NO$	0.0		E	(21)
279.	$C_2H_5SO+C_2H_5SO \rightarrow (C_2H_5SO)_2$	1.0×10^{-12}		E	(21)
280.	$C_2H_5SO+NO_2 \rightarrow C_2H_5SONO_2$	0.0		E	(21)
281.	$C_2H_5SO_2 +OH \rightarrow C_2H_5SO_3H$	1.0×10^{-11}		E	(21)
282.	$C_2H_5SO_2 +NO \rightarrow C_2H_5SO+NO_2$	2.0×10^{-13}		E	(21)
283.	$C_2H_5SO_2 (+M) \xrightarrow{O_2} C_2H_5O_2 +SO_2 (+M)$	1.2×10^{1}		E	(23)
284.	$C_2H_5SO_2 +O_2 \rightarrow C_2H_5SO_4$	4.9×10^{-19}		E	(21)
285.	$C_2H_5SO_2 +O_3 \rightarrow C_2H_5SO_3 +O_2$	6.8×10^{-14}		E	(21)
286.	$C_2H_5SO_2 +CH_3SH \rightarrow P$	0.0		E	(21)
287.	$C_2H_5SO_3 +H_2O \rightarrow C_2H_5SO_3H+OH$	5.0×10^{-13}		E	(21)
288.	$C_2H_5SO_3 +HCHO \xrightarrow{O_2} HO_2+CO+C_2H_5SO_3H$	6.0×10^{-16}		E	(21)
289.	$C_2H_5SO_3 +CH_3CHO \xrightarrow{O_2} CH_3CO_3+C_2H_5SO_3H$	2.0×10^{-15}		E	(21)
290.	$C_2H_5SO_3 +C_2H_5SC_2H_5 \rightarrow C_2H_5SO_3H +C_2H_5SCHCH_3$	6.8×10^{-14}		E	(21)
291.	$C_2H_5SO_3 + NO \rightarrow C_2H_5SO_2 +NO_2$	0.0		E	(21)
292.	$C_2H_5SO_3 (+M) \xrightarrow{O_2} C_2H_5O_2 +SO_3$	1.0×10^{-4}	1.2×10^{4}	E	(21)
293.	$C_2H_5SO_3 +NO_2 \rightarrow C_2H_5SO_3NO_2$	0.0		E	(21)
294.	$C_2H_5SO_3 + NO \rightarrow C_2H_5SO_3NO$	0.0		E	(21)
295.	$C_2H_5SO_4 \rightarrow CH_3CHO+ OH +SO_2$	2.5×10^{0}		E	(21)
296.	$C_2H_5SO_4 + NO \rightarrow C_2H_5SO_3 +NO_2$	6.8×10^{-15}		E	(21)
297.	$C_2H_5SO_4 +CH_3SH \rightarrow P$	0.0		E	(21)
298.	$C_2H_5SO_4 +(C_2H_5S)_2 \rightarrow P$	0.0		E	(21)
299.	$C_2H_5SO_4 +C_2H_5SO_4 \rightarrow 2\ C_2H_5SO_3 +O_2$	6.8×10^{-12}		E	(21)

Table 5. Reactions Common to All Organosulfur Reaction Mechanisms:

SO_x Chemistry and Chamber Wall Reactions

	REACTION	RATE CONSTANT[a]	ACTIVATION ENERGY(K)	REF.	NOTE
	SO_x Reactions				
300.	$SO + O_2 \rightarrow SO_2 + O(^3P)$	6.7×10^{-17}	2.275×10^3	6	
301.	$SO + NO_2 \rightarrow SO_2 + NO$	1.4×10^{-11}		6	
302.	$SO + O_3 \rightarrow SO_2 + O_2$	8.9×10^{-14}	1.17×10^3	6	
303.	$SO + O(^3P) \rightarrow SO_2$	2.2×10^{-11}		12	
304.	$SO + OH \xrightarrow{O_2} SO_2 + HO_2$	1.1×10^{-10}		12	
305.	$SO + SO_3 \rightarrow SO_2 + SO_2$	2.0×10^{-15}		12	
306.	$SO_2 + OH \rightarrow HSO_3$	1.1×10^{-12}	-2.31×10^2	17	(24)
307.	$SO_2 + O(^3P) \rightarrow SO_3$	3.4×10^{-14}	1.0×10^3	6	
308.	$SO_2 + HO_2 \rightarrow SO_3 + OH$	1.0×10^{-18}		2,5	
309.	$SO_2 + CH_3O_2 \rightarrow CH_3O + SO_3$	5.0×10^{-17}		2,6	
310.	$SO_2 + CH_3O(+M) \rightarrow CH_3OSO_2 (+M)$	5.5×10^{-13}		7	
311.	$SO_2 + CH_3 \rightarrow CH_3SO_2$	2.9×10^{-13}		12	
312.	$SO_2 + h\nu \rightarrow SO_2^*$	$2.0k_{NO_2}$		12	
313.	$SO_2^* + (M) \rightarrow SO_2$	3.7×10^6		12	
314.	$SO_2^* + SO_2 \rightarrow SO_3 + SO$	6.3×10^{-13}		12	
315.	$SO_2^* + CO \rightarrow SO + CO_2$	1.1×10^{-14}		12	
316.	$HSO_3 + O_2 \rightarrow SO_3 + HO_2$	4.0×10^{-13}	1.0×10^3	17	
317.	$HSO_3 + OH \rightarrow H_2SO_4$	1.0×10^{-11}		E13[b]	
318.	$SO_3 + H_2O(+M) \rightarrow H_2SO_4(+M)$	9.1×10^{-13}		2,17	
319.	$SO_3 + O(^3P) \rightarrow SO_2 + O_2$	5.6×10^{-17}		12	
	Wall Effects				
320.	$HNO_3 \rightarrow$ Wall	5.8×10^{-5}		E	(20)
321.	$O_3 \rightarrow$ Wall	8.5×10^{-6}		16	
322.	$NO_2 + H_2O +$ Wall $\rightarrow$ HONO	6.8×10^{-24}		19	
323.	$NO_2 +$ Wall $\rightarrow$ HONO	6.5×10^{-7}		19	

a. Rate constants are at 298 K, 1 atm in units of molecule, cm^3 and sec.

b. 'E' is used to indicate the rate constant was estimated in the reference whose number follows 'E'. In the absence of a number following 'E', the rate constant has been estimated in the present work.

References

1. Atkinson et al. [1980].
2. Atkinson and Lloyd [1984b].
3. Atkinson et al. [1984c].
4. Balla and Heicklen [1984].

5. Baulch et al. [1982].
6. Baulch et al. [1984].
7. Calvert and Stockwell [1984].
8. Cvetanović et al. [1981].
9. Demore et al. [1982].
10. Friedl et al. [1985].
11. Graham et al. [1964].
12. Graedel [1977].
13. Graedel [1979].
14. Grosjean [1984a].
15. Grosjean [1984b].
16. Grosjean [1985].
17. Kerr and Calvert [1984].
18. Leone and Seinfeld [1984].
19. Leone et al. [1985].
20. Martin et al. [1985].
21. Nip et al. [1981].
22. Semmes et al. [1985].
23. Wine et al. [1981].

Notes:

1. k_{NO_2} was estimated theoretically [Demerjian et al., 1980] for simulation of the experiments of Grosjean and Lewis, and measured for the work of Hatakeyama et al.. See text for discussion.
2. The rate constant data of reaction between HO_2 and HO_2 were fit by the expression [Atkinson and Lloyd, 1984b],

$$k = [2.2 \times 10^{-13} \exp(620/T) + 1.9 \times 10^{-33} [M] \exp(980/T)] \times [1 + 1.4 \times 10^{-21} [H_2O] \exp(2200/T)]$$

$cm^3 molecule^{-1} s^{-1}$, which can be expressed by reactions of (13)–(16).
3. Reaction (18) is the combination of the following three reactions,

$$\begin{aligned} O_3 + h\nu &\rightarrow O(^1D) + O_2 \\ O(^1D) + O_2 &\rightarrow O(^3P) + O_2 \\ O(^1D) + H_2O &\rightarrow 2\ OH \end{aligned}$$

4. These reactions are only applicable to $C_2H_5SC_2H_5$ photooxidation and $CH_3SCH_3 - C_2H_5ONO$ photooxidation.
5. CH_3ONO and C_2H_5ONO are assumed to have the same photolysis rate as HONO. Therefore, in the simulation of the experiments of Grosjean and Lewis, we use

$$k_{RONO} = 0.17 \times k_{NO_2} \qquad (R = CH_3, C_2H_5)$$

to which the results are not sensitive. The values of k_{RONO} were determined from concentration profiles of RONO of the experiments of Hatakeyama and Akimoto [1983].

$$k_{C_2D_5ONO} = 0.27 \times k_{NO_2}$$
$$k_{CH_3ONO} = 0.40 \times k_{NO_2}$$

6. See text for detailed discussion.
7. These reactions are assumed to be negligible.
8. These unimolecular reactions are assumed to decompose rapidly and the simulations are not sensitive to them.
9. These unimolecular reactions are assumed to decompose rapidly, however, the system reactivity and the product distribution are sensitive to these rate constants, which are estimated mainly based on the product studies.
10. $k_{SO_2H+O_2}$ and $k_{HSO_2+O_2}$ are estimated by assuming that they are similar to the reaction of $SO_3H + O_2$. $k_{CH_3SCH_2O+O_2}$ is estimated from the similar reaction of $RO + O_2$.
11. Hatakeyama and Akimoto [1983] suggested that this reaction is a facile reaction and is assumed to be fast in the simulations.
12. The rate constants are estimated from the similar reactions of $R + O_2$.
13. Considering the similarity with the reactions of $RO_2 + NO$, these rate constants are estimated.
14. Since the photolysis rate of the similar species, CH_3OCH_2O, is unknown, the photolysis rate of CH_3CHO is used in our simulations.
15. These reactions, especially the radical recombination reactions, are assumed to be fast and the simulations are not sensitive to these rate constants.
16. This rate constant is estimated from the similar reaction of $HS + NO_2$.
17. The rate constants are estimated by assuming that these reactions are analogous to the reaction of $SO + O_3$.
18. The rate constants are estimated from the similar reactions of $HS + O_2$ and $SO + O_2$.
19. The rate constant was expressed as

$$k_{CH_3SH} = 1.52 \times 10^{-12} + 64 \times 10^{-12}\exp(-1673/T)$$

$cm^3molecule^{-1}s^{-1}$ by Nip et al. [1981].
20. The rate constant is estimated from the product study.
21. For these reactions in the mechanisms for methanethiol and ethyl sulfide, the rate constants are assumed to be the same as the analogous reactions in the mechanism for methyl sulfide.
22. k_{CH_3SNO} was evaluated from the concentration-time profile of CH_3SNO for the simulation of $CH_3SH - CH_3ONO - NO$–air, and $k_{CH_3SNO} = 5.0 \times k_{NO_2}$.
23. Based on the product study of Grosjean [1984a], C_2H_5SO and $C_2H_5SO_2$ are assumed to decompose faster than CH_3SO and CH_3SO_2.
24. The temperature coefficient, which is a function of the total pressure, has been expressed for the temperature range 200–300 K by Kerr and Calvert [1984] as

$$-(E/R)/K = 3.6896 \times 10^{-4} \times (P/Torr)^2 - 6.793 \times 10^{-1} \times (P/Torr) + 5.3374 \times 10^2$$

Table 6. Product Distribution

SYSTEM	SO_2%	RSO_3H%	H_2SO_4%	REF.
$CH_3SCH_3 - C_2D_5ONO - NO - air$	21	> 50	–	b
$CH_3SCH_3 - C_2H_5ONO - NO - air$	20–25	–	–	d
$CH_3SCH_3 - NO_x - air$	20.7	> 50	< 2	a,b
	29	> 50	–	c
	30–94	0.6–13.4	1–17.0	e,f
$CH_3SH - CH_3ONO - NO - air$	29	40	≤ 2	b
$CH_3SH - NO_x - air$	46–100	–	–	f
$CH_3SSCH_3 - air$	> 90	< 10	–	b
$CH_3SSCH_3 - CH_3ONO - NO - air$	22	60	< 2	b
$C_2H_5SC_2H_5 - NO_x - air$	46.3–54.3	0.7–6.3	1.8–3.9	f

References:

a. Hatakeyama et al. [1982].
b. Hatakeyama and Akimoto [1983].
c. Hatakeyama at al. [1985].
d. Niki et al. [1983b].
e. Grosjean and Lewis [1982]*.
f. Grosjean [1984a]*.

* For experiments of Grosjean and Lewis [1982] and Grosjean [1984a], RSO_3H was measured in particulate phase only and was not corrected for aerosol loss to the reactor walls.

Table 7. Initial Conditions for CH_3SCH_3–NO_x–AIR

EXPERIMENT	G39[a]	G47	G77	G113	H82	H831	H85
Irrad. Time (min)	240	240	360	360	40	5	240
Ave. Temp. (K)	298	298	298	298	303	303	303
Humidity (%)	30–40	30–40	3.3	3.3	–	6.1×10^{-3}	–
k_{NO_2} (min^{-1})	b	b	b	b	0.28	0.28	0.34
Initial Conc. (ppm)							
H_2O	1.1×10^4	1.1×10^4	1.0×10^3	1.0×10^3	–	2.55	< 1
NO	0.28	0.355	0.360	0.240	14.2	18.4	0.75
NO_2	0.24	0.135	0.020	0.00	0.29	0.00	0.00
CH_3SCH_3	1.0	1.5	0.330	0.680	20.3	20.1	1.30
SO_2	0.027	0.030	0.005	–	–	–	–
C_2D_5ONO	–	–	–	–	–	34.5	–

Table 8. Initial Conditions for RSR′–NO_x–AIR

EXPERIMENT	G114 $C_2H_5SC_2H_5$	G116 $C_2H_5SC_2H_5$	G112 CH_3SH	H832 CH_3SH
Irrad. Time (min)	285	300	195	12.5
Ave. Temp. (K)	294	297	298	303
Humidity (%)	4.6	4.2	15.0	6.1×10^{-3}
k_{NO_2} (min^{-1})	b	b	b	0.28
Initial Conc. (ppm)				
H_2O	1.1×10^3	1.2×10^3	4.7×10^3	2.55
NO	0.252	0.280	0.302	10.9
NO_2	0.0	0.0	0.0	0.0
RSR′	0.364	0.462	0.99	19.5
CH_3ONO	–	–	–	36.8

a. Experimental data are obtained from the work of Hatakeyama et al.[1982, 1983 and 1985], Grosjean and Lewis [1982] and Grosjean [1984a].
G39 and G47: Experimental data of 4/17/81 and 6/17/81 from Grosjean and Lewis [1982].
G77, G113, G114, G116 and G112: Experimental data of Runs 77, 113, 114, 116, 112 [Grosjean, 1984a].
H82: Experimental data of Hatakeyama et al. [1982].
H831, H832: Figures 12 and 4 from the paper of Hatakeyama and Akimoto [1983].
H85: Experimental data of Hatakeyama et al. [1985].

b. The photolysis rate profiles of NO_2 are calculated theoretically.

Table 9. Comparison of Predicted and Measured Product Yields

EXPER.	SO_2%		H_2SO_4%		RSO_3H%[c]	
	predic.	measur.	predic.	measur.	predic.	measur.
G39[a]	44.8	39.4	10.0	4	30.7	—
G47[a]	44.9	74.1	7.2	14.7	32.9	—
G77	48.9	51.6	16.8	16.9	22.5	13.4
G113	56.7	34.9	8.2	2.6	26.9	4.5
H82[b]	29.0	30.6	4.8	< 2	39.5	> 50
H831[b]	21.4	21.7	2.5	—	36.9	> 50
H85[b]	46.1	23.0	7.6	—	30.6	> 50
G114	65.7	46.3	2.5	1.8	19.8	0.7
G116	65.2	54.3	3.5	3.9	19.9	6.3
H832[b]	23.9	27.0	10.9	< 2	26.7	40

a. Assuming 90% CH_3SCH_3 was consumed.
b. The yield of CH_3SO_3H was measured in small reactors at much higher concentrations of reactants (10 - 830 ppm of CH_3SCH_3 and 45 ppm of CH_3ONO).
c. For experiments of Grosjean and Lewis [1982] and Grosjean [1984a], RSO_3H was measured in particulate phase only and was not corrected for aerosol loss to the reactor walls. R = C_2H_5 for the experiments G114 and G116, and R = CH_3 for all other experiments.

REFERENCES

Adams, D. F., S. O. Farwell, M. R. Pack, and W. L. Bamesberger, Preliminary measurements of biogenic sulfur-containing gas emissions from soil, *J. Air Pollut. Control Assoc., 29,* 380–383, 1979.

Andreae, M. O., and H. Raemdonck, Dimethyl sulfide in the surface ocean and the marine atmosphere: A global view, *Science, 221,* 744–747, 1983.

Andreae, M. O., and W. R. Barnard, The marine chemistry of dimethylsulfide, *Marine Chem., 14,* 267–279, 1984.

Aneja, V. P., A. P. Aneja, and D. F. Adams, Biogenic sulfur compounds and the global sulfur cycle, *J. Air Pollut. Control Assoc., 32,* 803–807, 1982.

Atkinson, R., R. A. Perry, and J. N. Pitts, Jr., Rate constants for the reaction of the OH radical with CH_3SH and CH_3NH_2 over the temperature range 299–426 K, *J. Chem. Phys., 66,* 1578–1581, 1977.

Atkinson, R., R. A. Perry, and J. N. Pitts, Jr., Rate constants for the reaction of OH radicals with COS, CS_2 and CH_3SCH_3 over the temperature range 299–430 K, *Chem. Phys. Lett., 54,* 14–18, 1978.

Atkinson, R., W. P. L. Carter, K. R. Darnall, A. M. Winer, and J. N. Pitts, Jr., A smog chamber and modeling study of the gas phase NO_x–air photooxidation of toluene and the cresols, *Int. J. Chem. Kinet., 12,* 779–836, 1980.

Atkinson, R., J. N. Pitts, Jr., and S. M. Aschmann, Tropospheric reactions of dimethyl sulfide with NO_3 and OH radicals, *J. Phys. Chem., 88,* 1584–1587, 1984a.

Atkinson, R., and A. C. Lloyd, Evaluation of kinetic and mechanistic data for modeling of photochemical smog, *J. Phys. Chem. Ref. Data, 13,* 315–444, 1984b.

Atkinson, R., C. N. Plum, W. P. L. Carter, A. M. Winer, and J. N. Pitts, Jr., Rate constants for the gas-phase reactions of nitrate radicals with a series of organics in air at 298 ± 1 K, *J. Phys. Chem., 88,* 1210–1215, 1984c.

Balla, R. J., and J. Heicklen, Oxidation of sulfur compounds. II. Thermal reactions of NO_2 with aliphatic sulfur compounds, *J. Phys. Chem., 88,* 6314–6317, 1984.

Balla, R. J., and J. Heicklen, Oxidation of sulfur compounds III: The photolysis of $(CH_3S)_2$ in the presence of O_2, *J. Photochem., 29,* 297–310, 1985.

Baulch, D. L., R. A. Cox, P. J. Crutzen, R. F. Hampson, Jr., J. A. Kerr, J. Troe, and R. T. Watson, Evaluated kinetic and photochemical data for atmospheric chemistry: Supplement I, *J. Phys. Chem. Ref. Data, 11,* 327–496, 1982.

Baulch, D. L., R. A. Cox, R. F. Hampson, Jr., J. A. Kerr, J. Troe, and R. T. Watson, Evaluated kinetic and photochemical data for atmospheric chemistry: Supplement II, *J. Phys. Chem. Ref. Data, 13,* 1259–1380, 1984.

Black, G., Reactions of HS with NO and NO_2 at 298 K, *J. Chem. Phys., 80,* 1103–1107, 1984.

Calvert, J. G., and Stockwell, W. R., The mechanism and rates of the gas phase oxidations of sulfur dioxide and nitrogen oxides in the atmosphere, *SO_2, NO and NO_2 Oxidation Mechanisms: Atmospheric Considerations,* J. G. Calvert (Ed.), Butterworth, Boston, 1–62, 1984.

Chatfield, R. B., and P. J. Crutzen, Sulfur dioxide in remote oceanic air: Cloud transport of reactive precursors, *J. Geophys. Res., 89,* 7111–7132, 1984.

Cox, R. A., and D. Sheppard, Reactions of OH radicals with gaseous sulphur compounds, *Nature, 284,* 330–331, 1980.

Cvetanović, R. J., D. L. Singleton, and R. S. Irwin, Gas-phase reactions of $O(^3P)$ atoms with methanethiol, ethanethiol, methyl sulfide, and dimethyl disulfide. 2. Reaction products and mechanisms, *J. Am. Chem. Soc., 103,* 3530–3539,

1981.

Daum, K. A., M. F. Massoglia, and A. D. Shendrikar, An analysis of sulfur control strategies for the oil shale industry, *J. Air Pollut. Control Assoc., 32,* 391–392, 1982.

Demerjian, K. L., K. L. Schere, and J. T. Peterson, Theoretical estimates of actinic (spherically integrated) flux and photolytic rate constants of atmospheric species in the lower troposphere, *Adv. Environ. Sci. Technol., 10,* 369–459, 1980.

Demore, W. B., R. T. Watson, D. M. Golden, R. F. Hampson, M. Kurylo, C. J. Howard, M. J. Molina, and A. R. Ravishankara, *Chemical Kinetics and Photochemical Data for Use in Stratospheric Modeling,* JPL Report 82-57, July 15, 1982.

Friedl, R. R., W. H. Brune, and J. G. Anderson, Kinetics of SH with NO_2, O_3, O_2, and H_2O_2, *J. Phys. Chem., 89,* 5505–5510, 1985.

Galloway, J. N., G. E. Likens, W. C. Keene, and J. M. Miller, The composition of precipitation in remote areas of the world, *J. Geophys. Res., 87,* 8771–8786, 1982.

Graedel, T. E., The homogeneous chemistry of atmospheric sulfur, *Rev. Geophys. Space Phys., 15,* 421–428, 1977.

Graedel, T. E., Reduced sulfur emission from the open oceans, *Geophy. Res. Lett., 6,* 329–331, 1979.

Graham, D. M., R. L. Mieville, R. H. Pallen, and C. Sivertz, Photo-initiated reactions of thiols and olefins II. The addition of methanethiol to unconjugated olefins, *Can. J. Chem., 42,* 2250–2255, 1964.

Grosjean, D., and R. Lewis, Atmospheric photooxidation of methyl sulfide, *Geophys Res. Lett., 9,* 1203–1206, 1982.

Grosjean, D., Photooxidation of methyl sulfide, ethyl sulfide, and methanethiol, *Environ. Sci. Technol., 18,* 460–468, 1984a.

Grosjean, D., Gas phase chemistry of organo-sulfur compounds, paper presented at the *Conference on Gas-Liquid Chemistry of Natural Waters,* Brookhaven, NY, April, 1984b.

Grosjean, D., Wall loss of gaseous pollutants in outdoor teflon Chambers, *Environ. Sci. Technol., 19,* 1059–1065, 1985.

Haines, B., C. Jordan, H. Clark, and K. E. Clark, Acid rain in an Amazon rainforest, *Tellus, 35B,* 77–80, 1983.

Harvey, G. R., and R. F. Lang, Dimethylsulfoxide and dimethylsulfone in the marine atmosphere, *Geophys. Res. Lett., 13,* 49–51, 1986.

Hatakeyama, S., M. Okuda, and H. Akimoto, Formation of sulfur dioxide and methanesulfonic acid in the photooxidation of dimethyl sulfide in the air, *Geophys. Res. Lett., 9,* 583–586, 1982.

Hatakeyama, S., and H. Akimoto, Reactions of OH radicals with methanethiol, dimethyl sulfide, and dimethyl disulfide in air, *J. Phys. Chem., 87,* 2387–2395, 1983.

Hatakeyama, S., K. Izumi, and H. Akimoto, Yield of SO_2 and formation of aerosol in the photo-oxidation of DMS under atmospheric conditions, Atmos. Environ., 19, 135–141, 1985.

Herron, M. M., Impurity sources of F^-, Cl^-, NO_3^- and SO_4^{2-} in Greenland and Antarctic precipitation, *J. Geophys. Res., 87,* 3052–3060, 1982.

Kerr, J. A., and J. G. Calvert, *Chemical Transformation Modules For Eulerian Acid Deposition Models,* Volume I: The gas-phase chemistry, Boulder, Colorado, December, 1984.

Kurylo, M. J., Flash photolysis resonance fluorescence investigation of the reaction

of OH radicals with dimethyl sulfide, *Chem. Phys. Lett., 58,* 233–237, 1978.

Lee, J. H., R. B. Timmons, and L. J. Stief, Absolute rate parameters for the reaction of ground state atomic oxygen with dimethyl sulfide and episulfide, *J. Chem. Phys., 64,* 300–305, 1976.

Leone, J. A., and J. H. Seinfeld, Updated chemical mechanism for atmospheric photooxidation of toluene, *Int. J. Chem. Kinet., 16,* 159–193, 1984.

Leone, J. A., R. C. Flagan, D. Grosjean, and J. H. Seinfeld, An outdoor smog chamber and modeling study of toluene–NO_x Photooxidation, *Int. J. Chem. Kinet., 17,* 177–216, 1985.

Logan, J. A., M. B. McElroy, S. C. Wofsy, and M. J. Prather, Oxidation of CS_2 and COS: Sources for atmospheric SO_2, *Nature, 281,* 185–188, 1979.

Mac Leod, H., J. L. Jourdain, G. Poulet, and G. Le Bras, Kinetic study of reactions of some organic sulfur compounds with OH radicals, *Atmos. Environ., 18,* 2621–2626, 1984.

Maroulis, P. J., and A. R. Bandy, Estimate of the contribution of biologically produced dimethyl sulfide to the global sulfur cycle, *Science, 196,* 647–648, 1977.

Martin, D., J. L. Jourdain, and G. Le Bras, Kinetic study for the reactions of OH radicals with dimethylsulfide, diethylsulfide, tetrahydrothiophene, and thiophene, *Int. J. Chem. Kinet., 17,* 1247–1261, 1985.

Möller, D., On the global natural sulphur emission, *Atmos. Environ., 18,* 29–39, 1984.

Nguyen, B. C., B. Bonsang, and A. Gaudry, The role of the ocean in the global atmospheric sulfur cycle, *J. Geophys. Res., 88,* 10,903–10,914, 1983.

Niki, H., P. D. Maker, C. M. Savage, and L. P. Breitenbach, Spectroscopic and photochemical properties of CH_3SNO, *J. Phys. Chem., 87,* 7–9, 1983a.

Niki, H., P. D. Maker, C. M. Savage, and L. P. Breitenbach, An FTIR study of

the mechanism for the reaction HO + CH_3SCH_3, *Int. J. Chem. Kinet., 15,* 647–654, 1983b.

Nip, W. S., D. L. Singleton, and R. J. Cvetanović, Gas-phase reactions of $O(^3P)$ atoms with methanethiol, ethanethiol, methyl sulfide, and dimethyl disulfide. 1. Rate constants and Arrhenius parameters, *J. Am. Chem. Soc., 103,* 3526–3530, 1981.

Panter, R., and R. D. Penzhorn, Alkyl sulfonic acids in the atmosphere, *Atmos. Environ., 14,* 149–151, 1980.

Saltzman, E. S., D. L. Savoie, R. G. Zika, and J. M. Prospero, Methane sulfonic acid in the marine atmosphere, *J. Geophys. Res., 88,* 10,897–10,902, 1983.

Semmes, D. H., A. R. Ravishankara, C. A. Gump-perkins, and P. H. Wine, Kinetics of the reactions of hydroxyl radical with aliphatic aldehydes, *Int. J. Chem. Kinet., 17,* 303–313, 1985.

Sklarew, D. S., D. J. Hayes, M. R. Petersen, K. B. Olsen, and C. D. Pearson, Trace sulfur-containing species in the offgas from two oil shale retorting processes, *Environ. Sci. Technol., 18,* 592–600, 1984.

Slagle, I. R., R. E. Graham, and D. Gutman, Direct identification of reactive routes and measurement of rate constants in the reactions of oxygen atoms with methanethiol, ethanethiol, and methylsulfide, *Int. J. Chem. Kinet., 8,* 451–458, 1976.

Sze, N. D., and M. K. W. Ko, Photochemistry of COS, CS_2, CH_3SCH_3 and H_2S: Implications for the atmospheric sulfur cycle, *Atmos. Environ., 14,* 1223–1239, 1980.

Wine, P. H., N. M. Kreutter, C. A. Gump, and A. R. Ravishankara, Kinetics of OH reactions with the atmospheric sulfur compounds H_2S, CH_3SH, CH_3SCH_3, and CH_3SSCH_3, *J. Phys. Chem., 85,* 2660–2665, 1981.

Wine, P. H., Laboratory investigations of OH reactions with tropospheric sulfur compounds, paper presented at the meeting of the Division of Environmental Chemistry, American Chemical Society, Washington, D.C., September, 1982.

Wine, P. H., R. J. Thompson, and D. H. Semmes, Kinetics of OH reactions with aliphatic thiols, *Int. J. Chem. Kinet., 16,* 1623–1636, 1984.

Wong, C. M., R. W. Crawford, and A. K. Burnham, Determination of sulfur-containing gases from oil shale pyrolysis by triple quadrupole mass spectrometry, *Anal. Chem., 56,* 390–395, 1984.

FIGURE CAPTIONS

Figure 1. Mechanism for CH_3SCH_3 – OH reaction.

Figure 2. Mechanism for CH_3SH – OH reaction.

Figure 3. Mechanism for $C_2H_5SC_2H_5$ – OH reaction.

Figure 4. Observed and predicted concentration-time profiles for $CH_3SCH_3 - NO_x$ – air experiment G77.

Figure 5. Observed and predicted concentration-time profiles for $CH_3SCH_3 - NO_x$ – air experiment H82.

Figure 6. Observed and predicted concentration-time profiles for $CH_3SCH_3 - NO_x$ – air experiment G77. Competition between $RS + NO_x$ and $RS + O_2$. k_{113}/k_{115} and k_{114}/k_{115}: (a) 0.6, 1.13; (b) 0.07, 0.13. (Ratios are multiplied by 1.0×10^{-6}).

Figure 7. Observed and predicted concentration-time profiles for $CH_3SCH_3 - NO_x$ – air experiment G77. Competition between $RSO_x + O_2$ and RSO_x decomposition. k_{130}/k_{128} and k_{137}/k_{138} (ppm): (a) 0.44, 2.1; (b) 0.05, 0.24. (Ratios are multiplied by 1.0×10^{-6}).

Figure 8. Observed and predicted concentration-time profiles for $CH_3SCH_3 - NO_x$ – air experiment G77. The relative importance between abstraction and addition. Ratios of $k_{84}/[k_{83} + k_{84}]$: (a) 0.10; (b) 0.50; (c) 0.90.

Figure 9. Observed and predicted concentration-time profiles for $C_2H_5SC_2H_5 - NO_x$ – air experiment G116.

Figure 10. Observed and predicted concentration-time profiles for CH_3SH – CH_3ONO – NO – air experiment H832.

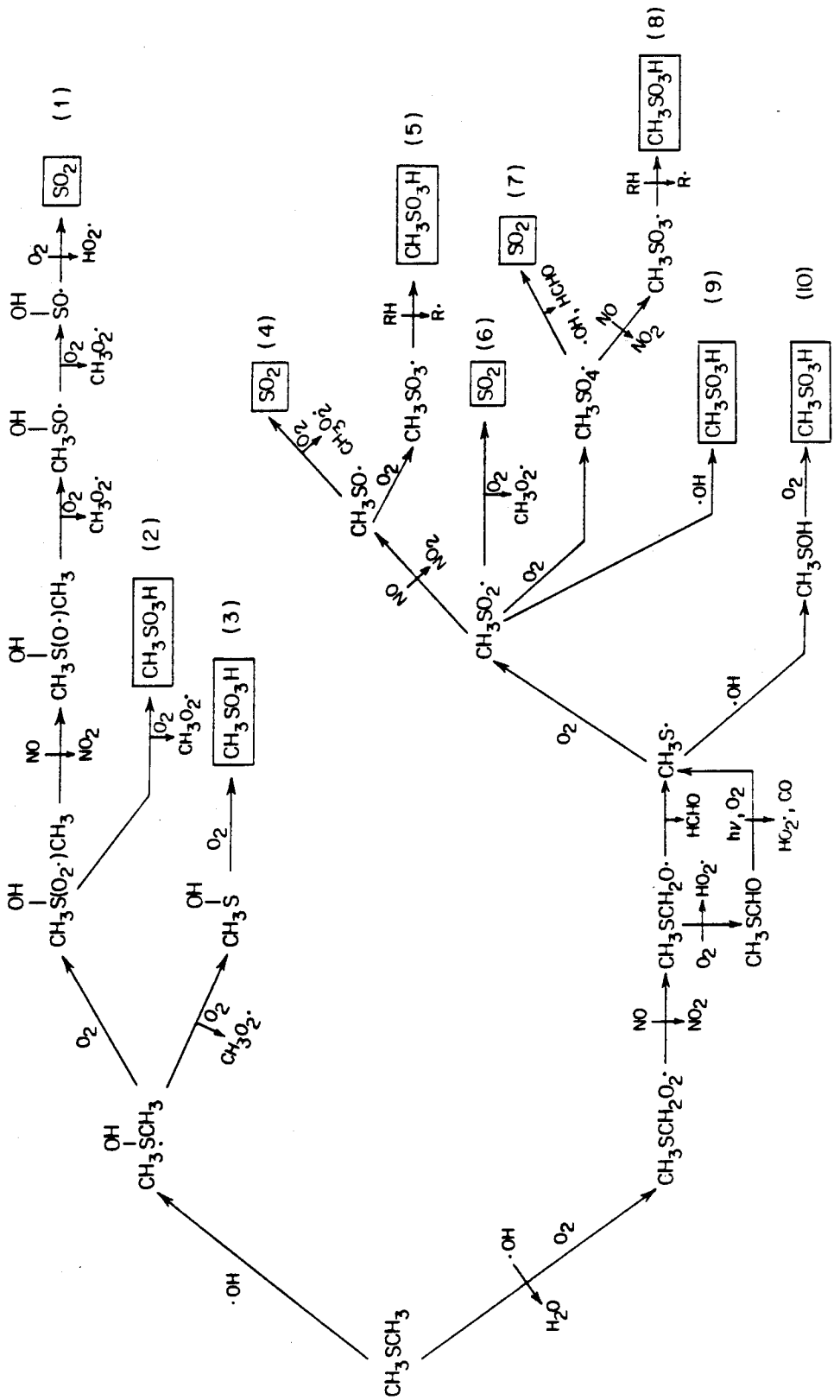

Figure 1

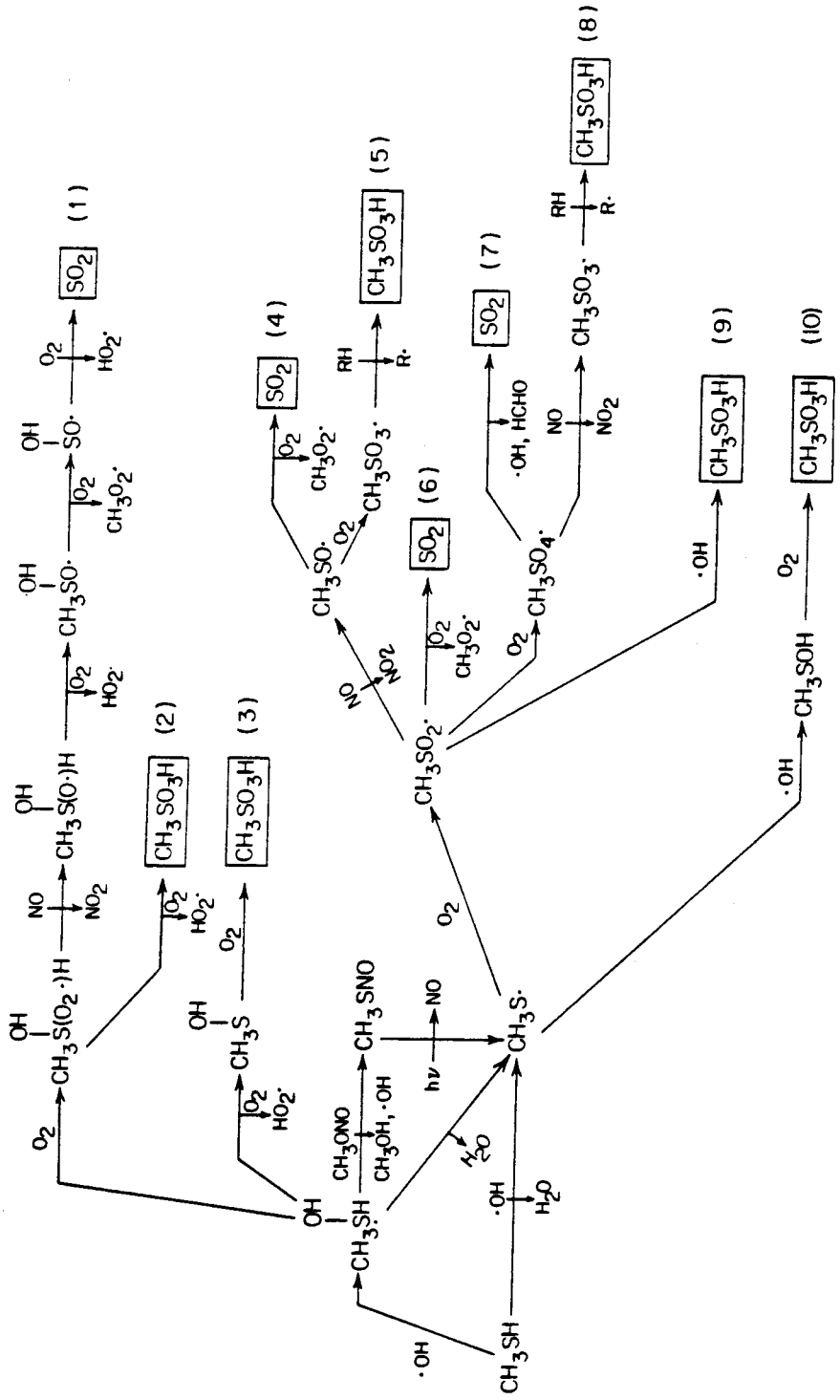

Figure 2

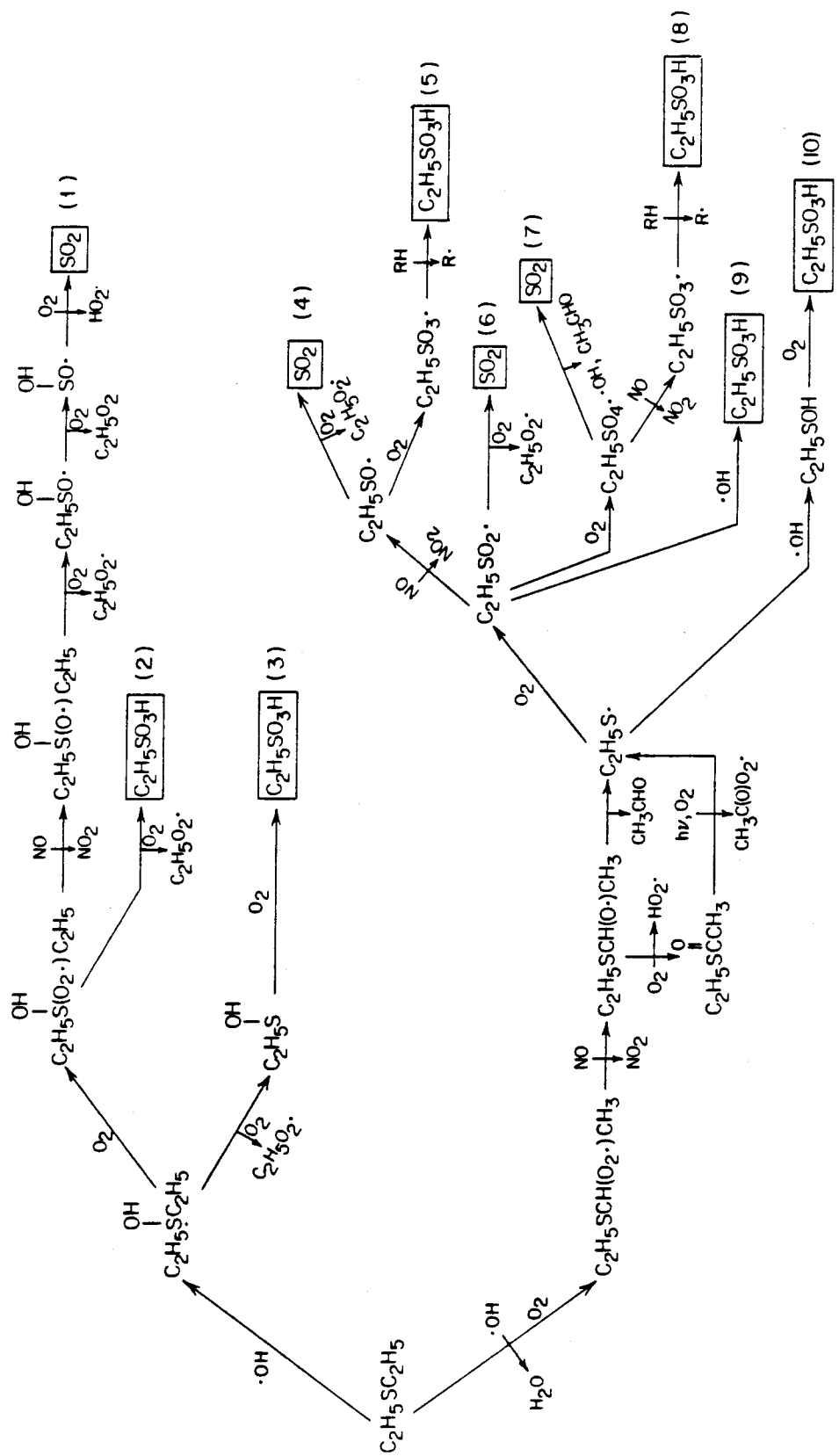

Figure 3

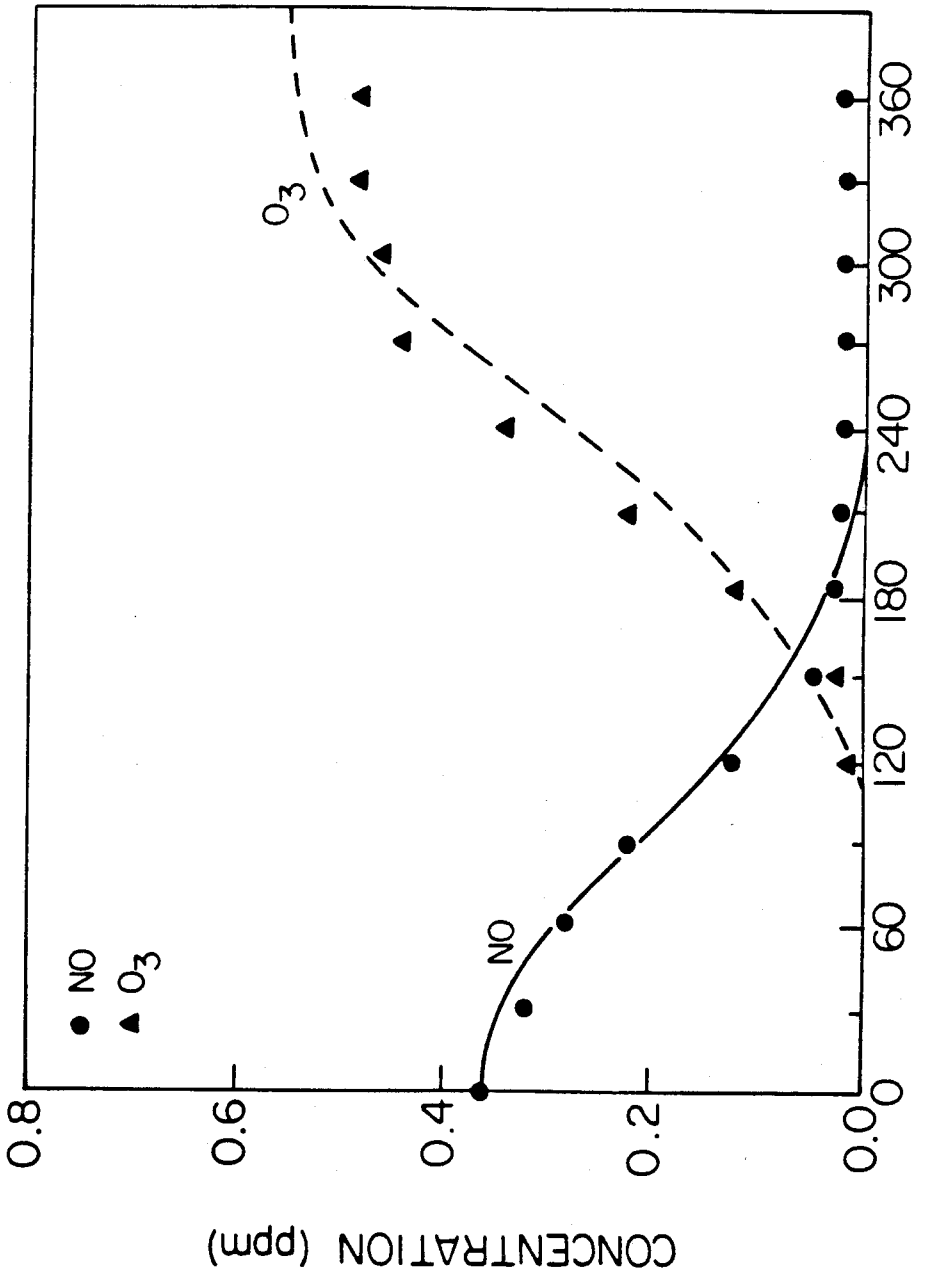
CONCENTRATION (ppm)
0.0
0.2
0.4
0.6
0.8
0
60
120
180
240
300
360
TIME (min)
NO
O_3
NO
O_3

Figure 4

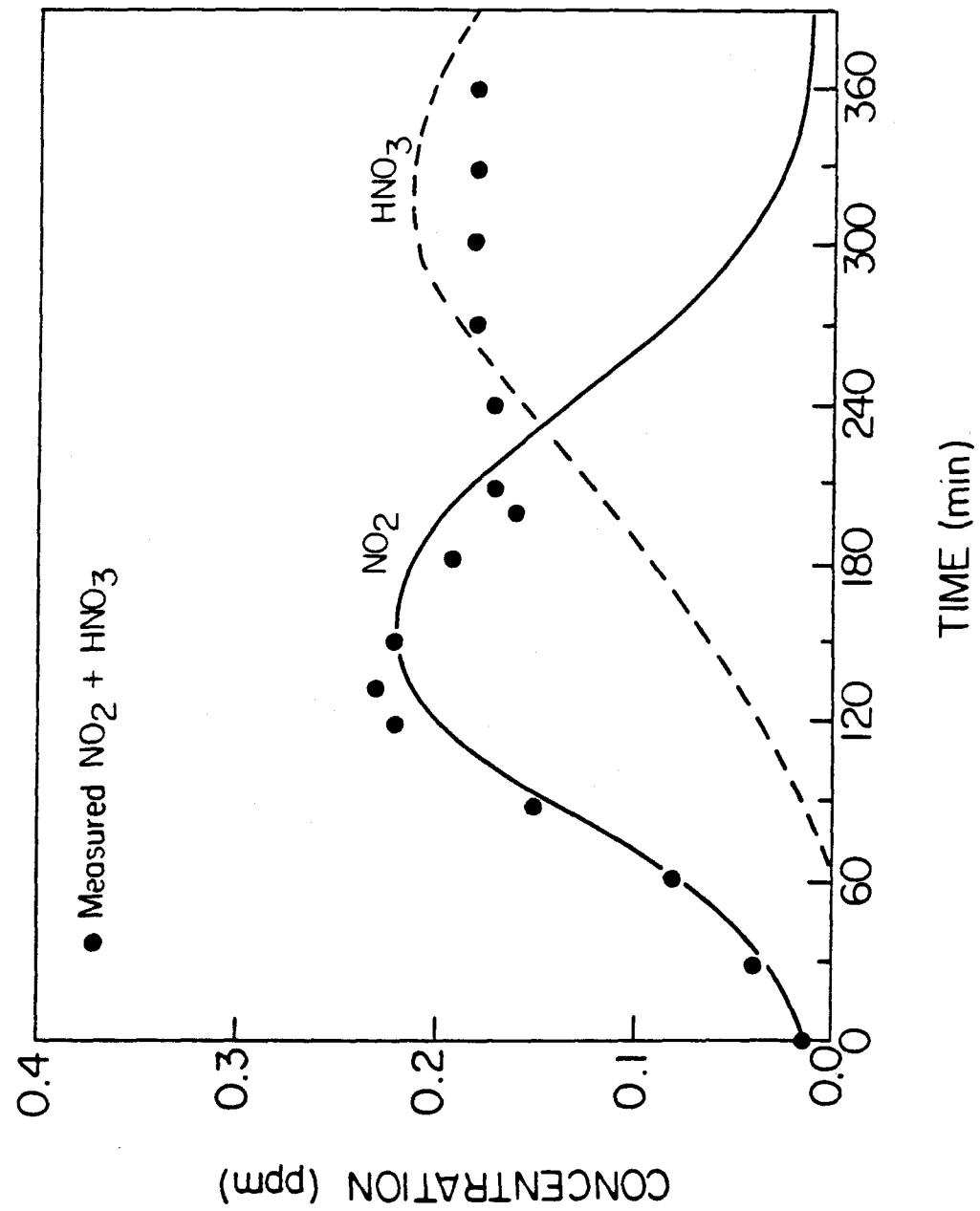
CONCENTRATION (ppm)
0.4
0.3
0.2
0.1
0.0
0
60
120
180
240
300
360
TIME (min)
HNO_3
NO_2
● Measured NO_2 + HNO_3

Figure 4

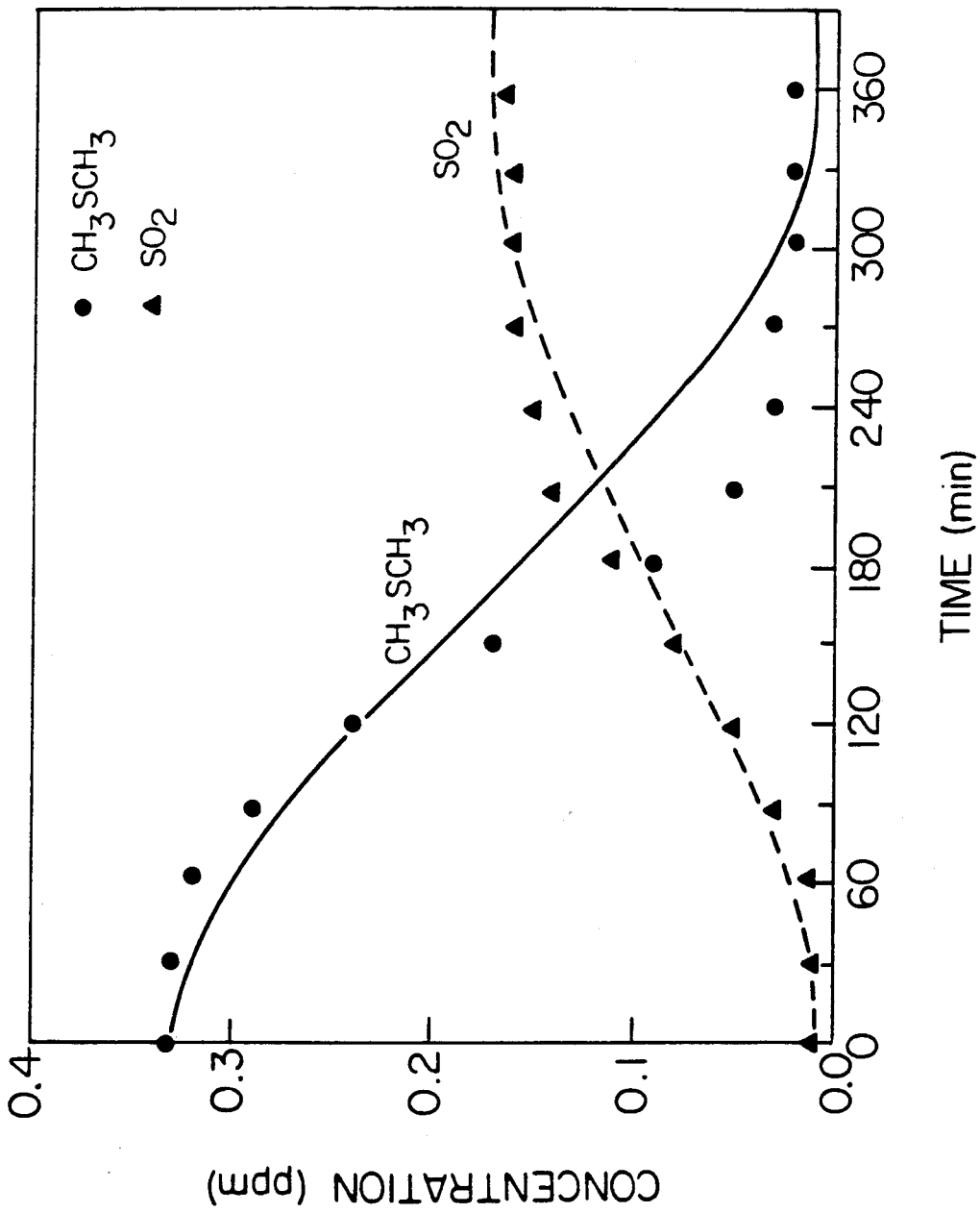
CONCENTRATION (ppm)
0.4
0.3
0.2
0.1
0.0
0
60
120
180
240
300
360
TIME (min)
CH_3SCH_3
SO_2
SO_2
CH_3SCH_3

Figure 4

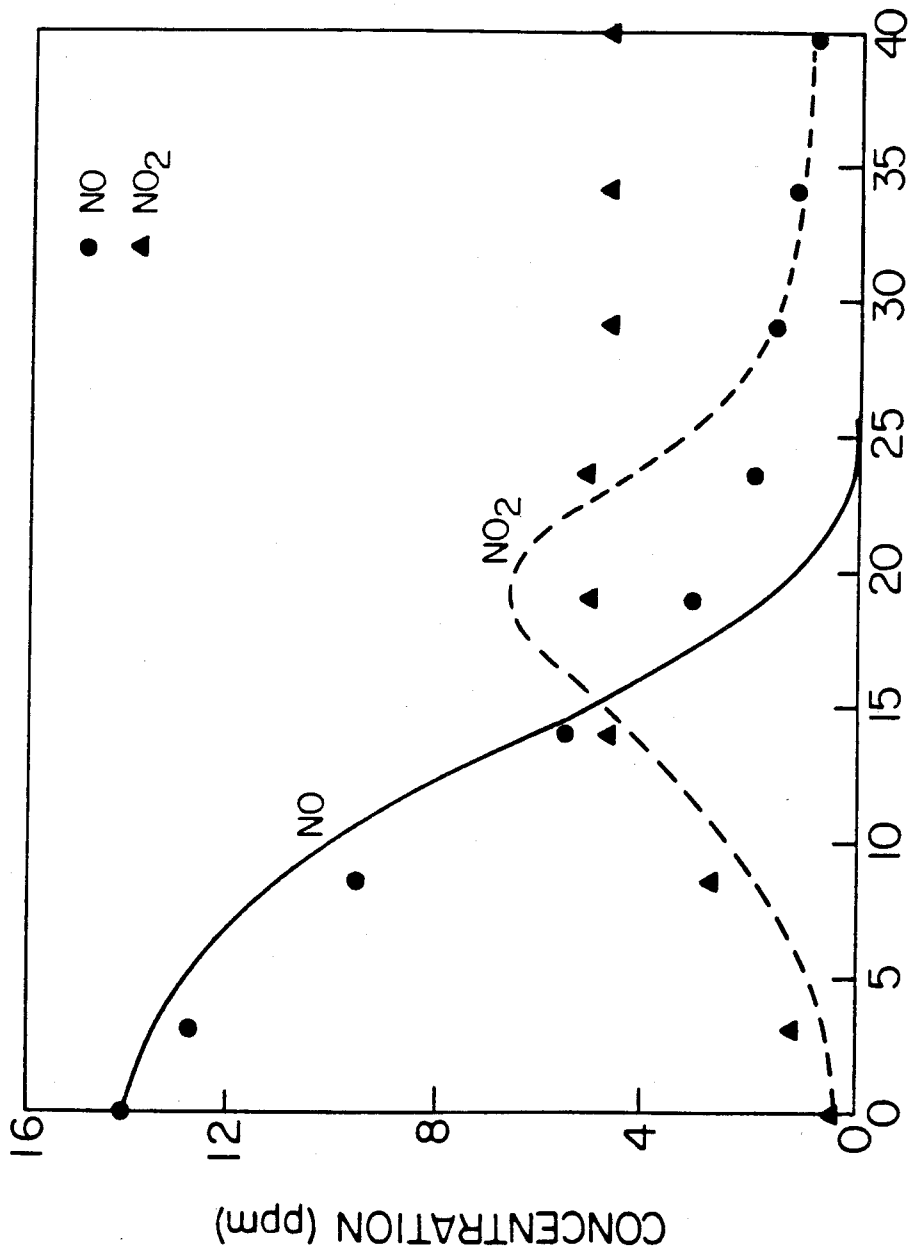
NO
NO2
NO
NO2
CONCENTRATION (ppm)
TIME (min)
0
4
8
12
16
0
5
10
15
20
25
30
35
40

Figure 5

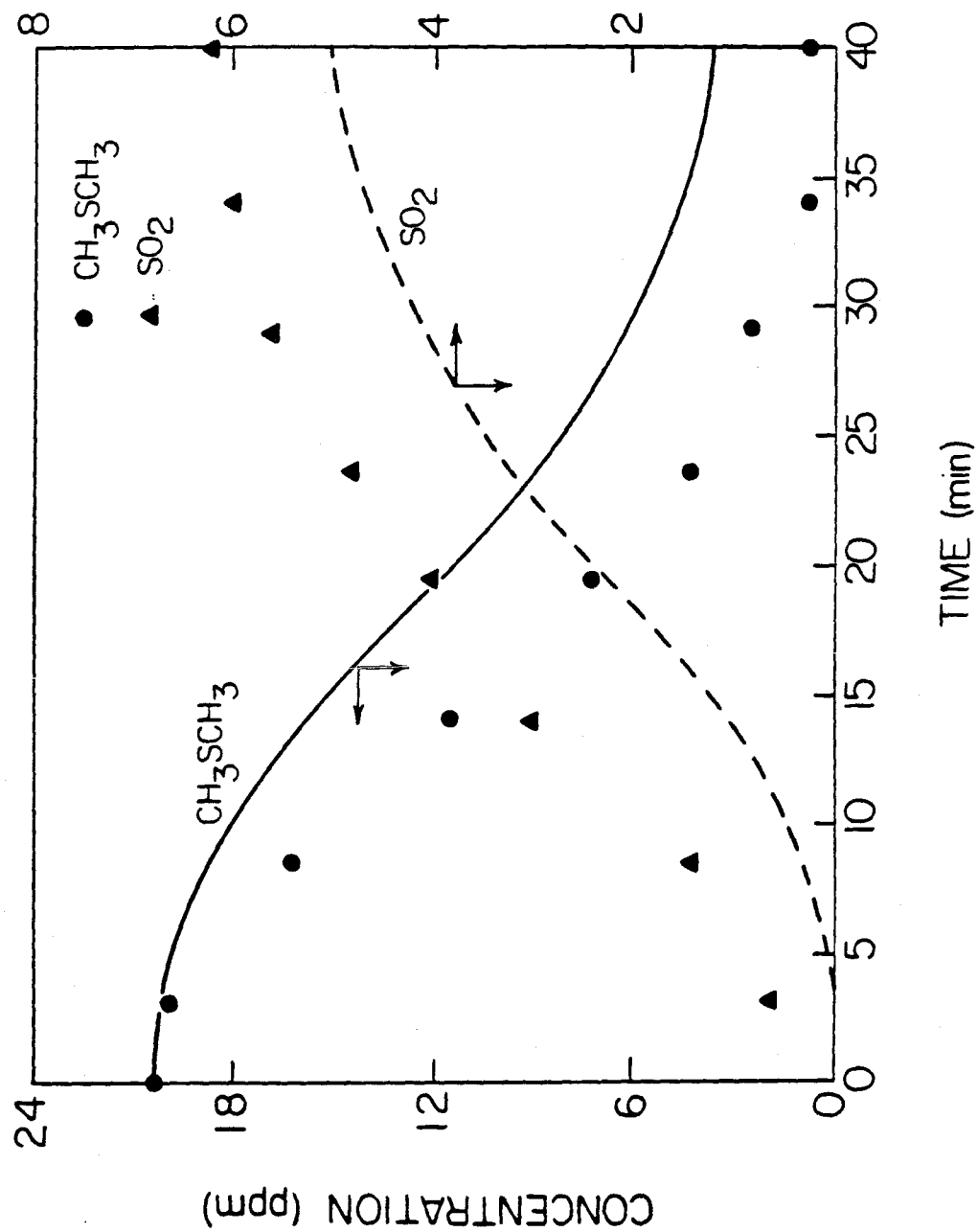
CONCENTRATION (ppm)
TIME (min)
CH_3SCH_3
SO_2
SO_2
CH_3SCH_3
0
6
12
18
24
0
2
4
6
8
0
5
10
15
20
25
30
35
40

Figure 5

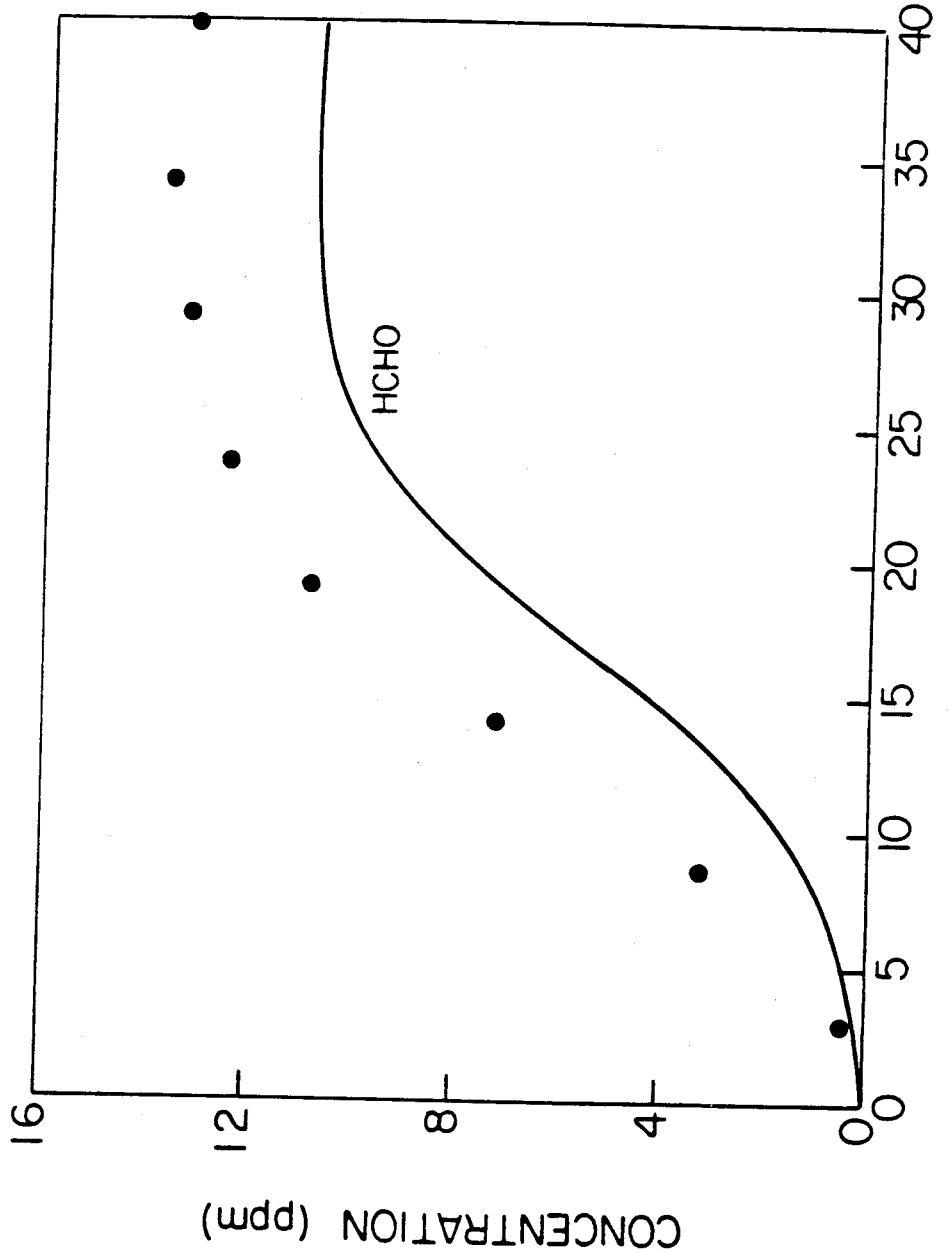
HCHO
CONCENTRATION (ppm)
TIME (min)
0
4
8
12
16
0
5
10
15
20
25
30
35
40

Figure 5

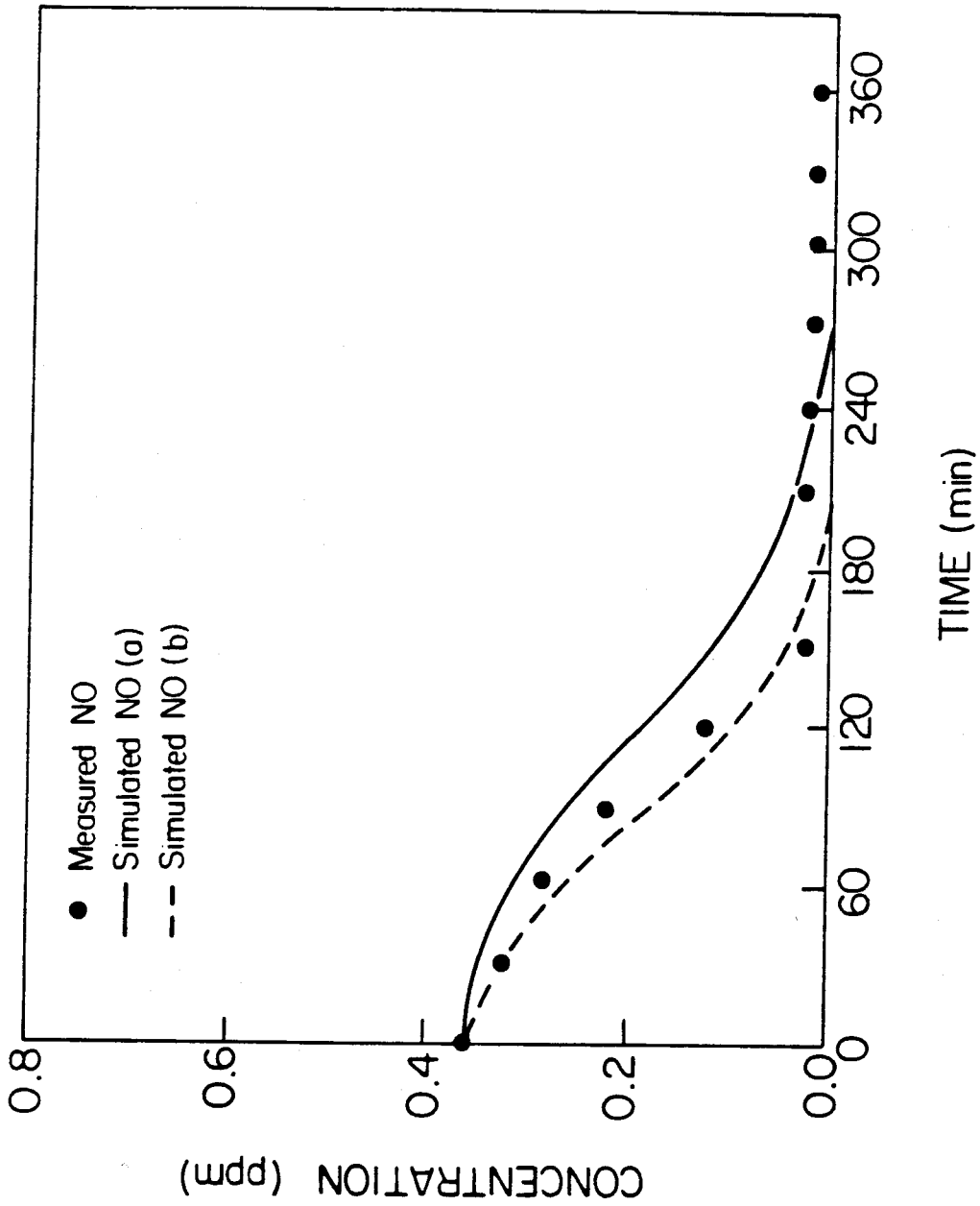
Measured NO
Simulated NO (a)
Simulated NO (b)
CONCENTRATION (ppm)
0.0
0.2
0.4
0.6
0.8
0
60
120
180
240
300
360
TIME (min)

Figure 6

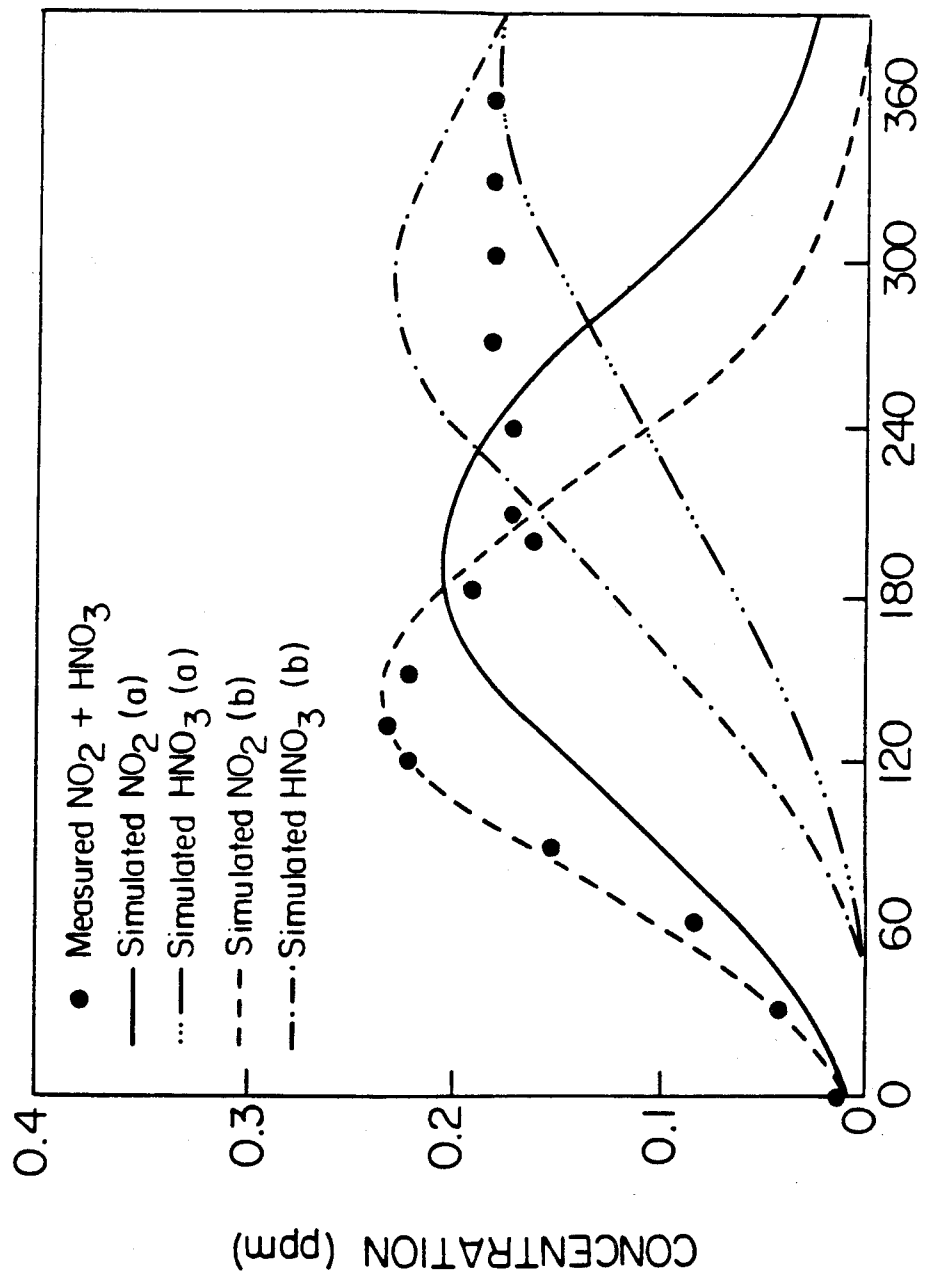
Measured $NO_2 + HNO_3$
Simulated NO_2 (a)
Simulated HNO_3 (a)
Simulated NO_2 (b)
Simulated HNO_3 (b)
CONCENTRATION (ppm)
0.4
0.3
0.2
0.1
0
0
60
120
180
240
300
360
TIME (min)

Figure 6

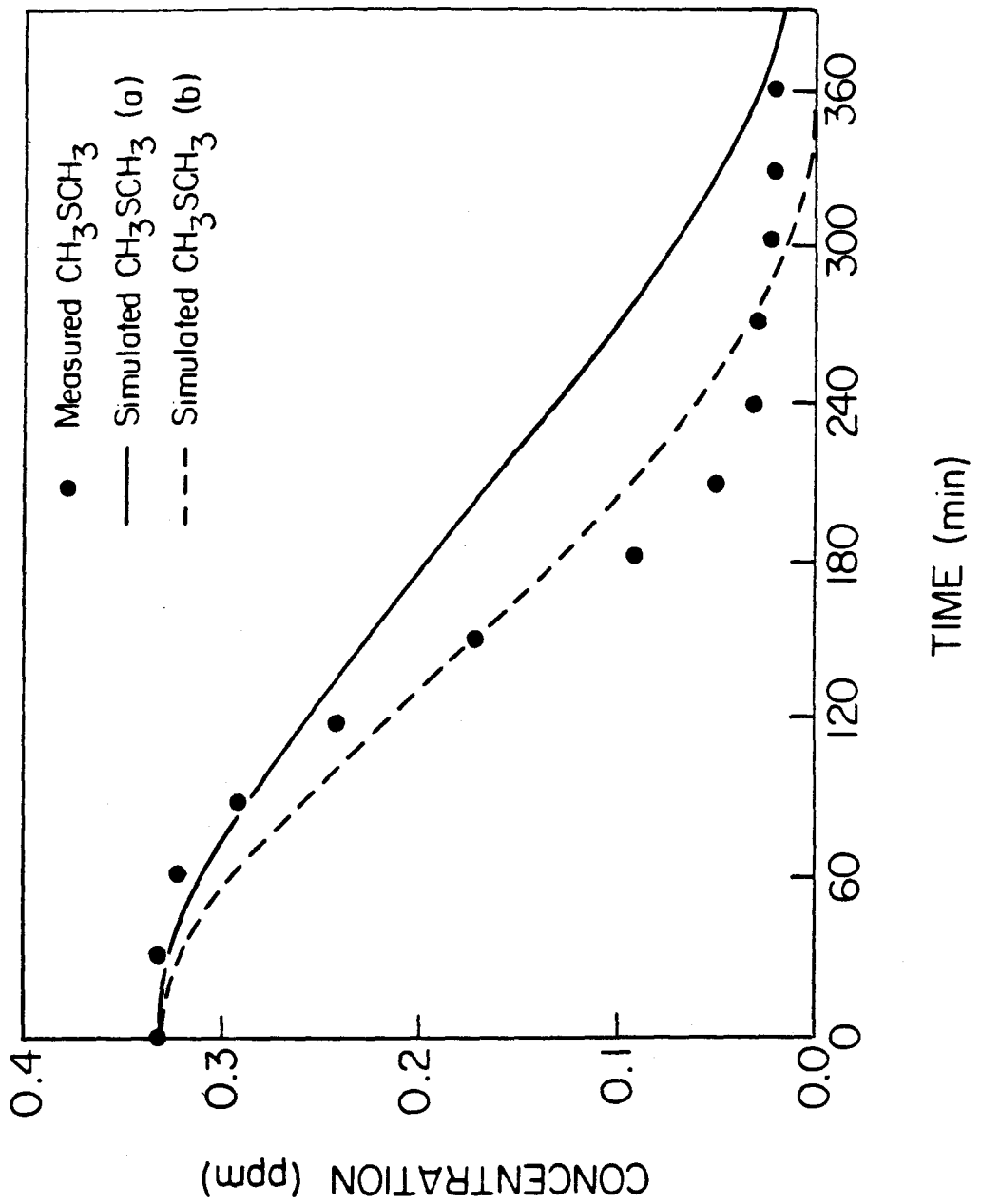
Measured CH_3SCH_3
Simulated CH_3SCH_3 (a)
Simulated CH_3SCH_3 (b)
CONCENTRATION (ppm)
0.0
0.1
0.2
0.3
0.4
0
60
120
180
240
300
360
TIME (min)

Figure 6

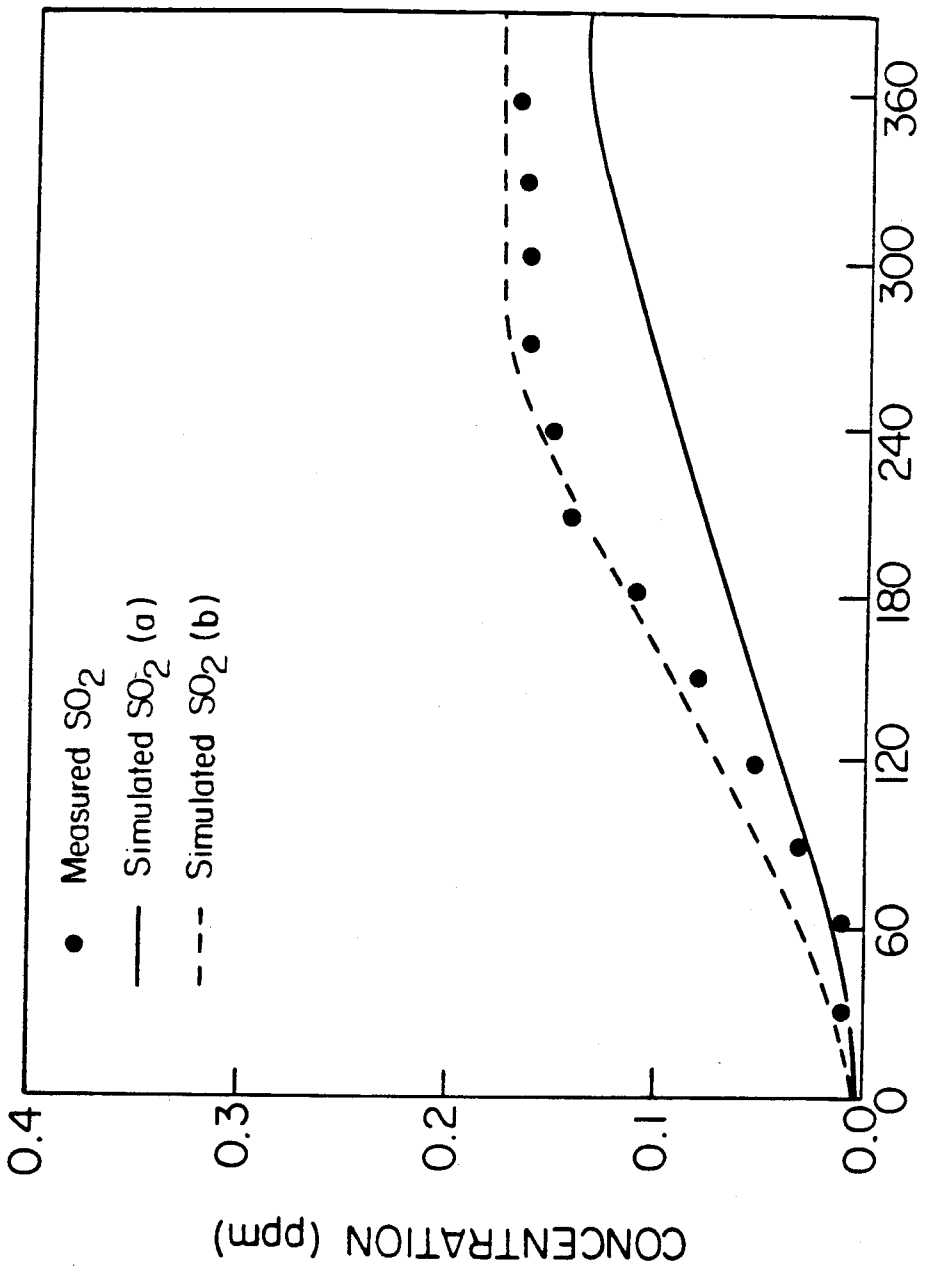
Measured SO_2
Simulated SO_2 (a)
Simulated SO_2 (b)
CONCENTRATION (ppm)
0.0
0.1
0.2
0.3
0.4
0
60
120
180
240
300
360
TIME (min)

Figure 6

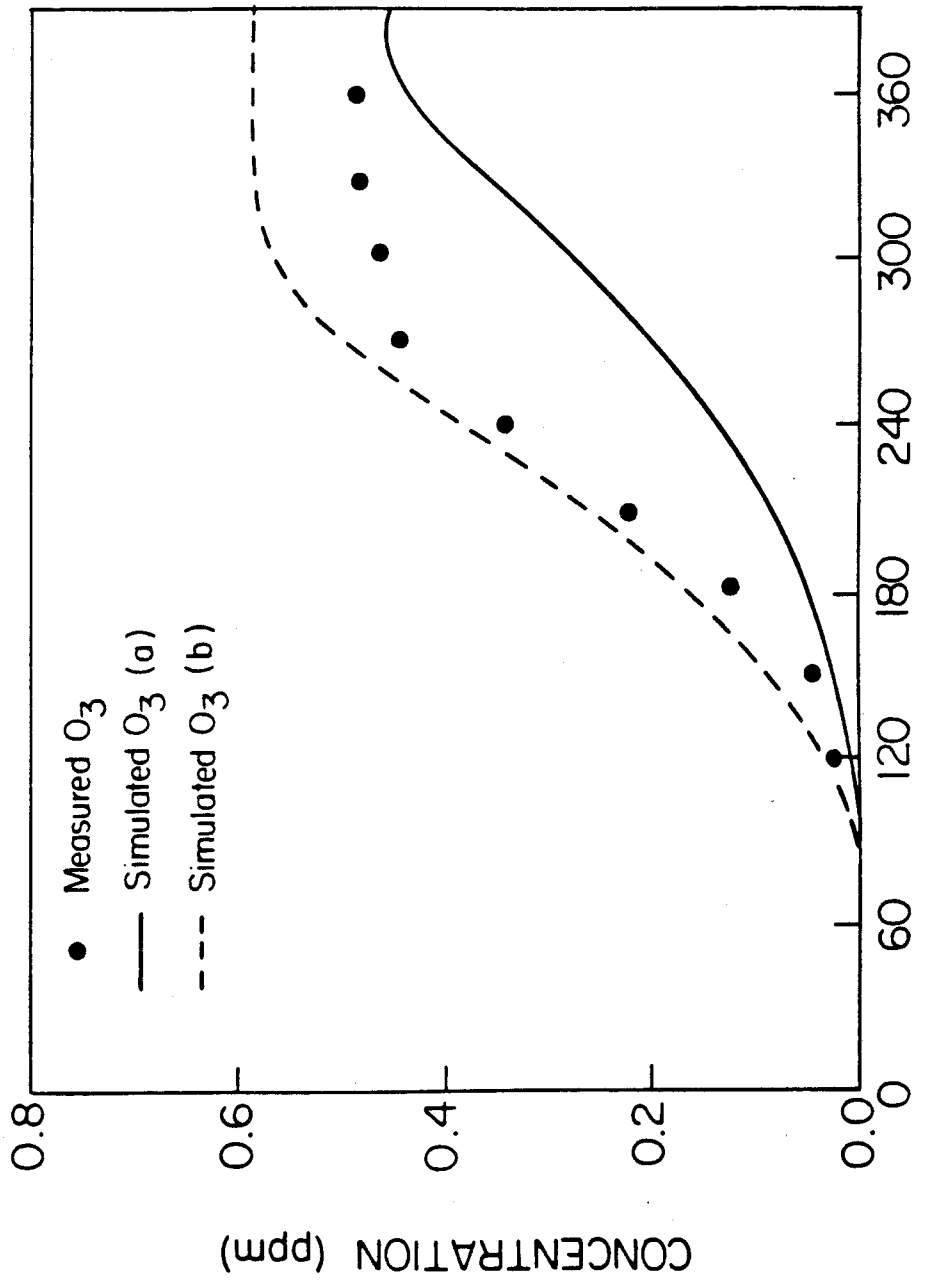
Measured O_3
Simulated O_3 (a)
Simulated O_3 (b)
CONCENTRATION (ppm)
0.0
0.2
0.4
0.6
0.8
0
60
120
180
240
300
360
TIME (min)

Figure 6

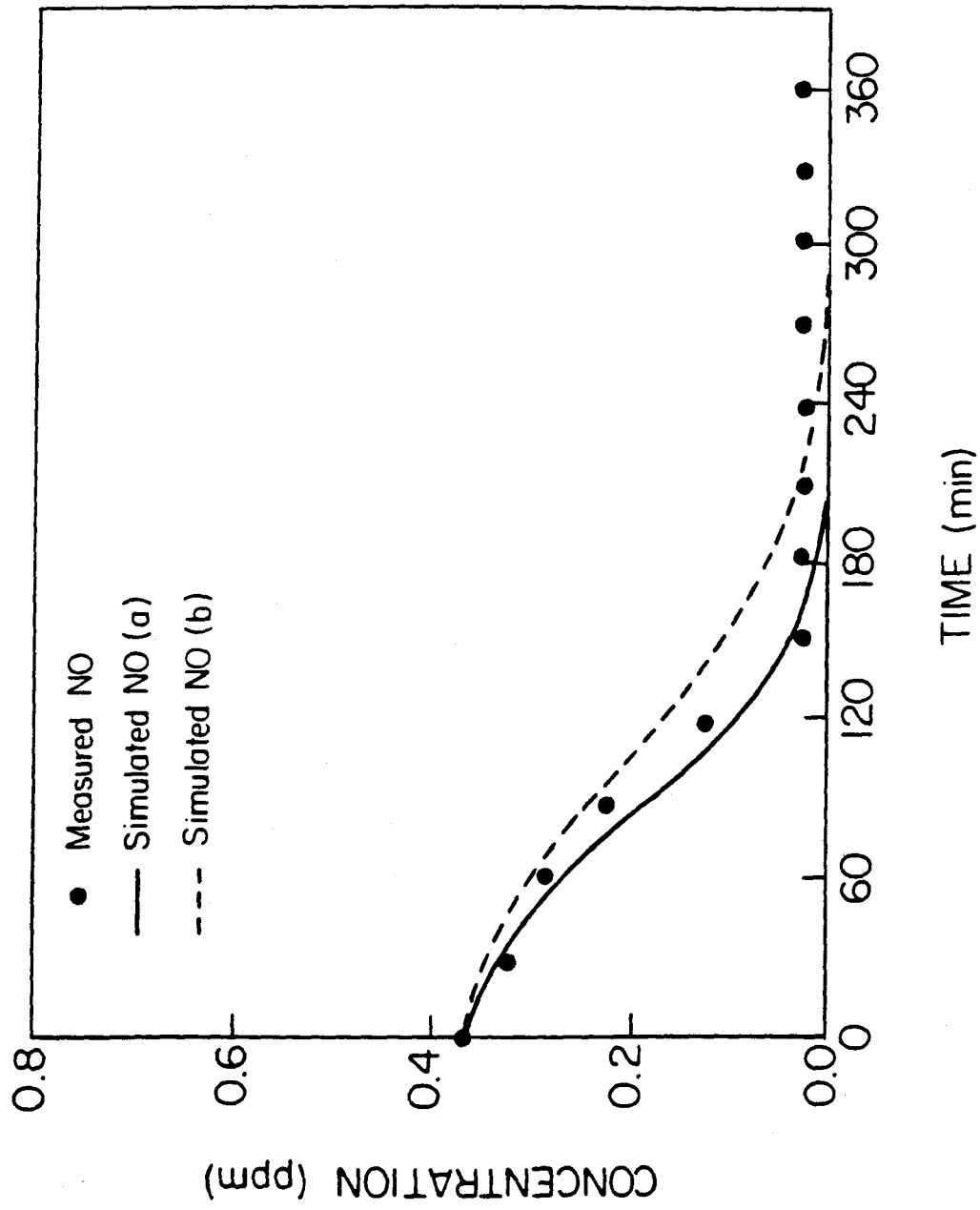
Measured NO
Simulated NO (a)
Simulated NO (b)
CONCENTRATION (ppm)
0.0
0.2
0.4
0.6
0.8
0
60
120
180
240
300
360
TIME (min)

Figure 7

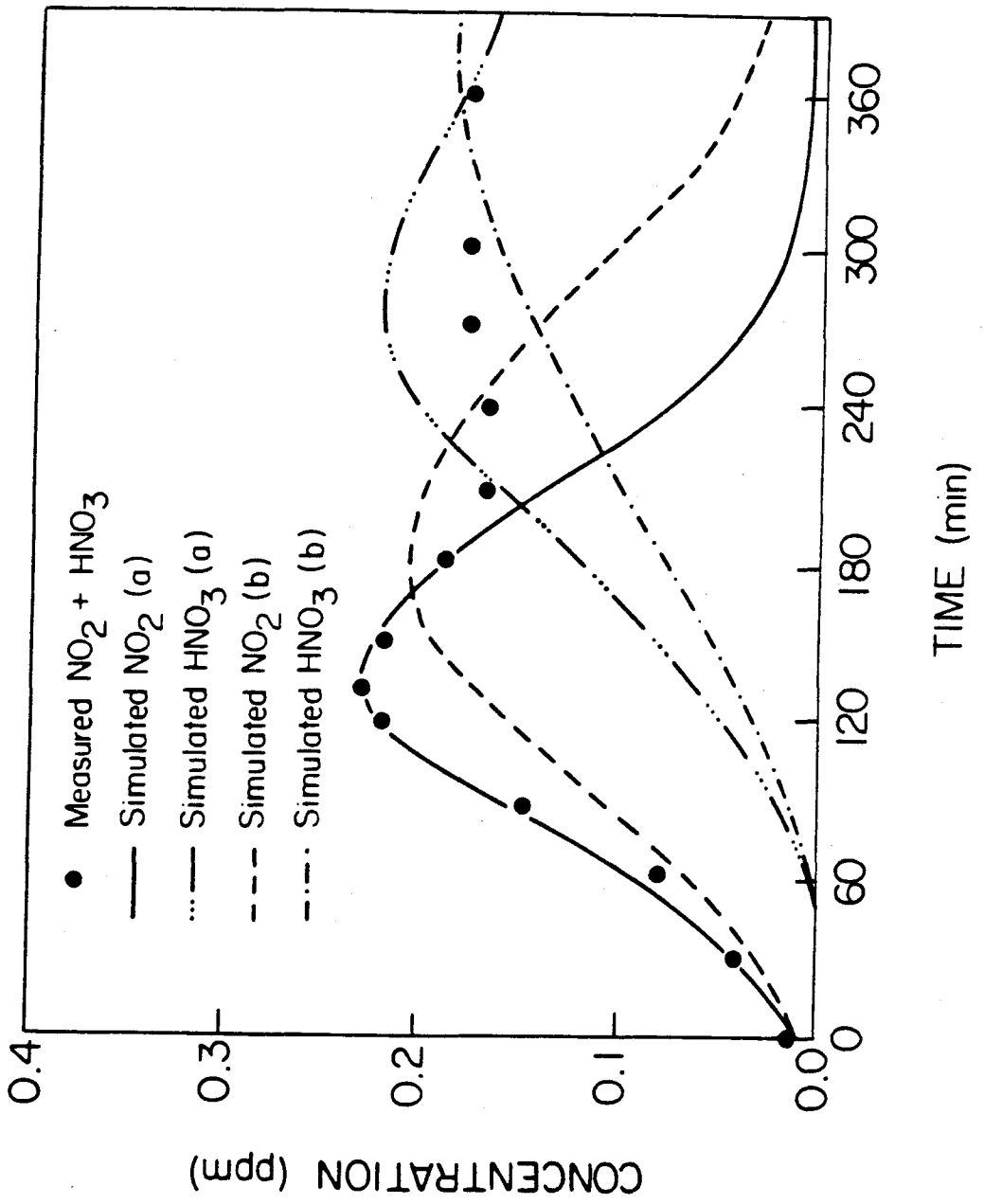
Measured NO_2 + HNO_3
Simulated NO_2 (a)
Simulated HNO_3 (a)
Simulated NO_2 (b)
Simulated HNO_3 (b)
CONCENTRATION (ppm)
0.0
0.1
0.2
0.3
0.4
0
60
120
180
240
300
360
TIME (min)

Figure 7

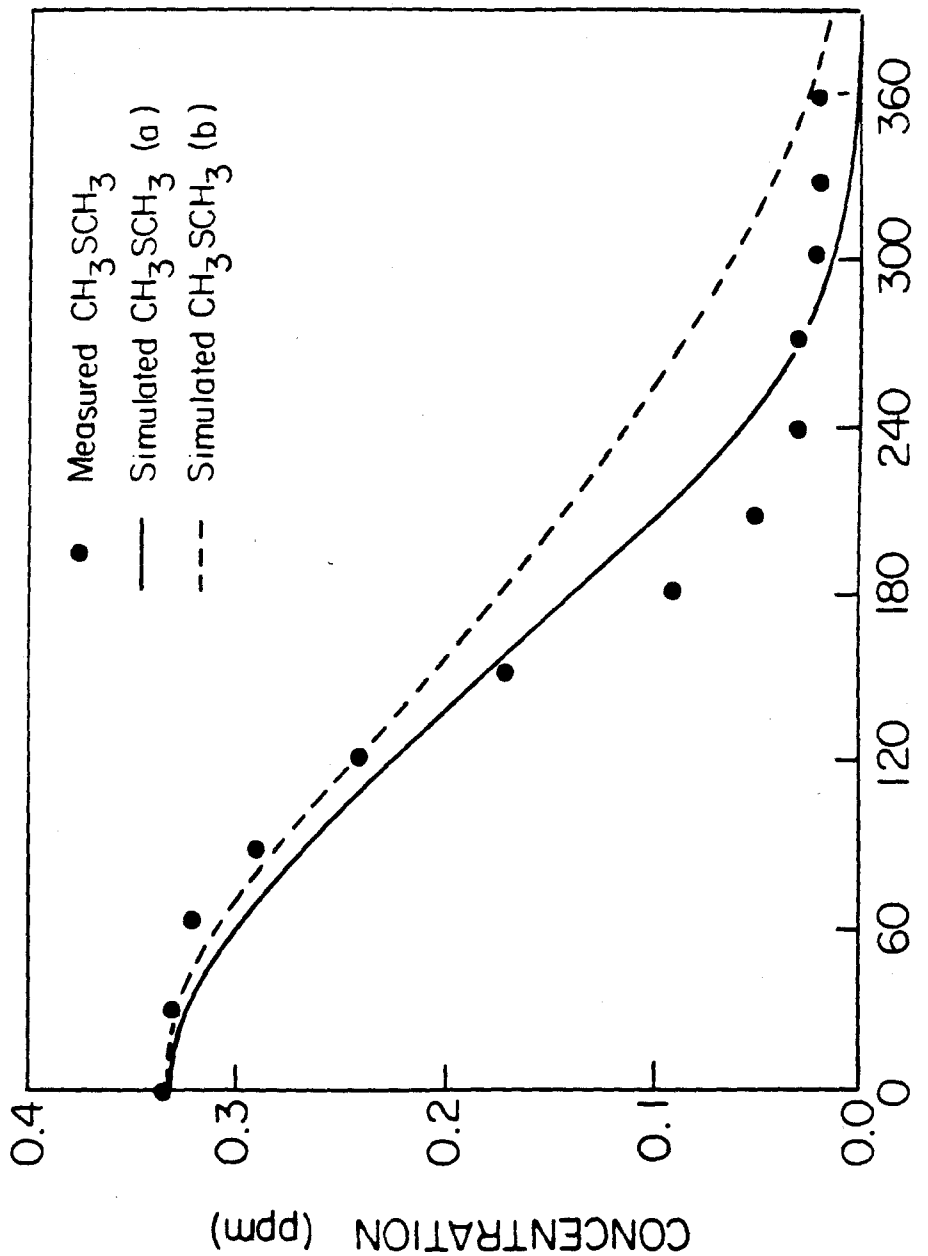
Measured CH_3SCH_3
Simulated CH_3SCH_3 (a)
Simulated CH_3SCH_3 (b)
CONCENTRATION (ppm)
0.4
0.3
0.2
0.1
0.0
0
60
120
180
240
300
360
TIME (min)

Figure 7

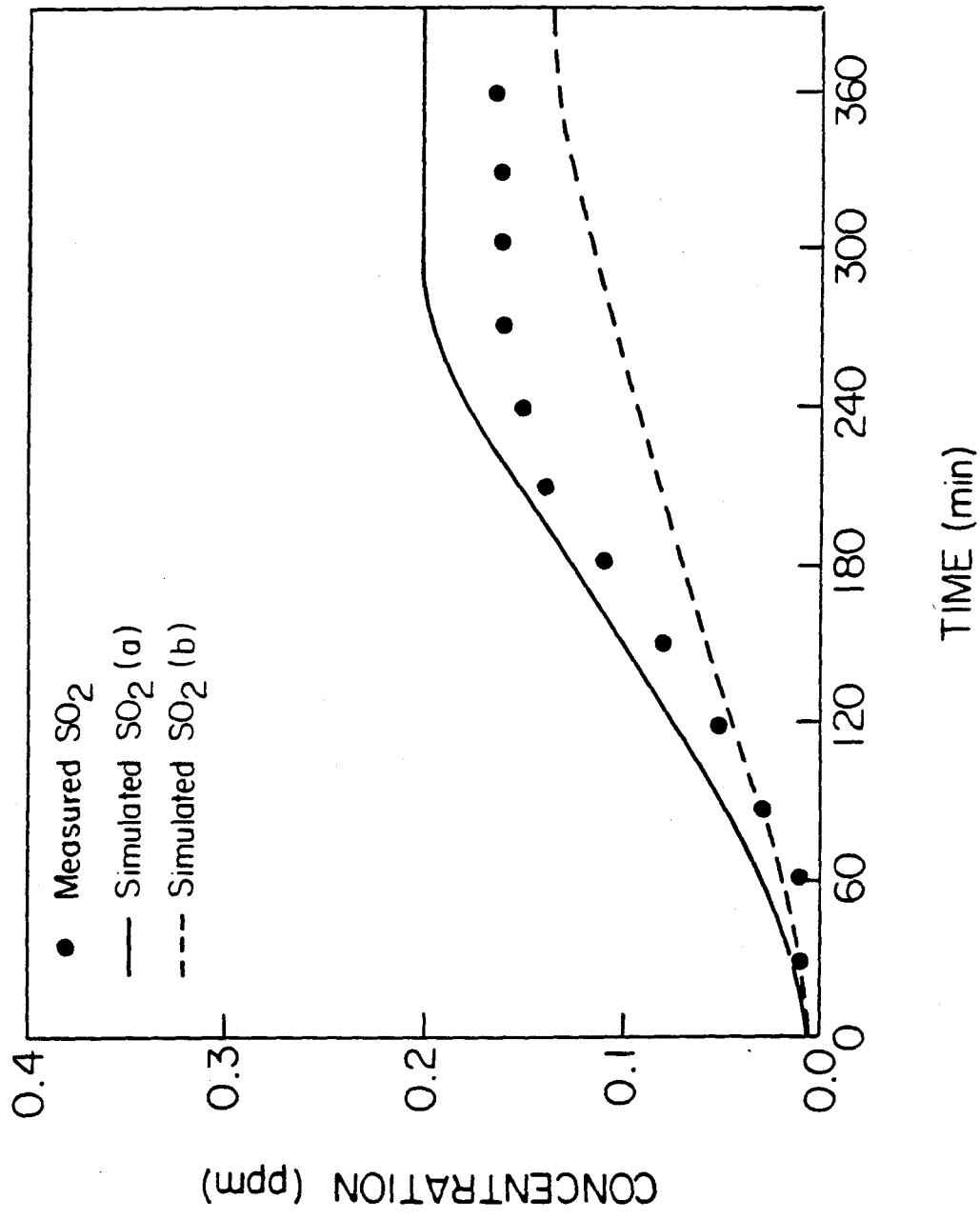
Measured SO_2
Simulated SO_2 (a)
Simulated SO_2 (b)
0.4
0.3
0.2
0.1
0.0
0
60
120
180
240
300
360
TIME (min)
CONCENTRATION (ppm)

Figure 7

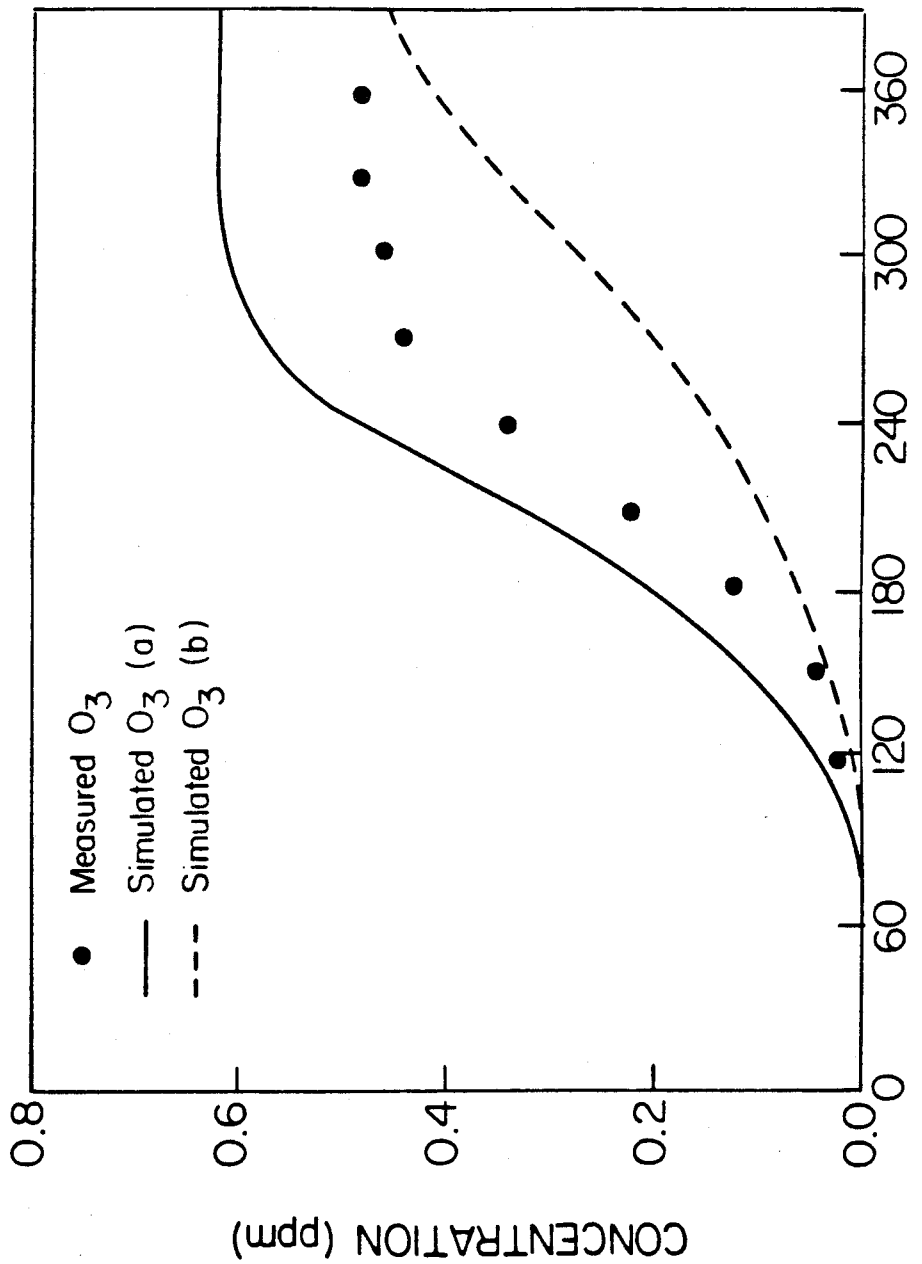
Measured O_3
Simulated O_3 (a)
Simulated O_3 (b)
CONCENTRATION (ppm)
0.0
0.2
0.4
0.6
0.8
0
60
120
180
240
300
360
TIME (min)

Figure 7

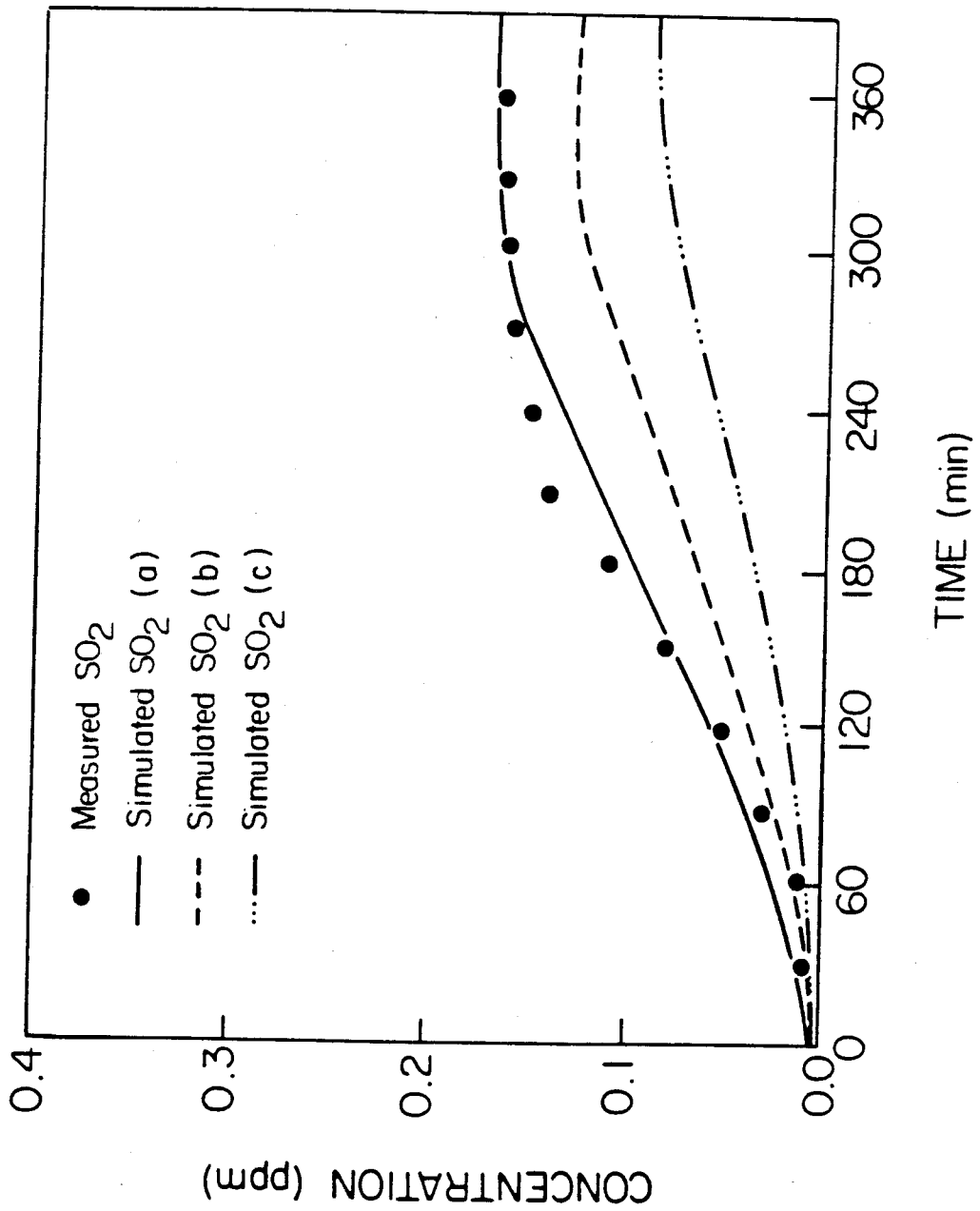
Measured SO_2
Simulated SO_2 (a)
Simulated SO_2 (b)
Simulated SO_2 (c)
CONCENTRATION (ppm)
0.0
0.1
0.2
0.3
0.4
0
60
120
180
240
300
360
TIME (min)

Figure 8

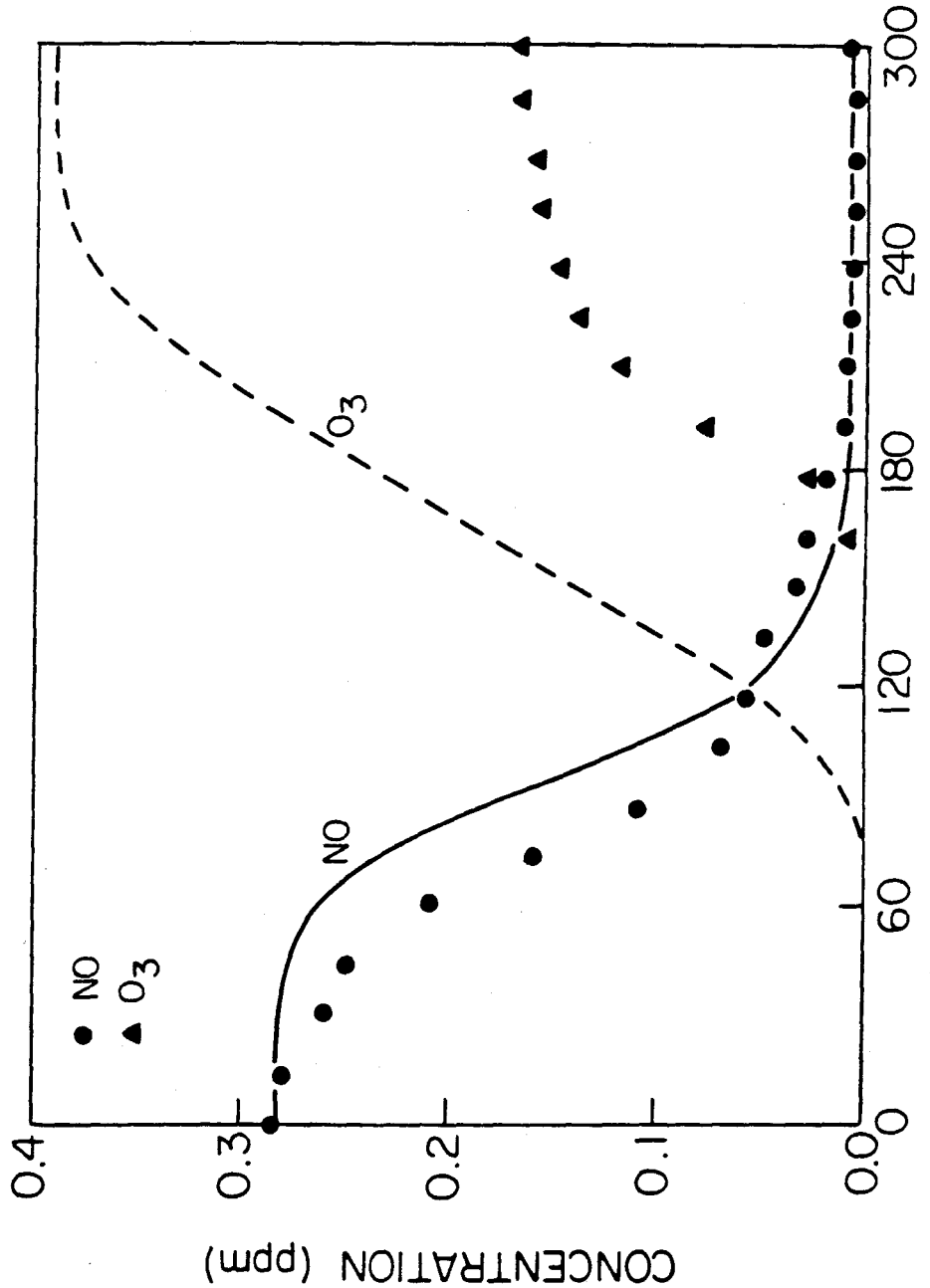
CONCENTRATION (ppm)
0.4
0.3
0.2
0.1
0.0
0
60
120
180
240
300
TIME (min)
NO
O_3
NO
O_3

Figure 9

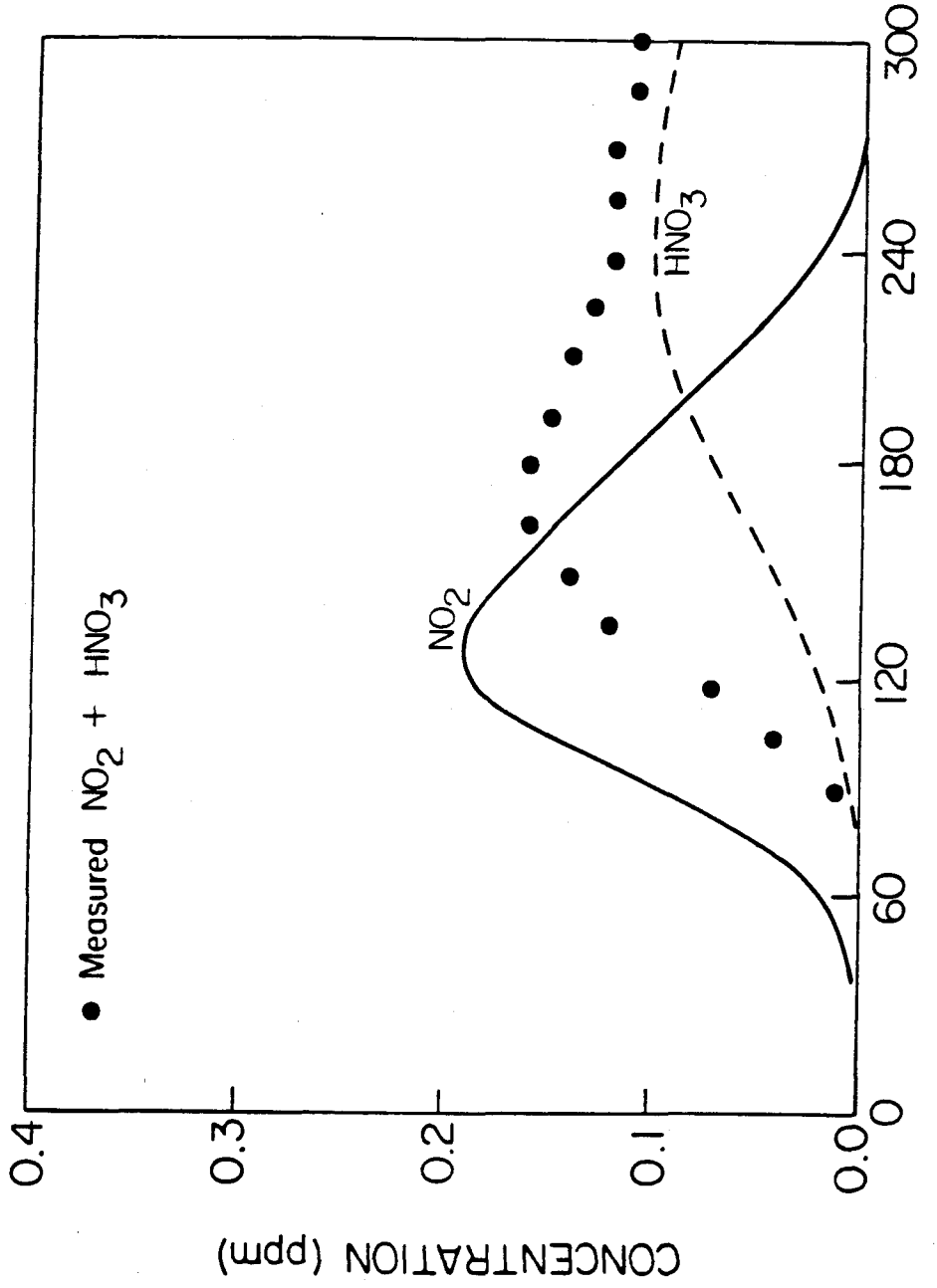
CONCENTRATION (ppm)
0.0
0.1
0.2
0.3
0.4
0
60
120
180
240
300
TIME (min)
● Measured NO_2 + HNO_3
NO_2
HNO_3

Figure 9

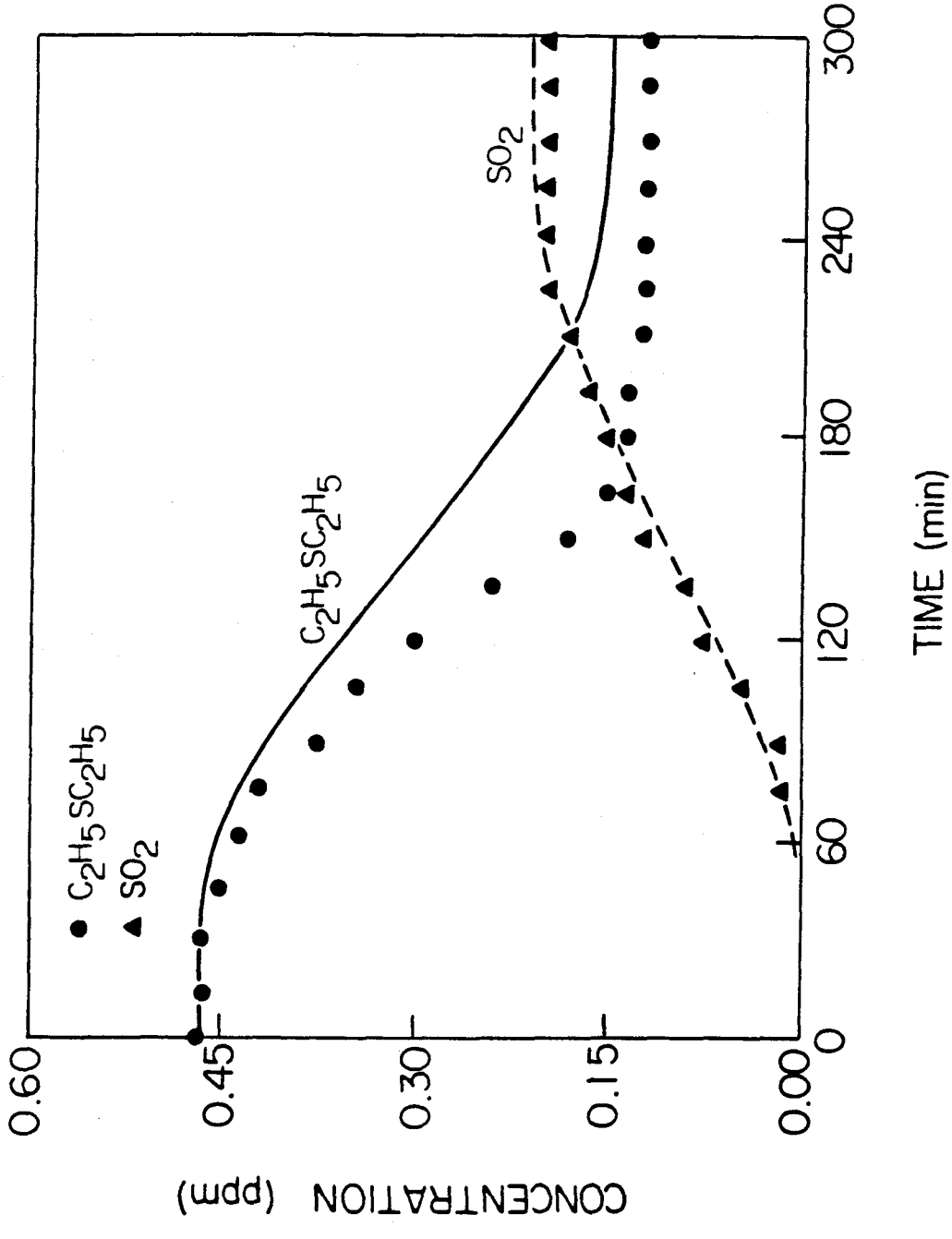
0.60
0.45
0.30
0.15
0.00
0
60
120
180
240
300
TIME (min)
CONCENTRATION (ppm)
$C_2H_5SC_2H_5$
SO_2
$C_2H_5SC_2H_5$
SO_2

Figure 9

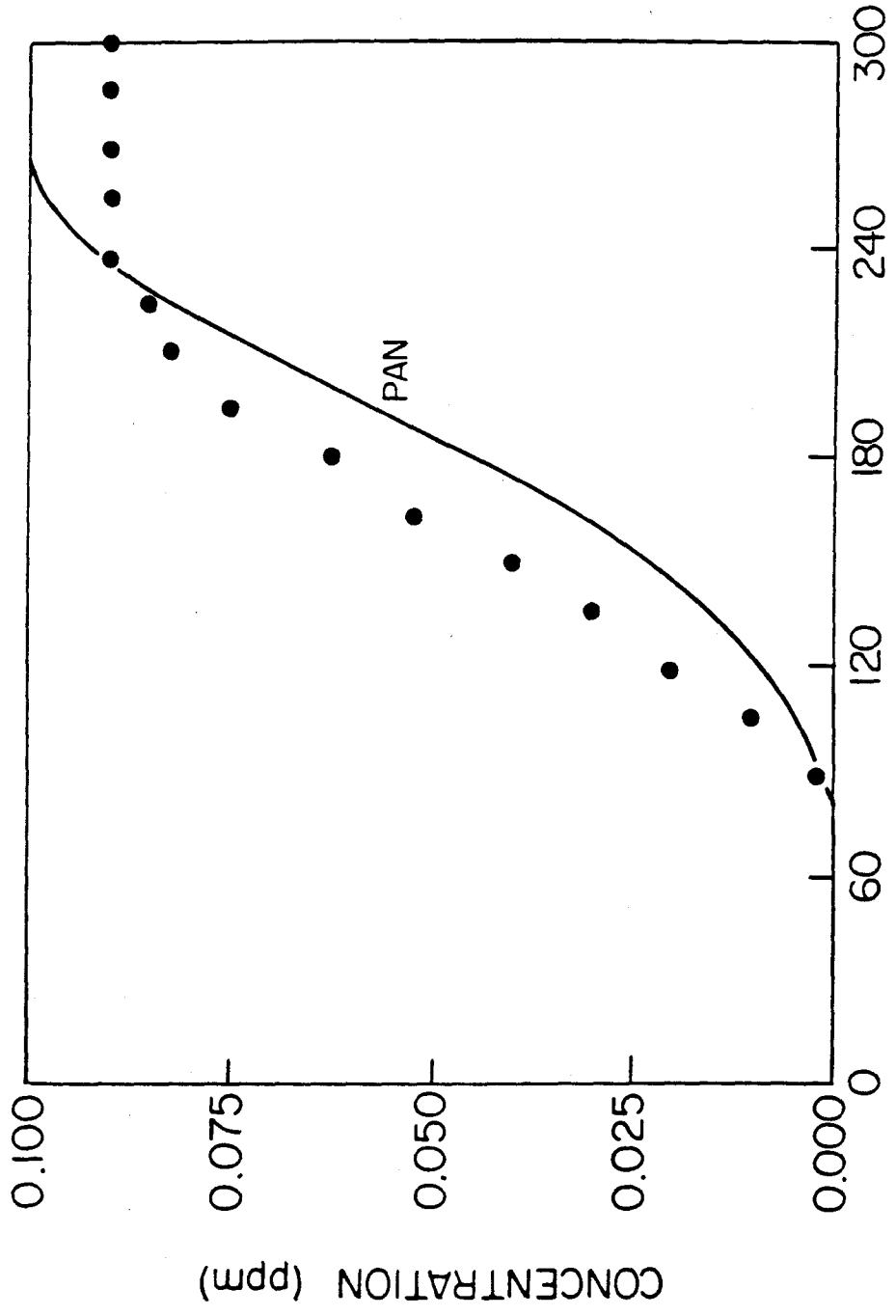
0.100
0.075
0.050
0.025
0.000
0
60
120
180
240
300
PAN
CONCENTRATION (ppm)
TIME (min)

Figure 9

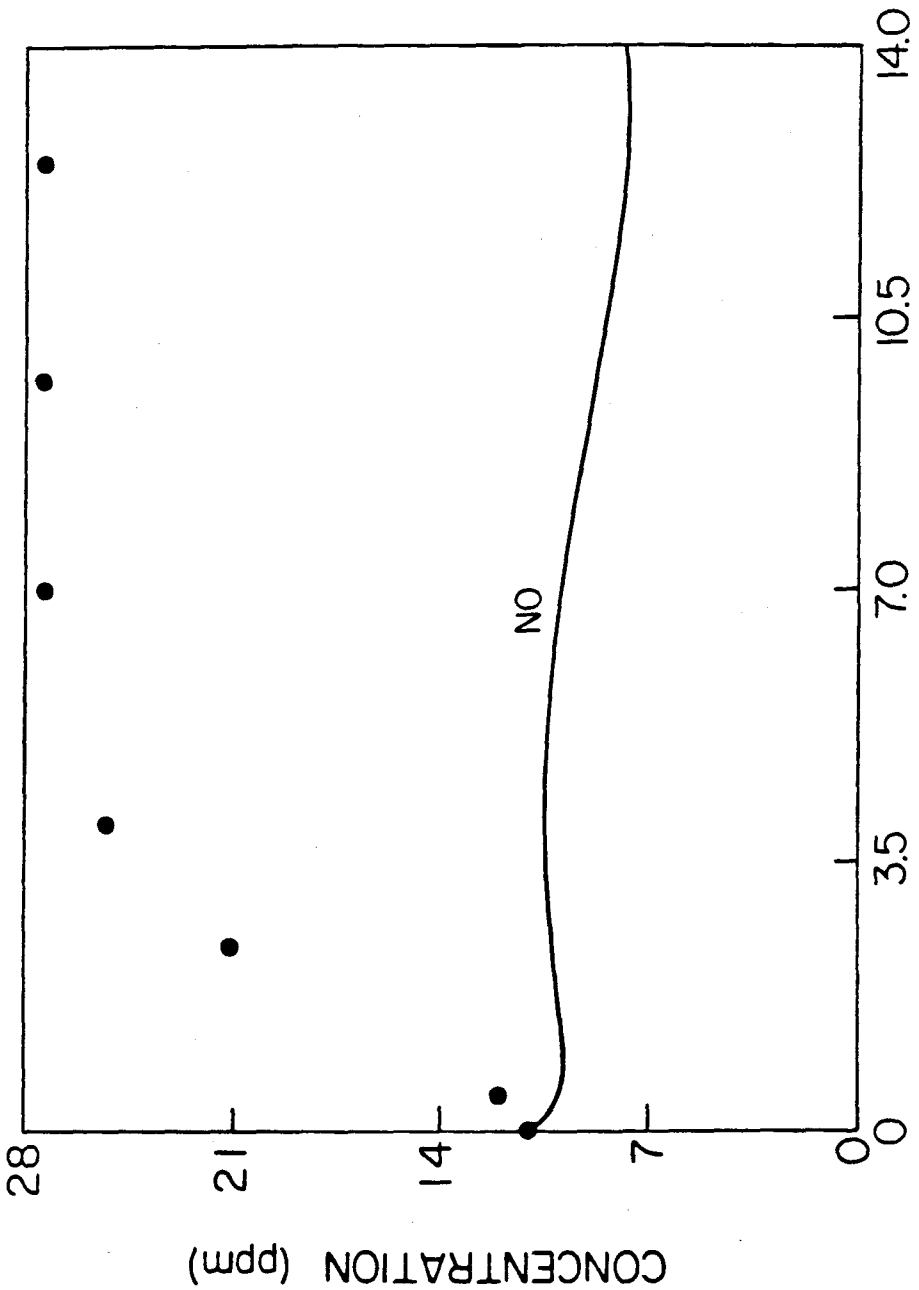

Figure 10

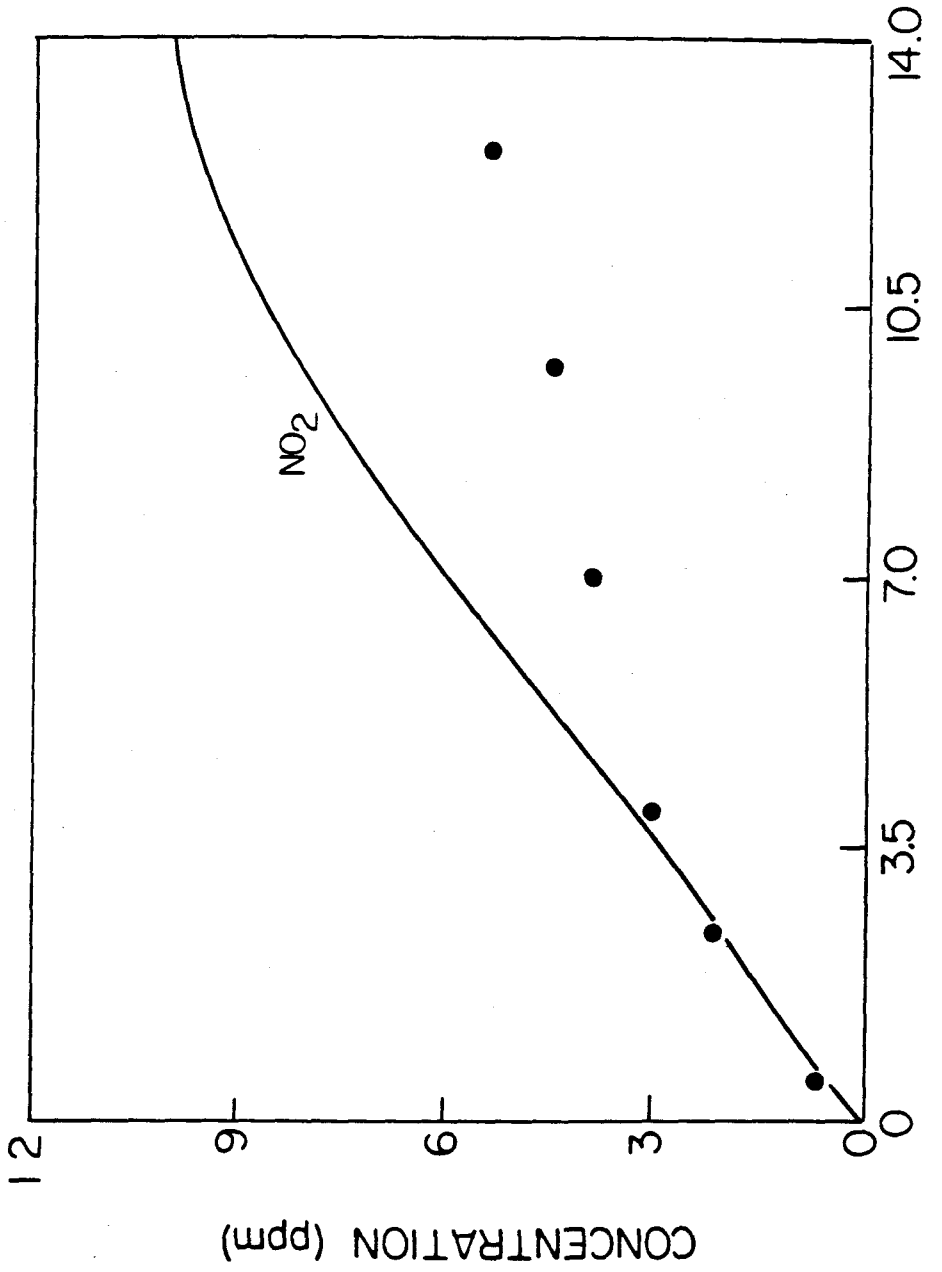

Figure 10

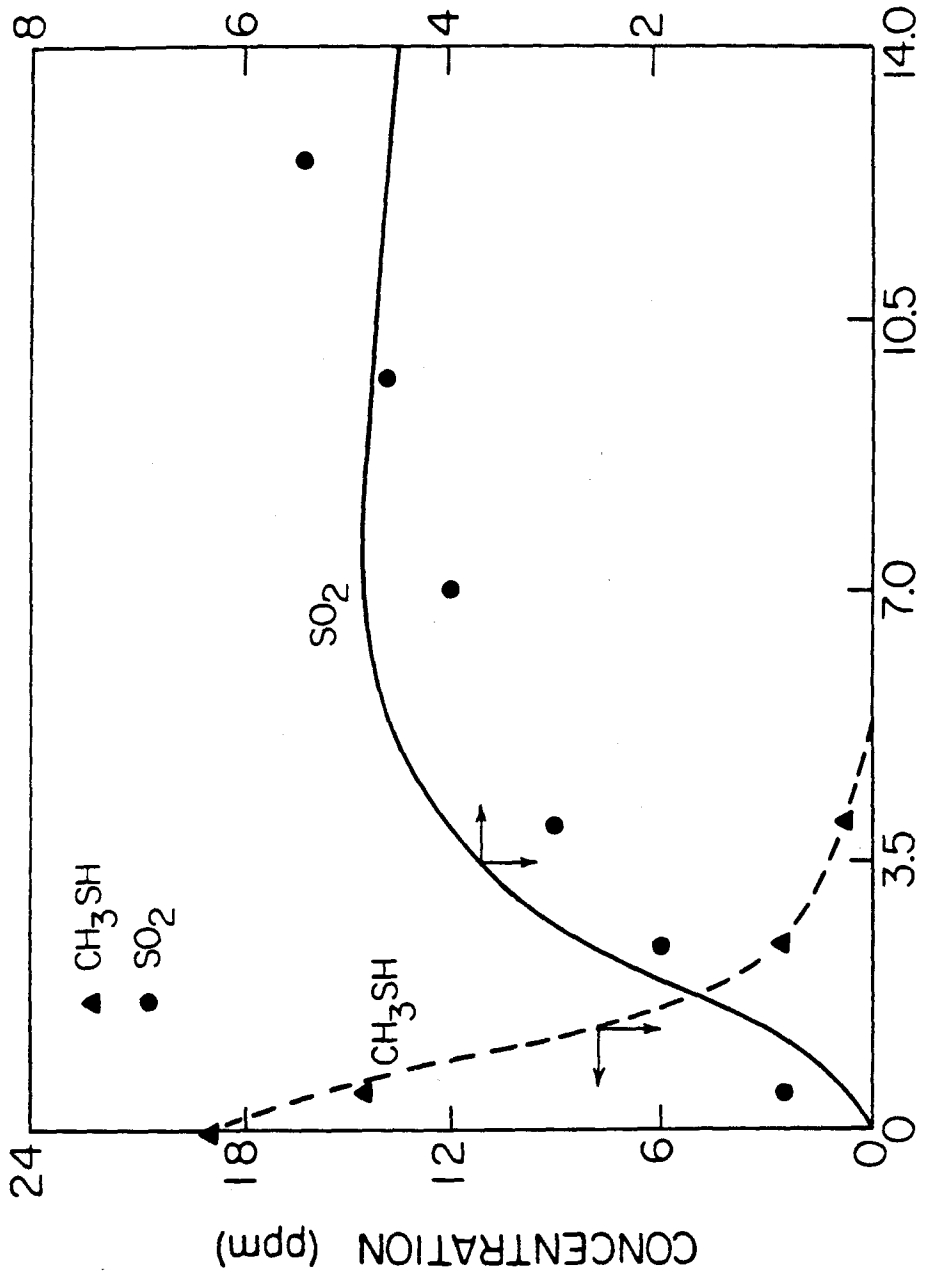
CONCENTRATION (ppm)
TIME (min)
CH_3SH
SO_2
SO_2
CH_3SH
0
3.5
7.0
10.5
14.0
0
6
12
18
24
2
4
6
8

Figure 10

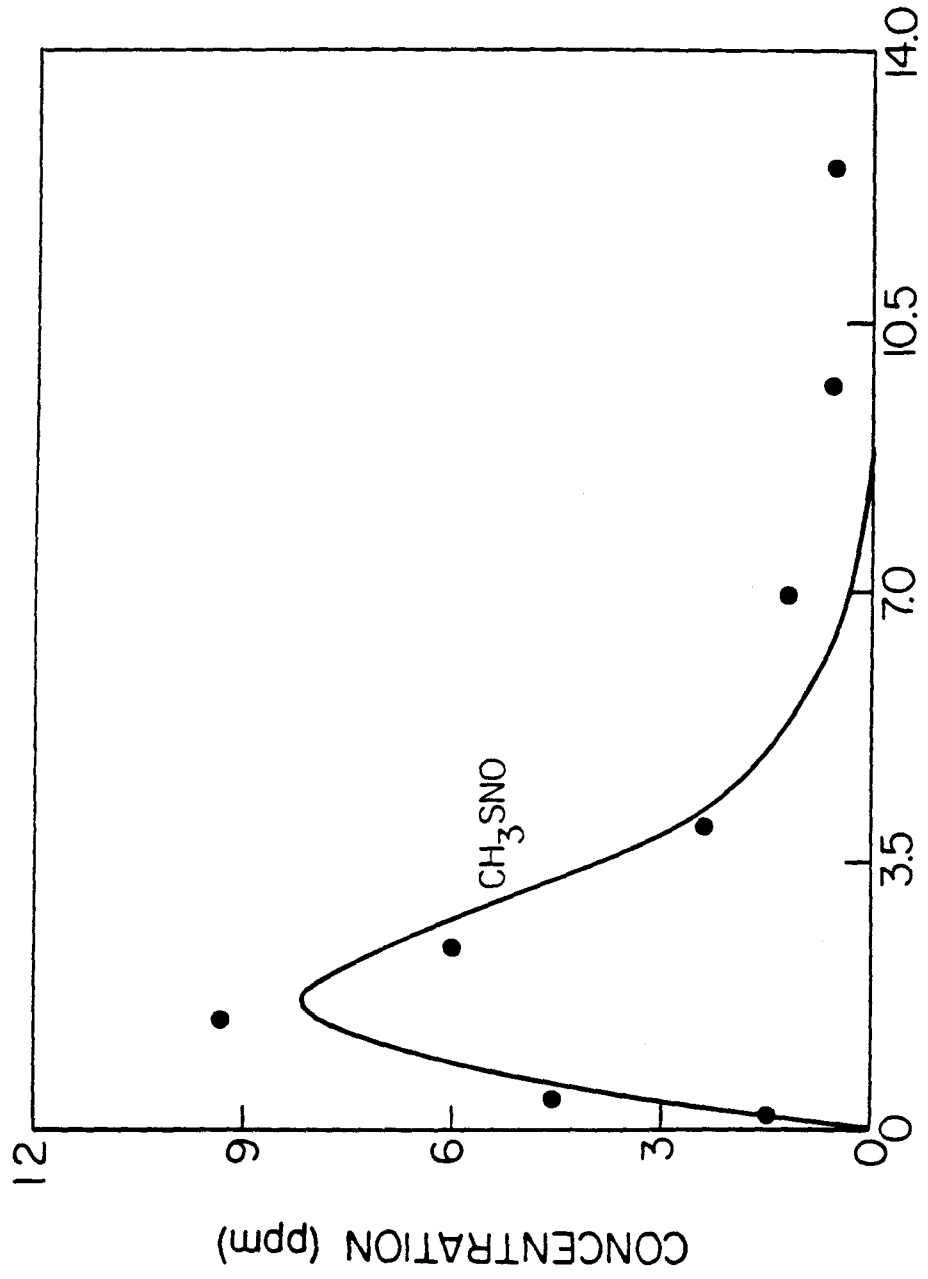

Figure 10

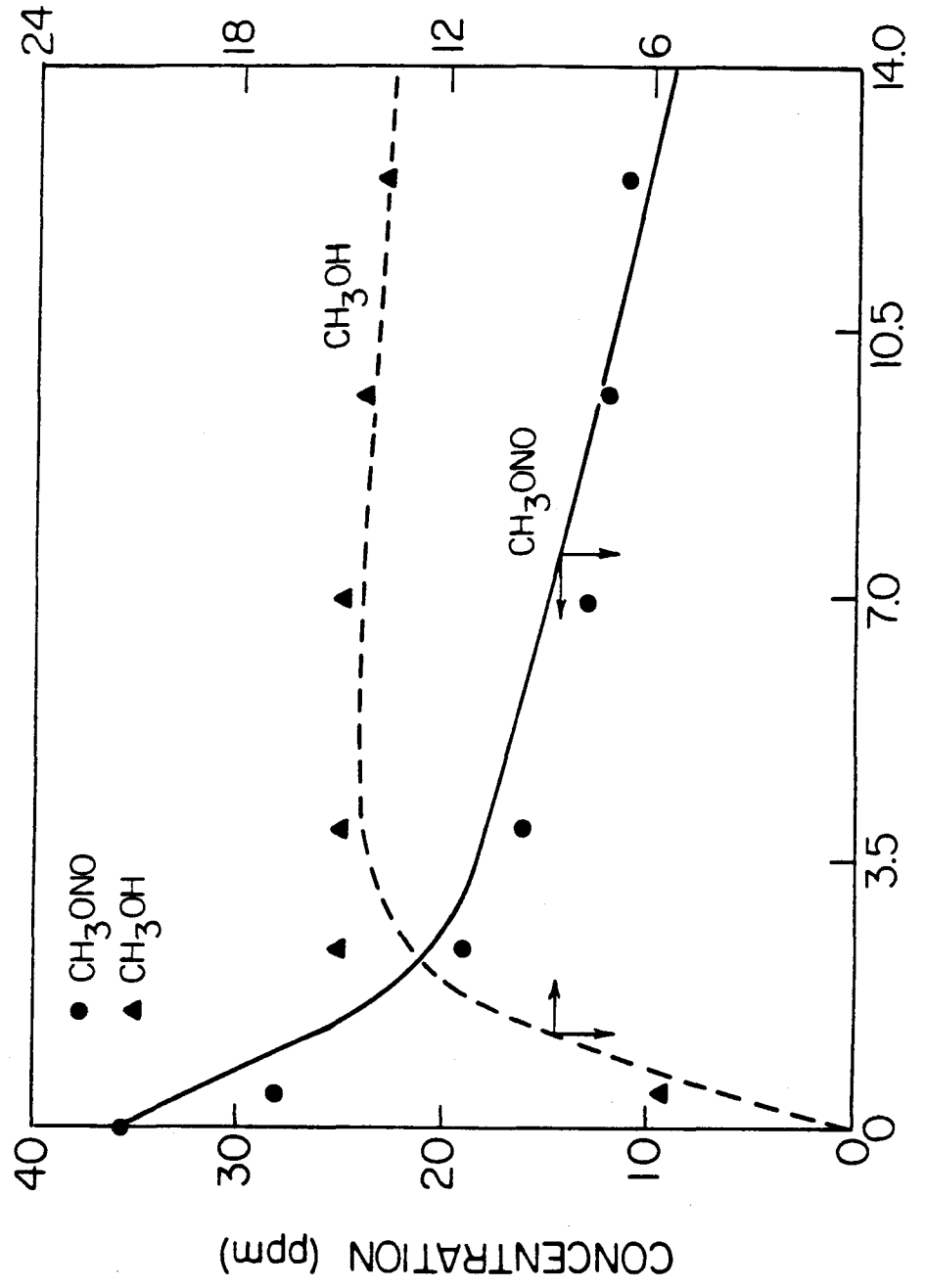
CONCENTRATION (ppm)
TIME (min)
CH_3ONO
CH_3OH
CH_3OH
CH_3ONO
0
10
20
30
40
6
12
18
24
3.5
7.0
10.5
14.0

Figure 10

CHAPTER III

ATMOSPHERIC PHOTOOXIDATION OF DIMETHYL SULFIDE AND DIMETHYL DISULFIDE: I. Mechanism Development.

ATMOSPHERIC PHOTOOXIDATION OF DIMETHYL SULFIDE AND DIMETHYL DISULFIDE: Mechanism Development.

ABSTRACT

Detailed theoretical (Part I, this article) and experimental (Part II) investigations are presented for the mechanism of the atmospheric photooxidation of dimethyl sulfide (CH_3SCH_3) and dimethyl disulfide (CH_3SSCH_3). In this paper comprehensive mechanisms for the atmospheric chemistry of CH_3SCH_3 and CH_3SSCH_3 are developed based on fundamental considerations of all available kinetic and mechanistic information.

Key Words:

Dimethyl sulfide; dimethyl disulfide; photooxidation mechanism.

1. Introduction

Reduced sulfur compounds, including hydrogen sulfide (H_2S), carbonyl sulfide (COS), carbon disulfide (CS_2), methanethiol (CH_3SH), dimethyl sulfide (CH_3SCH_3), and dimethyl disulfide (CH_3SSCH_3), are released from the ocean to the atmosphere. Among these compounds, dimethyl sulfide (CH_3SCH_3) is of major importance in the global sulfur cycle, with an estimated flux of about 40 Tg S yr^{-1} from the oceans and a mean concentration of about 100 ppt in the marine atmosphere [Andreae and Raemdonck, 1983; Andreae et al., 1985]. Thus, a better understanding of the atmospheric chemistry of reduced sulfur compounds, including dimethyl sulfide and dimethyl disulfide, is directly relevant to a number of important issues such as

SO_2 formation, deposition acidity, and global tropospheric sulfur budget.

In an earlier study [Yin et al., 1986], we proposed reaction mechanisms for the atmospheric oxidation of several organosulfur compounds including dimethyl sulfide. These mechanisms accounted for the major features of the few experimental studies then available [e.g., Hatakeyama et al., 1983 and 1985; Grosjean and Lewis, 1982; Grosjean, 1984] and outlined major areas of uncertainty in the tropospheric chemistry of organosulfur compounds. As more experimental studies have become available in recent years, especially regarding the kinetics of initial reactions of reduced sulfur compounds and the subsequent reactions of the CH_3S radical, it is now possible to develop and test updated mechanisms of the atmospheric oxidation of dimethyl sulfide and dimethyl disulfide. These new mechanisms are summarized conceptually in Figure 1 and Figure 2, respectively. In this article, Part I, we present, based on chemical considerations, a theoretical investigation of the possible CH_3SCH_3 and CH_3SSCH_3 oxidation pathways that are consistent with kinetic and mechanistic information now available. The proposed mechanisms are evaluated in a companion article, Part II, with new experimental data obtained in sunlight-irradiated CH_3SCH_3–NO_x–air, CH_3SSCH_3-air and CH_3SSCH_3–NO_x–air mixtures.

In the following sections, a comprehensive analysis of all available experimental information relevant to the chemistry of CH_3SCH_3 and CH_3SSCH_3 is carried out along the reaction sequences shown in Figure 1 and Figure 2, i.e., initial reactions with OH, NO_3, $O(^3P)$ and IO radicals, unimolecular decomposition and bimolecular reactions of the corresponding adducts, structures of CH_3SO_x and $CH_3S(O)_xOO$ radicals, detailed reactions of CH_3SOH and $CH_3S(O)_xCH_3$, oxidations of CH_3SO_x radicals and reductions of $CH_3S(O)_xOO$ radicals, and major formation pathways of SO_2 and CH_3SO_3H products and possible "missing " products. Finally, the new mechanisms are contrasted to those developed in earlier studies.

2. Initial Reactions

Atmospheric removal of organosulfur compounds is initiated by their reactions with OH, NO_3, IO and $O(^3P)$ radicals. The critical issue regarding these initial reactions is the extent of competition between addition and abstraction pathways. Although numerous kinetic studies of these reactions have been carried out, these studies have shed little light on the corresponding reaction mechanisms, especially as to the trends of observed rate constants and to the various "effects" due to secondary reactions. In this section, the general character of the initial reactions, i.e., addition and/or abstraction, will be analysed in terms of fundamental chemistry, as well as on the basis of available experimental data. Although our study focuses on CH_3SCH_3 and CH_3SSCH_3, initial reactions of other reduced sulfur compounds including H_2S and CH_3SH will also be included for comparison.

2.1. Initial Reaction Mechanisms

The initial reactions of reduced sulfur compounds with free radicals may involve two pathways, abstraction and addition. Hydrogen atom abstraction may proceed through C–H or S–H bond scission. Alternatively, the initial reaction may involve electrophilic addition onto the S atom. The corresponding energy-rich adduct may be collisionally stabilized or may unimolecularly decompose, either back to the reactants or to yield new products. These initial reactions can be represented by:

$$\begin{aligned}
RSR' + X &\longrightarrow RSR'' + HX && k_{abs} \\
&\xrightarrow{M} \text{Adduct} && k_{add},\ k_{-add} \\
\text{Adduct} &\xrightarrow{M} \text{Product} \\
\text{Adduct} + Y &\longrightarrow \text{Products}
\end{aligned}$$

(R = H, CH_3; R′ = H, CH_3, CH_3S; X = OH, NO_3, $O(^3P)$, IO; Y= reactive species such as O_2, NO_2 in the system)

The overall observed rate constant of the initial reaction, k_{obs}, is the net of all three reactions, i.e.,

$$k_{obs} = k_{abs} + (k_{add} - k_{-add})$$

The general trends of observed rate constants can be discussed in terms of the general trends of the molecular properties of reduced sulfur compounds and radicals.

From the trend of the bond dissociation energy (BDE) (kcal/mole) of C–H and S–H bonds [Hwang and Benson, 1979; Shum and Benson, 1983; Shum and Benson, 1985]:

CH_3S–H,	HS–H	<	H–CH_2SH,	H–CH_2SCH_3,	H–CH_2SSCH_3
88.6±1	90.5 ± 1.1		96±1	96.6 ± 1.0	97 (estimated)

the order of rate constants for the abstraction pathway can be expected to be:

$$k_{CH_3S-H},\ k_{HS-H} > k_{H-CH_2SH},\ k_{H-CH_2SCH_3},\ k_{H-CH_2SSCH_3}$$

Importantly, the rate constants for the abstraction pathways involving C–H and S–H bond scission are not expected to span several orders of magnitude (see Table 1), since the difference of bond dissociation energies for C–H and S–H bonds is about 6–8 kcal/mole although the H-atoms bonded to S could be more readily abstracted than those bonded to C.

The relative reactivity of different radicals towards reduced sulfur compounds by H-atom abstraction can be evaluated from the strength of the newly formed H - X bond (kcal/mole) [Kerr, 1985; Baulch et al., 1984],

HO–H	>	H–O	>	$H–ONO_2$,	H–OI
119±1		102.2		101.2±0.5	(101)

that is,

$$k_{OH} > k_{O(^3P)} > k_{NO_3}, k_{OI}$$

Considering the difference of bond dissociation energy between broken and formed bonds, it is anticipated that, among the four radicals, OH will be the most likely to react with reduced sulfur compounds by H-atom abstraction.

Theoretically, the intrinsic addition reaction is the addition of radicals to the S atom to form an energy-rich adduct. Due to the short lifetime of the adduct and the difficulty of detecting such an adduct, however, the addition pathway actually involves two steps, addition and subsequent unimolecular decomposition. Therefore, practically, the observed addition pathway can be envisioned as involving two steps, adduct formation and subsequent unimolecular decomposition. Adduct formation involves an electrophilic addition reaction, and is mainly determined by the electron density on the S atom. The electron-donating capability of substituted groups on the S atom is in the order:

$$CH_3S > CH_3 > H$$

Thus, the tendency for radical addition to the S atom is in the order:

$$CH_3SSCH_3 > CH_3SCH_3 > CH_3SH > H_2S$$

The rate and selectivity of the subsequent adduct unimolecular decomposition step depend on the bond dissociation energies of broken and formed bonds as well as on the stability of the radicals produced. The overall addition reaction rate may

be controlled by addition, unimolecular decomposition, or both. The adduct may also react with other reactive species in the system, thus affecting the observed rate constants; see section 2.4.

2.2. Observed Rate Constant Trends

Rate constants for the reactions of OH, NO_3, IO and $O(^3P)$ with reduced sulfur compounds are given in Table 1. These rate constants may include contributions from both abstraction and addition pathways. The rate constant trends are discussed below with respect to the relative importance of these two pathways.

2.2.1. Reaction with $O(^3P)$ Radical

The observed rate constants for the reactions of RSR′ with $O(^3P)$ are in the order:

$$k_{H_2S} << k_{CH_3SH} < k_{CH_3SCH_3} < k_{CH_3SSCH_3}$$

and span some four orders of magnitude [Cvetanović et al., 1981; Baulch et al., 1984]. This trend is consistent with addition being the major pathway. Cvetanović et al. [1981] studied the reactions of $O(^3P)$ with CH_3SH, CH_3SCH_3 and CH_3SSCH_3 and found that addition of $O(^3P)$ to the S atom followed by rapid unimolecular decomposition (see Table 1) was the dominant pathway, although abstraction may account for as much as 10% of the total reaction in the case of CH_3SH. The small negative activation energy for the reaction of $O(^3P)$ with CH_3SCH_3 and CH_3SSCH_3 is also consistent with an addition mechanism. The $H_2S+O(^3P)$ reaction is believed to proceed mostly by abstraction; this is supported by the positive activation energy of about 3.8 kcal/mole [Baulch et al., 1984].

2.2.2. Reaction with OH Radical

The trend of rate constants for the RSR′+OH reaction is similar to that for $O(^3P)$, with the exception of CH_3SCH_3:

$$k_{H_2S} < k_{CH_3SCH_3} < k_{CH_3SH} < k_{CH_3SSCH_3}$$

Hynes et al. [1986] estimated that, for the $OH + CH_3SCH_3$ reaction under atmospheric conditions at 300 K, the *effective* branching ratio is 0.75 abstraction, and 0.25 addition.

It will be shown below, however, that the observed trend of OH rate constants is consistent with addition being the dominant pathway, even for the $OH + CH_3SCH_3$ reaction. Although the *effective or apparent* pathway (considering only the formed adducts that are scavenged by O_2) for the $OH+CH_3SCH_3$ reaction is dominated by abstraction, 0.75 at 300 K as estimated by Hynes et al. [1986], the *actual or intrinsic* branching ratios of abstraction vs. addition (i.e., without considering the reverse reaction of addition) are 0.12 to 0.88 for CD_3SCD_3 at 261 K [Hynes et al., 1986], and 0.33 to 0.67 for CH_3SCH_3 at 298 K [Barnes et al., 1988], indicating that addition is the dominant pathway for the $OH + CH_3SCH_3$ reaction, although the abstraction pathway is not negligible. Furthermore, despite that the observed $k_{OH+CH_3SCH_3}$ is almost a factor of 10 lower than the observed k_{OH+CH_3SH}, the difference is much smaller if we define

$$k_{initial} = k_{abs} + k_{add}$$

and remove the effect of the reverse reaction of addition pathway. Estimates of k_{add} and k_{-add} have been made by Hynes et al. [1986] and Barnes et al. [1988]. For the $CD_3SCD_3 + OH$ reaction at 261 K in 700 torr $N_2 + O_2$ [Hynes et al., 1986],

$$k_{OH} = (1.6 \pm 0.2) \times 10^{-12} + (1.15 \pm 0.20) \times 10^{-11}$$
$$= (1.31 \pm 0.22) \times 10^{-11} \quad (cm^3\ molecule^{-1}\ s^{-1})$$

and for CH_3SCH_3 + OH at 298 K in 760 torr air [Barnes et al., 1988],

$$k_{OH} = (4.4 \pm 0.4) \times 10^{-12} + (9.0 \pm 0.5) \times 10^{-12}$$
$$= (1.34 \pm 0.09) \times 10^{-11} \quad (cm^3\ molecule^{-1}\ s^{-1})$$

Comparing with the corresponding value of $k_{OH+CH_3SH} = 3.3 \times 10^{-11}$ cm^3 $molecule^{-1}$ s^{-1} at 298 K [Hynes and Wine, 1987], both rate constants are now of the same magnitude, although k_{OH+CH_3SH} is still larger than $k_{OH+CH_3SCH_3}$. Since the trend for the abstraction pathway is $CH_3SH > CH_3SCH_3$ (see Section 2.1.), and the contribution of H-atom abstraction by the OH radical is increased relative to that by the $O(^3P)$ radical and also is comparable to that from addition, therefore, the reason that $k_{OH+CH_3SH} > k_{OH+CH_3SCH_3}$ can be explained by the contribution from the abstraction pathway, or more likely through the following mechanism:

$$CH_3S\text{–}H + OH \rightarrow CH_3\overset{\overset{H}{\overset{O}{|}}}{S}\text{–}H \rightarrow CH_3S\cdots H \rightarrow CH_3S\cdot + H_2O$$

Intramolecular H-bonding as well as the weaker S–H bond than C–H bond by 6–8 kcal/mole BDE facilitates the H-atom abstraction by OH radical, and the contribution of reverse decomposition is small compared to that for CH_3SCH_3. The formation of such a nonlinear transient state is consistent with the near-zero isotopic effect observed by Wine et al. [1984] for the CH_3SD + OH reaction. The lack of O_2 effect observed for $CH_3S(OH)H$ by Hynes and Wine [1987] is consistent with a relatively short lifetime for the $CH_3S(OH)H$ adduct and also supports the above mechanism. For CH_3SSCH_3, the effect of the reverse reaction is negligible since the

tendency of OH addition toward CH_3SSCH_3, whose rate constant is almost a factor of 10 higher, is much stronger than that for other reduced sulfur compounds.

In summary, the reaction of OH with organosulfur compounds involves addition as the dominant pathway, although abstraction also contributes to the overall reaction in the case of CH_3SH and CH_3SCH_3. Due to the reverse reaction of the adduct $CH_3S(OH)CH_3$, the OH + CH_3SCH_3 reaction is apparently dominated by abstraction at temperature larger than 285 K in the atmosphere (estimated by Hynes et al. [1986]).

2.2.3. Reactions with NO_3 and IO Radicals

As discussed in section 2.1, the NO_3 reaction is expected to involve abstraction only as a minor pathway, i.e., much smaller than that for OH and similar to that of $O(^3P)$. However, NO_3 reaction rate constants exhibit a totally different trend from those for $O(^3P)$ and OH; see Table 1. The NO_3-organosulfur rate constants are similar with the exception of that for $k_{NO_3+CH_3SSCH_3}$ [MacLeod et al., 1986], which will be discussed later. The rate constant of $H_2S + NO_3$ is at least 3 orders of magnitude smaller [Dlugokencky and Howard, 1988], indicating that in this case abstraction may be the dominant pathway. From Table 1, it can be seen that the rate constant for NO_3 radical is always a factor of 10 or more lower than that for other radicals. One possible explanation is that the unpaired electron on O atom of NO_3 is delocalized and forms a large π bond over the whole NO_3 radical, leading to its lower reactivity, while for other radicals the unpaired electron is localized on the O atom of each radical.

Comparison of CH_3SCH_3 and CH_3OCH_3 also supports the fact that addition is the dominant pathway for $NO_3 + RSR'$ [Wallington et al., 1986b and 1986c; Dlugokencky and Howard, 1988]:

			k_{298} (cm^3 $molecule^{-1}$ s^{-1})
$NO_3 + CH_3SCH_3$	→	Product	$7.7 - 10.9 \times 10^{-13}$
$NO_3 + CH_3OCH_3$	→	$HNO_3 + CH_3O\dot{C}H_2$	$< 0.03 \times 10^{-13}$

although C–H BDE are similar for the two compounds, i.e., 96.6 ± 1.0and 93 ± 1 kcal/mole for CH_3SCH_2–H and CH_3OCH_2–H, respectively [Shum and Benson, 1985; McMillen and Golden, 1982].

The observed similarity among NO_3 rate constants is not inconsistent with addition being the dominant reaction pathway if the observed rate constants are actually determined by the subsequent reactions of the adducts and the energy changes associated with them are of similar magnitude. Basically, the formed adducts, $CH_3S(ONO_2)X$ where X = H, CH_3 or SCH_3, can undergo unimolecular decomposition,

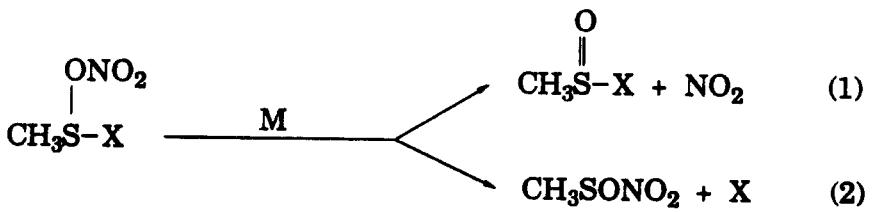

or intramolecular H-atom abstraction.

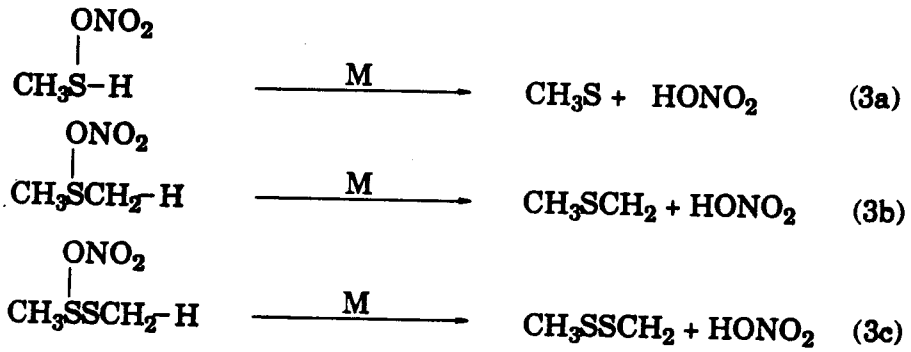

For pathway (1), the rates of adduct decomposition are expected to be similar for CH_3SH, CH_3SCH_3 and CH_3SSCH_3 since each of them involves similar O–NO_2 bond scission. Since it is difficult to evaluate the bond dissociation energies of adducts for pathway (2), a rough comparison of bond dissociation energy (kcal/mole) from the corresponding reactants can be made as follows [Benson, 1978; Shum and Benson, 1983]:

CH_3–S–H		H_3C–S–CH_3	CH_3S–S–CH_3	
74.2 ± 1	88.6 ± 1	75.0 ± 1	67.8 ± 2	57 ± 1.5

If the broken bonds are C–S in the CH_3SH and CH_3SCH_3 adducts and S–S in the CH_3SSCH_3 adducts, the difference between those bond dissociation energies is small and similar rate constants will be expected. C–S bond scission is indeed expected for the CH_3SH adduct. In order to explain the decomposition of the CH_3SSCH_3 adduct, the small bond dissociation energy of the C–S bond in CH_3SSCH_3 must be explained first. The bond dissociation energy of the C–S bond in CH_3SSCH_3 is about 18 kcal/mole less than that in CH_3SCH_3. This is due to the higher stability of the produced radical, $CH_3S\dot{S}$, because of the partial double or π bond formed in the radical [Benson, 1978; Shum and Benson, 1983]. However, if the adduct, $CH_3SS(ONO_2)CH_3$, decomposes by C–S bond scission instead of forming the $CH_3S\dot{S}$ radical, the molecule CH_3SS–ONO_2 will be formed, that is

$$CH_3S\dot{S}(ONO_2)CH_3 \rightarrow CH_3SS\text{–}ONO_2 + \dot{C}H_3 \quad \text{S–C bond scission}$$
$$\rightarrow CH_3S\text{–}ONO_2 + CH_3\dot{S} \quad \text{S–S bond scission}$$

and the corresponding special stability of $CH_3S\dot{S}$ is no longer involved. Although no thermodynamic data are available for CH_3SS–ONO_2 and CH_3S–ONO_2, their bond

dissociation energies are expected to be in the order

$$BDE(CH_3S\text{–}ONO_2) > BDE(CH_3SS\text{–}ONO_2)$$

since $BDE(CH_3S\text{–}CH_3) > BDE(CH_3SS\text{–}CH_3)$, and the S–S bond scission in adduct $CH_3SS(ONO_2)CH_3$ is therefore expected to be dominant.

The energy change for reaction pathway (3) is not available at the present since the bond dissiciation energies of C–H and S–H bonds of the *adducts* are unknown. It is expected that the adduct $CH_3S(ONO_2)H$ may undergo intramolecular H-atom abstraction faster than either $CH_3S(ONO_2)CH_3$ or $CH_3SS(ONO_2)CH_3$ due to its weaker S–H bond. However, other factors including the stability of the formed products and the energy strain between five-, six- and seven-member rings may compensate the favourable BDE for $CH_3S(ONO_2)H$. In summary, the observed trend of rate constants alone cannot distinguish the proposed three possible reaction pathways for the adduct $CH_3S(ONO_2)R'$ since each of them could lead to similar rate constants for $CH_3S(ONO_2)H$, $CH_3S(ONO_2)CH_3$ and $CH_3S(ONO_2)SCH_3$ adducts.

Why the rate constants for NO_3 + RSR' reactions appear to be determined by the unimolecular decomposition step rather than by the addition step is not evident. One possible explanation is the relatively large size of the NO_3 adduct, which would allow for easy dispersion of this excess energy over the whole radical.

Turning now to IO, only one reaction rate constant has been measured, that for CH_3SCH_3. [Martin et al., 1987; Barnes et al., 1987a]. Both studies showed that addition of IO to the S atom is the dominant pathway, followed by unimolecular decomposition through I–O bond cleavage. The trend of the rate constants for the IO radical is expected to be similar to that for $O(^3P)$ radical if the addition of IO to the S atom is the rate-limiting step.

In summary, analysis of observed reaction rate constant trends strongly sug-

gests that addition is the dominant pathway for the initial reactions of $O(^3P)$, OH, NO_3 and IO radicals with organosulfur compounds, which is mainly due to the unsaturated nature of the S atom and the relatively high electron density on the S atom of organosulfur compounds.

2.3. Unimolecular Decomposition of the Adducts

Reactants and the corresponding adducts are listed in Table 2. The discussion in this section will focus on the elucidation of the dominant adduct decomposition pathways, which depend on the relative strength of the bonds in the adducts and on the stability of the radicals and molecules produced.

The unimolecular decomposition of the $O(^3P) + RSR'$ adducts is reasonably well understood from the work of Cvetanović et al. [1981]. The dominant decomposition reaction is C–S bond scission for $CH_3S(O)H$ and $CH_3S(O)CH_3$, and S–S bond scission for $CH_3SS(O)CH_3$, although S–H bond cleavage is also important for $CH_3S(O)H$. No experimental observations are available for the decomposition of all other adducts listed in Table 2. Therefore the fate of those adducts is discussed here based mainly on thermodynamic considerations. Indirect experimental evidence will also be examined when available.

With respect to the adducts produced from the reactions between RSR' and OH radical, it is generally assumed that the adduct $CH_3S(OH)SCH_3$ undergoes rapid unimolecular decomposition to CH_3SOH and CH_3S [Wine et al., 1981; Hatakeyama and Akimoto, 1983; Atkinson, 1985], although no direct evidence is yet available. The fate of $CH_3S(OH)CH_3$ may be examined by comparison with that of the adduct $CH_3SS(OH)CH_3$:

$$CH_3SSCH_3 + OH \longrightarrow CH_3\overset{H}{\underset{|}{\overset{O}{\underset{|}{\dot{S}}}}}SCH_3 \xrightarrow{M} CH_3SOH + CH_3S\cdot$$

$$CH_3SCH_3 + OH \longrightarrow CH_3\overset{H}{\underset{|}{\overset{O}{\underset{|}{\dot{S}}}}}CH_3 \xrightarrow{M} CH_3SOH + CH_3\cdot$$

The energy changes of decomposition for above two adducts depend on the bond dissociation energies as well as the stability of the formed radicals. The difference in the formation enthalpy between CH_3S (31.0 kcal/mole) and CH_3 (34.8 kcal/mole) [Shum and Benson, 1983; Baulch et al., 1984] is small, and the bond dissociation energies between S–C and S–S bonds of the *adducts* are not expect to be very large (considering their corresponding reactants and the similar reasoning discussed in Section 2.2.3.). Thus, the unimolecular decomposition of $CH_3S(OH)CH_3$ to CH_3SOH and CH_3 is probably not negligible, and may contribute partially to $k_{CH_3SCH_3+OH}$ measured in the *absence* of O_2. Also the mechanism

$$CH_3S(OH)CH_3 + O_2 \rightarrow CH_3SOH + CH_3O_2$$

proposed by Hynes and Wine [1989] is more likely to proceed first through unimolecular decomposition of $CH_3S(OH)CH_3$ followed by addition of CH_3 to O_2, i.e., same as that in the absence of O_2. The adduct $CH_3S(OH)H$ may mainly undergo unimolecular decomposition to CH_3S and H_2O via intramolecular H-bonding. Given the structural similarity of all four CH_3SH adducts, one may also expect the $O(^3P)$, NO_3 and IO adducts to form intramolecular H-bonding and to decompose further to CH_3S and HO, $HONO_2$ or HOI, respectively, although the ability to form such H-bonding and to abstract an H atom is quite different among those four radicals. In fact, the observed 10% S–H bond cleavage for the $O(^3P) + CH_3SH$ reaction may be explained in terms of such H-bonding formation rather than by direct H-atom

abstraction.

As discussed in Section 2.2.3., the NO_3+RSR$'$ reaction adduct, $CH_3-\overset{R'}{\underset{|}{\dot{S}}}-ONO_2$, may undergo three possible reaction pathways. Since no NO_2 was observed by Tyndall et al. [1986] and Dlugokencky and Howard [1988] in the time scale of 100–200 ms, and no $CH_3S(O)CH_3$ was detected in FT–IR product studies [Tyndall et al., 1986; MacLeod et al., 1986], the adduct appears to decompose by pathways other than those involving O–N bond scission. In addition to the reaction between adducts and other species, another possible reaction for the adduct $CH_3S(ONO_2)R'$ is decomposition by breaking S–H, C–S and S–S bonds to produce $R'SONO_2$. It is interesting to note that an unidentified product containing a nitrate group was observed for the $NO_3+CH_3SCH_3$ reaction [Tyndall et al., 1986] although it may also be formed through secondary reactions. The product, $R'SONO_2$, may be thermally unstable and further decompose to R$'$SO and NO_2, which is also mentioned by Dlugokencky and Howard [1988] for the HSO–NO_2 adduct. Finally, the adduct $CH_3S(ONO_2)R'$ may undergo intramolecular H-atom abstraction through a five-, six- or seven-member ring, which is more favourable since only $HONO_2$, not NO_2, is formed. The simulation of smog chamber data also supports this pathway as dominant (see Part II).

The dominant reaction for adduct $CH_3S(OI)CH_3$ is the unimolecular decomposition to $CH_3S(O)CH_3$ by breaking the O–I bond since the yield of $CH_3S(O)CH_3$ was observed to be close to unity for the IO + CH_3SCH_3 reaction by Barnes et al. [1987a].

2.4. Adduct Bimolecular Reactions

Depending on adduct lifetime and on the time resolution of the experimental

techniques used, secondary reactions may contribute to the observed rate constants. Possible adduct bimolecular reactions are discussed in this section along with other secondary reactions and their possible effects on the observed reaction rate constants.

2.4.1. Adduct Reaction with Oxygen

Rate constants for the reactions of free radicals with organosulfur compounds have been observed to vary with oxygen concentration. This "O_2 effect" usually refers to the reaction,

$$\text{Adduct} + O_2 \rightarrow \text{Product}$$

The "O_2 effect" has been confirmed experimentally for only one reaction among H_2S, CH_3SH, CH_3SCH_3 and CH_3SSCH_3, that of OH with CH_3SCH_3 [Hynes et al., 1986; Barnes et al., 1988], although it has also been reported in studies of other organosulfur compounds [Barnes et al., 1986a]. The following possible reactions have been proposed for the $CH_3S(OH)CH_3$ adduct:

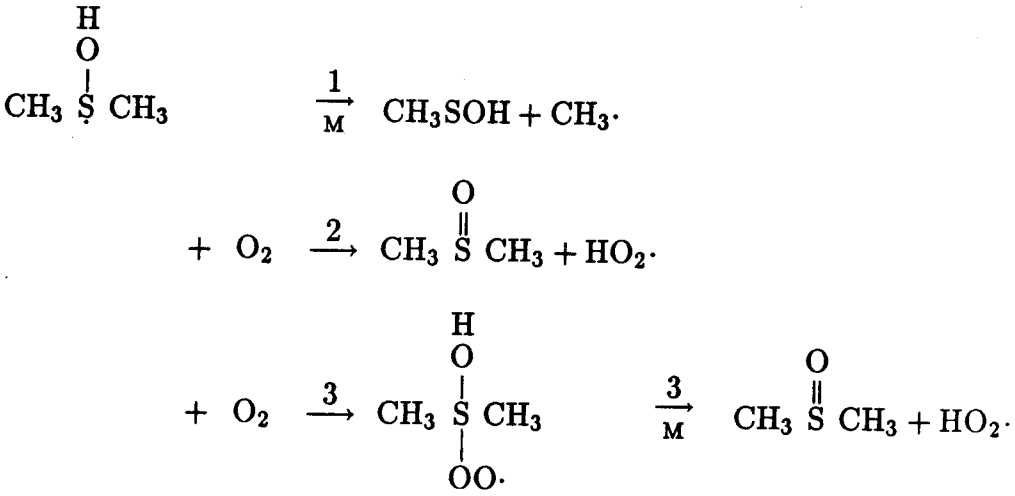

$$\xrightarrow[M]{4} \quad CH_3\overset{\overset{O}{\|}}{\underset{\underset{O}{\|}}{S}}CH_3 + OH$$

Note that reaction (1) is not related to "O_2 effect." Reaction (3) may proceed by addition to the S atom followed by H-atom abstraction via a five-member intramolecular ring. Although $CH_3S(O)_2CH_3$ has been observed [Barnes et al., 1988], it is not likely to form directly through reaction (4) since it is less likely to be a one-step reaction. The production of $CH_3S(O)_2CH_3$ in the CH_3SCH_3–H_2O_2–air system may result from the further oxidation of $CH_3S(O)CH_3$, which is supported by the fact that $k_{OH+CH_3S(O)CH_3} = 5.8 \pm 2.3 \times 10^{-11}$ cm^3 molecule^{-1} s^{-1} and by a preliminary product study of the $CH_3S(O)CH_3 + OH$ reaction in which $CH_3S(O)_2CH_3$ was found to be one of the major products [Barnes et al., 1986b].

No O_2 effect should be observed for the $CH_3S(OH)H$ adduct because of the formation of intramolecular H-bonding, which is consistent with the experimental observation by Hynes and Wine [1987]. The reason that no O_2 effect was observed for the $CH_3SS(OH)CH_3$ adduct may be that the *observed* rate constant for the $OH + CH_3SSCH_3$ reaction is already near the collision limit or may be that the adduct decomposition is fast enough that the reaction of adduct with O_2 cannot compete with it.

No data are available for the adducts formed in the reactions of RSR′ with radicals other than OH. An "O_2 effect" may also exist, depending mainly on the lifetime of the adduct.

2.4.2. NO_x Effect

Rate constants of initial reactions for organosulfur compounds have also been found to depend on the NO_x concentration. The observed increase of the rate

constant due to NO_x, observed only for OH+RSR′ reactions, is usually associated with conditions of high concentrations of NO_x, RSR′ and O_2, and with long reaction times [Cox and Sheppard, 1980; Atkinson et al., 1984a; Barnes et al., 1984; Nielsen et al., 1986; Barnes et al., 1986a; Wallington et al., 1986a]. More specifically, rate constants for the reactions of OH with CH_3SH, CH_3SCH_3 and $C_2H_5SC_2H_5$ were found to increase with increasing NO concentration [Barnes et al., 1986a; Nielsen et al., 1986]. Many secondary reactions may be responsible for this NO_x or NO effect. Of these, the reaction between CH_3SO_3 and RSR′ is probably the most important in view of the high reactivity of the CH_3SO_3 radical:

$$\begin{aligned} CH_3SO_3 + RSR' &\rightarrow CH_3SO_3H + RSR'' \\ &\rightarrow \text{Adduct} \end{aligned}$$

The detailed mechanism relating NO and CH_3SO_3 will be discussed in Section 7. The adduct $CH_3S(OH)(OO)CH_3$ formed from reaction (3) in section 2.4.1. may also react with NO. Other species that may contribute to the NO_x effect include $O(^3P)$, CH_3O_x, NO_3, Criegee radicals (when an alkene is used as reference reactant) and CH_3SO_x radicals. Although many of these species will mainly react with O_2 under atmospheric conditions, their reactions with RSR′ may become important at high concentrations of RSR′.

Considering the different OH sources used in the measurements, some special secondary reactions in addition to a NO_x effect may exist when using CH_3ONO + air+$h\nu$ as the OH source. Hatakeyama and Akimoto [1983] proposed the reaction

$$CH_3S(OH)H + CH_3ONO \rightarrow CH_3SNO + CH_3OH + OH$$

to explain their experimental observations. However, according to the principle

of microscopic reversibility, this reaction is unlikely to be an elementary reaction. Evidence suggests that the above reaction may be unimportant under their conditions. The heterogeneous reaction between CH_3ONO and CH_3SH [Niki et al., 1983a; Hatakeyama and Akimoto, 1983] may be enhanced under the irradition, which may contribute partially to the observed formation of CH_3SNO and CH_3OH. Also the confirmation of no reaction between O_2 and $CH_3S(OH)H$ [Hynes and Wine, 1987] suggested the lifetime of $CH_3S(OH)H$ may be very short due to the formation of intramolecular H-bonding since the similar adduct, $CH_3S(OH)CH_3$, reacted with O_2 very fast [Hynes et al., 1986].

Comparing the reactions between HO_2 and IO radicals with CH_3SCH_3,

$$\begin{array}{lll} & & \Delta H_{298}\ (\text{kcal/mole}) \\ CH_3SCH_3 + IO \rightarrow CH_3\overset{\overset{O}{\|}}{S}CH_3 + I & & -42.7 \\ + HOO \rightarrow CH_3\overset{\overset{O}{\|}}{S}CH_3 + OH & & -20.3 \end{array}$$

[Benson, 1978; Baulch et al., 1984] although the reaction of $HO_2 + CH_3SCH_3$ may be slower than the reaction of $IO + CH_3SCH_3$, in the absence of NO_x and in the presence of high concentration of HO_2, as in the case of studying the $OH + CH_3SCH_3$ reaction using H_2O_2 photolysis as the OH source [Barnes et al., 1988], the reaction $HO_2 + CH_3SCH_3$ may contribute partially to the high yield of $CH_3S(O_2)CH_3$ observed in their experiment.

2.4.3. RS Effect

The reaction between RS and RSR′ is another possible secondary reaction responsible for the observed rate constant enhancement. However, considering the

enthalpy changes of all the possible reactions of CH_3SH, CH_3SCH_3 and CH_3SSCH_3 with CH_3S [Benson, 1978; Baulch et al., 1984; Shum and Benson, 1983; Shum and Benson, 1985] (ΔH_{298}: kcal/mole),

					ΔH_{298}
CH_3SH	+ OH	→ $CH_3S(OH)H$	→	$CH_3S + H_2O$	−30.7
	+ CH_3S	→ $CH_3S(SCH_3)H$	→	$CH_3SSCH_3 + H$	+20.7
			→	$CH_3SSH + CH_3$	+8.6
CH_3SCH_3	+ OH		→	$CH_3SCH_2 + H_2O$	−22.6
	+ CH_3S		→	$CH_3SCH_2 + CH_3SH$	+8.1
	+ CH_3S	→ $CH_3S(SCH_3)CH_3$	→	$CH_3SSCH_3 + CH_3$	+6.9
CH_3SSCH_3	+ OH	→ $CH_3SS(OH)CH_3$	→	$CH_3SOH + CH_3S$	
	+ CH_3S		→	$CH_3SSCH_2 + CH_3SH$	
	+ CH_3S	→ $CH_3SS(SCH_3)CH_3$	→	$CH_3SSSCH_3 + CH_3$	

the reactions between RS and RSR′ are all endothermic (6.9–20.7 kcal/mole) except that of CH_3SSCH_3 with $CH_3S\cdot$ (whose enthalpy change cannot be estimated due to the lack of data on formation enthalpies for CH_3SOH, CH_3SSCH_2 and CH_3SSSCH_3). Compared to the large negative enthalpy change [(-22.6)–(-30.7) kcal/mole] for the OH+CH_3SH and OH+CH_3SCH_3 reactions, the reactions between $CH_3S\cdot$ and CH_3SH or CH_3SCH_3 are expected to be negligible under both laboratory and atmospheric conditions, especially considering the competition between $CH_3S\cdot$+RSR′ and OH+RSR′ and between CH_3S + RSR′ and CH_3S+NO_x. The effect of secondary reactions due to the $CH_3S\cdot$ radical has been found to be negligible for CH_3SCH_3 by Nielsen et al. [1986], who observed no additional loss of CH_3SCH_3 when photolyzing CH_3SSCH_3 in the presence of CH_3SCH_3 in either N_2 or air.

While the reaction between RS and RSR′ is negligible, the RS radical will have an effect on the observed rate constants when an alkene is used as a reference reactant. This is due to the addition of RS to the alkene double bond, a reaction well-documented in the liquid phase. An alkene has been used as reference reactant in both OH and NO_3 kinetic measurements by the relative rate method [Cox and Sheppard, 1980; Atkinson et al., 1984a; Barnes et al., 1984; Barnes et al., 1986a; MacLeod et al., 1986; Nielsen et al., 1986; Barnes et al., 1988; Atkinson et al., 1988] and in product studies [Hatakeyama and Akimoto, 1983]. The following mechanism is proposed to explain the possible effect of the RS radical in these studies (NO_3 radical and $CH_2{=}CH_2$ are used as examples).

NO_3	+	RSR'	→	Adduct	k_1
	+	$CH_2 = CH_2$	→	Product	k_2
CH_3S	+	$CH_2 = CH_2$	→	$CH_3SCH_2\dot{C}H_2$	k_3
	+	NO_2	→	$CH_3SO + NO$	k_4
	+	NO	→	CH_3SNO	k_5

Since studies involving the NO_3 radical are carried out in the dark, the photolysis of CH_3SNO is negligible. Usually the equation used to analyse the experimental data obtained by a relative rate technique is expressed as

$$\ln \frac{[RSR']_o}{[RSR']} = \frac{k_1'}{k_2} \ln \frac{[C_2H_4]_o}{[C_2H_4]} \qquad (a)$$

where k_1' is the observed rate constant without considering reaction (3). If reaction (3) is included,

$$\ln \frac{[RSR']_o}{[RSR']} = \frac{k_1}{k_2} (\ln \frac{[C_2H_4]_o}{[C_2H_4]} - C) \qquad (b)$$

where k_1 is the rate constant when reaction (3) is considered, and

$$C = \int_{[RSR']}^{[RSR']_o} \frac{d[RSR']}{k_3[C_2H_4] + k_4[NO_2] + k_5[NO]} > 0$$

Dividing equation (a) by equation (b),

$$\frac{k_1'}{k_1} = \frac{\ln[C_2H_4]_o/[C_2H_4] - C}{\ln[C_2H_4]_o/[C_2H_4]} < 1$$

i.e., the observed rate constant k_1' is smaller than the actual rate constant k_1 if reaction (3) is important compared to reaction (2). The following conditions need to be satisfied in order for reaction (3) to be important:

1). CH_3S (or RS) radical has to be generated. For the reactions between OH and RSR', the CH_3S radical is generated from CH_3SH, CH_3SCH_3 and CH_3SSCH_3. For reactions of NO_3 with RSR', CH_3S may be generated only from CH_3SSCH_3.

2). k_2/k_3 is close to one, or smaller than one. Since $k_{OH+RSR'}$ is much larger than $k_{NO_3+RSR'}$, the effect of the CH_3S radical on observed rate constants will be much larger for the NO_3 + RSR' reactions than for the OH + RSR' reactions.

3). [Alkene]/[NO_x] is close to one, or larger than one, which is usually the case at the beginning of the experiment.

Based on the above considerations, the $NO_3 + CH_3SSCH_3$ reaction is the most likely candidate to exhibit a CH_3S effect, in agreement with the observation of

MacLeod et al. [1986] and Atkinson et al. [1988]. MacLeod et al. [1986] measured the rate constants of the $CH_3SH + NO_3$ and $CH_3SSCH_3 + NO_3$ reactions, and obtained a much smaller $k_{NO_3+CH_3SSCH_3}$ than those measured by an absolute method [Wallington et al., 1986c; Dlugokencky and Howard, 1988], however the rate constant of $k_{NO_3+CH_3SH}$ agrees reasonably well with other measurements [Wallington et al., 1986c; Rahman et al., 1988; Dlugokencky and Howard, 1988]. Another study showed that the observed rate constant for the $NO_3 + CH_3SSCH_3$ reaction increased in the later stages of the reaction [Atkinson et al., 1988], indicating that the competitive reaction of CH_3S + alkene, i.e., reaction (3), was important in the early stage of the experiment. The alkenes used in these experimental studies were propene and trans–2–butene. The rate constants listed below for the CH_3S + alkene reactions are compared to those for the NO_3 + alkene reactions. [MacLeod et al., 1986; Graham et al., 1964a; Atkinson, 1985; Balla et al., 1987]:

				k_{298} (cm^3 $molecule^{-1}$ s^{-1})
$CH_3CH{=}CH_2$	+ NO_3	→	Product	7.6×10^{-15}
	+ OH	→	Product	2.63×10^{-11}
	+ CH_3S	→	Adduct	$1.0 \pm 0.4 \times 10^{-14}$
trans-2-butene	+ NO_3	→	Product	3.8×10^{-13}
	+ OH	→	Product	6.37×10^{-11}
2-butene	+ CH_3S	→	$CH_3CH(CH_3S)CHCH_3$	3.32×10^{-14}
cis-2-butene	+ CH_3S	→	Adduct	$< 5.5 \times 10^{-15}$

Therefore the effect of the CH_3S radical on the measured $CH_3SSCH_3 + NO_3$ rate constant cannot be neglected. The competition between reactions of OH and CH_3S with alkenes is dominated by the OH radical since the OH rate constants are much

larger than those for CH_3S. Finally, the addition of the CH_3SO_2 radical to alkene double bonds, similar to the addition of the CH_3S radical, may also have similar effects on the observed rate constants.

Also it should be pointed that when using alkene as the reference reactant, the adduct formed from the reactions between alkene and radicals including OH, NO_3 and RS may have O_2 effect or some other secondary reactions. The Criegee radical may also involved if O_3 existed in the system. Therefore it seems clear that secondary reactions are more likely to be involved when an alkene is used as a reference reactant for kinetic study of organosulfur compounds.

3. Structure of RSO_x and $RS(O)_xOO$ Radicals

The sulfinyl radical, RSO, sulfonyl radical, RSO_2, sulfur peroxyl radicals, $RS(O)_x$–OO, and possibily several other oxygen-containing sulfur radicals are involved as intermediates in the photooxidation of organosulfur compounds. In order to better understand the reactions of these species, it is necessary to discuss the structures of the following radicals and to estimate their reactivity from the corresponding structural properties:

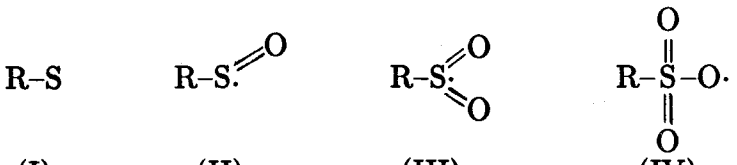

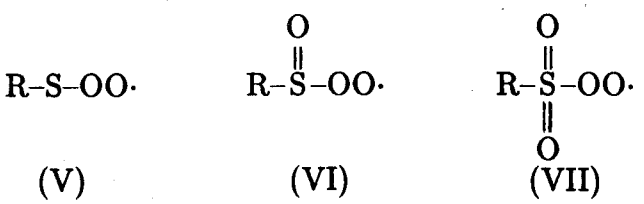

Sulfinyl radicals, RSO (II), are formal analogues of peroxyl (ROO) and perthiyl

(RSS) radicals. The π nature of the RSO radical results in enhanced stability relative to that of either the thiyl RS (I) or sulfonyl RSO_2 (III) radicals. This is reflected in the corresponding bond dissociation energies, i.e., BDE($CH_3S(O)$–CH_3) = 55 ± 2 kcal/mole is about 13–20 kcal/mole lower than BDE(CH_3S–CH_3) = 75.0 ± 1 kcal/mole and BDE($CH_3S(O)_2$–CH_3) = 68 kcal/mole [Benson, 1978; Shum and Benson, 1983].

Considering the sulfur peroxyl radicals, some confusion has been caused by the radical representation. Methanethiyl peroxyl radical, the adduct of methanethiyl radical (CH_3S) to molecular oxygen, should be represented as CH_3SOO rather than CH_3SO_2, which is the methanesulfonyl radical (III). Evidence for the thiol peroxyl radical (RSOO) has been recently observed by electron spin resonance in the liquid phase [Swarts et al., 1989]. Likewise, the adducts of O_2 to CH_3SO and CH_3SO_2 should be represented as $CH_3S(O)OO$ and $CH_3S(O)_2OO$, respectively. This distinction between sulfur and sulfur peroxy radicals is very important since these radicals have quite different chemical properties. The enthalpy change for the reaction $CH_3S + O_2$, which was incorrectly based on the formation enthalpy of the CH_3SO_2 radical [Hatakeyama and Akimoto, 1983], is about −89 kcal/mole. However, the *correct* enthalpy change for this reaction is in fact much less than −89 kcal/mole since CH_3SOO is much less stable than CH_3SO_2. This downward revision is entirely consistent with experimental observations of a very slow reaction between CH_3S and O_2 [Balla et al., 1986; Tyndall and Ravishankara, 1988].

4. Reactions of CH_3SOH and $CH_3S(O)_xCH_3$

Although CH_3SOH, $CH_3S(O)CH_3$ and $CH_3S(O)_2CH_3$ are proposed to be the addition pathway products of the OH+RSR′ reaction, only $CH_3S(O)_2CH_3$ has been observed experimentally [Barnes et al., 1988]. $CH_3S(O)CH_3$ and $CH_3S(O)_2CH_3$

have been detected in marine air and rain water [Harvey and Lang, 1986], suggesting that both are possible oxidation products of CH_3SCH_3. Only one kinetic study has been carried out for the reaction of $OH+CH_3S(O)CH_3$ [Barnes et al., 1986b] and no kinetic data are available for CH_3SOH and $CH_3S(O)_2CH_3$. Therefore the following discussion is based mainly on thermochemistry and on comparison of reactivity in the gas phase and liquid phase.

4.1. Reactions of CH_3SOH

Methanesulfenic acid, CH_3SOH, has not been directly detected but is believed to form by unimolecular decomposition of the adducts of $CH_3S(OH)CH_3$ and $CH_3SS(OH)CH_3$. It was proposed first by Hatakeyama and Akimoto [1983] that CH_3SOH reacts with O_2 to form CH_3SO_3H:

$$CH_3SOH + O_2 \xrightarrow{M} CH_3SO_3H$$

However, this one-step reaction is not consistent with the structual difference between CH_3SOH and CH_3SO_3H:

The structure of CH_3SOH has been confirmed by microwave spectroscopy to have form (A) rather than form (B) [Penn et al., 1978],

(A) (B)

By further examining the possibility of the reactions between CH_3SOH and O_2, it is concluded that O_2 cannot abstract a hydrogen from CH_3SOH to produce two radicals from two molecules since the H–OO bond is about 10* kcal/mole weaker than the CH_3SO–H bond (see discussion later). Also the addition of O_2 to the S atom on CH_3SOH will not be important since the similar reactions between O_2 and CH_3SCH_3 should be faster because of the electrophilic nature of O_2. However, due to the extremely large O_2/radicals concentration ratio in the atmosphere, the reaction between O_2 and CH_3SOH cannot be ruled out completely although it is clear that CH_3SO_3H cannot be formed directly from $CH_3SOH + O_2$.

Although the importance of sulfenic acid (RSOH) intermediate in mechanistic organic sulfur chemistry is well recognized, simple alkanesulfenic acids are extremely reactive and unstable and only a few of them have been isolated and detected [Davis et al.,1981]. Sulfenic acids readily undergo hydrogen atom transfer to free radicals and they have been found to be active radical scavengers for peroxy radicals [Koelewijn and Berger, 1972], indicating that the bond dissociation energy of the RSO–H bond is less than that of the ROO–H bond, about 87 kcal/mole. The efficiency of sulfenic acids as hydrogen atom donors is undoubtedly a consequence of the appreciable stability of the sulfinyl radical, RSO, due to its delocalized π-structure.

In the liquid phase, both sulfenic acids and sulfinic acids undergo facile H-atom abstraction by either alkoxy or OH radicals [Gilbert et al., 1975b; Block, 1978; Lunazzi and Pedulli, 1985]. Based on these experimental studies in the liquid phase,

---

* Since the BDE(CH_3SO–H) is estimated from the BDE(HOSO–H), the absolute value is less accurate than the relative trend. The importance of the $O_2 + CH_3SOH$ reaction will be determined by the relative strength of CH_3SO–H and OO-H bonds, which is unknown at this time.

we propose that H-atom abstraction is also a dominant atmospheric reaction pathway for both CH_3SOH and CH_3SO_2H (a possible product of the $CH_3S(O)CH_3$+OH reaction). Thus, possible H-atom abstraction reactions for CH_3SOH and the bond dissociation energies of the corresponding formed H–X bonds are listed below:

				BDE (kcal/mole)
CH_3SOH	+ OH	→	$CH_3SO + H_2O$	119
	+ CH_3SO_3	→	$CH_3SO + CH_3SO_3H$	(104)
	+ CH_3O	→	$CH_3SO + CH_3OH$	104.4
	+ $O(^3P)$	→	$CH_3SO + OH$	102.2
	+ NO_3	→	$CH_3SO + HONO_2$	101.2
	+ CH_3O_2	→	$CH_3SO + CH_3OOH$	87.2
	+ HO_2	→	$CH_3SO + H_2O_2$	87.2
	+ NO_2	→	$CH_3SO + HONO$	78.3

[Benson, 1978; McMillen and Golden, 1982; Baulch et al., 1984; Kerr, 1985]. Of the reactions listed above, those with OH and CH_3SO_3 radicals, and with peroxy radicals at low NO_x concentration are important. These reactions may in fact be quite fast since the bond dissociation energy of CH_3SO–H is expected to be much less than 87 kcal/mole.

Although no data are available for the BDE of O–H bond in $CH_3S(O)_xO$–H compounds, some estimates can be obtained from the structurally similar species $HOS(O)_xO$–H [Benson, 1978] (BDE: kcal/mole):

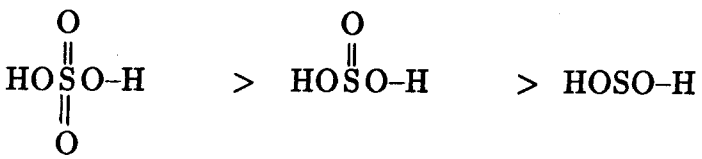

104 ± 3 81 59

Therefore, a similar bond strength trend can be expected for $CH_3S(O)_xO$–H acids, i.e.,

$$CH_3\overset{\overset{O}{\|}}{\underset{\underset{O}{\|}}{S}}O\text{–}H \;>\; CH_3\overset{\overset{O}{\|}}{S}O\text{–}H \;>\; CH_3SO\text{–}H$$

and the effect of CH_3 and OH groups on the bond dissociation energy is expected to be small compared to that of the group $S(O)_x$ since the bond dissociation energy of $HOS(O)_x$–H species varies about 44 kcal/mole from HOSO–H to $HOS(O)_2O$–H although an OH group is attached to each of $HOS(O)_x$–H. As a starting point, the bond dissociation energy of $CH_3S(O)_x$–H can be assumed to be the same as that for the corresponding acids of $HOS(O)_x$–H. This would assign 59 kcal/mole to the CH_3SO–H bond, a value consistent with our earlier estimate, i.e., much less than 87 kcal/mole. Since the bond dissociation energy of $CH_3S(O)O$–H is higher than that of CH_3SO–H, the H-atom abstraction from $CH_3S(O)OH$ is expected to be correspondingly slower. However, the O–H bond in $CH_3S(O)_2OH$ is much stronger than those in $CH_3S(O)OH$ and CH_3SOH; thus these compounds are expected to react rapidly with CH_3SO_3 by H-atom abstraction.

It should be pointed out that the electrophilic addition of radicals such as OH and NO_3 to the S atom in CH_3SOH, although it is minor, may not be negligible since the adduct of OH + CH_3SOH is stabilized by the resonance effect of OH in CH_3SOH, although the weak electron-withdrawing resulting from OH inductive effect could decrease the tendency of OH addition to CH_3SOH.

4.2. Reaction of $CH_3S(O)_xCH_3$

While $CH_3S(O)CH_3$ was not observed as a product by Barnes et al. [1988], they suggested that $CH_3S(O)CH_3$ was likely to be produced and further oxidized

rapidly to $CH_3S(O)_2CH_3$ and SO_2. The rate constant for $OH + CH_3S(O)CH_3$ has been measured to be $(5.8 \pm 2.3) \times 10^{-11}$ cm^3 $molecule^{-1}$ s^{-1} and $(6.2 \pm 2.2) \times 10^{-11}$ cm^3 $molecule^{-1}$ s^{-1} [Barnes et al., 1986b; Barnes et al., 1989], with SO_2 and $CH_3S(O)_2CH_3$ yields of 60% and 30%, respectively [Barnes et al., 1988]. The formation of SO_2 indicates that the addition pathway is not necessarily related only to the formation of CH_3SO_3H, and could also leads to the production of SO_2 as well. The same reaction has been studied by Meissner at al. [1967] in aqueous solutions of sulfoxides and a similar reaction rate constant of 1.2×10^{-11} cm^3 $molecule^{-1}$ s^{-1} has been reported [Gilbert et al., 1975a].

While $CH_3S(O)CH_3$ and $CH_3S(O)_2CH_3$ may react with a number of radicals in the atmosphere, their reaction with OH is likely to be the most important chemical loss process, and their reactions with NO_3 could also be important at nighttime in the atmosphere. The reaction of $CH_3S(O)CH_3$ with OH may involve abstraction or addition as follows:

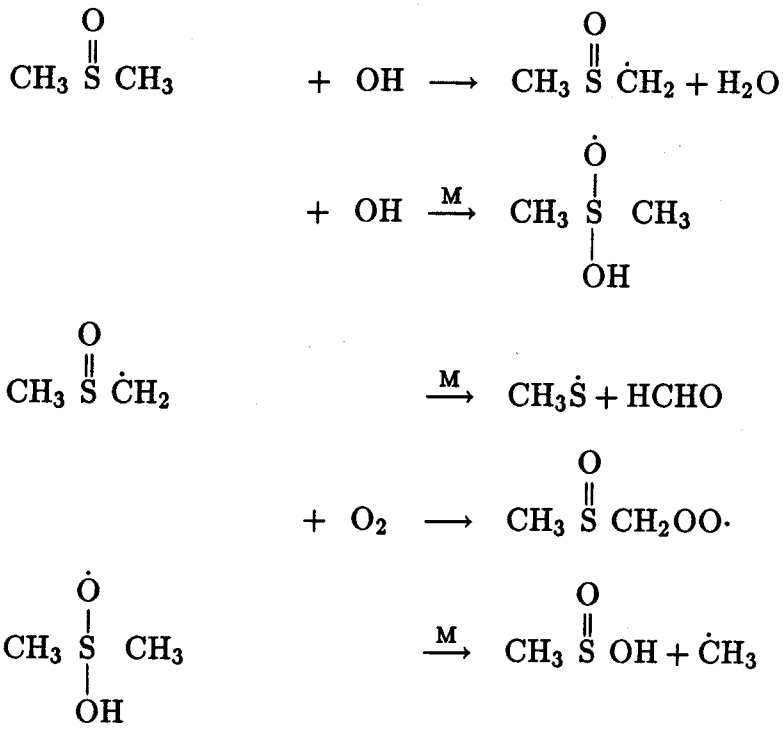

$$+ \ O_2 \longrightarrow CH_3\overset{\overset{O}{\|}}{\underset{\underset{O}{\|}}{S}}CH_3 + HO_2$$

In turn, methanesulfinic acid, $CH_3S(O)OH$, may be further oxidized to SO_2 or CH_3SO_3H. Although no information is available regarding the relative importance of addition and abstraction pathways for the $OH + CH_3S(O)CH_3$ reaction, some indication can be obtained from studies in the liquid phase. In a photolysis study of $CD_3S(O)CD_3$ in various nondeuterated solvents, Gollnick and Schade [1973] observed the formation of CD_3H to the virtual exclusion of CD_4 by the following reactions,

$$CD_3\overset{\overset{O}{\|}}{S}CD_3 + h\nu \rightarrow CD_3SO + CD_3$$

$$CD_3 + RH \rightarrow CD_3H + R$$

$$CD_3 + CD_3\overset{\overset{O}{\|}}{S}CD_3 \rightarrow CD_4 + CD_3\overset{\overset{O}{\|}}{S}CD_2$$

which suggested that hydrogen abstraction from dimethyl sulfoxide is energetically unfavorable. For H-atom abstraction by the phenyl radical, the relative reactivity per H-atom is [Block, 1978]:

$$\underset{1.89}{CH_3SCH_2\text{–}H} > \underset{1.2}{CH_3SSCH_2\text{–}H} > \underset{0.08}{CH_3S(O)CH_2 - H}$$

This indicates that the bond dissociation energy of $CH_3S(O)CH_2$–H is much higher than that of CH_3SCH_2–H of 96.6 ± 1.0 kcal/mole [Shum and Benson, 1985], but lower than that of Ph–H of 110.9 ± 2 kcal/mole [McMillen and Golden, 1982]. This is also true for $CH_3S(O)_2CH_3$ since the reaction

$$CH_3S(O)_2CH_3 + C_6H_5 \rightarrow CH_3S(O)_2CH_2 + C_6H_6$$

takes place readily in the liquid phase. Thus, H-atom abstraction by OH is expected to be much slower for $CH_3S(O)CH_3$ and $CH_3S(O)_2CH_3$ than for CH_3SCH_3. Since the observed rate constant of $CH_3S(O)CH_3$ with OH is about a factor of 10 higher than that of CH_3SCH_3+OH, addition is therefore expected to be the major pathway for $CH_3S(O)CH_3$ + OH.

Studies by Norman and Pritchett [1965] and Lagercrantz and Forshult [1969] indicate that the reaction of OH with dialkyl sulfoxides involves addition onto the sulfur atom rather than H-atom abstraction. Gilbert et al. [1975a] studied the reaction of OH with $CH_3S(O)CH_3$ in aqueous solution at ambient temperature and found that the addition of OH to $CH_3S(O)CH_3$, followed by rapid decomposition of the adduct $CH_3S(O\cdot)(OH)CH_3$ is the dominant pathway. The adduct, $CH_3S(O\cdot)(OH)CH_3$, once formed, may either react with O_2 to produce $CH_3S(O)_2CH_3$ or undergo unimolecular decomposition to $CH_3S(O)OH$:

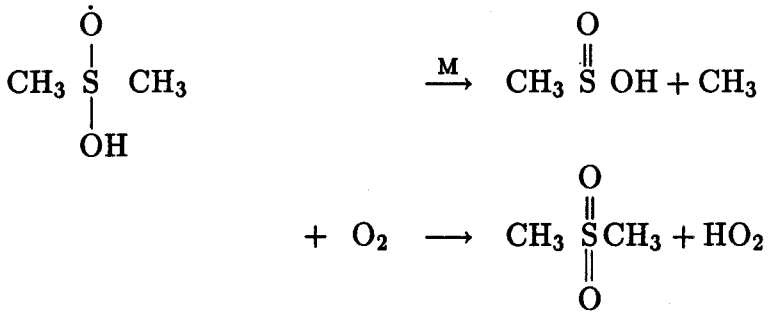

The above decomposition may be faster than that of the adduct $CH_3S(OH)CH_3$ since BDE($\dot{C}H_3S(O)$–CH_3) = 55 ± 2 is much smaller than BDE(CH_3S–CH_3) = 75.0 ± 1 [Benson, 1978; Shum and Benson, 1983]. This may be one of the reasons that $k_{CH_3S(O)CH_3+OH}$ is about a factor of 10 higher than $k_{CH_3SCH_3+OH}$. The rate constant of decomposition of the adduct, $CH_3S(\dot{O})(OH)CH_3$, is 1.5×10^7 s^{-1} [Veltwisch et al., 1980] in aqueous solution. Thus, if the aqueous phase rate con-

stant is used as a guide for estimating gas phase reactivity, the rate constant for $O_2 + CH_3S(\dot{O})(OH)CH_3$ would need to be about 3×10^{-12} cm^3 $molecule^{-1}$ s^{-1} to be competitive with the unimolecular decomposition of adduct $CH_3S(\dot{O})(OH)CH_3$ to form $CH_3S(O)_2CH_3$ in the atmosphere.

The hypothesis of addition being the dominant pathway for $OH + CH_3S(O)CH_3$ reaction is consistent with the fact that $CH_3S(O)_2CH_3$ was observed as one of the major product only when O_2 was present for CH_3SCH_3 + OH reaction [Barnes et al., 1988]. The independence of the rate constant for the reaction of $CH_3S(OH)CH_3$ with OH on O_2 concentration, observed by Barnes et al. [1986b], indicates that the reverse reaction of the adduct $CH_3S(O)(OH)CH_3$ is much slower than its decomposition to $CH_3S(O)OH + CH_3$. Notice that the observation of SO_2 as the major product for the $CH_3S(O)CH_3$ + OH reaction does not necessarily support the abstraction pathway since addition can also lead to SO_2 formation. The high yield of $CH_3S(O)_2CH_3$ observed by Barnes et al. [1988] indicates that $CH_3S(O)_2CH_3$ is relatively unreactive toward OH. This is not unexpected, since (a) the S atom in $CH_3S(O)_2CH_3$ is hexavalent and no further addition of OH to S is possible, and (b) H-atom abstraction is expected to be slow as a result of the polar effects of the $CH_3S(O)_2$ group.

The rate constant for $NO_3 + CH_3S(O)CH_3$ has been measured to be $(1.7 \pm 0.3) \times 10^{-13}$ cm^3 $molecule^{-1}$ s^{-1} [Barnes et al., 1989], and $CH_3S(O)_2CH_3$ and $HONO_2$ were observed from a preliminary product study on system $CH_3S(O)CH_3$–N_2O_5–air in the dark. Elucidation of the $CH_3S(O)CH_3 + NO_3$ reaction is not possible at present, and further experimental studies are needed.

The above discussion indicates that CH_3SOH does not necessarily lead to the formation of CH_3SO_3H, and that both SO_2 and CH_3SO_3H can be produced by further oxidation of CH_3SOH and $CH_3S(O)_xCH_3$. Thus, there is no direct relation

between the yields of SO_2 and CH_3SO_3H and the relative importance of OH addition and abstraction pathways.

5. Reactions of RSO_x Radicals

CH_3SO_x and $CH_3S(O)_xOO$ radicals have not been detected in product studies. Only indirect evidence suggests their existence. That of CH_3S is suggested by the observation of CH_3SNO [Niki et al., 1983b; Hatakeyama and Akimoto, 1983; MacLeod et al., 1986; Barnes et al., 1987b]. The tentative identification of $CH_3S(O)OO–NO_2$ by Barnes et al. [1987b] suggests that CH_3SO and $CH_3S(O)OO$ radicals are involved as well. The recent study of the $CH_3S + NO_2$ reaction by Tyndall and Ravishankara [1988] suggests the formation of both CH_3SO and CH_3SO_2 radicals. In the present sections, possible reactions of CH_3SO_x radicals are discussed, with focus on their further oxidation and unimolecular decomposition.

5.1. Reactions of RSO_x Radicals with O_2

The addition of molecular oxygen to CH_3S is arguably the most important reaction for CH_3S in the atmosphere. It is also the least characterized reaction of the CH_3S radical. Balla and Heicklen [1985] studied the photolysis of CH_3SSCH_3 in the presence of O_2 and proposed the following mechanism to explain the formation of SO_2,

$$\begin{aligned} CH_3S + O_2 &\rightarrow CH_3SOO \\ CH_3SOO + O_2 &\rightarrow CH_3SO_4 \\ CH_3SO_4 &\rightarrow HO + HCHO + SO_2 \end{aligned}$$

with the structure of the CH_3SO_4 radical given as

$$CH_3 - S\begin{matrix}O - O\cdot \\ O - O\cdot\end{matrix}$$

This structure is not correct, i.e., there should be another single unpaired electron (plus a pair of lone electrons) on the S atom. The CH_3SO_4 radical structure proposed by Balla and Heicklen would therefore include three single unpaired electrons, which is very unlikely. The structurally correct adduct of O_2 to CH_3SOO should be CH_3SOO–OO, which is very unstable and thermodynamically unfavorable. Furthermore, Tyndall and Ravishankara [1988] did not detect OH as a product in the reaction of CH_3S with O_2, thus suggesting that SO_2 is not produced from the CH_3SO_4 radical.

The rate constant of the $CH_3S + O_2$ reaction has been measured, and only upper limits have been determined. These range from 2×10^{-17} to 2.5×10^{-18} cm^3 $molecule^{-1}$ s^{-1}. [Balla et al., 1986; Tyndall and Ravishankara, 1988]. Considering $k_{CH_3+O_2} = 1.0 \times 10^{-12}$ cm^3 $molecule^{-1}$ s^{-1}, and the strong electrophilic character of O_2, the reaction of CH_3S with O_2 seems unexpectedly slow. Before we attempt to explain this result, let us consider in more detail the bonding between S and O atoms in CH_3SOO. The isoelectronics of CH_3SOO are CH_3OOO and CH_3SSS, with estimated BDE of -22 to -11.8 kcal/mole for the CH_3O–OO bond and $+41$ kcal/mole for the CH_3S–SS bond [Benson and Shaw, 1970; Francisco and Williams, 1988; Benson, 1978]. It can be seen that the adduct CH_3OOO is unstable and decomposes rapidly to CH_3O and O_2, which may be consistent with observation of the fast reaction between CH_3 and O_3 [Paltenghi et al., 1984] since this reaction may also involve the adduct CH_3OOO. The relatively strong bond of CH_3S–SS may reflect more resonance structures. Therefore the S–O bond in CH_3SOO is expected to be weak and the lifetime of the $CH_3S + O_2$ adduct will correspondingly be short. Based on these considerations, we suggest the following mechanism for the reaction

between CH_3S and O_2:

$$
\begin{aligned}
CH_3S + O_2 &\longrightarrow CH_3SOO \\
CH_3SOO &\xrightarrow{M} CH_3S + O_2 \\
&\xrightarrow{M} CH_3SO_2 \\
+ CH_3S &\longrightarrow CH_3SO + CH_3SO \\
+ NO &\longrightarrow CH_3SO + NO_2
\end{aligned}
$$

Further reactions of CH_3SO produce SO_2 and CH_3SO_3H. In the above scheme, the addition of O_2 to CH_3S is fast (with a rate constant about one order of magnitude smaller than that for the $CH_3 + O_2$ reaction), but the unstable adduct CH_3SOO, either rapidly decomposes back to CH_3S and O_2 or oxidizes reduced species in the system including CH_3S (or NO when NO_x is used). The rearrangement from CH_3SOO to CH_3SO_2 is slower than all other reactions.

The above mechanism is speculative, but is consistent with many experimental observations. For example, the apparent slow reaction observed by Balla et al. [1986] and Tyndall and Ravishankara [1988] is consistent with fast decomposition of the adduct back to the reactants. The observed decay of CH_3S is the net effect of adduct decomposition and adduct reactions with other species. Our mechanism also predicts that the observed reaction rate should *increase* with *increasing* concentrations of species consuming the adduct and/or with any factor that stabilize the adduct, i.e., that decreases its rate of reverse decomposition. Balla and Heicklen [1985] reported increasing SO_2 yields with increasing light intensity, which is inconsistent with their mechanism. The observed SO_2 yield increase may be simply due to the increased steady state concentration of CH_3S. Black et al. [1988b] studied the reaction between C_2H_5S and O_2 by laser induced fluorescence and estimated an upper limit of 2×10^{-17} cm^3 $molecule^{-1}$ s^{-1} for the rate constant. In contrast,

the liquid phase rate constant for this reaction is 5.6×10^{-13} cm^3 $molecule^{-1}$ sec^{-1} [Schäfer et al., 1978], which is comparable to the rate constant for addition of O_2 to C_2H_5, 1.0×10^{-12} cm^3 $molecule^{-1}$ s^{-1} [Atkinson and Lloyd, 1984b]. The observed high rate constant in solution may reflect solvent stabilization of the adduct and/or rapid removal by other species, in this case, possibly by C_2H_5SH as follows,

$$C_2H_5SOO + C_2H_5SH \rightarrow C_2H_5SOOH + C_2H_5S$$

The large rate constants for the i-C_3H_7S+O_2 reaction (1.1×10^{-14} cm^3 $molecule^{-1}$ s^{-1}, [Black et al., 1988a]) and the C_6H_5S+O_2 reaction (2.52×10^{-12} cm^3 $molecule^{-1}$ s^{-1}, [Shibuya et al., 1988]) are also consistent with stabilization of the RSOO adduct by the substituted groups, although abstraction may also be involved in the i-C_3H_7S+O_2 reaction.

The attachment of electron-withdrawing groups to the adduct S atom stabilizes the adduct and increases its lifetime. The tentative identification of $CH_3S(O)OO$–NO_2 in the CH_3SSCH_3–NO_2–air system [Barnes et al., 1987b] suggests a reasonably long lifetime for the $CH_3S(O)OO$ radical. Interestingly, the same set of IR peaks assigned to $CH_3S(O)OONO_2$ by Barnes et al. [1987b] was also detected by MacLeod et al. [1986] in mixtures of both CH_3SSCH_3–N_2O_5–NO_2–air and CH_3SH–N_2O_5–NO_2–air, indicating $CH_3S(O)OO$–NO_2 may also be involved. The adduct $CH_3S(O)_2OO$ should be even more stable, and the *apparent* addition of O_2 to CH_3SO_3 should be faster. A bond strength of about 16 kcal/mole can be estimated for the $CH_3S(O)_2$–OO bond by comparison with the similar bond in $HOS(O)_2$–OO (BDE($HOS(O)_2$–OO = 16 kcal/mole [Benson, 1978]), which is stronger than the S–O bond in CH_3SOO radical. The reaction mechanisms for CH_3SO and CH_3SO_2 radicals with O_2 are similar to the mechanism for CH_3S with

O_2 as discussed above.

CH_3SOO may also rearrange to form the CH_3SO_2 radical. However, this rearrangement is expected to be unimportant. No decay of CH_3S was observed by Tyndall and Ravishankara [1988] in the CH_3SSCH_3–O_2 system on the time scale of milliseconds. This intramolecular rearrangement, proceeding by a three-member ring, should be hindered by ring strain and by the large lone-pair repulsion involving six lone-pairs of electrons in the CH_3SOO radical. Another point that argues against such intramolecular conversion is that similar rearrangement from $CH_3S(O)OO$ to $CH_3S(O)_2O$ is expected to be faster due to the effect of electron-withdrawing by attached oxygen on sulfur in $CH_3S(O)OO$ radical, and CH_3SO_3H is predicted to be the major product from reactions $CH_3SO_x + O_2$, which is contrary to the experimental results [Hatakeyama and Akimoto, 1983; Yin et al., 1989].

The analogous reaction of $HOS(O)_2$ with O_2, which is confirmed by several experiments to be

$$HOSO_2 + O_2 \rightarrow SO_3 + HO_2$$

[Margitan, 1984; Martin et al., 1986; Gleason et al., 1987] despite the unfavorable enthalpy change, may proceed as addition followed by unimolecular decomposition. The adduct formed may rapidly decompose through the formation of intromolecular H-bonding by a five-member ring before the vibrationally exicted $HOS(O)_2OO$ collisionally stabilized since the intramolecular rearrangement is much faster than the intermolecular reaction. And also the entropy change from adduct to the transient state will be less than zero. This may help to explain the discrepancy between the thermochemical prediction and the kinetic observation for this reaction.

5.2. Reaction of RSO_x radicals

CH_3SO_x radicals can be readily oxidized in the atmosphere,

$$CH_3S + O\text{–}Y \rightarrow [CH_3SO\text{–}Y]^* \rightarrow CH_3SO + Y$$
$$CH_3SO + O\text{–}Y \rightarrow [CH_3S(O)O\text{–}Y]^* \rightarrow CH_3SO_2 + Y$$
$$CH_3SO_2 + O\text{–}Y \rightarrow [CH_3S(O)_2O\text{–}Y]^* \rightarrow CH_3SO_3 + Y$$

and undergo direct or intramolecular (via six-member ring) H-atom abstraction

$$CH_3S + O\text{–}Y \rightarrow [CH_3SO\text{–}Y]^* \rightarrow CH_2S + H\text{–}OY$$
$$CH_3SO + O\text{–}Y \rightarrow [CH_3SOO\text{–}Y]^* \rightarrow CH_2SO + H\text{–}OY$$
$$CH_3SO_2 + O\text{–}Y \rightarrow [CH_3S(O)_2O\text{–}Y]^* \rightarrow CH_2SO_2 + H\text{–}OY$$

(H–OY will be HO + Y for O_3) or regenerate CH_3S and CH_3SO (Notice that the resonance structures of $CH_3\dot{S}O$ and $CH_3\dot{S}O_2$ are $CH_3S\dot{O}$ and $CH_3S(O)\dot{O}$):

$$CH_3S\dot{O} + O\text{–}Y \rightarrow [CH_3SOO\text{–}Y]^* \rightarrow CH_3S + O_2 + Y$$
$$CH_3S(O)\dot{O} + O\text{–}Y \rightarrow [CH_3S(O)OO\text{–}Y]^* \rightarrow CH_3SO + O_2 + Y$$

where Y includes NO for ONO, NO_2 for ONO_2, OH for HOO, CH_3O for CH_3OO, O_2 for O_3, and $CH_3S(O)_xO$ for $CH_3S(O)_xOO$, respectively. The relative importance of these oxidative species will depend on their ambient concentrations.

Several experimental studies have recently become available regarding the reactions of CH_3SO_x radicals. Tyndall and Ravishankara [1988] identified NO as the major product of the $CH_3S + NO_2$ reaction, with a yield of 0.80 ± 0.20. They also observed a secondary production of NO and suggested that the CH_3SO radical formed could be oxidized further to CH_3SO_2 by NO_2. The CH_3SO radical was indeed detected in another study of the $CH_3S + NO_2$ reaction by mass spectrometry [Mellouki et al., 1988]. Regarding the reactions of CH_3S with O_3, Domine et al.

[1989] have identified CH_3SO as one of the products with a yield of (0.156 ± 0.04). Also CH_2SO and OH were detected in the CH_3S/O_3 system, possibly via H-atom abstraction as shown above. Their preliminary data also indicated that CH_3SO reacts with O_3 to regenerate CH_3S with a yield of about 0.22. Furthermore, both our experimental observations and computer simulation for CH_3SSCH_3 photooxidation (see datailed discussion in Part II) indicate that the reactions of CH_3SO_x with O_3 are very important, and the rate constant of $CH_3S + O_3$, 6×10^{-12} cm^{-3} $molecule^{-1}$ s^{-1} estimated entirely from the simulation of our experimental data, agrees reasonably well with the first reported rate constant, $(4.1 \pm 2.0) \times 10^{-12}$ cm^{-3} $molecule^{-1}$ s^{-1} [Tyndall and Ravishankara, 1989] and better with the more recently reported value, $(5.7 \pm 1.5) \times 10^{-12}$ cm^{-3} $molecule^{-1}$ s^{-1} [Domine et al., 1989].

With the exception of limited data for the $RSO_x + NO_2$ and $RSO_x + O_3$ reactions, kinetic data are not available for RSO_x reactions. In order to estimate the reactivity of CH_3S, CH_3SO and CH_3SO_2 radicals towards oxidants, let us compare the reaction enthalpies between the analogous reactions. Table 3 lists enthalpy changes for all oxidation reactions except those for $CH_3S(O)_xOO$ radicals, which will be discussed later. Examination of the data in Table 3 reveals two important features. First, for a given oxidant species the reaction enthalpy decreases from CH_3S to CH_3SO_2 radicals, indicating that the tendency of CH_3SO_x radicals toward oxidation is in the order

$$CH_3S > CH_3SO > CH_3SO_2$$

Second, for a given sulfur radical all oxidation reactions are considerably exothermic with similar enthalpy changes, thus suggesting that all these reactions are expected to proceed rapidly in the atmosphere. For comparison, Table 4 presents the rate constants as well as the reaction enthalpies for CH_3SO_x oxidation by NO_2 and O_3 and

for HSO_x reactions. For both CH_3SO_x and HSO_x radicals, the observed trend in kinetic data is quite consistent with that predicted from thermodynamic considerations. The rate constants for CH_3SO_x radicals are similar to those for HSO_x radicals, and so are the corresponding enthalpy changes. Therefore, rate constants for CH_3SO_x oxidation can be estimated from those of the corresponding HSO_x reactions. While no rate constant is available, the oxidation of the CH_3SO_2 radical by NO_2 may be fast since the similar reaction

$$HOSO_2 + NO_2 \rightarrow HOS(O)_2\text{–}ONO \rightarrow HOS(O)_2O + NO$$

was estimated to be relatively fast at 300 K [Benson, 1978]. Although no rate constants are available for the reactions of peroxy radicals with CH_3SO_x, they should be of a similar magnitude as those for the reaction with NO_2 since reaction enthalpies for the analogous reactions between NO_2 and peroxy radicals are similar. The observations of a high SO_2 yield in the photolysis of CH_3SCH_3-H_2O_2 mixtures in air [Barnes et al., 1988] and in the photolysis of CH_3SSCH_3 in air [Hatakeyama and Akimoto, 1983; Yin et al., 1989] are consistent with a rapid oxidation of CH_3S and CH_3SO by HO_2 and CH_3OO. Furthermore, the enthalpy changes listed in Table 4 for all the possible pathways of $CH_3SO_x + O_3$ reactions indicate that oxidation is thermodynamically most favourable, although H-atom abstraction is also significantly exothermic.

In experiments carried out at high NO_x concentrations [Hatakeyama et al., 1982; Hatakeyama and Akimoto, 1983; Grosjean, 1984; Barnes et al., 1987b], CH_3SO_x radicals are oxidized mainly by NO_2. At much lower NO_x concentrations, e.g., in the marine atmosphere, reactions of CH_3SO_x with ozone may become the most important pathway for CH_3SO_x radicals.

Finally, the addition of NO_2 (or NO_3) to CH_3SO_x may also be a minor path-

way for CH_3SO_x radicals. Although CH_3SNO_2 has been tentatively identified as a reaction product in several studies [Niki et al., 1983a; Grosjean, 1984; MacLeod et al., 1986; Barnes et al., 1987b], the corresponding addition pathway is probably only a minor component of the $CH_3SO_x + NO_2$ reaction, which proceeds mainly via oxidation. Comparing the NO_2 reactions of CH_3O and CH_3S:

$CH_3O + NO_2 \rightarrow$	$CH_3O\text{–}NO_2$	major
$\rightarrow$	$CH_3O\text{–}ONO$	negligible
$CH_3S + NO_2 \rightarrow$	$CH_3S\text{–}NO_2$	minor
$\rightarrow$	$CH_3S\text{–}ONO$	major

the CH_3O–ONO bond is very weak and no CH_3OONO has been observed to form. In contrast, the CH_3S–ONO bond is expected to be stronger than that in $CH_3S\text{–}NO_2$ because of the larger difference of electronegativity. Thus, the dominant pathway in this case is the formation of the adduct CH_3SONO, which is thermally unstable and further decomposes rapidly to CH_3SO and NO. This may explain the relative difficulty of detecting CH_3SNO_2 in the experiments, which may also be true for the analogous species of $CH_3S(O)NO_2$ and $CH_3S(O)_2NO_2$.

5.3. Decomposition of RSO_x Radicals

Unimolecular decomposition reactions of CH_3SO_x radicals and the corresponding estimated bond dissociation energies are given below,

	ΔH°_{298} (kcal/mole)
$CH_3SO \xrightarrow{M} CH_3 + SO$	50 ± 2
$CH_3SO_2 \xrightarrow{M} CH_3 + SO_2$	17.2
$CH_3SO_3 \xrightarrow{M} CH_3 + SO_3$	22

[Benson, 1978; Kerr and Calvert, 1984]. Examination of BDE values suggests that the CH_3SO radical should be stable with respect to its decomposition, and that CH_3SO_2 and CH_3SO_3 radicals should decompose rapidly. According to the above mechanism, the CH_3 radical is postulated to form, but experimental studies so far have yield conflicting results. On the one hand, MacLeod et al. [1986] studied the reactions of $CH_3SH + NO_3$ and $CH_3SSCH_3 + NO_3$ in the dark and observed CH_3ONO_2 in both systems, strongly suggesting that the CH_3 radical was the intermediate species. CH_3ONO_2 was also observed in the $CH_3SSCH_3 + NO_2$ study of Barnes et al. [1987b], clearly indicating the formation of CH_3 radicals. On the other hand, the absence of CH_3ONO in the photolysis of CH_3SNO in air with light above 500 nm [Hatakeyama and Akimoto, 1983; Hatakeyama, 1987] was cited as an evidence for lack of CH_3 formation in their system, where CH_3ONO would be formed by:

$$CH_3 + O_2 \xrightarrow{M} CH_3O_2$$
$$CH_3O_2 + NO \longrightarrow CH_3O + NO_2$$
$$CH_3O + NO \xrightarrow{M} CH_3ONO$$

However, the same authors observed CH_3ONO in the system of $CH_3SSCH_3 + C_2H_5ONO + NO + h\nu$ [Hatakeyama and Akimoto, 1983]. In this system, CH_3ONO is unlikely to form from CH_3CHO since in analogous system of CH_3SCH_3–C_2H_5ONO–NO–$h\nu$ Niki et al. [1983b] measured a lower limit of 25% of CH_3ONO without consuming the formed CH_3CHO.

It should be pointed out that the lack of observation of CH_3ONO and CH_3ONO_2 does not necessarily indicate the absence of the formation of the CH_3 radical since the rate constants of $CH_3O + NO_x$ are uncertain and the competitive reaction of $CH_3O + O_2$ is the major loss pathway for CH_3O radical.

Another observation which has been used to argue against the formation of CH_3 radical by Hatakeyama and Akimoto [1983] is that little CH_3OH was formed from the photolysis of CH_3SSCH_3 in air although HCHO yield was more than 90% because from following mechanism and available rate constants,

$$\begin{aligned} CH_3 + O_2 &\xrightarrow{M} CH_3O_2 \\ CH_3O_2 + CH_3O_2 &\longrightarrow 2\ CH_3O + O_2 \\ &\longrightarrow HCHO + CH_3OH + O_2 \\ CH_3O + O_2 &\longrightarrow HCHO + HO_2 \end{aligned}$$

a yield of 46% CH_3OH was expected. However, such result not only was consistent with the generation of CH_3 radical in the system, but also was a clear evidence that $CH_3O_2 + CH_3S$ reaction occured, i.e.,

$$CH_3O_2 + CH_3S \rightarrow CH_3O + CH_3SO$$

therefore, HCHO should be expected to form, but not CH_3OH.

Mellouki et al. [1988] studied the decomposition of the CH_3SO_2 radical by a discharge flow-EPR-mass spectrometric technique and estimated $k_{CH_3SO_2}$ to be about 10 s^{-1} at room temperature and 0.33 Torr pressure. This rate constant may be higher in the atmosphere since the reaction is probably pressure dependent. Moreover, the decomposition rate of CH_3SO_2 radical may be enhanced in sunlight because CH_3SO_2 absorbs strongly in the 300–600 nm region with a maximum at ca. 350 nm [Chatgilialogou et al., 1987].

In summary, thermodynamic, kinetic and some (but not all) product data indicate that unimolecular decomposition is an important loss process for CH_3SO_x radicals.

5.4. Formation of CH_3SSCH_3

The formation of CH_3SSCH_3 has been observed in the systems of CH_3SNO–air–$h\nu$ [Niki et al., 1983a], CH_3SNO–NO_x–air–$h\nu$ [Hatakeyama, 1987] and CH_3SH–N_2O_5–air in the dark [MacLeod et al., 1986]. The formation of CH_3SSCH_3 is puzzling since CH_3S radical recombination to produce CH_3SSCH_3 ($k = 4.1\times10^{-11}$ cm^3 $molecule^{-1}$ s^{-1} [Graham et al., 1964b]) is too slow to compete with the CH_3S+ NO_2 reaction ($k = 6.1\times10^{-11}$ cm^3 $molecule^{-1}$ s^{-1} [Tyndall and Ravishankara, 1987]) at the high level of NO_2 used in the above studies. Therefore, there must be other routes to produce CH_3SSCH_3. Based on thermochemistry considerations, the following reaction is proposed to account for the formation of CH_3SSCH_3,

$$CH_3SNO + CH_3S \rightarrow \underset{\displaystyle CH_3S}{\overset{\displaystyle |}{CH_3S\text{–}NO}} \rightarrow CH_3S\text{–}SCH_3 + NO$$

Since $BDE(CH_3S\text{–}NO) = 25 \pm 1$ kcal/mole is much less than $BDE(CH_3S\text{–}SCH_3) = 74 \pm 2$ kcal/mole [Benson, 1978], the above reaction is expected to be fast. In fact, from the experimental data of $CH_3S^{14}NO + {}^{15}NO + N_2$ system obtained by Niki et al. [1983a] and using a simple mechanism including CH_3S radical, NO , CH_3SNO and CH_3SSCH_3 species, we estimate a value of 5.5×10^{-12} cm^3 $molecule^{-1}$ s^{-1} for the rate constant of the $CH_3S + CH_3SNO$ reaction. The validity of our proposed mechanism for formation of CH_3SSCH_3 can be further tested using Hatakeyama's [1987] experimental data for the CH_3SNO–NO_x–air–$h\nu$ system. Assuming CH_3S is mainly consumed by the following two reactions,

$$CH_3S + CH_3SNO \longrightarrow CH_3SSCH_3 + NO \qquad a$$

$$+ NO_2 \longrightarrow CH_3SO + NO \qquad b$$

and that the reaction between CH_3S and CH_3SNO is the sole reaction responsible for the production of CH_3SSCH_3, the CH_3SSCH_3 yield is therefore proportional to the ratio of reaction rates, R_a/R_b, or to the ratio of $[CH_3SNO]/[NO_2]$, i.e.,

$$\frac{R_a}{R_b} = \frac{5.5 \times 10^{-12}}{6.1 \times 10^{-11}} \times \frac{[CH_3SNO]}{[NO_2]}$$

As a first approximation, the yield of CH_3SSCH_3 should be roughly proportional to the initial concentration ratio, $[CH_3SNO]_o/[NO_2]_o$ (no time profiles of CH_3SNO and NO_2 were available). Initial concentration and CH_3SSCH_3 yields are listed in Table 5, and indeed show a high degree of correlation. It should be pointed out that the CH_3SSCH_3 yield does not anticorrelate with the initial O_2 concentration directly, which was interpreted by Hatakeyama originally, because the consumption of CH_3S due to $CH_3S + O_2$ reaction is minor under such high concentration of NO_2 (1.3–10.5 ppm) according to the apparent rate constant of 2.5×10^{-18} cm^3 $molecule^{-1}$ s^{-1} [Tyndall and Ravishankara, 1988]. However, the presence of high O_2 concentration in the system is necessary to reconvert NO to NO_2 and maintain the high NO_2 concentration by following reactions,

$$\begin{aligned}
CH_3 + O_2 &\xrightarrow{M} CH_3O_2 \\
CH_3O_2 + NO &\longrightarrow CH_3O + NO_2 \\
CH_3O + O_2 &\longrightarrow HCHO + HO_2 \\
HO_2 + NO &\longrightarrow OH + NO_2 \\
CH_3SSCH_3 + OH &\longrightarrow CH_3S + CH_3SOH
\end{aligned}$$

and also the reaction of $CH_3SSCH_3 + OH$ decreases the product yield of CH_3SSCH_3. The high CH_3SSCH_3 yield observed in the absence of O_2 (which is shown in Table

5 at last line), despite the relatively low ratio of $[CH_3SNO]_o/[NO_2]_o$, is not inconsistent with our mechanism since the competition cannot be maintained in this case.

In the dark reaction of CH_3SH with N_2O_5 in air [MacLeod et al., 1986], several reactions may be responsible for the formation of CH_3SSCH_3. The formation of CH_3SSCH_3 was only observed in the presence of O_2 and CH_3 was also produced, as indicated by the observation of CH_3ONO_2. Thus, it is likely that OH was produced from CH_3O_2. Therefore, CH_3S could have formed by reaction of CH_3SH with OH, and could have further reacted with CH_3SNO_x or CH_3SONO_2 to produce CH_3SSCH_3:

$$\begin{aligned} CH_3S + CH_3SNO &\rightarrow CH_3SSCH_3 + NO \\ + CH_3SNO_2 &\rightarrow CH_3SSCH_3 + NO_2 \\ + CH_3SONO_2 &\rightarrow CH_3SSCH_3 + NO_3 \end{aligned}$$

Although no bond dissociation energies are available for CH_3S–NO_2 and CH_3S–ONO_2 bonds, the S–N and S–O bonds in the above three species are expected to be weaker than the S–S bond of CH_3S–SCH_3

Due to the rapid photolysis of CH_3SNO, CH_3SSCH_3 formation by the reaction of CH_3S with CH_3SNO will *not* be important in the daytime atmosphere.

6. Reaction of $RS(O)_xOO$ Radicals

The reactivity of $CH_3S(O)_xOO$ radicals may be more similar to that of peroxy radicals than to that of sulfur radicals. This is consistent with the prediction, from a recent ab initio molecular orbital calculation, that the electron spin density on O atoms in CH_3SOO is similar to that in CH_3OO [Swarts et al., 1989]. In fact,

$CH_3S(O)_xOO$ radicals may be even more reactive than peroxy radicals by virtue of the weaker O–O bonds. Although no thermodynamic data are available, the relative reactivity of $CH_3S(O)_xOO$ radicals is expected to be:

$$CH_3SOO > CH_3S(O)OO > CH_3S(O)_2OO$$

since the relative strength of O–O bond is in the order:

$$CH_3SO–O < CH_3S(O)O–O < CH_3S(O)_2O–O$$

The major loss process for $CH_3S(O)_xOO$ radicals will be reduction reactions involving NO or CH_3SO_x, although self-reaction and H-atom abstraction may also be important. Thus, for NO and CH_3S:

$$\begin{aligned}
CH_3SOO \quad &+ NO \quad \rightarrow CH_3SO + NO_2 \\
&+ CH_3S \rightarrow CH_3SO + CH_3SO \\
CH_3S(O)OO \quad &+ NO \quad \rightarrow CH_3SO_2 + NO_2 \\
&+ CH_3S \rightarrow CH_3SO_2 + CH_3SO \\
CH_3S(O)_2OO \quad &+ NO \quad \rightarrow CH_3SO_3 + NO_2 \\
&+ CH_3S \rightarrow CH_3SO_3 + CH_3SO
\end{aligned}$$

These reactions are expected to be fast and comparable to the reaction of CH_3O_2 with NO, $k = 7.6\times10^{-12}$ cm^3 $molecule^{-1}$ s^{-1}. At high NO concentration, $CH_3S(O)_xOO$ will oxidize NO to NO_2; at low NO_x concentration, the reactions between $CH_3S(O)_xOO$ and CH_3SO_x radicals become important, competing with the reactions between other peroxy radicals and CH_3SO_x radicals.

The tentative identification of $CH_3S(O)OONO_2$ by Barnes et al. [1987b] suggests that the competition reaction of NO_2 for $CH_3S(O)OO$ is important; this may

also hold true for the $CH_3S(O)_2OO$ radical.

7. Formation of SO_2 and CH_3SO_3H

Although SO_2 and CH_3SO_3H have been identified as major reaction products in several studies [Grosjean and Lewis, 1982; Hatakeyama et al., 1982; Hatakeyama and Akimoto, 1983; Grosjean, 1984; Hatakeyama et al., 1985; Barnes et al., 1987b; Barnes et al., 1988], their formation pathways are still poorly characterized. In this section, we discuss SO_2 and CH_3SO_3H formation pathways, and examine the effects of high or low NO_x concentration on the yield distribution of SO_2 and CH_3SO_3H.

The analysis presented in the preceding sections makes it clear that SO_2 and CH_3SO_3H can be produced in both addition or abstraction pathways. The major formation pathways for SO_2 and CH_3SO_3H are compiled below:

$$
\begin{aligned}
CH_3SO_2 \quad &\xrightarrow{M} SO_2 + CH_3 \\
CH_3SO_3 + HCHO \quad &\longrightarrow CH_3SO_3H + HCO \\
+ CH_3SCH_3 \quad &\longrightarrow CH_3SO_3H + CH_3SCH_2 \\
+ CH_3SH \quad &\longrightarrow CH_3SO_3H + CH_3S \\
+ CH_3SOH \quad &\longrightarrow CH_3SO_3H + CH_3SO \\
+ CH_3SO_2H \quad &\longrightarrow CH_3SO_3H + CH_3SO_2 \\
+ HONO \quad &\longrightarrow CH_3SO_3H + NO_2 \\
+ H_2O_2 \quad &\longrightarrow CH_3SO_3H + HO_2 \\
+ CH_3OH \quad &\longrightarrow CH_3SO_3H + CH_2OH \\
+ HO_2 \quad &\longrightarrow CH_3SO_3H + O_2
\end{aligned}
$$

The unimolecular decomposition of CH_3SO_2 is the dominant reaction pathway for SO_2 production, and may be enhanced in sunlight as discussed earlier. The

bond dissociation energies of the C–H, S–H and O–H bonds in the H-donors listed above are in the range 49–96 kcal/mole [Benson, 1978; McMillen and Golden, 1982; Shum and Benson, 1983 and 1985; Kerr, 1985] and are much smaller than that for $CH_3S(O)_2O$–H bond of about 104 kcal/mole or more. In smog chamber experiments, especially at high concentrations of RSR′, the reactions of CH_3SO_3 with RSR′ (including CH_3SOH) and with HCHO will be the dominant pathways for CH_3SO_3H formation compared with the decomposition of the CH_3SO_3 radical.

The relative importance of addition and abstraction is still uncertain for the reaction of CH_3SO_3 with organosulfur compounds. Considering the relatively strong C–H bonds in CH_3SCH_3 and CH_3SSCH_3 (about 97 kcal/mole) and the relatively high electron density on S atom, electrophilic addition of CH_3SO_3 to CH_3SCH_3 and CH_3SSCH_3 is probably more important than H-atom abstraction, as is the case for other free radicals including OH, NO_3, $O(^3P)$ and IO.

Since SO_2 and CH_3SO_3H are produced mainly from CH_3SO_2, the competition between CH_3SO_2 decomposition and further oxidation to CH_3SO_3 will determine their yield distribution, which is shown schematically as follows:

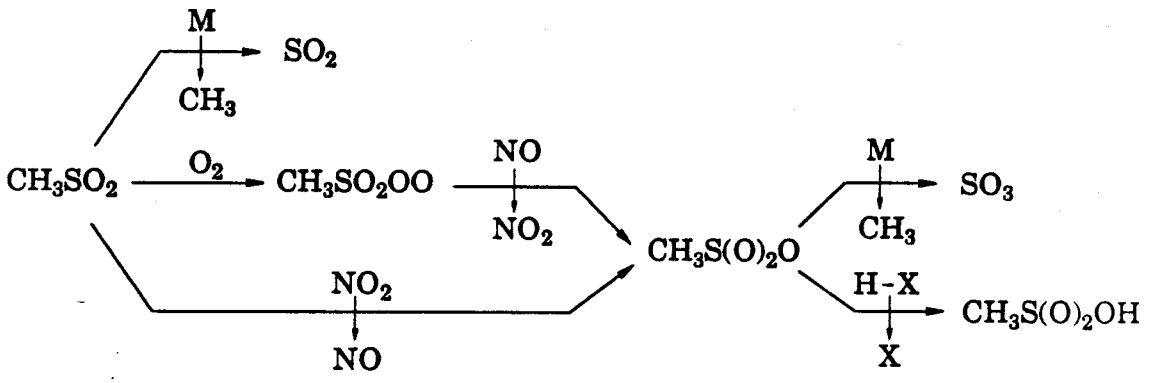

In the absence of NO_x or at very low NO_x concentration, neither the oxidation of CH_3SO_2 by peroxy radicals nor the reduction of $CH_3S(O)_2OO$ by CH_3SO_x radicals will be fast since the concentrations of those radicals are very low. In this case, the competition is dominated by the unimolecular decomposition of the CH_3SO_2 radical to form SO_2. This is consistent with the observation of high SO_2 yield in systems of CH_3SCH_3–H_2O_2–air–$h\nu$ [Barnes et al., 1988], and CH_3SSCH_3–air–$h\nu$ [Hatakeyama and Akimoto, 1983; Yin et al., 1989]. At higher NO_x concentrations (> 0.1 ppm), the reactions $CH_3SO_2 + NO_2$ and $CH_3S(O)_2OO + NO$, especially the later, compete effectively with CH_3SO_2 decomposition. In this case, the yield of SO_2 decreases and that of CH_3SO_3H increases, in agreement with experimental observations [Grosjean and Lewis, 1982; Hatakeyama et al., 1982; Hatakeyama and Akimoto, 1983; Grosjean, 1984; Hatakeyama et al., 1985; Barnes et al., 1987b, Yin et al., 1989].

The effects of NO_x on the yield distribution of SO_2 and CH_3SO_3H can be used to explain the NO_x effects on the observed rate constants of initial reactions mentioned in section 2.4.2. As the NO_x concentration increased in the systems, the formation rate of CH_3SO_3 is increased, and so is the rate of CH_3SO_3H formation. Also in those experiments, the concentration of CH_3SH and CH_3SCH_3 were very high and the reaction between CH_3SO_3 and CH_3SH or CH_3SCH_3 should be the dominant one for CH_3SO_3H formation. Therefore, the observed decay rate of CH_3SH or CH_3SCH_3 will be enhanced and the measured rate constants of the initial reactions will depend on the NO_x concentration. It should be mentioned that, although the difference between the bond dissociation energy of $CH_3S(O)_2O$–H and CH_3SCH_2–H bonds is relatively small (about 8 kcal/mole or more), the addition of CH_3SO_3 to CH_3SCH_3 may also contribute to the enhanced decay rate of CH_3SCH_3 since the CH_3SO_3 radical is analogous to NO_3 radical.

It should be pointed out that the formation mechanisms of SO_2 proposed by

Balla and Heicklen [1985] and Hatakeyama [1987] do not predict SO_2 production in the absence of O_2, in contradiction with the observations of Barnes et al. [1987b] for the CH_3SSCH_3–NO_2–N_2 system.

8. Missing Products

Experimental studies of organosulfur oxidation have so far yielded poor sulfur, nitrogen and carbon mass balances. Although concentrations of many measured compounds, including H_2SO_4, CH_3SO_3H, HNO_3 and HCHO, may usually be underestimated due to wall losses, other unidentified products may also be produced, especially condensible species with high molecular weight. A speculative list of such products is given below:

$$\begin{aligned}
CH_3S(O)OO &+ NO_2 \xrightarrow{M} CH_3S(O)OONO_2 \\
CH_3S(O)_2OO &+ NO_2 \xrightarrow{M} CH_3S(O)_2OONO_2 \\
CH_3SO_2 &+ RSR' \xrightarrow{M} \text{Adduct} \\
CH_3SO_3 &+ RSR' \xrightarrow{M} \text{Adduct} \\
&+ NO \xrightarrow{M} CH_3S(O)_2ONO \\
&+ NO_2 \xrightarrow{M} CH_3S(O)_2ONO_2 \\
CH_3SO_2 &+ NO_2 \xrightarrow{M} CH_3S(O)_2ONO
\end{aligned}$$

The peroxynitrate compounds may be thermally unstable and serve as a reservoir for both sulfur and nitrogen compounds. The CH_3SO_3 radical, which is analogous to NO_3, may not only abstract hydrogen from RSR′ or hydrocarbons but also add to RSR′ or unsaturated hydrocarbons in the atmosphere. The adduct may undergo unimolecular decomposition to form condensible species. The possible $CH_3S(O)_2ONO_x$ products, which are similar to $HOS(O)_2ONO_x$ discussed by

Benson [1978], may be easily absorbed on the reactor surfaces and exothermically hydrolyzed to CH_3SO_3H, HONO, or $HONO_2$. Two other condensible species, CH_3SOH and CH_3SO_2H, may also be lost on the reactor walls, although they could be further oxidized to SO_2 and CH_3SO_3H.

9. New mechanisms for Atmospheric Oxidation of CH_3SCH_3 and CH_3SSCH_3

Based on the comprehensive analysis presented in the preceding sections, new mechanisms have been developed to describe atmospheric chemistry of CH_3SCH_3–NO_x–air–$h\nu$ (Tables 6, 7 and 9) and CH_3SSCH_3–NO_x–air–$h\nu$ (Table 8). The difference between these two mechanisms lies mostly in their initial reactions. A detailed mechanism for CH_3SH photooxidation in the atmosphere could readily be developed using the appropriate initial reactions, with subsequent reactions identical to those presented here for CH_3SSCH_3.

Major differences between the mechanisms presented here and those developed in our earlier work [Yin et al., 1986] including the following:

1. Detailed reaction mechanisms for $CH_3S(O)CH_3$, $CH_3S(O)_2CH_3$ and CH_3SOH.
2. Clear distinction between CH_3SO_x and $CH_3S(O)_xOO$ radicals.
3. Detailed elucidation of CH_3SO_x reaction mechanisms.
4. Delineation of the major pathways for SO_2 and CH_3SO_3H formation.

In order to evaluate the proposed new mechanisms and to determine the yield distribution of SO_2 and CH_3SO_3H under low NO_x conditions, a series of outdoor smog chamber experiments has been carried out for CH_3SCH_3–NO_x–air–$h\nu$ and CH_3SSCH_3–(NO_x)–air–$h\nu$ mixtures. The results of these experiments are presented in our companion paper, Part II.

ACKNOWLEDGMENT

This work was supported by National Science Foundation grant ATM–8503103. We thank Dr. Barnes, Dr. Becker, Dr. Balla, Dr. Black, Dr. Hatakeyama and Dr. Akimoto, Dr. Hynes, Dr. Wine, and Dr. Tyndall and Dr. Ravishankara for communicating their results to us prior to publication.

Table 1 Summary of Kinetic Data for Reduced Sulfur Compounds

	Initial Reaction		$k_{298} \times 10^{11}$ (cm^3 $molecule^{-1}$ s^{-1})
$O(^3P)$ + H_2S	→ HS + OH		0.0022
+ CH_3SH	→ CH_3S + OH		0.18
	→ $CH_3S(O)H$	→ HSO + CH_3	
		→ CH_3SO + H	
+ CH_3SCH_3	→ $CH_3S(O)CH_3$	→ CH_3SO + CH_3	5.0
+ CH_3SSCH_3	→ $CH_3S(O)SCH_3$	→ CH_3SO + CH_3S	10–13
OH + H_2S	→ HS + H_2O		0.48
+ CH_3SH	→ CH_3S + H_2O		3.3
	→ $CH_3S(OH)H$		
+ CH_3SCH_3	→ CH_3SCH_2 + H_2O		0.44–0.63
	→ $CH_3S(OH)CH_3$		
+ CH_3SSCH_3	→ $CH_3S(OH)SCH_3$	→ CH_3SOH + CH_3S	21
NO_3 + H_2S	→ HS + $HONO_2$		< 0.00008–0.003
	$HS(ONO_2)H$		
+ CH_3SH	→ CH_3S + $HONO_2$		0.077–0.109
	→ $CH_3S(ONO_2)H$		
+ CH_3SCH_3	→ CH_3SCH_2 + $HONO_2$		0.075–0.106
	→ $CH_3S(ONO_2)CH_3$		
+ CH_3SSCH_3	→ CH_3SSCH_2 + $HONO_2$		0.0739
	→ $CH_3SS(ONO_2)CH_3$		
IO + CH_3SSCH_3	→ $CH_3S(OI)CH_3$	→ $CH_3S(O)CH_3$ + I	1.5–3.0

Notes:

1. The rate constants are measured at room temperature and at both low or high pressure by various techniques.
2. Usually both abstraction and addition pathways are presented. In the case where the information on the mechanism is available, the dominant reaction is given.

References:

$O(^3P)$:

Nip et al., 1981; Cvetanović et al., 1981; Baulch et al., 1984.

OH:

Atkinson et al., 1977; Wine et al., 1981; Wine et al., 1984; Hynes and Wine, 1987; Baulch et al., 1984; Martin et al., 1985; Wallington et al., 1986a; Nielsen et al., 1986; Hynes et al., 1986; Hsu et al., 1987; Barnes et al;., 1988; Cox and Sheppard, 1980.

NO_3:

Atkinson et al., 1984a; MacLeod et al., 1986; Wallington et al., 1986b; Wallington et al., 1986c; Tyndall et al., 1986; Dlugokencky and Howard, 1988.

IO:

Barnes et al., 1987a; Martin et al., 1987.

Table 2 Structures of Initial Reaction Adducts

	H_3C-S-H	H_3C-S-CH_3	CH_3-S-S-CH_3
BDE: (kcal/mole)	74.2 88.6	75.0	67.8 57
	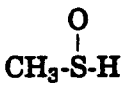	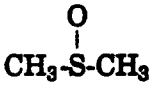	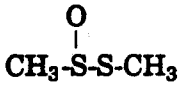
	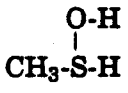	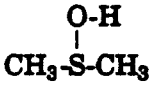	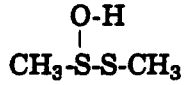
	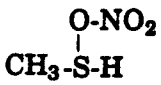	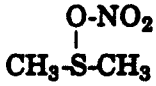	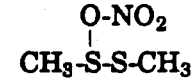
	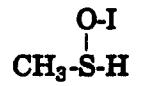	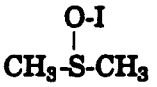	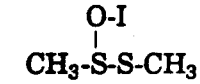

Note: The bond dissociation energies of organosulfur compounds are from Benson [1978] and Shum and Benson [1983].

Table 3 Summary of Reaction Enthalpies for CH_3SO_x Oxidation

Oxidation Reaction	ΔH°_{298} (kcal/mole)
$CH_3S + O\text{–}NO \longrightarrow CH_3SO + NO$	−32
$+ O\text{–}OH \longrightarrow CH_3SO + OH$	−39
$+ O\text{–}OCH_3 \longrightarrow CH_3SO + OCH_3$	−46
$+ O\text{–}OO \longrightarrow CH_3SO + O_2$	−80
$+ O\text{–}NO_2 \longrightarrow CH_3SO + NO_2$	−55
$CH_3SO + O\text{–}NO \longrightarrow CH_3SO_2 + NO$	−26
$+ O\text{–}OH \longrightarrow CH_3SO_2 + OH$	−33
$+ O\text{–}OCH_3 \longrightarrow CH_3SO_2 + OCH_3$	−40
$+ O\text{–}OO \longrightarrow CH_3SO_2 + O_2$	−74
$+ O\text{–}NO_2 \longrightarrow CH_3SO_2 + NO_2$	−49
$CH_3SO_2 + O\text{–}NO \longrightarrow CH_3SO_3 + NO$	−13
$+ O\text{–}OH \longrightarrow CH_3SO_3 + OH$	−20
$+ O\text{–}OCH_3 \longrightarrow CH_3SO_3 + OCH_3$	−27
$+ O\text{–}OO \longrightarrow CH_3SO_3 + O_2$	−61
$+ O\text{–}NO_2 \longrightarrow CH_3SO_3 + NO_2$	−36

Note: The formation enthalpies of CH_3SO_x radicals are estimated from the bond dissociation energies of corresponding species estimated by Benson [1978] and Kerr and Calvert [1984]. The formation enthalpies of other species are from Shum and Benson [1983] and Baulch et al. [1984].

Table 4 Summary of Kinetic Data for NO_2 and O_3 Reaction

Reaction		k $\times 10^{11}$ (cm^3 molecule^{-1} s^{-1})	ΔH°_{298} (kcal/mole)
NO_2 Reaction			
NO_2 + HS	→ HSO + NO	2.4–8.6	−25.0
+ CH_3S	→ CH_3SO + NO	5.1–11.0	−32
+ C_2H_5S	→ C_2H_5SO + NO	9.2	∼ −30
+ i-C_3H_7S	→ i-C_3H_7SO + NO	5.9	∼ −30
NO_2 + HSO	→ HSO_2 + NO	0.41–0.96	−23.3
+ CH_3SO	→ CH_3SO_2 + NO	0.8–3	−26
NO_2 + HSO_2	→ Product		
+ CH_3SO_2	→ CH_3SO_3 + NO		−13
O_3 Reaction			
O_3 + HS	→ HSO + O_2	0.29–0.32	−72.7
+ CH_3S	→ CH_3SO + O_2	0.41–0.57	−80
	→ CH_2S + O_2 + OH		−31
O_3 + HSO	→ HSO_2 + O_2	0.001–0.01	−71
	→ HS + $2O_2$		+5.9
+ CH_3SO	→ CH_3S + O_2 + O_2	∼ 0.06	+12
+ CH_3SO	→ CH_3SO_2 + O_2		−74
	→ CH_2SO + OH + O_2		−22
O_3 + HSO_2	→ Product		
+ $CH_3S(O)O$	→ CH_3SO + O_2 + O_2		+6
+ CH_3SO_2	→ CH_3SO_3 + O_2		−61
+ CH_3SO_2	→ CH_2SO_2 + OH + O_2		−39

Notes:

1. The rate constants were measured at room temperature and at low or high pressure by various techniques.
2. Only the dominant pathway is given for each reaction.

References:

NO_2 *reactions*:

Black, 1984; Bulatov et al., 1984; Friedl et al., 1985; Wang et al., 1987; Schönle et al., 1987; Stachnik and Molina, 1987, Lovejoy et al., 1987 Balla et al., 1986; Tyndall and Ravishankara, 1988; Black et al., 1988a and 1988b; Mellouki et al., 1988; Domine et al., 1989.

O_3 *reactions*:

Friedl et al., 1985; Schönle et al., 1987; Tyndall and Ravishankara, 1987; Tyndall and Ravishankara, 1989; Domine et al., 1989.

Reaction enthalpy:

The formation enthalpies of CH_3SO_x radicals are estimated from the bond dissociation energies of corresponding species estimated by Benson [1978] and Kerr and Calvert [1984]. The formation enthalpy of HSO radical is uncertain within the range of (-5 ± 4)-(-0.4 ± 2) kcal/mole [Slagle et al., 1978; Benson, 1978; Davidson et al., 1982; Luke and McLean, 1985] and the value estimated by Benson [1978] was used. The formation enthalpies of other species are obtained from Benson [1978], Hwang and Benson [1979], Shum and Benson [1983], and Baulch et al. [1984]. The enthalpy changies for $C_2H_5S + NO_2$ and i-$C_3H_7S + NO_2$ reactions are estimated by Balck et al. [1988a and 1988b].

Table 5 Correlation between CH_3SSCH_3 Yield and Initial Concentration

$[CH_3SNO]_o/[NO_2]_o$	CH_3SSCH_3 Yield	$[O_2]_o$ (Torr)
7.97	0.67	152
6.75	0.52	76
6.24	0.54	152
4.94	0.42	380
4.09	0.20	760
1.85	0.18	152
1.09	0.13	152
0.74	—	152
5.96	0.71	~ 0

Note: The CH_3SSCH_3 yield is measured from the photolysis of CH_3SNO–NO_x–air mixtures by Hatakeyama [1987].

Table 6 Inorganic and Aldehyde Chemistry Common to Mechanisms of Organosulfur Species

	REACTION	RATE CONSTANT[a]	ACTIVATION ENERGY(K)	REF.	NOTE
	Inorganic Reactions				
1.	$NO_2 + h\nu \rightarrow NO + O(^3P)$	*			(1)
2.	$O(^3P) + O_2 \xrightarrow{M} O_3$	1.5×10^{-14}	-5.60×10^2	2,17	
3.	$O_3 + NO \rightarrow NO_2 + O_2$	1.8×10^{-14}	1.43×10^3	2	
4.	$O(^3P) + NO \xrightarrow{M} NO_2$	2.1×10^{-12}		3	
5.	$O(^3P) + NO_2 \rightarrow NO + O_2$	9.7×10^{-12}	-1.2×10^2	3	
6.	$O(^3P) + NO_2 \xrightarrow{M} NO_3$	1.8×10^{-12}	-4.2×10^2	6,17	
7.	$O(^3P) + NO_3 \rightarrow NO_2 + O_2$	1.0×10^{-11}		3	
8.	$O(^3P) + O_3 \rightarrow 2\ O_2$	8.0×10^{-15}	2.06×10^3	3	
9.	$O_3 + NO_2 \rightarrow NO_3 + O_2$	3.2×10^{-17}	2.45×10^3	3	
10.	$O_3 + NO_2 \rightarrow NO + 2\ O_2$	9.7×10^{-19}	2.45×10^3	17	
11.	$O_3 + OH \rightarrow HO_2 + O_2$	6.7×10^{-14}	1.0×10^3	3	
12.	$O_3 + HO_2 \rightarrow OH + 2\ O_2$	2.0×10^{-15}	6.0×10^2	3	
13.	$O_3 + h\nu \rightarrow O(^3P) + O_2$	$4.0 \times 10^{-2} k_{NO_2}$		1,19	
14.	$O_3 + H_2O + h\nu \rightarrow 2\ OH + O_2$	$9.34 \times 10^{-22} k_{NO_2}$		1,9	(3)
15.	$HO_2 + OH \rightarrow O_2 + H_2O$	1.1×10^{-10}	-2.5×10^2	3	
16.	$HO_2 + HO_2 \rightarrow H_2O_2 + O_2$	1.8×10^{-12}	-6.2×10^2	2	(2)
17.	$HO_2 + HO_2 \rightarrow H_2O_2 + O_2$	1.3×10^{-12}	-9.8×10^2	2	(2)
18.	$HO_2 + HO_2 + H_2O \rightarrow H_2O_2 + O_2 + H_2O$	4.0×10^{-30}	-2.8×10^3	2	(2)
19.	$HO_2 + HO_2 + H_2O \rightarrow H_2O_2 + O_2 + H_2O$	2.8×10^{-30}	-3.2×10^3	2	(2)
20.	$H_2O_2 + OH \rightarrow HO_2 + H_2O$	1.7×10^{-12}	1.6×10^2	3	
21.	$H_2O_2 + h\nu \rightarrow 2\ OH$	$7.1 \times 10^{-4} k_{NO_2}$		1	
22.	$NO + HO_2 \rightarrow NO_2 + OH$	8.3×10^{-12}	-2.4×10^2	3	
23.	$NO + NO + O_2 \rightarrow 2\ NO_2$	2.0×10^{-38}	-5.3×10^2	3	
24.	$NO + OH \xrightarrow{M} HONO$	6.6×10^{-12}		2	
25.	$HONO + h\nu \rightarrow NO + OH$	$1.7 \times 10^{-1} k_{NO_2}$		1	
26.	$HONO + OH \rightarrow NO_2 + H_2O$	4.9×10^{-12}	3.9×10^2	3	
27.	$HNO + O_2 \rightarrow NO + HO_2$	2.1×10^{-20}	5.0×10^3	17	
28.	$NO_2 + OH \xrightarrow{M} HONO_2$	1.1×10^{-11}		2,17	
29.	$NO_2 + HO_2 \xrightarrow{M} HO_2NO_2$	1.4×10^{-12}		2	
30.	$HO_2NO_2 \xrightarrow{M} HO_2 + NO_2$	8.5×10^{-2}	1.042×10^4	2	
31.	$HO_2NO_2 + OH \rightarrow NO_2 + H_2O + O_2$	5.0×10^{-12}	-3.6×10^2	3,17	
32.	$NO_3 + OH \rightarrow NO_2 + HO_2$	2.3×10^{-11}		3	
33.	$NO_3 + NO \rightarrow 2\ NO_2$	2.7×10^{-11}	-1.5×10^2	3	
34.	$NO_3 + NO_2 \rightarrow NO + NO_2 + O_2$	4.0×10^{-16}	1.23×10^3	2	

(continued)

	REACTION	RATE CONSTANT[a]	ACTIVATION ENERGY(K)	REF. NOTE
35.	$NO_3 \xrightarrow{M} NO + O_2$	3.0×10^{-3}	6.84×10^{3}	17
36.	$NO_3 + HO_2 \rightarrow HONO_2 + O_2$	4.3×10^{-12}		3
37.	$NO_3 + h\nu \rightarrow 0.3\ NO + 0.7\ NO_2 + 0.7\ O(^3P)$	$1.55 \times 10^{1} k_{NO_2}$		18
38.	$NO_3 + NO_2 \xrightarrow{M} N_2O_5$	1.2×10^{-12}	6.0×10^{1}	2,17
39.	$N_2O_5 \xrightarrow{M} NO_2 + NO_3$	5.2×10^{-2}	1.084×10^{4}	5,17
40.	$N_2O_5 + H_2O \rightarrow 2\ HONO_2$	2.0×10^{-21}		3
41.	$HONO_2 + OH \rightarrow NO_3 + H_2O$	1.5×10^{-13}	-7.78×10^{2}	2,3,6
42.	$CO + OH \xrightarrow{O_2} CO_2 + HO_2$	2.4×10^{-13}		3
43.	$H_2 + OH \xrightarrow{O_2} HO_2 + H_2O$	6.7×10^{-15}	2.10×10^{3}	3
	Aldehyde Reactions			
44.	$HCHO + h\nu \rightarrow H_2 + CO$	$3.3 \times 10^{-3} k_{NO_2}$		19
45.	$HCHO + h\nu \xrightarrow{2O_2} 2\ HO_2 + CO$	$2.3 \times 10^{-3} k_{NO_2}$		19
46.	$HCHO + OH \xrightarrow{O_2} HO_2 + CO + H_2O$	1.1×10^{-11}	1.1×10^{2}	3
47.	$HCHO + NO_3 \xrightarrow{O_2} CO + HONO_2 + HO_2$	6.0×10^{-16}		3
48.	$HCHO + O(^3P) \xrightarrow{O_2} OH + HO_2 + CO$	1.6×10^{-13}	1.550×10^{3}	2
49.	$HCHO + HO_2 \xrightarrow{M} O_2CH_2OH$	7.9×10^{-14}	-6.25×10^{2}	3
50.	$O_2CH_2OH \xrightarrow{M} HCHO + HO_2$	1.5×10^{2}	7.0×10^{3}	3
51.	$O_2CH_2OH + NO \xrightarrow{O_2} HCOOH + NO_2 + HO_2$	7.6×10^{-12}	-1.8×10^{2}	2,17
52.	$O_2CH_2OH + HO_2 \rightarrow HO_2CH_2OH + O_2$	7.2×10^{-12}	-2.3×10^{3}	24,25
53.	$O_2CH_2OH + HO_2 \rightarrow HCOOH + H_2O + O_2$	4.8×10^{-12}	-2.3×10^{3}	24,25
54.	$2\ O_2CH_2OH \rightarrow HCOOH + CH_2(OH)_2 + O_2$	7.0×10^{-13}	-7.5×10^{2}	24,25
55.	$2\ O_2CH_2OH \rightarrow 2\ HCOOH + 2\ HO_2 + O_2$	5.5×10^{-12}		24,25
56.	$HCOOH + OH \xrightarrow{O_2} H_2O + HO_2 + CO_2$	4.8×10^{-13}	7.7×10^{1}	3,17
57.	$CH_3 + O_2 \xrightarrow{M} CH_3O_2$	1.0×10^{-12}		2
58.	$CH_3 + O_2 \rightarrow HCHO + OH$	5.0×10^{-17}		6
59.	$CH_3O_2 + NO \rightarrow NO_2 + CH_3O$	7.6×10^{-12}	-1.80×10^{2}	3
60.	$CH_3O_2 + NO_2 \xrightarrow{M} CH_3O_2NO_2$	4.1×10^{-12}		3
61.	$CH_3O_2NO_2 \xrightarrow{M} CH_3O_2 + NO_2$	1.8	1.06×10^{4}	3
62.	$CH_3O_2 + HO_2 \rightarrow CH_3OOH + O_2$	4.9×10^{-12}	-1.0×10^{3}	3
63.	$CH_3O_2H + OH \rightarrow CH_3O_2 + H_2O$	3.9×10^{-12}	-1.9×10^{2}	26
64.	$CH_3O_2H + OH \rightarrow HCHO + OH + H_2O$	1.5×10^{-12}	-1.9×10^{2}	26
65.	$CH_3O_2 + CH_3O_2 \rightarrow CH_3OH + HCHO + O_2$	2.1×10^{-13}	-2.2×10^{2}	3
66.	$CH_3O_2 + CH_3O_2 \rightarrow 2\ CH_3O + O_2$	1.3×10^{-13}	-2.2×10^{2}	3
67.	$CH_3O_2 + CH_3O_2 \rightarrow CH_3OOCH_3 + O_2$	3.0×10^{-14}	-2.2×10^{2}	3
68.	$CH_3O + O_2 \rightarrow HCHO + HO_2$	1.9×10^{-15}	1.08×10^{3}	3

(continued)

	REACTION	RATE CONSTANT*	ACTIVATION ENERGY(K)	REF.	NOTE
69.	$CH_3O + NO_2 \xrightarrow{M} CH_3ONO_2$	1.5×10^{-11}		2	
70.	$CH_3O + NO_2 \rightarrow HCHO + HONO$	3.0×10^{-13}		3	
71.	$CH_3O + NO \xrightarrow{M} CH_3ONO$	3.0×10^{-11}		2	
72.	$CH_3ONO + h\nu \rightarrow CH_3O + NO$	$0.17k_{NO_2}$		E	(4)
73.	$CH_3O + NO \rightarrow HCHO + HNO$	1.3×10^{-12}		2	
74.	$CH_3OH + OH \xrightarrow{O_2} HCHO + HO_2 + H_2O$	9.0×10^{-13}	6.9×10^2	3,17	

* References and notes of Tables 6–8 are listed at the bottom of Table 9.

TABLE 7. Atmospheric Photooxidation Mechanism for Dimethyl Sulfide

	REACTION	RATE CONSTANT[a]	ACTIVATION ENERGY(K)	REF.	NOTE
	Initial Reactions				
75.	$CH_3SCH_3 + OH \rightarrow CH_3SCH_2 + H_2O$	4.4×10^{-12}	2.34×10^{2}	3	(6)
76.	$CH_3SCH_3 + OH \xrightarrow{M} CH_3S(OH)CH_3$	1.7×10^{-12}		3	(6)
77.	$CH_3SCH_3 + O(^3P) \rightarrow CH_3SO + CH_3$	5.0×10^{-11}	-4.09×10^{2}	3,8,20	
78.	$CH_3SCH_3 + O(^3P) \rightarrow CH_3S + CH_3O$	0.0		E	(7)
79.	$CH_3SCH_3 + NO_3 \rightarrow CH_3SCH_2 + HONO_2$	0.0		E	(6)
80.	$CH_3SCH_3 + NO_3 \xrightarrow{M} CH_3S(ONO_2)CH_3$	7.5×10^{-13}	-5.00×10^{2}	3,27	(6)
81.	$CH_3SCH_3 + NO_2 \rightarrow CH_3S(O)CH_3 + NO$	9.0×10^{-21}		4	
82.	$CH_3SCH_3 + O_3 \rightarrow$ Product	0.0		E	(7)
	Adduct Reactions and other Radical Reactions				
83.	$CH_3S(OH)CH_3 \xrightarrow{M} CH_3SOH + CH_3$	5.0×10^{5}		E	(6)
84.	$CH_3S(OH)CH_3 + O_2 \rightarrow CH_3S(O)CH_3 + HO_2$	2.0×10^{-12}		E	(6)
85.	$CH_3S(OH)CH_3 + O_2 \xrightarrow{M} CH_3S(OH)(OO)CH_3$	1.0×10^{-12}		E	(6)
86.	$CH_3S(OH)(OO)CH_3 \xrightarrow{M} CH_3S(O)CH_3 + HO_2$	1.0×10^{1}		E	(6)
87.	$CH_3S(OH)(OO)CH_3 + NO \rightarrow CH_3S(OH)(O)CH_3 + NO_2$	5.0×10^{-12}		E	(6)
88.	$CH_3SCH_2 + O_2 \xrightarrow{M} CH_3SCH_2OO$	7.3×10^{-13}		15	
89.	$CH_3SCH_2OO + NO \rightarrow CH_3SCH_2O + NO_2$	8.0×10^{-12}		E	(11)
90.	$CH_3SCH_2OO + CH_3S \rightarrow CH_3SCH_2O + CH_3SO$	6.1×10^{-11}		E	(11)
91.	$CH_3SCH_2OO + CH_3SO \rightarrow CH_3SCH_2O + CH_3SO_2$	4.0×10^{-12}		E	(11)
92.	$CH_3SCH_2OO + CH_3SO_2 \rightarrow CH_3SCH_2O + CH_3SO_3$	2.5×10^{-13}		E	(11)
93.	$CH_3SCH_2OO + HO_2 \rightarrow CH_3SCH_2OOH + O_2$	1.5×10^{-12}		E	(11)
94.	$CH_3SCH_2OO + CH_3O_2 \rightarrow CH_3SCH_2O + CH_3O + O_2$	1.8×10^{-13}		E	(11)
95.	$2\ CH_3SCH_2OO \rightarrow 2\ CH_3SCH_2O + O_2$	8.6×10^{-14}		E	(11)
96.	$CH_3SCH_2O \xrightarrow{M} CH_3S + HCHO$	1.0×10^{1}		E	(8)
97.	$CH_3S(ONO_2)CH_3 \xrightarrow{M} CH_3SCH_2 + HONO_2$	1.0×10^{2}		E	(6)
98.	$CH_3S(ONO_2)CH_3 + O_2 \rightarrow$ Product	0.0		E	(7)
99.	$CH_3SONO_2 \xrightarrow{M} CH_3SO + NO_2$	1.0×10^{0}		E	(8)
	$CH_3S(O)CH_3$ Reactions				
100.	$CH_3S(O)CH_3 + OH \rightarrow CH_3S(O)CH_2 + H_2O$	0.0		E	(7)
101.	$CH_3S(O)CH_3 + OH \xrightarrow{M} CH_3S(OH)(O)CH_3$	5.8×10^{-11}		14	(6)

(continued)

	REACTION	RATE CONSTANT[a]	ACTIVATION ENERGY(K)	REF.	NOTE
102.	$CH_3S(OH)(O)CH_3 \xrightarrow{M} CH_3SO_2H + CH_3$	1.5×10^{7}	22	(6)	
103.	$CH_3S(OH)(O)CH_3+O_2 \rightarrow CH_3S(O)_2CH_3+HO_2$	1.2×10^{-12}	E	(6)	
104.	$CH_3S(O)CH_2 \xrightarrow{M} CH_3S + HCHO$	1.0×10^{2}	E	(8)	
105.	$CH_3S(O)CH_2 + O_2 \xrightarrow{M} CH_3S(O)CH_2OO$	1.0×10^{-12}	E	(10)	
106.	$CH_3S(O)CH_2OO+NO \rightarrow CH_3S(O)CH_2O+NO_2$	6.0×10^{-12}	E	(11)	
107.	$CH_3S(O)CH_2OO + CH_3S \rightarrow CH_3S(O)CH_2O + CH_3SO$	5.0×10^{-11}	E	(11)	
108.	$CH_3S(O)CH_2OO + CH_3SO \rightarrow CH_3S(O)CH_2O + CH_3SO_2$	4.0×10^{-12}	E	(11)	
109.	$CH_3S(O)CH_2OO + CH_3SO_2 \rightarrow CH_3S(O)CH_2O + CH_3SO_3$	2.5×10^{-13}	E	(11)	
110.	$CH_3S(O)CH_2OO + HO_2 \rightarrow CH_3S(O)CH_2OOH + O_2$	1.5×10^{-12}	E	(11)	
111.	$CH_3S(O)CH_2OO + CH_3O_2 \rightarrow CH_3S(O)CH_2O + CH_3O + O_2$	1.8×10^{-13}	E	(11)	
112.	$2\ CH_3S(O)CH_2OO \rightarrow 2\ CH_3S(O)CH_2O + O_2$	8.6×10^{-14}	E	(11)	
113.	$CH_3S(O)CH_2O \xrightarrow{M} CH_3SO + HCHO$	1.0×10^{2}	E	(8)	
	$CH_3S(O)_2CH_3$ Reactions				
114.	$CH_3S(O)_2CH_3 + OH \rightarrow CH_3S(O)_2CH_2 + H_2O$	1.0×10^{-14}	E	(6)	
115.	$CH_3S(O)_2CH_2 + O_2 \xrightarrow{M} CH_3S(O)_2CH_2OO$	7.3×10^{-13}	E	(10)	
116.	$CH_3S(O)_2CH_2OO+NO \rightarrow CH_3S(O)_2CH_2O+NO_2$	5.0×10^{-12}	E	(11)	
117.	$CH_3S(O)_2CH_2OO + CH_3S \rightarrow CH_3S(O)_2CH_2O + CH_3SO$	5.0×10^{-11}	E	(11)	
118.	$CH_3S(O)_2CH_2OO + CH_3SO \rightarrow CH_3S(O)_2CH_2O + CH_3SO_2$	4.0×10^{-12}	E	(11)	
119.	$CH_3S(O)_2CH_2OO + CH_3SO_2 \rightarrow CH_3S(O)_2CH_2O + CH_3SO_3$	2.5×10^{-13}	E	(11)	
120.	$CH_3S(O)_2CH_2OO + HO_2 \rightarrow CH_3S(O)_2CH_2OOH + O_2$	1.5×10^{-12}	E	(11)	
121.	$CH_3S(O)_2CH_2OO + CH_3O_2 \rightarrow CH_3S(O)_2CH_2O + CH_3O + O_2$	1.8×10^{-13}	E	(11)	
122.	$2\ CH_3S(O)_2CH_2OO \rightarrow 2\ CH_3S(O)_2CH_2O + O_2$	8.6×10^{-14}	E	(11)	
123.	$CH_3S(O)_2CH_2O \xrightarrow{M} CH_3SO_2 + HCHO$	1.0×10^{1}	E	(8)	
	CH_3SOH and CH_3SO_2H Reactions				
124.	$CH_3SOH + OH \rightarrow CH_3SO + H_2O$	1.1×10^{-10}	E	(6)	
125.	$CH_3SOH + CH_3SO_3 \rightarrow CH_3SO + CH_3SO_3H$	3.4×10^{-12}	E	(6)	

(continued)

	REACTION	RATE CONSTANT[a]	ACTIVATION ENERGY(K)	REF.	NOTE
126.	$CH_3SOH + CH_3O \rightarrow CH_3SO + CH_3OH$	3.4×10^{-12}		E	(5)
127.	$CH_3SOH + O(^3P) \rightarrow CH_3SO + OH$	3.4×10^{-12}		E	(5)
128.	$CH_3SOH + NO_3 \rightarrow CH_3SO + HONO_2$	3.4×10^{-12}		E	(5)
129.	$CH_3SOH + HO_2 \rightarrow CH_3SO + H_2O_2$	8.5×10^{-13}		E	(6)
130.	$CH_3SOH + CH_3O_2 \rightarrow CH_3SO + CH_3OOH$	8.5×10^{-13}		E	(6)
131.	$CH_3SOH + NO_2 \rightarrow CH_3SO + HONO$	0.0		E	(7)
132.	$CH_3SOH + O_3 \rightarrow CH_3SO + OH + O_2$	0.0		E	(7)
133.	$CH_3SOH + CH_3SOH \rightarrow CH_3SS(O)CH_3 + H_2O$	3.6×10^{-18}		E	
134.	$CH_3SO_2H + OH \rightarrow CH_3SO_2 + H_2O$	1.6×10^{-11}		E	(6)
135.	$CH_3SO_2H + CH_3SO_3 \rightarrow CH_3SO_2 + CH_3SO_3H$	1.0×10^{-13}		E	(6)
136.	$CH_3SO_2H + CH_3O \rightarrow CH_3SO_2 + CH_3OH$	1.0×10^{-13}		E	(5)
137.	$CH_3SO_2H + O(^3P) \rightarrow CH_3SO_2 + OH$	1.0×10^{-13}		E	(5)
138.	$CH_3SO_2H + NO_3 \rightarrow CH_3SO_2 + HONO_2$	1.0×10^{-13}		E	(5)
139.	$CH_3SO_2H + HO_2 \rightarrow CH_3SO_2 + H_2O_2$	1.0×10^{-15}		E	(5)
140.	$CH_3SO_2H + CH_3O_2 \rightarrow CH_3SO_2 + CH_3OOH$	1.0×10^{-15}		E	(5)
	CH_3SO_x and $CH_3S(O)_xOO$ Reactions				
141.	$CH_3S + O_2 \xrightarrow{M} CH_3SOO$	5.8×10^{-17}		E	(6)
142.	$CH_3SOO \xrightarrow{M} CH_3S + O_2$	6.0×10^{2}		E	(6)
143.	$CH_3S + NO_2 \rightarrow CH_3SO + NO$	6.1×10^{-11}		21	(6)
144.	$CH_3S + NO_2 \xrightarrow{M} CH_3SNO_2$	6.1×10^{-13}		E	(6)
145.	$CH_3S + NO_3 \rightarrow CH_3SO + NO_2$	6.4×10^{-11}		E	(5)
146.	$CH_3S + O_3 \rightarrow CH_3SO + O_2$	6.0×10^{-12}		E	(6)
147.	$CH_3S + HO_2 \rightarrow CH_3SO + OH$	3.0×10^{-11}		E	(6)
148.	$CH_3S + CH_3O_2 \rightarrow CH_3SO + CH_3O$	6.1×10^{-11}		E	(6)
149.	$CH_3S + NO \xrightarrow{M} CH_3SNO$	2.87×10^{-11}		10	
150.	$CH_3SNO + h\nu \rightarrow CH_3S + NO$	$0.5k_{NO_2}$		E	
151.	$CH_3S + CH_3S \xrightarrow{M} CH_3SSCH_3$	4.15×10^{-11}		11	
152.	$CH_3S + CH_3SNO \rightarrow CH_3SSCH_3 + NO$	1.4×10^{-12}		E	(6)
153.	$CH_3S + OH \xrightarrow{M} CH_3SOH$	5.0×10^{-11}		E	(5)
154.	$CH_3SOO + NO \rightarrow CH_3SO + NO_2$	1.4×10^{-11}		E	(11)
155.	$CH_3SOO + CH_3S \rightarrow CH_3SO + CH_3SO$	8.0×10^{-11}		E	(11)
156.	$CH_3SOO + CH_3SO \rightarrow CH_3SO + CH_3SO_2$	9.0×10^{-12}		E	(11)
157.	$CH_3SOO + CH_3SO_2 \rightarrow CH_3SO + CH_3SO_3$	3.0×10^{-13}		E	(11)
158.	$CH_3SOO + HO_2 \rightarrow CH_3SOOH + O_2$	4.0×10^{-12}		E	(11)
159.	$CH_3SOO + CH_3O_2 \rightarrow CH_3SO + CH_3O + O_2$	5.5×10^{-12}		E	(11)
160.	$CH_3SOO + CH_3SOO \rightarrow 2\ CH_3SO + O_2$	6.0×10^{-12}		E	(11)

(continued)

	REACTION	RATE CONSTANT[a]	ACTIVATION ENERGY(K)	REF.	NOTE
161.	$CH_3SO \xrightarrow{M} SO + CH_3$	5.0×10^{-5}	2.52×10^{4}	E	(6)
162.	$CH_3SO + O_2 \xrightarrow{M} CH_3S(O)OO$	7.7×10^{-18}		E	(6)
161.	$CH_3SO \xrightarrow{M} SO + CH_3$	5.0×10^{-5}	2.52×10^{4}	E	(6)
162.	$CH_3SO + O_2 \xrightarrow{M} CH_3S(O)OO$	7.7×10^{-18}		E	(6)
163.	$CH_3S(O)OO \xrightarrow{M} CH_3SO + O_2$	1.7×10^{2}		E	(6)
164.	$CH_3SO + NO_2 \rightarrow CH_3SO_2 + NO$	3.0×10^{-12}		E	(6)
165.	$CH_3SO + NO_2 \xrightarrow{M} CH_3S(O)NO_2$	0.0		E	(7)
166.	$CH_3SO + NO_3 \rightarrow CH_3SO_2 + NO_2$	8.0×10^{-12}		E	
167.	$CH_3SO + O_3 \rightarrow CH_3SO_2 + O_2$	2.0×10^{-12}		E	(6)
168.	$CH_3SO + HO_2 \rightarrow CH_3SO_2 + OH$	1.5×10^{-12}		E	(6)
169.	$CH_3SO + CH_3O_2 \rightarrow CH_3SO_2 + CH_3O$	3.0×10^{-12}		E	(6)
170.	$CH_3SO + NO \xrightarrow{M} CH_3S(O)NO$	0.0		E	(7)
171.	$CH_3SO + CH_3SO \rightarrow CH_3S + CH_3SO_2$	7.5×10^{-12}		E	
172.	$CH_3SO + CH_3SNO \rightarrow CH_3S(O)SCH_3 + NO$	6.8×10^{-13}		E	
173.	$CH_3SO + OH \xrightarrow{M} CH_3SO_2H$	5.0×10^{-11}		E	(5)
174.	$CH_3S(O)OO + NO \rightarrow CH_3SO_2 + NO_2$	8.0×10^{-12}		E	(11)
175.	$CH_3S(O)OO + CH_3S \rightarrow CH_3SO_2 + CH_3SO$	7.0×10^{-11}		E	(11)
176.	$CH_3S(O)OO + CH_3SO \rightarrow CH_3SO_2 + CH_3SO_2$	8.1×10^{-12}		E	(11)
177.	$CH_3S(O)OO + CH_3SO_2 \rightarrow CH_3SO_2 + CH_3SO_3$	3.0×10^{-13}		E	(11)
178.	$CH_3S(O)OO + HO_2 \rightarrow CH_3S(O)OOH + O_2$	3.0×10^{-12}		E	(11)
179.	$CH_3S(O)OO + CH_3O_2 \rightarrow CH_3SO_2 + CH_3O + O_2$	5.5×10^{-12}		E	(11)
180.	$CH_3S(O)OO + CH_3S(O)OO \rightarrow 2\ CH_3SO_2 + O_2$	6.0×10^{-12}		E	(11)
181.	$CH_3S(O)OO + NO_2 \xrightarrow{M} CH_3S(O)OONO_2$	1.0×10^{-12}		E	(11)
182.	$CH_3S(O)OONO_2 \xrightarrow{M} CH_3S(O)OO + NO_2$	4.2×10^{-3}		E	(9)
183.	$CH_3S(O)OO + CH_3SOH \rightarrow CH_3S(O)OOH + CH_3SO$	4.0×10^{-13}		E	(11)
184.	$CH_3SO_2 \xrightarrow{M} SO_2 + CH_3$	1.1×10^{1}	8.656×10^{3}	E	(6)
185.	$CH_3SO_2 + O_2 \xrightarrow{M} CH_3S(O)_2OO$	2.6×10^{-18}		E	(6)
186.	$CH_3S(O)_2OO \xrightarrow{M} CH_3SO_2 + O_2$	3.3×10^{0}		E	(6)
187.	$CH_3SO_2 + NO_2 \rightarrow CH_3SO_3 + NO$	1.0×10^{-14}		E	(6)
188.	$CH_3SO_2 + NO_2 \xrightarrow{M} CH_3S(O)_2NO_2$	0.0		E	(7)
189.	$CH_3SO_2 + NO_3 \rightarrow CH_3SO_3 + NO_2$	1.0×10^{-14}		E	(5)
190.	$CH_3SO_2 + O_3 \rightarrow CH_3SO_3 + O_2$	5.0×10^{-15}		E	(6)
191.	$CH_3SO_2 + HO_2 \rightarrow CH_3SO_3 + OH$	2.5×10^{-13}		E	(6)
192.	$CH_3SO_2 + CH_3O_2 \rightarrow CH_3SO_3 + CH_3O$	2.5×10^{-13}		E	(6)

(continued)

	REACTION	RATE CONSTANT[a]	ACTIVATION ENERGY(K)	REF.	NOTE
193.	$CH_3SO_2 + NO \xrightarrow{M} CH_3S(O)_2NO$	0.0		E	(7)
194.	$CH_3SO_2 + CH_3S \rightarrow CH_3S(O)_2SCH_3$	4.2×10^{-11}		E	(5)
195.	$CH_3SO_2 + CH_3SO_2 \rightarrow CH_3SO + CH_3SO_3$	7.5×10^{-12}		E	(5)
196.	$CH_3SO_2 + CH_3SNO \rightarrow CH_3S(O)_2SCH_3 + NO$	6.8×10^{-13}		E	
197.	$CH_3SO_2 + OH \xrightarrow{M} CH_3SO_3H$	5.0×10^{-11}		E	(5)
198.	$CH_3S(O)_2OO + NO \rightarrow CH_3SO_3 + NO_2$	1.0×10^{-11}		E	(11)
199.	$CH_3S(O)_2OO + CH_3S \rightarrow CH_3SO_3 + CH_3SO$	6.0×10^{-11}		E	(11)
200.	$CH_3S(O)_2OO + CH_3SO \rightarrow CH_3SO_3 + CH_3SO_2$	8.0×10^{-12}		E	(11)
201.	$CH_3S(O)_2OO + CH_3SO_2 \rightarrow CH_3SO_3 + CH_3SO_3$	3.0×10^{-13}		E	(11)
202.	$CH_3S(O)_2OO + HO_2 \rightarrow CH_3S(O)_2OOH + O_2$	2.0×10^{-12}		E	(11)
203.	$CH_3S(O)_2OO + CH_3O_2 \rightarrow CH_3SO_3 + CH_3O + O_2$	5.5×10^{-12}		E	(11)
204.	$CH_3S(O)_2OO + CH_3S(O)_2OO \rightarrow 2CH_3SO_3 + O_2$	6.0×10^{-12}		E	(11)
205.	$CH_3S(O)_2OO + NO_2 \xrightarrow{M} CH_3S(O)_2OONO_2$	1.0×10^{-12}		E	(11)
206.	$CH_3S(O)_2OONO_2 \xrightarrow{M} CH_3S(O)_2OO + NO_2$	4.2×10^{-3}		E	(9)
207.	$CH_3S(O)_2OO + CH_3SOH \rightarrow CH_3S(O)_2OOH + CH_3SO$	4.0×10^{-13}		E	(11)
	CH_3SO_3H Formation				
208.	$CH_3SO_3 \xrightarrow{M} SO_3 + CH_3$	1.6×10^{-1}		E	(6)
209.	$CH_3SO_3 + HCHO \xrightarrow{O_2} CH_3SO_3H + HO_2 + CO$	1.6×10^{-15}		E	(6)
210.	$CH_3SO_3 + CH_3SCH_3 \rightarrow CH_3SO_3H + CH_3SCH_2$	6.8×10^{-14}		E	(6)
211.	$CH_3SO_3 + CH_3SCH_3 \xrightarrow{M}$ Adduct	0.0		E	(6)
212.	$CH_3SO_3 + HO_2 \rightarrow CH_3SO_3H + O_2$	5.0×10^{-11}		E	
213.	$CH_3SO_3 + HONO \rightarrow CH_3SO_3H + NO_2$	6.6×10^{-16}		E	
214.	$CH_3SO_3 + H_2O_2 \rightarrow CH_3SO_3H + HO_2$	3.0×10^{-16}		E	
215.	$CH_3SO_3 + CH_3OOH \rightarrow CH_3SO_3H + CH_3O_2$	3.0×10^{-16}		E	
216.	$CH_3SO_3 + CH_3OH \xrightarrow{O_2} CH_3SO_3H + HO_2 + HCHO$	1.0×10^{-16}		E	
217.	$CH_3SO_3 + NO_2 \xrightarrow{M} CH_3S(O)_2ONO_2$	3.0×10^{-15}		E	(6)
218.	$CH_3S(O)_2ONO_2 + H_2O \rightarrow CH_3SO_3H + HONO_2$	1.0×10^{-15}		E	(5)
219.	$CH_3SO_3 + NO \xrightarrow{M} CH_3S(O)_2ONO$	3.0×10^{-15}		E	(6)
220.	$CH_3S(O)_2ONO + H_2O \rightarrow CH_3SO_3H + HONO$	1.0×10^{-15}		E	(5)

TABLE 8. Atmospheric Photooxidation Mechanism for Dimethyl Disulfide

REACTION	RATE CONSTANT[a]	ACTIVATION ENERGY(K)	REF.	NOTE
Initial Reactions				
221. $CH_3SSCH_3 + OH \rightarrow CH_3SSCH_2 + H_2O$	0.0		E	(6)
222. $CH_3SSCH_3 + OH \rightarrow CH_3SOH + CH_3S$	2.0×10^{-10}	-3.80×10^{2}	3	(6)
223. $CH_3SSCH_3 + O(^3P) \rightarrow CH_3SO + CH_3S$	1.3×10^{-10}	-2.50×10^{2}	3,8,20	
224. $CH_3SSCH_3 + NO_3 \rightarrow CH_3SSCH_2 + HONO_2$	0.0		E	(7)
225. $CH_3SSCH_3 + NO_3 \xrightarrow{M} CH_3S(ONO_2)SCH_3$	7.0×10^{-13}	0.0	3	(6)
226. $CH_3SSCH_3 + h\nu \rightarrow CH_3S + CH_3S$	$5.0\times10^{-3}k_{NO_2}$		E	(6)
Adduct Reactions and other Radical Reactions				
227. $CH_3S(ONO_2)SCH_3 \xrightarrow{M} CH_3SONO_2 + CH_3S$	1.0×10^{2}		E	(8)
228. $CH_3S(ONO_2)SCH_3 + O_2 \rightarrow$ Product	0.0		E	(7)
229. $CH_3SONO_2 \xrightarrow{M} CH_3SO + NO_2$	1.0×10^{0}		E	(8)
CH_3SOH and CH_3SO_2H Reactions				
230. $CH_3SOH + OH \rightarrow CH_3SO + H_2O$	1.1×10^{-10}		E	(6)
231. $CH_3SOH + CH_3SO_3 \rightarrow CH_3SO + CH_3SO_3H$	3.4×10^{-12}		E	(6)
232. $CH_3SOH + CH_3O \rightarrow CH_3SO + CH_3OH$	3.4×10^{-12}		E	(5)
233. $CH_3SOH + O(^3P) \rightarrow CH_3SO + OH$	3.4×10^{-12}		E	(5)
234. $CH_3SOH + NO_3 \rightarrow CH_3SO + HONO_2$	3.4×10^{-12}		E	(5)
235. $CH_3SOH + HO_2 \rightarrow CH_3SO + H_2O_2$	8.5×10^{-13}		E	(6)
236. $CH_3SOH + CH_3O_2 \rightarrow CH_3SO + CH_3OOH$	8.5×10^{-13}		E	(6)
237. $CH_3SOH + NO_2 \rightarrow CH_3SO + HONO$	0.0		E	(7)
238. $CH_3SOH + O_3 \rightarrow CH_3SO + OH + O_2$	0.0		E	(7)
239. $CH_3SOH + CH_3SOH \rightarrow CH_3SS(O)CH_3 + H_2O$	3.6×10^{-18}		E	
240. $CH_3SO_2H + OH \rightarrow CH_3SO_2 + H_2O$	1.6×10^{-11}		E	(6)
241. $CH_3SO_2H + CH_3SO_3 \rightarrow CH_3SO_2 + CH_3SO_3H$	1.0×10^{-13}		E	(6)
242. $CH_3SO_2H + CH_3O \rightarrow CH_3SO_2 + CH_3OH$	1.0×10^{-13}		E	(5)
243. $CH_3SO_2H + O(^3P) \rightarrow CH_3SO_2 + OH$	1.0×10^{-13}		E	(5)
244. $CH_3SO_2H + NO_3 \rightarrow CH_3SO_2 + HONO_2$	1.0×10^{-13}		E	(5)
245. $CH_3SO_2H + HO_2 \rightarrow CH_3SO_2 + H_2O_2$	1.0×10^{-15}		E	(5)
246. $CH_3SO_2H + CH_3O_2 \rightarrow CH_3SO_2 + CH_3OOH$	1.0×10^{-15}		E	(5)
CH_3SO_x and $CH_3S(O)_xOO$ Reactions				
247. $CH_3S + O_2 \xrightarrow{M} CH_3SOO$	5.8×10^{-17}		E	(6)
248. $CH_3SOO \xrightarrow{M} CH_3S + O_2$	6.0×10^{2}		E	(6)

(continued)

	REACTION	RATE CONSTANT[a]	ACTIVATION ENERGY(K)	REF.	NOTE
249.	$CH_3S + NO_2 \rightarrow CH_3SO + NO$	6.1×10^{-11}		21	(6)
250.	$CH_3S + NO_2 \xrightarrow{M} CH_3SNO_2$	6.1×10^{-13}		E	(6)
251.	$CH_3S + NO_3 \rightarrow CH_3SO + NO_2$	6.4×10^{-11}		E	(5)
252.	$CH_3S + O_3 \rightarrow CH_3SO + O_2$	6.0×10^{-12}		E	(6)
253.	$CH_3S + HO_2 \rightarrow CH_3SO + OH$	3.0×10^{-11}		E	(6)
254.	$CH_3S + CH_3O_2 \rightarrow CH_3SO + CH_3O$	6.1×10^{-11}		E	(6)
255.	$CH_3S + NO \xrightarrow{M} CH_3SNO$	2.87×10^{-11}		10	
256.	$CH_3SNO + h\nu \rightarrow CH_3S + NO$	$0.5k_{NO_2}$		E	
257.	$CH_3S + CH_3S \xrightarrow{M} CH_3SSCH_3$	4.15×10^{-11}		11	
258.	$CH_3S + CH_3SNO \rightarrow CH_3SSCH_3 + NO$	1.4×10^{-12}		E	(6)
259.	$CH_3S + OH \xrightarrow{M} CH_3SOH$	5.0×10^{-11}		E	(5)
260.	$CH_3SOO + NO \rightarrow CH_3SO + NO_2$	1.4×10^{-11}		E	(11)
261.	$CH_3SOO + CH_3S \rightarrow CH_3SO + CH_3SO$	8.0×10^{-11}		E	(11)
262.	$CH_3SOO + CH_3SO \rightarrow CH_3SO + CH_3SO_2$	9.0×10^{-12}		E	(11)
263.	$CH_3SOO + CH_3SO_2 \rightarrow CH_3SO + CH_3SO_3$	3.0×10^{-13}		E	(11)
264.	$CH_3SOO + HO_2 \rightarrow CH_3SOOH + O_2$	4.0×10^{-12}		E	(11)
265.	$CH_3SOO + CH_3O_2 \rightarrow CH_3SO + CH_3O + O_2$	5.5×10^{-12}		E	(11)
266.	$CH_3SOO + CH_3SOO \rightarrow 2\ CH_3SO + O_2$	6.0×10^{-12}		E	(11)
267.	$CH_3SO \xrightarrow{M} SO + CH_3$	5.0×10^{-5}	2.52×10^{4}	E	(6)
268.	$CH_3SO + O_2 \xrightarrow{M} CH_3S(O)OO$	7.7×10^{-18}		E	(6)
269.	$CH_3S(O)OO \xrightarrow{M} CH_3SO + O_2$	1.7×10^{2}		E	(6)
270.	$CH_3SO + NO_2 \rightarrow CH_3SO_2 + NO$	3.0×10^{-12}		E	(6)
271.	$CH_3SO + NO_2 \xrightarrow{M} CH_3S(O)NO_2$	0.0		E	(7)
272.	$CH_3SO + NO_3 \rightarrow CH_3SO_2 + NO_2$	8.0×10^{-12}		E	
273.	$CH_3SO + O_3 \rightarrow CH_3SO_2 + O_2$	2.0×10^{-12}		E	(6)
274.	$CH_3SO + HO_2 \rightarrow CH_3SO_2 + OH$	1.5×10^{-12}		E	(6)
275.	$CH_3SO + CH_3O_2 \rightarrow CH_3SO_2 + CH_3O$	3.0×10^{-12}		E	(6)
276.	$CH_3SO + NO \xrightarrow{M} CH_3S(O)NO$	0.0		E	(7)
277.	$CH_3SO + CH_3SO \rightarrow CH_3S + CH_3SO_2$	7.5×10^{-12}		E	
278.	$CH_3SO + CH_3SNO \rightarrow CH_3S(O)SCH_3 + NO$	6.8×10^{-13}		E	
279.	$CH_3SO + OH \xrightarrow{M} CH_3SO_2H$	5.0×10^{-11}		E	(5)
280.	$CH_3S(O)OO + NO \rightarrow CH_3SO_2 + NO_2$	8.0×10^{-12}		E	(11)
281.	$CH_3S(O)OO + CH_3S \rightarrow CH_3SO_2 + CH_3SO$	7.0×10^{-11}		E	(11)
282.	$CH_3S(O)OO + CH_3SO \rightarrow CH_3SO_2 + CH_3SO_2$	8.1×10^{-12}		E	(11)
283.	$CH_3S(O)OO + CH_3SO_2 \rightarrow CH_3SO_2 + CH_3SO_3$	3.0×10^{-13}		E	(11)
284.	$CH_3S(O)OO + HO_2 \rightarrow CH_3S(O)OOH + O_2$	3.0×10^{-12}		E	(11)
285.	$CH_3S(O)OO + CH_3O_2 \rightarrow CH_3SO_2 + CH_3O + O_2$	5.5×10^{-12}		E	(11)

(continued)

	REACTION	RATE CONSTANT[a]	ACTIVATION ENERGY(K)	REF.	NOTE
286.	$CH_3S(O)OO + CH_3S(O)OO \rightarrow 2\ CH_3SO_2 + O_2$	6.0×10^{-12}		E	(11)
287.	$CH_3S(O)OO + NO_2 \xrightarrow{M} CH_3S(O)OONO_2$	1.0×10^{-12}		E	(11)
288.	$CH_3S(O)OONO_2 \xrightarrow{M} CH_3S(O)OO + NO_2$	4.2×10^{-3}		E	(9)
289.	$CH_3S(O)OO + CH_3SOH \rightarrow CH_3S(O)OOH + CH_3SO$	4.0×10^{-13}		E	(11)
290.	$CH_3SO_2 \xrightarrow{M} SO_2 + CH_3$	1.1×10^{1}	8.656×10^{3}	E	(6)
291.	$CH_3SO_2 + O_2 \xrightarrow{M} CH_3S(O)_2OO$	2.6×10^{-18}		E	(6)
292.	$CH_3S(O)_2OO \xrightarrow{M} CH_3SO_2 + O_2$	3.3×10^{0}		E	(6)
293.	$CH_3SO_2 + NO_2 \rightarrow CH_3SO_3 + NO$	1.0×10^{-14}		E	(6)
294.	$CH_3SO_2 + NO_2 \xrightarrow{M} CH_3S(O)_2NO_2$	0.0		E	(7)
295.	$CH_3SO_2 + NO_3 \rightarrow CH_3SO_3 + NO_2$	1.0×10^{-14}		E	(5)
296.	$CH_3SO_2 + O_3 \rightarrow CH_3SO_3 + O_2$	5.0×10^{-15}		E	(6)
297.	$CH_3SO_2 + HO_2 \rightarrow CH_3SO_3 + OH$	2.5×10^{-13}		E	(6)
298.	$CH_3SO_2 + CH_3O_2 \rightarrow CH_3SO_3 + CH_3O$	2.5×10^{-13}		E	(6)
299.	$CH_3SO_2 + NO \xrightarrow{M} CH_3S(O)_2NO$	0.0		E	(7)
300.	$CH_3SO_2 + CH_3S \rightarrow CH_3S(O)_2SCH_3$	4.2×10^{-11}		E	(5)
301.	$CH_3SO_2 + CH_3SO_2 \rightarrow CH_3SO + CH_3SO_3$	7.5×10^{-12}		E	(5)
302.	$CH_3SO_2 + CH_3SNO \rightarrow CH_3S(O)_2SCH_3 + NO$	6.8×10^{-13}		E	
303.	$CH_3SO_2 + OH \xrightarrow{M} CH_3SO_3H$	5.0×10^{-11}		E	(5)
304.	$CH_3S(O)_2OO + NO \rightarrow CH_3SO_3 + NO_2$	1.0×10^{-11}		E	(11)
305.	$CH_3S(O)_2OO + CH_3S \rightarrow CH_3SO_3 + CH_3SO$	6.0×10^{-11}		E	(11)
306.	$CH_3S(O)_2OO + CH_3SO \rightarrow CH_3SO_3 + CH_3SO_2$	8.0×10^{-12}		E	(11)
307.	$CH_3S(O)_2OO + CH_3SO_2 \rightarrow CH_3SO_3 + CH_3SO_3$	3.0×10^{-13}		E	(11)
308.	$CH_3S(O)_2OO + HO_2 \rightarrow CH_3S(O)_2OOH + O_2$	2.0×10^{-12}		E	(11)
309.	$CH_3S(O)_2OO + CH_3O_2 \rightarrow CH_3SO_3 + CH_3O + O_2$	5.5×10^{-12}		E	(11)
310.	$CH_3S(O)_2OO + CH_3S(O)_2OO \rightarrow 2CH_3SO_3 + O_2$	6.0×10^{-12}		E	(11)
311.	$CH_3S(O)_2OO + NO_2 \xrightarrow{M} CH_3S(O)_2OONO_2$	1.0×10^{-12}		E	(11)
312.	$CH_3S(O)_2OONO_2 \xrightarrow{M} CH_3S(O)_2OO + NO_2$	4.2×10^{-3}		E	(9)
313.	$CH_3S(O)_2OO + CH_3SOH \rightarrow CH_3S(O)_2OOH + CH_3SO$	4.0×10^{-13}		E	(11)
	CH_3SO_3H Formation				
314.	$CH_3SO_3 \xrightarrow{M} SO_3 + CH_3$	1.6×10^{-1}		E	(6)
315.	$CH_3SO_3 + HCHO \xrightarrow{O_2} CH_3SO_3H + HO_2 + CO$	1.6×10^{-15}		E	(6)
316.	$CH_3SO_3 + CH_3SSCH_3 \rightarrow CH_3SO_3H + CH_3SSCH_2$	0.0		E	(6)
317.	$CH_3SO_3 + CH_3SSCH_3 \xrightarrow{M}$ Adduct	0.0		E	(6)

(continued)

	REACTION	RATE CONSTANT[a]	ACTIVATION ENERGY(K)	REF.	NOTE
318.	$CH_3SO_3 + HO_2 \rightarrow CH_3SO_3H + O_2$	5.0×10^{-11}		E	
319.	$CH_3SO_3 + HONO \rightarrow CH_3SO_3H + NO_2$	6.6×10^{-16}		E	
320.	$CH_3SO_3 + H_2O_2 \rightarrow CH_3SO_3H + HO_2$	3.0×10^{-16}		E	
321.	$CH_3SO_3 + CH_3OOH \rightarrow CH_3SO_3H + CH_3O_2$	3.0×10^{-16}		E	
322.	$CH_3SO_3 + CH_3OH \xrightarrow{O_2} CH_3SO_3H + HO_2 + HCHO$	1.0×10^{-16}		E	
323.	$CH_3SO_3 + NO_2 \xrightarrow{M} CH_3S(O)_2ONO_2$	3.0×10^{-15}		E	(6)
324.	$CH_3S(O)_2ONO_2 + H_2O \rightarrow CH_3SO_3H + HONO_2$	1.0×10^{-15}		E	(5)
325.	$CH_3SO_3 + NO \xrightarrow{M} CH_3S(O)_2ONO$	3.0×10^{-15}		E	(6)
326.	$CH_3S(O)_2ONO + H_2O \rightarrow CH_3SO_3H + HONO$	1.0×10^{-15}		E	(5)

Table 9 Reactions Common to Organosulfur Mechanisms:

SO_x Chemistry and Chamber Wall Reactions

	REACTION	RATE CONSTANT[a]	ACTIVATION ENERGY(K)	REF.	NOTE
	SO_x Reactions				
327.	$SO + O_2 \rightarrow SO_2 + O(^3P)$	6.7×10^{-17}	2.275×10^3	3	
328.	$SO + NO_2 \rightarrow SO_2 + NO$	1.4×10^{-11}		3	
329.	$SO + O_3 \rightarrow SO_2 + O_2$	8.9×10^{-14}	1.17×10^3	3	
330.	$SO + O(^3P) \xrightarrow{M} SO_2$	2.2×10^{-11}		12	
331.	$SO + OH \xrightarrow{O_2} SO_2 + HO_2$	1.1×10^{-10}		12	
332.	$SO + SO_3 \rightarrow SO_2 + SO_2$	2.0×10^{-15}		12	
333.	$SO_2 + OH \xrightarrow{M} HOSO_2$	1.1×10^{-12}	-2.31×10^2	3,17	(12)
334.	$SO_2 + O(^3P) \xrightarrow{M} SO_3$	3.4×10^{-14}	1.0×10^3	6,17	
335.	$SO_2 + HO_2 \rightarrow SO_3 + OH$	1.0×10^{-18}		2,3	
336.	$SO_2 + CH_3O_2 \rightarrow CH_3O + SO_3$	5.0×10^{-17}		2,3	
337.	$SO_2 + CH_3O \xrightarrow{M} CH_3OSO_2$	5.5×10^{-13}		7	
338.	$SO_2 + CH_3 \xrightarrow{M} CH_3SO_2$	2.9×10^{-13}		12	
339.	$SO_2 + h\nu \rightarrow SO_2^*$	$2.0k_{NO_2}$		12	
340.	$SO_2^* \xrightarrow{M} SO_2$	3.7×10^6		12	
341.	$SO_2^* + SO_2 \rightarrow SO_3 + SO$	6.3×10^{-13}		12	
342.	$SO_2^* + CO \rightarrow SO + CO_2$	1.1×10^{-14}		12	
343.	$HOSO_2 + O_2 \rightarrow SO_3 + HO_2$	4.0×10^{-13}	1.0×10^3	3,17	
344.	$HOSO_2 + OH \xrightarrow{M} H_2SO_4$	1.0×10^{-11}		E13[b]	
345.	$SO_3 + H_2O \xrightarrow{M} H_2SO_4$	9.1×10^{-13}		2,17	
346.	$SO_3 + O(^3P) \rightarrow SO_2 + O_2$	7.0×10^{-13}		28	
	Wall Effects				
347.	$CH_3SCH_3 \rightarrow$ Wall	1.5×10^{-6}		23	
348.	$CH_3SSCH_3 \rightarrow$ Wall	1.6×10^{-6}		23	
349.	$SO_2 \rightarrow$ Wall	3.0×10^{-6}		23	
350.	$O_3 \rightarrow$ Wall	4.5×10^{-6}		23	
351.	$HNO_3 \rightarrow$ Wall	5.8×10^{-5}		16	
352.	$NO_2 + H_2O +$ Wall $\rightarrow$ HONO	6.8×10^{-24}		19	
353.	$NO_2 +$ Wall $\rightarrow$ HONO	6.5×10^{-7}		19	
354.	$N_2O_5 +$ Wall(or aerosol) $\rightarrow$ 2 HONO2	8.3×10^{-3}		E	

a. Rate constants are at 298 K, 1 atm in units of molecule, cm^3 and sec. See Part II for detailed discussion.

b. 'E' is used to indicate the rate constant was estimated in the reference whose number follows 'E'. In the absence of a number following 'E', the rate constant has been estimated in the present work.

References

1. Atkinson et al. [1980]; 2. Atkinson and Lloyd [1984b]; 3. Atkinson et al. [1989]; 4. Balla and Heicklen [1984]; 5. Baulch et al. [1982]; 6. Baulch et al. [1984]; 7. Calvert and Stockwell [1984]; 8. Cvetanović et al. [1981]; 9. Demore et al. [1982]; 10. Balla et al. [1986]; 11. Graham et al. [1964a]; 12. Graedel [1977]; 13. Graedel [1979]; 14. Barnes et al. [1986b]; 15. Schäfer et al. [1978]; 16. Grosjean [1985]; 17. Kerr and Calvert [1984]; 18. Leone and Seinfeld [1984]; 19. Leone et al. [1985]; 20. Nip et al. [1981]; 21. Tyndall and Ravishankara [1988]; 22. Veltwisch et al. [1980]; 23. Yin et al. [1989]; 24. Veyret et al. [1989]; 25. Burrows et al. [1989]; 26. Vaghjiani and Ravishankara [1989]; 27. Wallington et al. [1986b]; 28. Calvert et al. [1978].

Notes:

1. k_{NO_2} was estimated theoretically [Demerjian et al., 1980] for simulation of the experiments. See Part II for discussion.
2. The rate constant data of reaction between HO_2 and HO_2 were fit by the expression [Atkinson and Lloyd, 1984b],

$$k = [2.2 \times 10^{-13} \exp(620/T) + 1.9 \times 10^{-33} [M] \exp(980/T)] \times [1 + 1.4 \times 10^{-21} [H_2O] \exp(2200/T)]$$

$cm^3 molecule^{-1} s^{-1}$, which can be expressed by reactions of (16)–(19).
3. Reaction (14) is the combination of the following three reactions,

$$\begin{aligned} O_3 + h\nu &\rightarrow O(^1D) + O_2 \\ O(^1D) + O_2 &\rightarrow O(^3P) + O_2 \\ O(^1D) + H_2O &\rightarrow 2\ OH \end{aligned}$$

4. CH_3ONO is assumed to have the same photolysis rate as HONO.
5. The system reactivity and the product distribution are not sensitive to the values of these reactions.
6. See text of Part I and II for detailed discussion.
7. These reactions are assumed to be negligible.
8. These unimolecular reactions are assumed to decompose rapidly and the simulations are not sensitive to them.
9. These unimolecular reactions are assumed to decompose rapidly, however, the system reactivity and the product distribution are sensitive to these rate constants, which are estimated mainly based on the product studies.
10. The rate constants are estimated from the similar reactions of $R + O_2$.
11. These rate constants are basically estimated from the corresponding reactions of similar peroxy radicals. Also the structual difference of the peroxy radicals is considered.
12. The temperature coefficient, which is a function of the total pressure, has been expressed for the temperature range 200–300 K by Kerr and Calvert [1984] as

$$-(E/R)/K = 3.6896 \times 10^{-4} \times (P/Torr)^2 - 6.793 \times 10^{-1} \times (P/Torr) + 5.3374 \times 10^2$$

REFERENCES

Andreae, M. O., and H. Raemdonck, Dimethyl sulfide in the surface ocean and the marine atmosphere: A global view, *Science, 221,* 744–747, 1983.

Andreae, M. O., R. J. Ferek, F. Bermond, K. P. Byrd, R. T. Engstrom, S. Hardin, P. D. Houmira, F. Le Marrec, H. Raemdonck, and R. B. Chatfield, Dimethyl sulfide in the marine atmosphere, *J. Geophys. Res., 90,* 12891–12901, 1985.

Atkinson, R., R. A. Perry, and J. N. Pitts, Jr., Rate constants for the reaction of the OH radical with CH_3SH and CH_3NH_2 over the temperature range 299–426 K, *J. Chem. Phys., 66,* 1578–1581, 1977.

Atkinson, R., W. P. L. Carter, K. R. Darnall, A. M. Winer, and J. N. Pitts, Jr., A smog chamber and modeling study of the gas phase NO_x–air photooxidation of toluene and the cresols, *Int. J. Chem. Kinet., 12,* 779–836, 1980.

Atkinson, R., J. N. Pitts, Jr., and S. M. Aschmann, Tropospheric reactions of dimethyl sulfide with NO_3 and OH radicals, *J. Phys. Chem., 88,* 1584–1587, 1984a.

Atkinson, R., and A. C. Lloyd, Evaluation of kinetic and mechanistic data for modeling of photochemical smog, *J. Phys. Chem. Ref. Data, 13,* 315–444, 1984b.

Atkinson, R., Kinetics and mechanisms of the gas-phase reactions of the hydroxyl radical with organic compounds under atmospheric conditions, *Chem. Rev., 85,* 69–201, 1985.

Atkinson, R., S. M. Aschmann, and J. N. Pitts, Jr., Kinetics of the reaction of NO_3 radical with CH_3SSCH_3, *J. Geophys. Res., 93,* 7125–7126, 1988.

Atkinson, R., D. L. Baulch, R. A. Cox, R. F. Hampson, Jr., J. A. Kerr, and J. Troe, Evaluated kinetic and photochemical data for atmospheric chemistry:

Supplement III, *J. Phys. Chem. Ref. Data, 13,* 881–1097, 1989.

Balla, R. J., and J. Heicklen, Oxidation of sulfur compounds. II. Thermal reactions of NO_2 with aliphatic sulfur compounds, *J. Phys. Chem., 88,* 6314–6317, 1984.

Balla, R. J., and J. Heicklen, Oxidation of sulfur compounds III: The photolysis of $(CH_3S)_2$ in the presence of O_2, *J. Photochem., 29,* 297–310, 1985.

Balla, R. J., H. H. Nelson, and J. R. McDonald, Kinetics of the reaction of CH_3S with NO, NO_2 and O_2, *Chem. Phys., 109,* 101–107, 1986.

Balla, R. J., B. R. Weiner, and H. H. Nelson, Kinetics of the reaction of CH_3S with unsaturated hydrocarbons, *J. Am. Chem. Soc., 109,* 4804–4808, 1987.

Barnes, I., V. Bastian, and K. H. Becker, Reactions of OH radicals with reduced sulfur compounds under atmospheric conditions, *Physico-chemical behaviour of atmospheric pollutants,* pp. 149–157, Proceedings of the Third European Symposium, edited by Versino, B., and G. Angeletti, Varese, Italy, Apr. 1984.

Barnes, I., V. Bastian, K. H. Becker, E. H. Fink, and W. Nelsen, Oxidation of sulphur compounds in the atmosphere: I. Rate constants of OH radical reactions with sulphur dioxide, hydrogen sulphide, alipaatic thiols and thiophenol, *J. Atmos. Chem., 4,* 445–466, 1986a.

Barnes, I., V. Bastian, and K. H. Becker, Products and kinetics of the OH initiated oxidation of SO_2, CH_3SH, DMS, DMDS, DMSO, *Physico-chemical behaviour of atmospheric pollutants,* pp. 327–337, Proceedings of the Fourth European Symposium, edited by Angeletti, G., and G. Restelli, Stresa, Italy, Sept. 1986b.

Barnes, I., K. H. Becker, P. Carlier, and G. Mouvier, FTIR study of the DMS/NO_2 /I_2/N_2 photolysis system: The reaction of IO radcial with DMS, *Int. J. Chem. Kinet., 19,* 489–501, 1987a.

Barnes, I., V. Bastian, K. H. Becker, and H. Niki, FTIR spectroscopic studies of the CH_3S + NO_2 reaction under atmospheric conditions, *Chem. Phys. Lett.,*

140, 451–457, 1987b.

Barnes, I., V. Bastian, and K. H. Becker, Kinetics and mechanisms of the reaction of OH radicals with dimethyl sulfide, *Int. J. Chem. Kinet., 20,* 415–431, 1988.

Barnes, I., V. Bastian, K. H. Becker, and D. Martin, Fourier transform IR studies of the reactions of dimethyl sulfoxide with OH, NO_3, and Cl radicals, *Biogenic Sulfur in the Environment,* edited by Saltzman, E. S., and W. J. Cooper, American Chemical Society, Washington, DC, 476–488, 1989.

Baulch, D. L., R. A. Cox, P. J. Crutzen, R. F. Hampson, Jr., J. A. Kerr, J. Troe, and R. T. Watson, Evaluated kinetic and photochemical data for atmospheric chemistry: Supplement I, *J. Phys. Chem. Ref. Data, 11,* 327–496, 1982.

Baulch, D. L., R. A. Cox, R. F. Hampson, Jr., J. A. Kerr, J. Troe, and R. T. Watson, Evaluated kinetic and photochemical data for atmospheric chemistry: Supplement II, *J. Phys. Chem. Ref. Data, 13,* 1259–1380, 1984.

Benson, S. W., and R. Shaw, Thermochemistry of organic peroxides, hydroperoxides, polyoxides, and their radicals, *Organic peroxides, Vol. I,* edited by Swern, D., pp. 105–139, John Wiley & Sons, Inc., 1970.

Benson, S. W., Thermochemistry and kinetics of sulfur-containing molecules and radicals, *Chem. Rev., 78,* 23–35, 1978.

Black, G., Reactions of HS with NO and NO_2 at 298 K, *J. Chem. Phys., 80,* 1103–1107, 1984.

Black, G., L. E. Jusinski, and R. Patrick, Reactions of i-C_3H_7S with O_2, NO_2, and NO at 296 K, *J. Phys. Chem., 92,* 1134–1138, 1988a.

Black, G., L. E. Jusinski, and R. Patrick, Kinetics of the reactions of C_2H_5S with NO_2, NO, and O_2 at 296 K, *J. Phys. Chem., 92,* 5972–5977, 1988b.

Block, E., *Reactions of Organosulfur Componds,* Academic Press, New York, NY, 1978.

Burrows, J. P., G. K. Moortgat, G. S. Tyndall, R. A. Cox, M. E. Jenkin, G. D. Hayman, and B. Veyret, Kinetics and mechanism of the photoxidation of formaldehyde. 2. Molecular modulation studies, *J. Phys. Chem., 93,* 2375–2382, 1989.

Busfield, W. K., K. J. Ivin, H. Mackle, and P. A. G. O'Hare, Studies in the thermochemistry of sulphones, *Trans. Faraday Soc., 57,* 1064–1069, 1961.

Calvert, J. G., F. Su, J. W. Bottenheim, and O. P. Strausz, Mechanism of the homogeneous oxidation of sulfur dioxide in the troposphere, *Atmos. Environ., 12,* 197–226, 1978.

Calvert, J. G., and Stockwell, W. R., The mechanism and rates of the gas phase oxidations of sulfur dioxide and nitrogen oxides in the atmosphere, *SO_2, NO and NO_2 Oxidation Mechanisms: Atmospheric Considerations,* J. G. Calvert (Ed.), Butterworth, Boston, 1–62, 1984.

Carton, P. M., B. C. Gilbert, H. A. H. Laue, R. O. C. Norman, and R. C. Sealy, Electron spin resonance studies. Part XLVII. Sulphinyl- and sulphonyl-substituted aliphatic radicals, *J. Chem. Soc., Perkin Trans., 2,* 1245–1249, 1975.

Chatgilialoglu, C., D. Griller, and M. Guerra, Experimental and theoretical approaches to the optical absorption spectra of sulfonyl radicals, *J. Phys. Chem., 91,* 3747–3750, 1987.

Cox, R. A., and D. Sheppard, Reactions of OH radicals with gaseous sulphur compounds, *Nature, 284,* 330–331, 1980.

Cvetanović, R. J., D. L. Singleton, and R. S. Irwin, Gas-phase reactions of $O(^3P)$ atoms with methanethiol, ethanethiol, methyl sulfide, and dimethyl disulfide. 2. Reaction products and mechanisms, *J. Am. Chem. Soc., 103,* 3530–3539, 1981.

Davidson, F. E., A. R. Clemo, G. L. Duncan, R. J. Browett, J. H. Hobson, and R. Grice, Reactive scattering of a supersonic oxygen atom beam: O + H_2S, *Mol.*

Phys., 46, 33–40, 1982.

Davis, F. A., R. H. Jenkins, Jr.,S. Q. A. Rizvi, and S. G. Yocklovich, *J. Org. Chem., 46,* 3647–3474, 1981.

Demerjian, K. L., K. L. Schere, and J. T. Peterson, Theoretical estimates of actinic (spherically integrated) flux and photolytic rate constants of atmospheric species in the lower troposphere, *Adv. Environ. Sci. Technol., 10,* 369–459, 1980.

Demore, W. B., R. T. Watson, D. M. Golden, R. F. Hampson, M. Kurylo, C. J. Howard, M. J. Molina, and A. R. Ravishankara, *Chemical Kinetics and Photochemical Data for Use in Stratospheric Modeling,* JPL Report 82–57, July 15, 1982.

Dlugokencky, E. J., and C. J. Howard, Laboratory studies of NO_3 radical reactions with some atmospheric sulfur compounds, *J. Phys. Chem., 92,* 1188–1193, 1988.

Domine, F., A. R. Ravishankara, and C. J. Howard, Atmospheric reactions of some reduced sulfur radicals, *Trans. Am. Geophys. Union, 70,* 100, 1989.

Francisco, J. S., and I. H. Williams, The thermochemistry of polyoxides and polyoxy radicals, *Int. J. Chem. Kinet., 20,* 455–466, 1988.

Friedl, R. R., W. H. Brune, and J. G. Anderson, Kinetics of SH with NO_2, O_3, O_2, and H_2O_2, *J. Phys. Chem., 89,* 5505–5510, 1985.

Gilbert, B. C., R. O. C. Norman, and R. C. Sealy, Electron spin resonance studies. Part XLIII. Reaction of dimethyl sulphoxide with the hydroxyl radical, *J. Chem. Soc., Perkin Trans., 2,* 303–308, 1975a.

Gilbert, B. C., R. O. C. Norman, and R. C. Sealy, Electron spin resonance studies. Part XLIV. The formation of alkylsulphonyl radicals by the oxidation of aliphatic sulphoxides with the hydroxyl radical and by the reaction of alkyl

radicals with sulphur dioxide, *J. Chem. Soc., Perkin Trans., 2,* 308–312, 1975b.

Gleason, J. F., A. Sinha, and C. J. Howard, Kinetics of the gas-phase reaction $HOSO_2 + O_2 \rightarrow HO_2 + SO_3$, J. Phys. Chem., 91, 719–724, 1987.

Good, A., and J. C. J. Thynne, Reaction of free radicals with sulphur dioxide, *Trans. Faraday Soc., 63,* 2708–2719, 1967.

Graham, D. M., R. L. Mieville, and C. Sivertz, Photo-initiated reactions of thiols and olefins I. The thiyl radical catalyzed isomerization of butene-2 and 1,2-ethylene-d_2, *Can. J. Chem., 42,* 2239–2249, 1964a.

Graham, D. M., R. L. Mieville, R. H. Pallen, and C. Sivertz, Photo-initiated reactions of thiols and olefins II. The addition of methanethiol to unconjugated olefins, *Can. J. Chem., 42,* 2250–2255, 1964b.

Grosjean, D., and R. Lewis, Atmospheric photooxidation of methyl sulfide, *Geophys Res. Lett., 9,* 1203–1206, 1982.

Grosjean, D., Photooxidation of methyl sulfide, ethyl sulfide, and methanethiol, *Environ. Sci. Technol., 18,* 460–468, 1984.

Grosjean, D., Wall loss of gaseous pollutants in outdoor teflon Chambers, *Environ. Sci. Technol., 19,* 1059–1065, 1985.

Harvey, G. R., and R. F. Lang, Dimethylsulfoxide and dimethylsulfone in the marine atmosphere, *Geophys. Res. Lett., 13,* 49–51, 1986.

Hatakeyama, S., M. Okuda, and H. Akimoto, Formation of sulfur dioxide and methanesulfonic acid in the photooxidation of dimethyl sulfide in the air, *Geophys. Res. Lett., 9,* 583–586, 1982.

Hatakeyama, S., and H. Akimoto, Reactions of OH radicals with methanethiol, dimethyl sulfide, and dimethyl disulfide in air, *J. Phys. Chem., 87,* 2387–2395, 1983.

Hatakeyama, S., K. Izumi, and H. Akimoto, Yield of SO_2 and formation of aerosol in

the photo-oxidation of DMS under atmospheric conditions, *Atmos. Environ.*, 19, 135–141, 1985.

Hatakeyama, S., Mechanism for the reaction of CH_3S with NO_2, paper presented at the meeting of the Environmental Chemistry, American Chemical Society, New Orleans, Louisiana, Aug. 1987.

Horowitz, A., Radiolytic decomposition of methanesulfonyl chloride in liquid cycloexane. A kinetic determination of the bond dissociation energies D(Me–SO_2) and D(c–C_6H_{11}–SO_2), *Int. J. Chem. Kinet., 8,* 709–723, 1976.

Hsu, Y. C., D. S. Chen, and Y. P. Lee, Rate constant for the reaction of OH radicals with dimethyl sulfide, *Int. J. Chem. Kinet., 19,* 1073–1082, 1987.

Hwang, R. J., and S. W. Benson, Kinetics of iodination of hydrogen sulfide by iodine and the heat of the formation of the SH radical, *Int. J. Chem. Kinet., 11,* 579–583, 1979.

Hynes, A. J., P. H. Wine, and D. H. Semmes, Kinetics and mechanism of OH reactions with organic sulfides, *J. Phys. Chem., 90,* 4148–4156, 1986.

Hynes, A. J., and P. H. Wine, Kinetics of the OH + CH_3SH reaction under atmospheric conditions, *J. Phys. Chem., 91,* 3672–3676, 1987.

Hynes, A. J., and P. H. Wine, OH-initiated oxidation of biogenic sulfur compounds, *Biogenic Sulfur in the Environment,* edited by Saltzman, E. S., and W. J. Cooper, American Chemical Society, Washington, DC, 424–436, 1989.

Kerr, J. A., and J. G. Calvert, *Chemical Transformation Modules For Eulerian Acid Deposition Models,* Volume I: The gas-phase chemistry, Boulder, Colorado, December, 1984.

Kerr, J. A., Strengths of chemical bonds, *CRC handbook of chemistry and physics, 66th,* edited by Weast et al., F-174–F-193, CRC Press, Inc., Boca Raton, FL, 1985.

Koelewijn, P., and H. Berger, Mechanism of the antioxidant action of dialkyl sulfoxides, *Red. Trav. Chim. Pays-Bas., 91,* 1275–1286, 1972.

Lagercrantz, C., and S. Forshult, Trapping of short-lived free radicals as nitroxide radicals detected by ESR spectroscopy. The radicals formed in the reaction between OH-radicals and some sulphoxides and sulphones, *Acta Chem. Scand., 23,* 811–817, 1969.

Leone, J. A., and J. H. Seinfeld, Updated chemical mechanism for atmospheric photooxidation of toluene, *Int. J. Chem. Kinet., 16,* 159–193, 1984.

Leone, J. A., R. C. Flagan, D. Grosjean, and J. H. Seinfeld, An outdoor smog chamber and modeling study of toluene–NO_x Photooxidation, *Int. J. Chem. Kinet., 17,* 177–216, 1985.

Lovejoy, E. R., N. S. Wang, and C. J. Howard, Kinetic studies of the reactions of HSO with NO_2, NO, and O_2, *J. Phys. Chem., 91,* 5749–5755, 1987.

Luke, B. T., and A. D. McLean, A theoretical investigation of atmospheric sulfur chemistry. 1. The HSO/HOS energy separation and the heat of formation of HSO, HOS, and HS_2, *J. Phys. Chem., 89,* 4592–4596, 1985.

Lunazzi, L., and G. F. Pedulli, Structure and reactivity of sulphur containing organic free radicals: recent advances, *Studies in organic chemistry 19: Organic sulfur chemistry,* edited by Bernardi et al., pp. 484–567, Elsevier, New York, NY, 1985.

MacLeod, H., S. M. Aschmann, R. Atkinson, E. C. Tuazon, J. A. Sweetman, A. M. Winer, and J. N. Pitts, Jr., Kinetics and mechanisms of the gas phase reactions of the NO_3 radical with a series of raduced sulfur compounds, *J. Geophys. Res., 91,* 5338–5346, 1986.

Margitan, J. J., Mechanism of the atmospheric oxidation of sulfur dioxide. Catalysis by hydroxyl radicals, *J. Phys. Chem., 88,* 3314–3318, 1984.

Martin, D., J. L. Jourdain, and G. Le Bras, Kinetic study for the reactions of OH radicals with dimethylsulfide, diethylsulfide, tetrahydrothiophene, and thiophene, *Int. J. Chem. Kinet., 17,* 1247–1261, 1985.

Martin, D., J. L. Jourdain, and G. Le Bras, Discharge flow measurements of the rate constants for the reactions OH + SO_2 + He and $HOSO_2$ + O_2 in relation with the atmospheric oxidation of SO_2, *J. Phys. Chem., 90,* 4143–4147, 1986.

Martin, D., J. L. Jourdain, G. Laverdet, and G. Le Bras, Kinetic study of the reaction of IO with CH_3SCH_3, *Int. J. Chem. Kinet., 19,* 503–512, 1987.

Meissner, A. H., and G. Beck, Pulsradiolytische Untersuchung von Dimethylthioäther und Dimethylsulfoxyd in wäßriger Lösung, *Z. Naturforsch.,22b,* 13–19, 1967.

Mellouki, A., J. L. Jourdain, and G Le Bras, Discharge flow study of the CH_3S + NO_2 reaction mechanism using Cl + CH_3SH as the CH_3S source, *Chem. Phys. Lett., 148,* 231–236, 1988.

McMillen, D. F., and D. M. Golden, Hydrocarbon bond dissociation energies, *Ann. Rev. Phys. Chem., 33,* 493–532, 1982.

Nielsen, O. J., J. Treacy, L. Nelson, and H. Sidebottom, Photo-oxidation of sulphur containing compounds, *Physico-chemical behaviour of atmospheric pollutants,* pp. 205–211, Proceedings of the Fourth European Symposium, edited by Angeletti, G., and G. Restelli, Stresa, Italy, Sept. 1986.

Niki, H., P. D. Maker, C. M. Savage, and L. P. Breitenbach, Spectroscopic and photochemical properties of CH_3SNO, *J. Phys. Chem., 87,* 7–9, 1983a.

Niki, H., P. D. Maker, C. M. Savage, and L. P. Breitenbach, An FTIR study of the mechanism for the reaction HO + CH_3SCH_3, *Int. J. Chem. Kinet., 15,* 647–654, 1983b.

Nip, W. S., D. L. Singleton, and R. J. Cvetanović, Gas-phase reactions of $O(^3P)$ atoms with methanethiol, ethanethiol, methyl sulfide, and dimethyl disulfide.

1. Rate constants and Arrhenius parameters, *J. Am. Chem. Soc., 103,* 3526–3530, 1981.

Paltenghi, R., E. A. Ogryzlo, and Kyle D. Bayes, Rates of reaction of alkyl radicals with ozone, *J. Phys. Chem., 88,* 2595–2599, 1984.

Panter, R., and R. D. Penzhorn, Alkyl sulfonic acids in the atmosphere, *Atmos. Environ., 14,* 149–151, 1980.

Penn, R. E., E. Block, and L. K. Revelle, Methanesulfenic acid, *J. Am. Chem. Soc., 100,* 3622–3623, 1978.

Rahamàn, M. M., E. Becker, T. Benter, and R. N. Schindler, A gasphase kinetic investigation of the system F + HNO_3 and the determination of absolute rate constants for the reactions of the NO_3 radical with CH_3SH, 2-methylpropene, 1,3-butadiene and 2,3-dimethyl-2-butene, *Ber. Bunsenges. Phys. Chem., 92,* 91–100, 1988.

Saltzman, E. S., D. L. Savoie, R. G. Zika, and J. M. Prospero, Methane sulfonic acid in the marine atmosphere, *J. Geophys. Res., 88,* 10,897–10,902, 1983.

Schäfer, K., M. Bonifačić, D. Bahnemann, and K.-D. Asmus, Addition of oxygen to organic sulfur radicals, *J. Phys. Chem., 82,* 2777–2780, 1978.

Schönle, G., M. M. Rahman, and R. N. Schindler, Kinetics of the reaction of atmoic fluorine with H_2S and elementary reactions of the HS radical, *Ber. Bunsenges. Phys. Chem., 91,* 66–75, 1987.

Semmes, D. H., A. R. Ravishankara, C. A. Gump-Perkins, and P. H. Wine, Kinetics of the reactions of hydroxyl radical with aliphatic aldehydes, *Int. J. Chem. Kinet., 17,* 303–313, 1985.

Shibuya, K., M. Nemoto, A. Yanagibori, M. Fukushima, and K. Obi, Spectroscopy and kinetics of thiophenoxy radicals in the gas phase, *Chem. Phys., 121,* 237–244, 1988.

Shum, L. G. S., and S. W. Benson, Thermochemistry and kinetics of the reaction of methyl mercaptan with iodine, *Int. J. Chem. Kinet., 15,* 433–453, 1983.

Shum, L. G. S., and S. W. Benson, Iodine catalyzed pyrolysis of dimethyl sulfide. Heats of formation of CH_3SCH_2I, the CH_3SCH_2 radical, and the pibond energy in CH_2S, *Int. J. Chem. Kinet., 17,* 277–292, 1985.

Slagle, I. R., F. Baiocchi, and D. Gutman, Study of the reactions of oxygen atoms with hydrogen sulfide, methanethiol, ethanethiol, and methyl sulfide, *J. Phys. Chem., 82,* 1333–1336, 1978.

Stachnik, R. A., and M. J. Molina, Kinetics of the reactions of SH radicals with NO_2 and O_2, *J. Phys. Chem., 91,* 4603–4606, 1987.

Stern, J. E., R. C. Flagan, D. Grosjean, and J. H. Seinfeld, Aerosol formation and growth in atmospheric aromatic hydrocarbon, *Environ. Sci. Technol., 21,* 1224–1231, 1987.

Swarts, S. G., D. Becker, S. DeBolt, and M. D. Sevilla, An electron spin resonance investigation of the structure and formation of sulfinyl radicals: reaction of peroxyl radicals with thiols, *J. Phys. Chem, 93,* 155–161, 1989.

Tyndall, G. S., J. P. Burrows, W. Schneider, and G. K. Moortgat, Rate coefficient for the reaction between NO_3 radicals and dimethyl sulphide, *Chem. Phys. Lett., 130,* 463–466, 1986.

Tyndall, G. S., and A. R. Ravishankara, Atmospheric reactions of CH_3S radicals, Paper presented at the meeting of the Environmental Chemistry, American Chemical Society, New Orleans, Louisiana, Aug. 1987.

Tyndall, G. S., and A. R. Ravishankara, Kinetics and mechanisms of the reactions of CH_3S with O_2 and NO_2 at 298 K, *J. Phys. Chem.,* 1988 (in press).

Tyndall, G. S., and A. R. Ravishankara, Kinetics of the reactions of CH_3S with O_3 at 298 K, *J. Phys. Chem., 93,* 4707–4710, 1989.

Vaghjiani, G. L., and A. R. Ravishankara, Kinetics and mechanism of OH reaction with CH_3OOH, *J. Phys. Chem., 93,* 1948–1959, 1989.

Veltwisch, D., E. Janata, and K-D. Asmus, Primary processes in the reaction of OH-radicals with sulphoxides, *J. Chem. Soc., Perkin Trans., 2,* 146–153, 1980.

Veyret, B., R. Lesclaux, M-T. Rayez, J-C. Rayez, R. A. Cox, and G. K. Moortgat, Kinetics and mechanism of the photooxidation of formaldehyde. 1. Flash photolysis study, *J. Phys. Chem., 93,* 2368–2374, 1989.

Wallington, T. J., R. Atkinson, E. C. Tuazon, and S. M. Aschmann, The reaction of OH radical with dimethyl suulfide, *Int. J. Chem. Kinet., 18,* 837–846, 1986a.

Wallington, T. J., R. Atkinson, A. M. Winer, and J. N. Pitts, Jr., Absolute rate constants for the gas-phase reactions of the NO_3 radical with CH_3SCH_3, NO_2, CO, and a series of alkanes at 298±2 K, *J. Phys. Chem., 90,* 4640–4644, 1986b.

Wallington, T. J., R. Atkinson, A. M. Winer, and J. N. Pitts, Jr., Absolute rate constants for the gas-phase reactions of the NO_3 radical with CH_3SH, CH_3SCH_3, CH_3SSCH_3, H_2S, SO_2, and CH_3OCH_3 over the temperature range 280–350 K, *J. Phys. Chem., 90,* 5393–5396, 1986c.

Wang, N. S., E. R. Lovejoy, and C. J. Howard, Temperature dependence of the rate constant for the reaction $HS + NO_2$, *J. Phys. Chem., 91,* 5743–5749, 1987.

Wine, P. H., N. M. Kreutter, C. A. Gump, and A. R. Ravishankara, Kinetics of OH reactions with the atmospheric sulfur compounds H_2S, CH_3SH, CH_3SCH_3, and CH_3SSCH_3, *J. Phys. Chem., 85,* 2660–2665, 1981.

Wine, P. H., R. J. Thompson, and D. H. Semmes, Kinetics of OH reactions with aliphatic thiols, *Int. J. Chem. Kinet., 16,* 1623–1636, 1984.

Yin, F., D. Grosjean, and J. H. Seinfeld, Analysis of atmospheric photooxidation mechanisms for organosulfur compounds, *J. Geophys. Res., 91,* 14417–14438, 1986.

Yin, F., D. Grosjean, R. C. Flagan, and J. H. Seinfeld, Atmospheric photooxidation of dimethyl sulfide and dimethyl disulfide. II. Mechanism evaluation, *J. Atmos. Chem., this issue*, 1989.

Figure Caption

Figure 1. CH_3SCH_3 Atmospheric Photooxidation Mechanism.

Figure 2. CH_3SSCH_3 Atmospheric Photooxidation Mechanism.

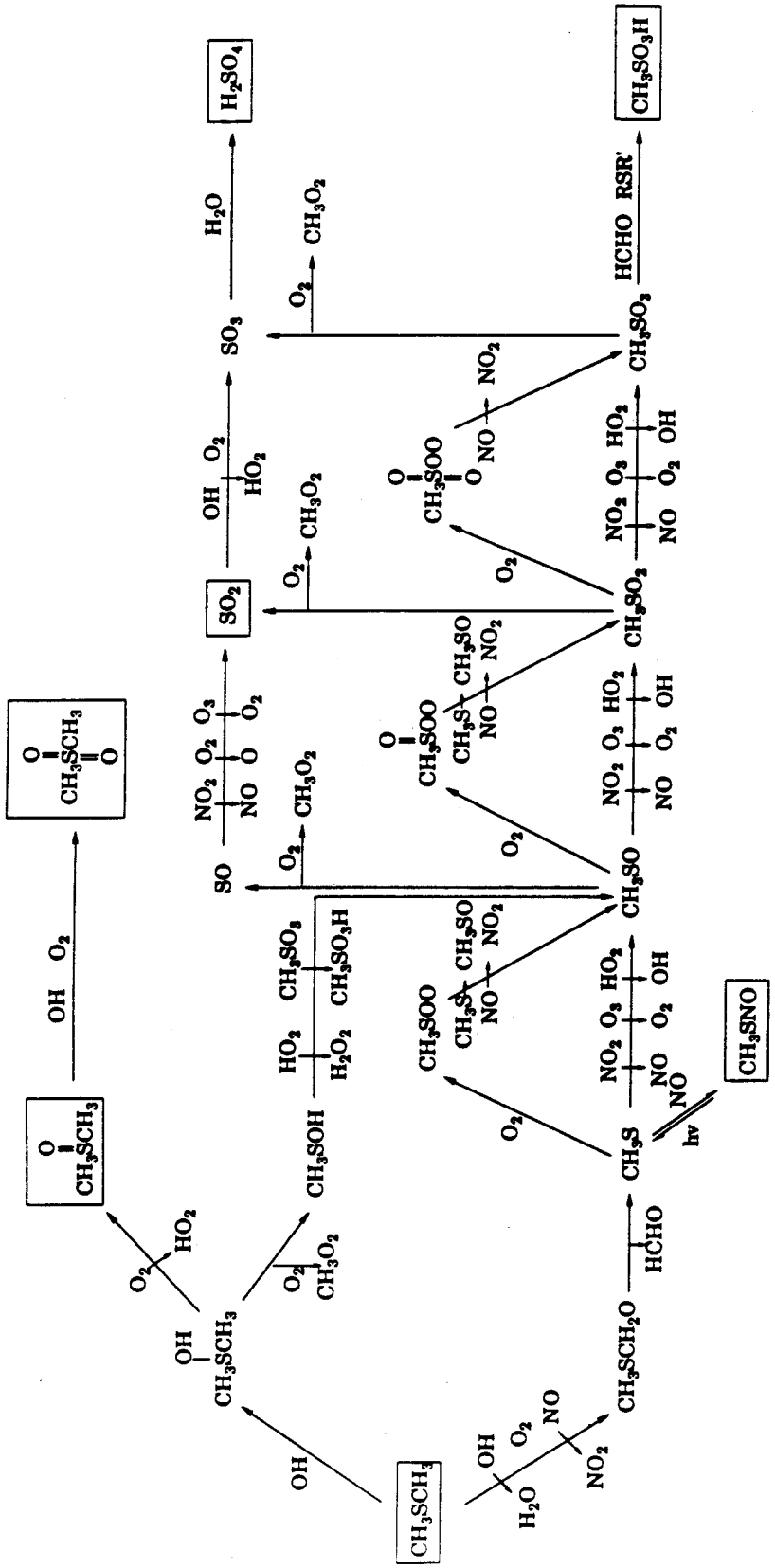

Figure 1. CH_3SCH_3 Photooxidation Mechanism

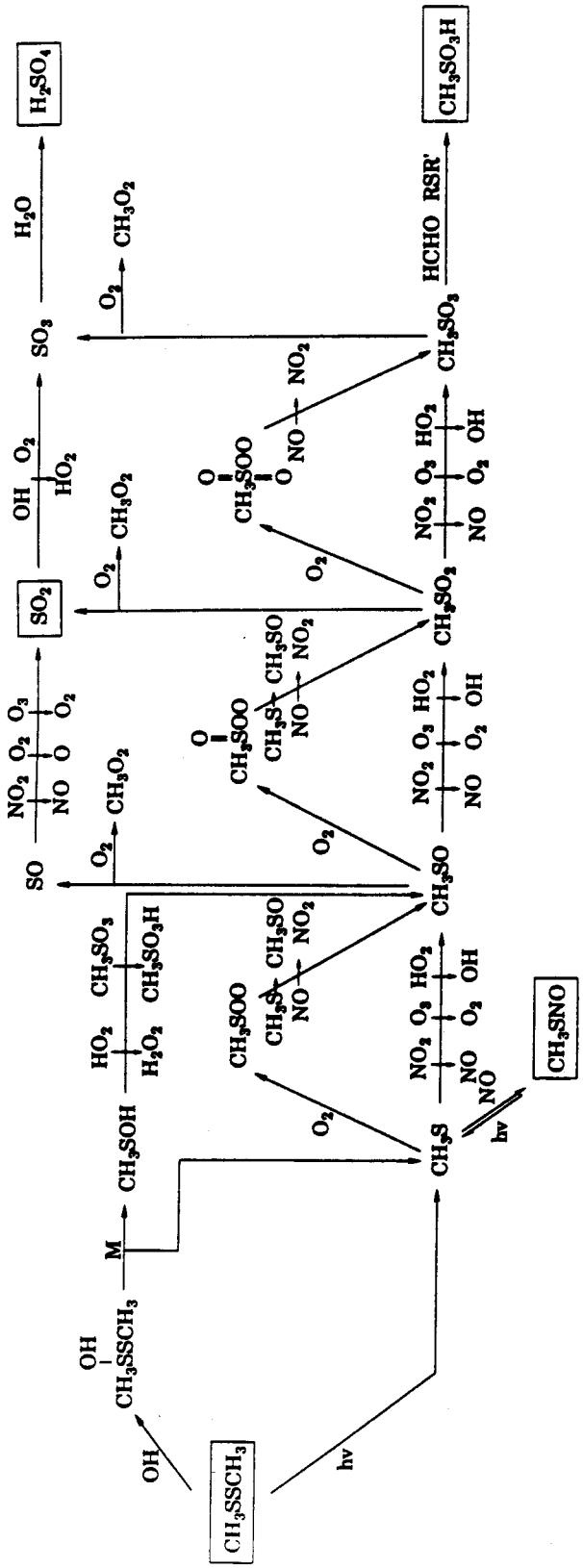

Figure 2. CH_3SSCH_3 Photooxidation Mechanism

CHAPTER IV

ATMOSPHERIC PHOTOOXIDATION OF DIMETHYL SULFIDE AND DIMETHYL DISULFIDE: Mechanism Evaluation.

ATMOSPHERIC PHOTOOXIDATION OF DIMETHYL SULFIDE AND DIMETHYL DISULFIDE: II. Mechanism Evaluation.

ABSTRACT

The mechanisms for atmospheric photooxidation of CH_3SCH_3 and CH_3SSCH_3 developed in Part I are evaluated by a series of outdoor smog chamber experiments. Measured product yields, including SO_2, H_2SO_4, CH_3SO_3H and HCHO, are reported. The predictions of the mechanisms developed in Part I are found to be in substantial agreement with the measured concentrations from the smog chamber. By comparison of mechanism predictions and observations, critical uncertainties in the mechanism are identified.

Key Words:

Dimethyl sulfide, dimethyl disulfide, photooxidation mechanism, outdoor smog chamber experiments, computer simulations.

1. Introduction

In Part I of this study, we developed kinetic mechanisms for the atmospheric photooxidation of dimethyl sulfide, CH_3SCH_3, and dimethyl disulfide, CH_3SSCH_3, in the presence of NO_x in air based on fundamental thermodynamic and kinetic considerations and all available information regarding reaction rates and products. In this article, Part II, our goal is to evaluate the mechanisms developed in Part I with a set of outdoor smog chamber studies of CH_3SCH_3 and CH_3SSCH_3 photooxidation in the presence and absence of NO_x. The corresponding experiments

were carried out using low levels of organo-sulfur compounds in pure air, with and without added NO_x, in the dark and in sunlight. Yields of the major gas-phase and aerosol-phase products, sulfur dioxide, formaldehyde, sulfuric acid and methanesulfonic acid, were determined for a range of initial conditions relevant to both the clean and polluted troposphere. Using the mechanisms presented in Part I, kinetic simulations are compared here to the experimental observations. The results of these comparisons are discussed with respect to our understanding of the atmospheric chemistry of organosulfur compounds. A study of the dynamics of aerosol formation in the smog chamber experiments will be reported elsewhere.

2. Experimental Methods

Photooxidations of CH_3SCH_3–NO_x–air and CH_3SSCH_3–NO_x–air mixtures have been carried out in an outdoor smog chamber. The all-Teflon chamber facility has been described by Leone et al. [1985] and Stern et al. [1987], and only a brief summary of the experimental protocol is given here. The chamber, constructed from 10 2-mil-thick FEP Teflon panels each of 1.2 m × 10.4 m, has a total volume of about 25 m^3 and 60 m^3 when operated as a dual or single reactor, respectively. The chamber was installed on a rooftop above a dark tarpaulin to minimize sunlight reflection from the surfaces below. Figure 1 shows the experimental system schematically. Four Teflon ports were installed at the bottom of the chamber for injection of the reactants and sampling of reactants and products.

With the chamber covered by a dark, opaque tarpaulin, NO, NO_2, organosulfur compound, and seed particles (if employed) were injected into the purified matrix air in the reaction chamber. After providing time for mixing, the opaque cover was removed, and the photooxidation of the mixture commenced. The RSR'–NO_x–air mixture was exposed to sunlight continuously for several hours, and monitored

by both gas- and aerosol-phase instruments. Gas-phase sampling was carried out through Teflon tubing extended approximately 30 cm into the chamber. Aerosol-phase sampling was conducted through separate copper lines extending about 15 cm into the chamber. The two Electrical Mobility Spectrometers were set immediately beneath the reaction chamber to minimize sampling line length. The copper lines used for aerosol sampling were all insulated to mininize changes of temperature and relative humidity along the lines. Filters and cartridges for off-line sampling were connected close to the reaction chamber (less than 50 cm) in order to minimize the sampling line losses. Parameters measured on-line included the concentrations of the organosulfur compound, sulfur dioxide, oxides of nitrogen, and ozone, relative humidity, temperatures of chamber and sampling line, solar ultraviolet radiation intensity and total solar radiation intensity, total condensation nuclei concentration, and aerosol size distribution. The signals from each of the on-line instruments were sent directly to several computers, including two PDP-11/03 mini-computers and three IBM PC's, for control of the instruments and data acquisition and processing. The course of the experiment could be followed in real time by displaying the parameter-time profile or size distribution of any of these parameters on several terminals.

The measured parameters and corresponding analytical methods are given in Table 1. A Hewlett-Packard model 5830A gas chromatograph equipped with a photoionization detector was used to measure CH_3SCH_3 and CH_3SSCH_3. The column used was a 30-in. $\times$ 1/8-in. Teflon column packed with 80/100 mesh Super Q operated isothermally at 373 K for CH_3SCH_3, and at 423 K for CH_3SSCH_3. The samples were introduced into the GC automatically by a Teflon sampling loop, a pneumatic solenoid valve, and a Valco 6-port sampling valve to optimize the reproducibility of the sampling volume. The gas chromatography and the pulsed

fluorescence SO_2 analyzer were calibrated with certified gas cylinders with a precision of ±2% (Scott-Marin Inc.). The calibration methods for ozone, oxides of nitrogen, temperatures, and relative humidity have been described by Leone et al. [1985]. The setup and configuation for the electrical aerosol analyzers and the optical particle counter were similar to those used by Stern et al. [1987]. The electrical mobility spectrometers and the differential mobility analyzer/CNC's were calibrated against an electrometer. One condensation nuclei counter [TSI, model 3020], which was available for measuring the total number concentration of the particles in the chamber, was calibrated by the manufacturer. For off-line sampling, Teflon and Nylon filters were used to collect samples of particulate sulfate, nitrate, and methanesulfonic acid, and gaseous nitric acid, respectively, and analyzed by Ion Chromatography. Formaldehyde was sampled using small C_{18} cartridges impregnated with DNPH, and measured by HPLC. The corresponding analytical methods have been described by Grosjean [1984].

Nitric oxide and nitrogen dioxide (600 ppm in ultrapure N_2, Scott-Marine Inc.), sulfur dioxide (1000 ppm in ultrapure N_2, Scott-Marine Inc.), dimethyl sulfide and dimethyl disulfide (> 99 % purity, Aldrich Chemical Co.) were used without further purification. The purity of each reagent was verified using the analytical methods described above, and additional impurities could not be detected.

3. Experimental Investigations and Results

Based on the comprehensive analysis of available kinetic and product information in Part I, a set of experimental product studies for atmospheric photooxidation of CH_3SCH_3 and CH_3SSCH_3 compounds were designed and conducted with emphasis on following objectives: (1) to evaluate the kinetic mechanisms developed in Part I; (2) to determine the product yield distributions of SO_2 and CH_3SO_3H; and

(3) to study the dynamics of sulfur-containing aerosols.

3.1. Experimental Investigations

Seventeen smog chamber experiments were carried out with mixtures of RSR′ and NO_x in air. Of the seventeen smog chamber experiments, eleven were run in dual mode; thus yielding a total of 28 sets of initial conditions. Table 2, 3 and 4 lists the experimental initial conditions, including initial concentrations of reactants, average temperature and humidity, and irradiation time. The experiments were performed under clear sky conditions to minimize cloud scattering of sunlight.

In order to evaluate the developed kinetic reaction mechanisms by providing the concentration profiles of reactants and products and to determine the yield distribution of products SO_2 and CH_3SO_3H and the effects of NO_x concentration on them, the photooxidation of four different organosulfur systems was studied in a wide range of initial conditions relevant to both clean and polluted troposphere. First, to measure the yields of SO_2 and CH_3SO_3H under NO_x-free (or very low NO_x) conditions, mixtures of CH_3SSCH_3–air were irradiated in the newly constructed Teflon chamber before introduction of any NO_x to avoid any trace contamination from NO_x species on the reactor surface. During these experiments, NO, NO_2 and NO_x were monitored and their concentrations were at all times below the detection limit of the instrument, i.e., 2 ppb. Also no nitric acid was found in the filter samples. Second, photooxidation of mixtures of CH_3SSCH_3–NO_x–air was carried out. The initial NO_x concentrations (0.045 to 0.661 ppm), the ratio of NO to NO_2 and the ratio of NO_x to CH_3SSCH_3 were varied to determine their effects on the yield distribution of SO_2 and CH_3SO_3H. Third, the system of CH_3SCH_3–NO_x–air was studied to determine the yields of SO_2 and CH_3SO_3H at low NO_x levels. Finally, the system CH_3SCH_3–NO_2–O_3–air was studied in the dark at night in order

to investigate the $CH_3SCH_3 + NO_3$ reaction. Although due to the detection limits of the analytical methods, the NO_x concentrations used in the experiments was still relatively high compared to those found in the clean atmosphere, the studies of NO_x effects on the yield distribution of SO_2 and CH_3SO_3H and the chemical mechanisms will enable us to extrapolate the observed yield distribution to clean atmospheric conditions.

3.2. Wall Loss

In order to characterize the chamber behavior, a series of control experiments were performed, including irradition of pure air, and measurement of the stability of both reactants and products in pure air both in the dark and in sunlight. Table 5 lists the observed loss rates of major species relevant to this study, including the organosulfur compounds, SO_2, NO_x and O_3. These loss rates are comparable to those measured by Grosjean [1985] for a similar outdoor smog chamber. The loss rates of the organosulfur compounds were negligible since they were about a factor of 100 smaller than those observed in the photooxidation experiments. If we assume that the observed removal rates of the organosulfur compounds and NO_2 in the control experiments are due entirely to reaction with the OH radical, an upper limit of about 10^5 molecule cm^{-3} can be estimated for the steady state concentration of OH radicals generated from the reactor surfaces. Because of the high reactivity of organosurfur compounds, a wall radical source of this magnitude is negligible compared with the major OH source from photooxidation of the organosulfur compounds with NO_x in air.

The wall loss rate of aerosol particles is a fuction of particle size, charge, chemical composition and physical properties. It should be pointed out that due to the limitation of our knowledge on the aerosol chemical composition, it is not possible

to take account of the effects of wall loss on measured product yields, and estimate the true aerosol product yields even if the wall loss rates of the particles are precisely measured.

3.3. Measured Product Yields

Product yields, including the maximum yields of SO_2 as well as the average yields of CH_3SO_3H, H_2SO_4, and HCHO, are listed in Table 6. For the CH_3SSCH_3–air system, the yield of SO_2 was usually about 90%, and the yields of CH_3SO_3H and H_2SO_4 were always less than 1%. As the initial NO concentration was increased from zero to about 0.040 ppm, the yield of SO_2 decreased to about 70%. Further increasing NO to 0.611 ppm resulted in an SO_2 yield of 56%, and CH_3SO_3H and H_2SO_4 yields of 6.9% and 6.8%, respectively.

For the CH_3SCH_3–NO_x–air system, the SO_2 yield ranged from 62% to 71% and the yields of CH_3SO_3H and H_2SO_4 were about 1 to 7% and 1 to 5%, respectively. SO_2 was also the major product in the dark CH_3SCH_3–NO_2–O_3–air system, with a yield of 55 to 68%, with negligible CH_3SO_3H observed from the analysis of the filter samples (less than 1%). To our best knowledge, this is the first time that the product yields has been reported for the atmospheric oxidation of CH_3SCH_3 initiated by NO_3 radical. Product yields measured by off-line techniques were averaged over the entire duration of the experiments before wall losses were accounted for. Therefore, these yields are lower limits for the actual average yields.

Under all experimental conditions studied, the major product of the photooxidation of CH_3SCH_3 and CH_3SSCH_3 was SO_2, and the yield distribution of SO_2, H_2SO_4 and CH_3SO_3H was dependent on the NO concentration level in the system.

The aerosol measurements and their analysis will be reported elsewhere.

4. Simulation of Organosulfur Photooxidation Experiments

Chemical reaction mechanisms for atmospheric photooxidation of CH_3SCH_3 and CH_3SSCH_3 are listed in Tables 6–9 in Part I. In this section, simulations of the outdoor smog chamber experiments are presented and discussed. Necessary inputs for the chemical mechanisms are the irradiation time, the chamber temperature, the NO_2 photolysis rate profile, and the initial concentrations of the reactants, which are listed in Tables 2, 3 and 4. The NO_2 photolysis rates are calculated theoretically as a function of date, time of day, and latitude assuming clear sky conditions [Demerjian et al., 1980].

Reaction rate constants for inorganic species, formaldehyde and SO_x species have been taken from the literature [Baulch et al., 1982 and 1984; Atkinson and Lloyd, 1984; Kerr and Calvert, 1984; Leone et al., 1985; etc.], and have been updated with the latest version of evaluated kinetic data reviewed by Atkinson et al. [1989]. Many rate constants for reactions involving organosulfur compounds and corresponding radicals have not yet been measured. They were first estimated by considering analogous reactions having measured rate constants (when available) and further evaluated through the simulation of the experimental data in the present study.

4.1. Photooxidation of CH_3SSCH_3

Although CH_3SSCH_3 appears to be only of minor importance in the global sulfur cycle, the elucidation of the chemsitry of CH_3SSCH_3 is directly relevant to achieving a better understanding of the atmospheric chemistry of CH_3SCH_3. Because of the relatively simple initial reactions of CH_3SSCH_3 and its function as a well-defined source of the CH_3S radical, simulation of CH_3SSCH_3 photooxidation

experiments will enable us to study the oxidation of the key CH_3S radical to SO_2 and sulfur-containing aerosols. In the following sections, the results of simulating the CH_3SSCH_3 photooxidation experiments are presented and the developed kinetic mechanism for CH_3SSCH_3 is investigated through computer simulation to elucidate the major chemical pathways of SO_2 and CH_3SO_3H formation in that system and to identify the critical uncertainties in kinetic data.

4.1.1. Simulation of CH_3SSCH_3 Photooxidation Experiments

Typical observed and predicted concentrations in CH_3SSCH_3 photooxidations in pure air and under low and high levels of NO_x concentrations are shown in Figures 2–4. The agreement between the predicted and observed concentration-time profiles of reactants and major products was usually good for all the simulations, especially the trends. The conversion of NO to NO_2, the decay of CH_3SSCH_3 and the production of SO_2 are well predicted by the mechanism for all photooxidation experiments, i.e., with and without added NO_x. Ozone formation is overpredicted for some of the simulations, however the time of the ozone appearance and its trends are predicted reasonably well. The predicted product yields of CH_3SO_3H, H_2SO_4 and HCHO were consistently higher than those observed. This is expected since the measured yields are the average yields exclusive of the wall losses. The good agreement between observed and predicted concentration-time profiles in CH_3SSCH_3 photooxidations indicates that the major assumptions made in developing the reaction mechanism for CH_3SSCH_3 (Table 8 in Part I) are reasonable, including addition as the dominant initial pathway for CH_3SSCH_3 + OH reaction, H-atom abstraction to be the major pathway for CH_3SOH, the neglect of the intramolecular rearrangement of CH_3SOO to CH_3SO_2, the importance of $CH_3SO_x + O_3$ reaction, and the major formation pathways for SO_2 and CH_3SO_3H (see Section 4.1.5. for more details).

In the CH_3SSCH_3–air system, about 60% of the observed CH_3SSCH_3 decay is predicted to be due to photolysis, and about 40% is due to the CH_3SSCH_3 + OH reaction. Consumption of CH_3SSCH_3 by reaction with OH is borne out by the experimental observations: in dual mode experiments, CH_3SSCH_3 in both sides of the reaction chamber decayed differently under different initial concentration levels (for example, 4.5×10^{-3} min^{-1} for experiment DDS4A and 5.7×10^{-3} min^{-1} for experiment DDS4B), although solar radiation intensity was identical. CH_3SO_x radicals are predicted to be oxidized mainly by HO_2, CH_3O_2 and $CH_3S(O)_xOO$ although the self reactions between peroxy radicals were also predicted to be important. At low radical concentrations, the competition between unimolecular decomposition of CH_3SO_2 and its further oxidation (either by peroxy radicals or addition of O_2 followed by reduction of CH_3SO_x) was dominated by CH_3SO_2 decomposition. As a result, SO_2 was observed as the major product with yields of about 90%.

As the initial NO_x concentration was increased to about 50 ppb, the reaction of OH+CH_3SSCH_3 becomes increasingly important and the contribution of CH_3SSCH_3 photolysis decreases to less than about 10%. The contribution of $O(^3P)$ and NO_3 to CH_3SSCH_3 decay was predicted to be about 2% and 1%, respectively. The oxidation of CH_3SO_x by NO_2 and O_3 and the addition of O_2 to CH_3SO_x followed by reduction with NO are both predicted to be important, however the oxidation of CH_3SO_x by peroxy radicals is predicted to be negligible. Since O_3 was consumed not only by NO, but also by CH_3SO_x radicals, O_3 could build up only after most of the CH_3SSCH_3 has reacted. When initial NO_x concentrations were increased to values exceeding 0.1 ppm, the contribution of CH_3SSCH_3 photolysis to the overall initial consumption was predicted to be less than 4%, and the contribution of both $O(^3P)$ and NO_3 radicals increases to about 5%. Since CH_3SSCH_3 is rapidly oxidized to SO_2 and CH_3SO_3H, O_3 could accumulate much earlier than

in the low NO_x concentration case. The CH_3SO_x radicals are in this case oxidized mainly by NO_2 and O_3, although addition of O_2 was also very important at the early stage of the experiment when the NO concentration was high. For CH_3SSCH_3–NO_x-air photooxidation, the contribution of $CH_3S(O)_2OO + NO$ was increased relative to CH_3SO_2 decomposition, thus leading to an increase of the observed CH_3SO_3H yield with increasing NO concentration.

4.1.2. Initial Reactions of CH_3SSCH_3

The rate constants for the initial reactions of CH_3SSCH_3 with OH, NO_3 and $O(^3P)$ are relatively well defined. The mechanisms are assumed to be dominated by addition reactions followed by rapid unimolecular decomposition. This assumption, although reasonable for OH and $O(^3P)$ initial reactions, has not been verified experimentally, especially for the $NO_3 + CH_3SSCH_3$ reaction. The overall dynamic behavior of the reaction mechanism is, however, not sensitive to the mechanism of the $NO_3 + CH_3SSCH_3$ reaction, i.e., addition or abstraction, since NO_3 initial reaction is much slower than that of OH, and the CH_3SSCH_3 consumption is dominated by OH reaction. From the absorption spectral data of CH_3SSCH_3 [Calvert and Pitts, 1966] and the calculated actinic flux of solar radiation at the Earth's surface [Demerjian et al., 1980], the rate constant for CH_3SSCH_3 photolysis is *roughly* estimated to be 2.5 $\times 10^{-3}$ min^{-1} at noon of July 1 at a latitude of 40° N for zero surface albedo assuming clear sky conditions. This rate constant is adjusted in our simulations due to the variation of sunlight intensity with date and time of the day. It is found that the decay of CH_3SSCH_3 is most sensitive to the change of its photolysis rate constant for CH_3SSCH_3 photooxidation in pure air, where the maximum contribution of CH_3SSCH_3 photolysis to the overall initial reaction is more than 50%. As the NO_x concentration increases, the dynamic behavior of

the reaction mechanism is much less dependent on CH_3SSCH_3 photolysis because of the rapid OH production from the $HO_2 + NO$ reaction.

4.1.3. Reactions of CH_3SOH

CH_3SOH is one of the two major intermediates from CH_3SSCH_3 photooxidation. Based mainly on information from liquid phase chemistry (discussed in Part I), the H-atom abstraction is presumed to be the dominant reaction pathway for CH_3SOH species. The rate constants for these H-atom abstractions are estimated by considering the relative strength of the formed H-X bonds (see Part I). Throughout the sensitivity analysis of the reaction mechanism it is found that OH, CH_3SO_3, HO_2 and CH_3O_2 are most important among those species possibly reacting with CH_3SOH:

$$CH_3SOH + OH \longrightarrow CH_3SO + H_2O \quad (1)$$

$$+ CH_3SO_3 \longrightarrow CH_3SO + CH_3SO_3H \quad (2)$$

$$+ HO_2 \longrightarrow CH_3SO + H_2O_2 \quad (3)$$

$$+ CH_3O_2 \longrightarrow CH_3SO + CH_3OOH \quad (4)$$

Since CH_3SOH acts basically as an active radical scavenger by donating its hydrogen atom, the dynamic behavior of the mechanism is controlled largely by its relative reactivity as well as the absolute values of the rate constants. Overall, the reaction with CH_3SO_3 is predicted to be the dominant chemical pathway for CH_3SOH and the reactions of CH_3SOH with OH, HO_2 and CH_3O_2 are also important. As the ratio of k_1/k_2 increases, the reaction of CH_3SOH with OH becomes important, thus competing with $OH + CH_3SSCH_3$ and decreasing the decay rate of CH_3SSCH_3, as well as affecting the time for O_3 build-up, especially at the latter

stage of the CH_3SSCH_3 consumption where the CH_3SOH concentration is relatively high. Variation of the ratios of k_3/k_2 and k_4/k_2 has an even larger effect on the reactivity of the system than that of k_1/k_2 since the termination of both HO_2 and CH_3O_2 radicals directly decreases the rate of formation of OH and HCHO, affecting CH_3SSCH_3 decay as well as SO_2 formation. Furthermore, the formation rates of the condensable species, H_2SO_4 and CH_3SO_3H, are altered significantly by varying these two ratios. A best fit to experimental data is obtained when the ratios are 0.25, as shown in Figure 5.

The possibility of electrophilic addition of radicals such as OH and CH_3SO_3 to the S atom in CH_3SOH as a minor reaction pathway has not been explored since the detailed mechanisms of the addition and subsequent reaction are not clear at the present time.

4.1.4. Reactions of CH_3SO_x and $CH_3S(O)_xOO$ Radicals

The reactions of CH_3SO_x and $CH_3S(O)_xOO$ radicals including CH_3S, CH_3SO, CH_3SO_2 and CH_3SO_3, are the most complicated reaction schemes in the reaction mechanism since their reactions involve many pathways such as oxidation, reduction, addition and decomposition. In this section, we focus on the competition between them through computer simulation in order to elucidate the major reaction pathways and to identify the critical uncertainties associated with them based on simulations of the smog chamber data.

4.1.4.1. Competition between O_2 Addition and Oxidation by peroxy Radicals

Three major uncertainties regarding the reaction of CH_3S with O_2 concern

(1) its mechanism, (2) its rate constant, and (3) intramolecular rearrangement of CH_3SOO to CH_3SO_2, which is assumed to be negligible in the simulation. The possible pathways for the $CH_3S + O_2$ reaction have been investigated in Part I, and are summarized as follows:

CH_3S	$+ O_2$	$\xrightarrow{M}$	CH_3SOO	(1)
CH_3SOO		$\xrightarrow{M}$	$CH_3S + O_2$	(2)
CH_3SOO		$\xrightarrow{M}$	CH_3SO_2	(3)
CH_3S	$+ CH_3SOO$	$\longrightarrow$	$CH_3SO + CH_3SO$	(4)
	$+ HO_2$	$\longrightarrow$	$CH_3SO + OH$	(5)
	$+ CH_3O_2$	$\longrightarrow$	$CH_3SO + CH_3O$	(6)
CH_3SOO	$+ CH_3SOO$	$\longrightarrow$	$CH_3SO + CH_3SO + O_2$	(7)
	$+ CH_3O_2$	$\longrightarrow$	$CH_3SO + CH_3O + O_2$	(8)
	$+ HO_2$	$\longrightarrow$	$CH_3SOOH + O_2$	(9)

At the present time, rate constants for the above reactions are essentially not available and must be estimated.

In order to evaluate the $CH_3SO_x + O_2$ reaction mechanism, the measured concentration-time profiles for CH_3SSCH_3 photooxidation in pure air are used. For the addition of O_2 to CH_3S, only upper limits of the *effective addition* (without considering the reverse reaction) rate constant have been determined [Balla et al., 1986; Tyndall and Ravishankara, 1988]. In the simulations of our experimental data, however, the reverse reactions of addition (i.e., reaction 2) (and analogous reactions for $CH_3S(O)OO$ and $CH_3S(O)_2OO$ radicals) are included because of the possible competition between adduct decomposition and reduction by CH_3S or NO, or addition of NO_2 to form PAN-like products. A direct consequence of considering such reverse reactions is that the *effective addition* rates of O_2 to CH_3SO_x radi-

cals will depend on the concentrations of CH_3SO_x radicals and NO_x present in the system (see Section 4.1.4.2. for more discussion).

Modelling of CH_3SSCH_3 photooxidation in pure air, as shown in Figure 2, indicates that the production of SO_2 on the time scale of a few minutes can be successfully simulated. This is not inconsistent with the fact that no decay of the CH_3S radical was observed on the time scale of milli-seconds in the kinetic study of the CH_3SSCH_3–O_2–$h\nu$ system [Tyndall and Ravishankara, 1988]. Through sensitivity analysis of the mechanism, it is found that a pseudo-equilibrium is quickly reached between CH_3S and CH_3SOO radicals. The steady state concentrations of CH_3S and CH_3SOO are not sensitive to the absolute values of k_1 and k_2, but are affected by the ratio k_1/k_2. Also variation of this ratio in a certain range has a negligible effect on the performance of the mechanism since the overall oxidation of CH_3S to CH_3SOO is limited by reactions (4) to (9). However, the dominant oxidation pathways for CH_3S to CH_3SOO could be altered from reactions (4)–(6) to reactions (7)–(9) when the ratio of k_1/k_2 increases. Therefore for oxidation of CH_3S to CH_3SO radicals, the competition is actually between the reactions of CH_3S with peroxy radicals (reactions 4–6) and the reactions among peroxy radicals (reactions 7–9), and there is no direct competition between the reactions of CH_3S with O_2 and peroxy radicals; and addition of O_2 to CH_3S only functions as a source of the CH_3SOO radical. It will be seen later that this conclusion has important implications to the clean atmospheric photooxidation of organosulfur compounds. Simulations of experimental data for CH_3SSCH_3 photooxidation in pure air indicate that the decay of CH_3SSCH_3 is sensitive to the rate constants of reactions of HO_2 with the CH_3S and CH_3SO radicals since they are the major OH sources in the system. Overall, a best fit for all the measured concentration-time profiles can be achieved when the reactions of CH_3S and CH_3SO with peroxy rad-

icals (HO_2, CH_3O_2 and $CH_3S(O)_xOO$) become the dominant pathways for their oxidation, although the reactions between peroxy radicals are also important.

It should be pointed out that the dynamic behavior described above is a direct result of an important assumption, i.e., the neglect of the intramolecular rearrangement of CH_3SOO to CH_3SO_2. Unfortunately, the available experimental data do not allow us to eliminate this reaction unambiguously.

4.1.4.2. Competition between O_2 addition and oxidation by NO_2 and O_3

In this section, experimental concentration profiles of CH_3SSCH_3 photooxidation with NO_x in air are simulated in order to assess (1) the importance of O_3 oxidation relative to other chemical pathways, and (2) the competition between O_2 addition and oxidation by NO_2 and O_3.

For the reactions of CH_3SO_x with NO_2, oxidation as the dominant pathways is supported by direct experimental observations (see Section 5.2. in Part I for detailed discussion). Regarding the reactions of CH_3SO_x with O_3, the oxidation reactions are tentatively assumed as the dominant pathways in the simulation because (1) although CH_2SO has been detected in the CH_3S/O_3 system [Domine et al., 1989], no information is available on the further reactions of CH_2SO; (2) under our experimental conditions, CH_3SO_x radicals are mainly oxidized to SO_2, CH_3SO_3H and H_2SO_4, not to CH_2SO, especially under low NO_x concentrations where the reactions of CH_3SO_x with O_3 are very important (see discussion below); and (3) in the case that CH_2SO is formed from $CH_3S(O)OOO$ through intramolecular H-atom abstraction via a six-member ring, $CH_3S(O)OO$ should also produce CH_2SO via a five-member ring. Instead, $CH_3S(O)OONO_2$ has been tentatively identified [Barnes et al. [1987]. It should be pointed out here, however, that the effect of CH_2SO on

product formation depends directly on the fate of CH_2SO, and that the importance of $CH_3S_x + O_3$ through pathways other than oxidation needs to be further studied experimentally, especially the yields of CH_2SO and its fate under atmospheric conditions. The reaction of CH_2SO with O_3 is probably one of the important removal processes for CH_2SO in the atmosphere.

Simulation of CH_3SSCH_3 photooxidation in air at low and high NO_x levels shows that the simulated O_3 concentration, as well as the time of O_3 appearance, is consistently overpredicted, as shown in Figure 6, unless the rate constants for the $CH_3SO_x + O_3$ reactions (CH_3S, CH_3SO and CH_3SO_2) are about the same order of magnitude as those of the corresponding NO_2 reactions. This indicates that the oxidation of CH_3SO_x by O_3 is comparable to that by NO_2, which is consistent with thermochemical considerations (see Part I). Notice that in both cases in Figure 6 there is little difference between the predicted NO_x concentrations, and both of them agree well with the observed data. This is important since the ozone concentration-time profile is expected to be well predicted as long as the conversion of NO to NO_2 is consistent with the experimental data. Furthermore, the examination of experimental data for CH_3SSCH_3 photooxidation conducted at low NO_x concentration (about 50 ppb) reveals that there is a delay of O_3 formation after NO is rapidly converted to NO_2, indicating O_3 may react with other species in the system. It was also observed that substantial amounts of ozone will not form until the SO_2 concentration has reached its maximum, suggesting reactions between some sulfur-containing species and O_3 in the system, i.e., $CH_3SO_x + O_3$ reactions. Regarding the possible competition between the oxidation of CH_3SO by O_3 and the H-atom abstraction of CH_3SO with O_3 to form CH_2SO, simulation of CH_3SSCH_3 photooxidation experiments reveals that the formation of CH_2SO has some significant effects on the final product yield distribution as well as the overall reactivity

of the reaction system. However, the importance of CH_2SO cannot be examined unambiguously by computer simulation since no experimental data of CH_2SO are currently available, and more importantly no information is available regarding the fate of CH_2SO in the atmosphere, although it is clear that the dominant fate of CH_3SO_x radicals is their oxidation to SO_2 and CH_3SO_3H under our experimental conditions.

Reactions of $CH_3S(O)_xOO$ with NO_x can compete with the adduct decompositions when NO_x is present in the system. Thus, addition of O_2 to CH_3SO_x radicals has a significant effect on the overall reactivity of the mechanism and product distribution. Considering oxidation of CH_3SO to CH_3SO_2 as an example, the possible major oxidation pathways for CH_3SO are:

$$CH_3SO + O_2 \xrightarrow{M} CH_3S(O)OO \quad (1)$$

$$+ NO_2 \longrightarrow CH_3SO_2 + NO \quad (2)$$

$$+ O_3 \longrightarrow CH_3SO_2 + O_2 \quad (3)$$

$$CH_3S(O)OO \xrightarrow{M} CH_3SO + O_2 \quad (4)$$

$$+ NO \longrightarrow CH_3SO_2 + NO_2 \quad (5)$$

$$+ NO_2 \longrightarrow CH_3S(O)OONO_2 \quad (6)$$

The CH_3SO radical can be oxidized either by NO_2 and O_3 directly or by addition of O_2 followed by reduction by NO, depending largely on the NO/NO_2 concentration ratio. Furthermore, the *effective addition* rate of O_2 to CH_3SO, i.e., the net rate of reactions (1) and (4), is a function of NO concentration in the system. Overall, the oxidation of CH_3SO by NO_2 and O_3 competes with either O_2 addition or further adduct reactions, depending on the present concentrations of NO_x. Figure 7 shows the effect on the overall reactivity of varying the ratios of O_2 addition to oxidation by

NO_2 and O_3 for CH_3SO. As the O_2 addition rate is decreased, more CH_3SO must be oxidized by NO_2 and O_3. Thus, the rate of NO to NO_2 conversion as well as O_3 formation is decreased. SO_2 production is also delayed since the yield of SO_2 depends strongly on the prediction of the NO profile.

Sensitivity analysis of the mechanism reveals that for CH_3S and CH_3SO radicals, O_2 addition and oxidation by NO_2 and O_3 are comparable when NO_x level is about 50 ppb, and the contribution of oxidation by NO_2 and O_3 is increased when NO_x reaches about 200 ppb. However, the addition of O_2 is still important at the early stage of the experiment since the initial high NO concentration also enhanced the *effective* addition pathways. For the CH_3SO_2 radical, the competition between O_2 addition and its oxidation by NO_2 and O_3 is dominated by the O_2 addition pathway for reasons as discussed in Part I. However, the competition between CH_3SO_2 unimolecular decomposition and its O_2 addition is quite important and will be discussed in Section 4.1.5.

The above discussion focused only on the two most important issues regarding the reactions of CH_3SO_x and $CH_3S(O)_xOO$ radicals. Many others, including the possible formation of CH_3SNO_2, the function of the reservoir species CH_3SNO, $CH_3S(O)OONO_2$ and $CH_3S(O)_2OONO_2$, the possible formation of $CH_3S(O)_xOOH$ and the regeneration of CH_3SSCH_3, also have minor, but not negligible, effects on both the dynamic behavior of the mechanism and the product yield distribution.

4.1.5. Formation of SO_2 and CH_3SO_3H

With respect to the formation of SO_2 and CH_3SO_3H, several uncertainties need to be addressed: (1) the importance of CH_3SO_x decomposition relative to further oxidation, (2) the effect of NO_x on the product yield distribution, and (3) the major formation pathways for SO_2 (including H_2SO_4) and CH_3SO_3H.

Because of the relatively high BDE of the CH_3–SO bond (see Part I), the unimolecular decomposition of CH_3SO is assumed to be negligible at atmospheric temperatures. Since the oxidation of CH_3SO_2 by NO_2 and O_3 is assumed to be relatively slow at concentrations < 1 ppm of both NO_2 and O_3, the reactions of the CH_3SO_2 radical are dominated by its unimolecular decomposition and O_2 addition. The reactions of the CH_3SO_3 radical may proceed via two pathways: H-atom abstraction to produce CH_3SO_3H and decomposition to form SO_3, contributing to H_2SO_4 production. Overall, the possible competitive pathways are:

$$CH_3SO_2 \xrightarrow{M} SO_2 + CH_3 \quad (1)$$

$$CH_3SO_2 + NO_2 \longrightarrow CH_3SO_3 + NO \quad (2)$$

$$CH_3SO_2 + O_3 \longrightarrow CH_3SO_3 + O_2 \quad (3)$$

$$CH_3SO_2 + O_2 \xrightarrow{M} CH_3S(O)_2OO \quad (4)$$

$$CH_3S(O)_2OO \xrightarrow{M} CH_3SO_2 + O_2 \quad (5)$$

$$CH_3S(O)_2OO + CH_3S \longrightarrow CH_3SO_3 + CH_3SO \quad (6)$$

$$CH_3S(O)_2OO + NO \longrightarrow CH_3SO_3 + NO_2 \quad (7)$$

$$CH_3S(O)_2OO + NO_2 \xrightarrow{M} CH_3S(O)_2OONO_2 \quad (8)$$

$$CH_3SO_3 \xrightarrow{M} SO_3 + CH_3 \quad (9)$$

$$CH_3SO_3 + HX \longrightarrow CH_3SO_3H + X \quad (10)$$

Simulations of CH_3SSCH_3 photooxidation experiments under zero, low and high levels of NO_x indicate that the system reactivity strongly depends on the competition between CH_3SO_2 decomposition and its oxidation. This is expected since generation of the CH_3 radical is the major sources for CH_3O_2, HO_2, OH radicals and HCHO. As shown in Figure 7, decreasing k_1/k_4 by 50% leads to a significant change in the product yield distribution of SO_2 relative to CH_3SO_3H (and H_2SO_4). Also, the rates of both NO to NO_2 conversion and O_3 formation are

decreased due to a lower CH_3 radical generation. Overall, the rate constant ratios k_1/k_4, k_4/k_5, and k_5/k_7 are adjusted to obtain the best fits of SO_2 concentration-time profiles. It is found in the simulation that in the absence of NO, the net rate of O_2 addition to CH_3SO_2 is slow since reaction (6) cannot compete with reaction (5) because of the low concentration of CH_3S radicals. Thus, unimolecular decomposition dominates the fate of the CH_3SO_2 radical, and SO_2 is observed as the major product. As the NO concentration increases, reaction (7) becomes more important, and the CH_3SO_3H yield increases. However, the CH_3SO_3H yield reaches only a certain level because reaction (4) will be the rate-limiting step at high NO levels and the product yield distribution will depend only on the relative rates of reactions (1) and (4), no longer on the rate of reaction (7). Although smog chamber studies of CH_3SSCH_3 photooxidation at levels of NO_x exceeding 10 ppm have not been conducted due to the limits of our instruments, computer simulation shows that when the concentration of NO_2 is large (e.g., above 10-20 ppm), the oxidation of CH_3SO_2 by NO_2 and O_3 could be important, leading to a decreasing SO_2 yield. This may be partially responsible for the relatively low SO_2 yield (49%) observed by Barnes et al. [1987].

Overall, the predicted concentration-time profiles of SO_2 are most sensitive to the rate constants k_1, k_4, k_5 and k_7. Furthermore, the effect of temperature on SO_2 yield through k_1 is important since k_1 could increase by a factor of about 2 when temperature is varied from 298 K to 308 K (the temperature range covered by the experiments).

The measured average yields for H_2SO_4 and CH_3SO_3H can be employed to estimate the rate constant ratio k_9/k_{10}. Simulation of the experimental data indicates that the dominant reaction pathway for the CH_3SO_3 radical is H-atom abstraction from CH_3SOH and HCHO, although the decomposition to form H_2SO_4 through the

$SO_3 + H_2O$ reaction is also important. The reactivity of the mechanism is relatively insensitive to the value of k_9 since reaction (9) contributes only a minor portion of the generated CH_3 radical. However, k_9 has a significant effect on predicted aerosol dynamics since it directly influences the formation rate of H_2SO_4, the major species for aerosol nucleation. Also reaction (10) needs to be examined in more detail since it, in fact, represents a group of about 10 reactions to form CH_3SO_3H, as listed in Table 8 in Part I. Concerning the chemical pathways for CH_3SO_3H formation, the following three major points have been studied through sensitivity analysis of the mechanism:

(1). The relative contribution of each H-atom donor to H-atom abstraction. Although it is clear that H-atom abstraction is the dominant reaction pathway for the CH_3SO_3 radical, the competition among H-donors is highly uncertain at the present time. Considering both the H-atom donating capability and the concentrations present in the reaction systems, the reactions of CH_3SO_3 with CH_3SOH, HCHO are assumed to be the dominant pathways for CH_3SO_3H formation under our experimental conditions. Increasing the rate constant of reactions of CH_3SO_3 with CH_3SOH, the CH_3SSCH_3 decay rate is increased since fewer OH radicals are consumed by CH_3SOH scavenging. Also the rate of accumulation of CH_3SOH is decreased, leading to a rapid oxidation of CH_3SSCH_3 to SO_2 and CH_3SO_3H. Variation of the rate constant of the $CH_3SO_3 + HCHO$ reaction affects the reactivity (e.g., the rates of organosulfur compound decay, NO to NO_2 conversion, O_3, HCHO and SO_2 formation) of the mechanism since HO_2 is directly generated from this reaction.

(2). The importance of CH_3SO_3 + CH_3SSCH_3 reaction. Because of the relatively high concentrations of CH_3SSCH_3, especially at the initial stage of the experiment, the reaction of CH_3SO_3 with CH_3SSCH_3 could be an important pathway

for the CH_3SO_3 radical. CH_3SO_3 can be considered to be roughly similar to the NO_3 radical, with a stronger tendency to abstract H-atoms (higher BDE) and to add to CH_3SSCH_3 (strong electrophilic radical). Thus, the rate constant of this reaction should be at least as high as that of NO_3 + CH_3SSCH_3, 7.4×10^{-13} cm^3 $molecule^{-1}$ s^{-1} [Dlugokencky and Howard, 1988]. Its reaction pathway would most likely be addition, especially considering the similar addition reactions of all other radicals with CH_3SSCH_3. When the estimated value is used in the simulation, the reaction has a noticeable effect on the reactivity of the mechanism. However, since no detailed kinetic mechanism can be developed regarding the addition of CH_3SO_3 to CH_3SSCH_3, a sensitivity analysis can not be carried out further at this time.

(3). Other chemical pathways. CH_3SO_3H can be formed, for example, through the addition of NO_x to the CH_3SO_3 radical followed by reactions of adducts with H_2O (see Table 8 in Part I). These reactions are more likely to proceed heterogeneously, either on the particle surface or on the reactor surface at relatively high humidity. Their importance is unknown, and more experimental data are needed to evaluate them.

It should be mentioned that the above uncertainties cannot be unambiguously resolved from the available product study data, and specific studies are clearly required for a better understanding of CH_3SO_3H formation in the atmosphere.

4.2. Photooxidation of CH_3SCH_3

Reaction mechanisms discussed above regarding oxidation of the CH_3S radical to SO_2 and CH_3SO_3H in the CH_3SSCH_3 mechanism are also applicable to CH_3SCH_3. Thus, the following discussion of the CH_3SCH_3 smog chamber experiments will focus on reactions specific to CH_3SCH_3, including (1) CH_3SCH_3 initial reactions,

(2) possible reactions of primary adducts, and (3) reactions of $CH_3S(O)CH_3$ and $CH_3S(O)_2CH_3$, and (4) reactions of $CH_3S(O)OH$.

Comparisons of observed and predicted concentrations from CH_3SCH_3–NO_x–air photooxidation experiments are shown in Figures 8 and 9. The simulated temporal profiles of NO, NO_2, O_3, CH_3SCH_3 and SO_2 were usually predicted quite well. The consistency between observed and predicted concentration-time profiles for CH_3SCH_3 photooxidation indicates that the major assumptions made in developing the mechanism (Part I) are reasonable, including H-atom abstraction as the major reaction pathway for CH_3SCH_3 + OH, addition followed by intramolecular H-atom abstraction to be the major pathway for the CH_3SCH_3 + NO_3 reaction, reaction of OH + $CH_3S(O)CH_3$ being dominated by the addition pathway, and slow H-atom abstraction for $CH_3S(O)_2CH_3$ + OH reaction. As in the case of CH_3SSCH_3, the product yields of CH_3SO_3H, H_2SO_4 and HCHO were consistently overpredicted.

4.2.1. Initial Reaction of CH_3SCH_3

The reactions of CH_3SCH_3 with OH, NO_3 and $O(^3P)$ radicals may proceed via two pathways: addition to the S atom, and H-atom abstraction from the CH_3 group. Although the addition pathway is by nature reversible, radical addition followed by adduct decomposition back to CH_3SCH_3 is not included in the initial reactions here. The *effective or apparent* addition pathway in the kinetic mechanism only represents those primary adducts that *actually* undergo secondary reactions in the system. Such treatment, however, implicitly assumes that the apparent addition pathway is independent of the concentrations of O_2 and other species (such as NO_x or CH_3SCH_3) in this system. This is a reasonable assumption for both the smog chamber experiments and the clean troposphere because of the relatively low concentrations of NO_x and CH_3SCH_3, and the constant O_2 concentration.

For the OH + CH_3SCH_3 reaction, the effect of the competition between addition and abstraction on the dynamic behavior of the mechanism can be examined by varying the branching ratio, as shown in Figure 11. As the addition pathway is increased, the yields of both SO_2 and CH_3SO_3H (and H_2SO_4) generally decrease because of the formation of $CH_3S(O)CH_3$ and $CH_3S(O)_2CH_3$. However, the product yield distribution between SO_2 and CH_3SO_3H is not directly related to the branching ratio (discussed in Part I), and the fate of the adducts play a more important role here (see discussion in next section). The negligible difference in the conversion of NO to NO_2 is due to the fact that the formation rates of peroxy radicals are similar in these three cases in Figure 10 despite large difference in the branching ratio. Since reactions of CH_3SO_x with O_3 are their dominant oxidation pathways at latter stages of the experiments (NO_2 is less important because of its low concentration), the O_3 formation rate is higher in case (c) than in case (b) because less O_3 is consumed by CH_3SO_x. Overall, it is found that H-atom abstraction is predicted to contribute about 75% to the initial CH_3SCH_3 + OH reaction. The temperature effect on the branching ratio of addition vs. abstraction is accounted for by considering the recommendation of Hynes et al. [1986]. Simulations of experimental data for CH_3SCH_3 photooxidation are not sufficient to test the temperature effect on the branching ratio since the average temperature variation between different experiments was less than 5 K under our experimental conditions.

The reactions of $O(^3P)$ and NO_3 with CH_3SCH_3 are predicted to contribute about 10% to the observed CH_3SCH_3 decay although in latter stages of the experiment when both NO_2 and O_3 are high, the $CH_3SCH_3 + NO_3$ reaction is predicted to become comparable to that of CH_3SCH_3 + OH. Also since the OH-NO_2 rate constant is twice that of OH-CH_3SCH_3, the consumption of CH_3SCH_3 is predicted to be slowed when NO_2 accumulates, in agreement with experimental observations.

For the $NO_3 + CH_3SCH_3$ reaction, addition is presumed to be the dominant pathway (see Part I). However, the fate of the adduct formed has an important effect on the reactivity of the mechanism (see next section for more discussion).

4.2.3. Competition between Adduct Decomposition and Bimolecular Reaction

The uncertainties of the initial reactions of CH_3SCH_3 consist of two issues: the branching ratio of addition vs. abstraction (discussed above), and the subsequent reactions of the primary adducts, the latter being in fact more important. Furthermore, these two issues interact on each other, and a well-defined (or meaningful) value of the branching ratio must be based on the elucidation of the chemical pathways of adducts. For the $CH_3S(OH)CH_3$ adduct, the possible reaction pathways are shown below:

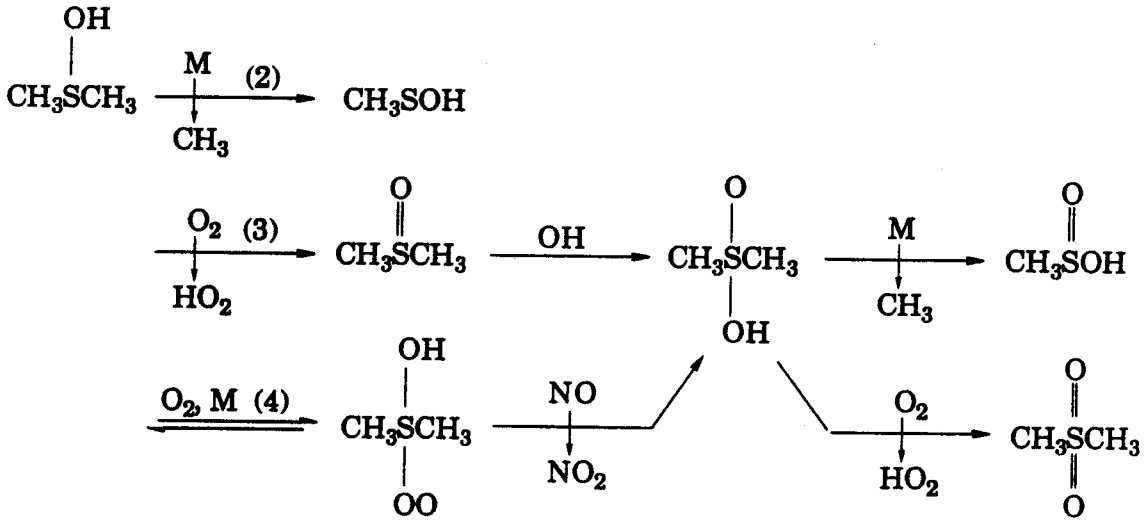

In the simulation of the CH_3SCH_3 photooxidation experiments, pathways (3) and (4) are considered to be the dominant reactions for the adduct $CH_3S(OH)CH_3$,

with the contribution of pathway (2) assumed to be less than 10% of the overall reaction of the adduct. Although reactions (3) and (4) are quite different, their effect on the reaction mechanism is the same if further reaction of $OH + CH_3S(O)CH_3$ is dominated by OH addition, which is the case in our simulation (see Section 4.2.4). Variation of the ratio $k_2/(k_3+k_4)$ has a noticeable effect on yield distribution of SO_2, CH_3SO_3H and $CH_3S(O)_2CH_3$, but not much on the reactivity of the mechanism. The small difference in reactivity is expected since the production rates of peroxy radicals (CH_3O_2 and HO_2) between pathways (2) and (3) or (4) is very similar. Furthermore the CH_3SCH_3 consumed through the addition pathway only represents a small portion of the total reacted CH_3SCH_3.

For the $CH_3S(ONO_2)CH_3$ adduct, three possible products of its unimolecular decomposition are examined by simulating the measured concentration-time profiles: (a) $CH_3SCH_2 + HONO_2$ through intramolecular H-atom abstration via a six-member ring, (b) $CH_3SONO_2 + CH_3$, and (c) $CH_3S(O)CH_3 + NO_2$, and As shown in Figure 12, pathway (a) gives the best prediction among the three, and pathway (a) is also consistent with all the available experimental evidence regarding the $CH_3SCH_3 + NO_3$ reaction (see Part I for details). Furthermore, pathway (a) is supported by the very recent experimental evidence that the reaction of CH_3SCH_3 with NO_3 does involve breaking a carbon-hydrogen bond [Daykin and Wine, 1990]. The major difference between pathway (a) and pathways (b) and (c) is that NO_2 is regenerated from pathways (b) and (c), thus leading to a cycle in which CH_3SCH_3 is consumed by NO_3. Notice that the overall reaction of NO_3 addition followed by pathway (a) is the same as the direct H-atom abstraction for $CH_3SCH_3 + NO_3$. Regarding the possible reactions of the adduct with O_2 and NO_x, they may be too slow to compete with reaction pathway (a) since the "*apparent*" rate constant of $CH_3SCH_3 + NO_3$, recently observed by Daykin and Wine [1990], is found to be the

same at 500 Torr air as at 19–500 Torr N_2.

4.2.4. Reactions of $CH_3S(O)CH_3$ and $CH_3S(O)_2CH_3$

Reaction of $CH_3S(O)CH_3$ with OH is assumed to be its major chemical removal process. The reaction between $CH_3S(O)CH_3$ and NO_3 is not included in the mechanism for simulation of our daytime smog chamber experiments, but it may be of importance for nighttime chemistry of $CH_3S(O)CH_3$ compound. Also reaction of $CH_3S(O)CH_3$ with CH_3SO_3 is probably important although the reaction mechanism is unknown at present. The branching ratio of addition to abstraction for the $OH + CH_3S(O)CH_3$ reaction has a large effect on the reactivity of the mechanism:

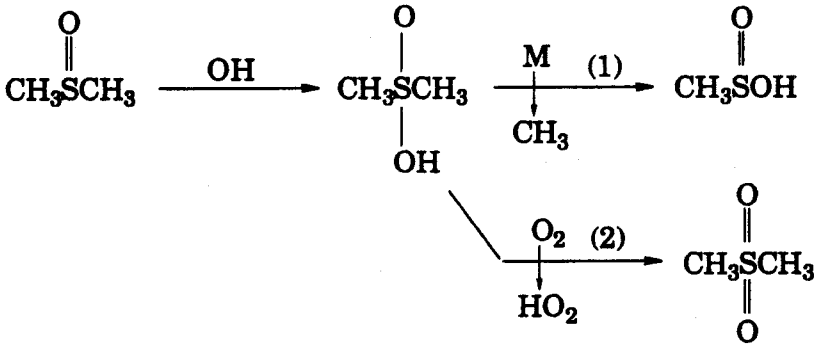

Simulations of the measured concentration-time profiles of CH_3SCH_3–NO_x-air system suggest that addition is the dominant pathway for the $CH_3S(O)CH_3 + OH$ reaction, which is consistent with the conclusion reached in Part I. The adduct $CH_3S(OH)(O)CH_3$ may either undergo unimolecular decomposition to CH_3SO_2H (reaction 1) or react with O_2 to produce $CH_3S(O)_2CH_3$ (reaction 2). The competition between these two pathways directly influences both the product yield distribution between SO_2, CH_3SO_3H and $CH_3S(O)_2CH_3$ and the reactivity of the mechanism. When the ratio of k_1/k_2 is increased, the yields of SO_2 and CH_3SO_3H are increased, and the reactivity of system is higher since more CH_3 is generated.

However, the effect of varing k_1/k_2 is small because CH_3SCH_3 consumed through the addition pathway represents only about 20% of the reacted CH_3SCH_3, and peroxy radicals are generated in both cases. Based mainly on the preliminary product studies of OH+$CH_3S(O)CH_3$ by Barnes et al. [1988] as well as the sensitivity analysis of the mechanism, the ratio k_1/k_2 is chosen to be 0.7/0.3 in our simulation, indicating that the overall yield of $CH_3S(O)_2CH_3$ for CH_3SCH_3 photooxidation is less than 10%, i.e., a minor product under our experimental conditions.

The only possible pathway for the OH+$CH_3S(O)_2CH_3$ reaction is the H-atom abstraction since the S atom in $CH_3S(O)_2CH_3$ is already saturated. Also because $CH_3S(O)_2CH_3$ is relatively unreactive towards OH, and the predicted yield of $CH_3S(O)_2CH_3$ is low and the CH_3SCH_3 concentration was still relatively high at the end of the experiments, the reactivity of the mechanism and the yield distribution of the products are insensitive to the value of $k_{OH+CH_3S(O)_2CH_3}$. Since the boiling point for $CH_3S(O)_2CH_3$ (511 K) is higher than that for CH_3SO_3H (440 K), it is expected that its condensation on aerosol particles and on the smog chamber wall are likely to be more important. Therefore, for $CH_3S(O)_2CH_3$ in the atmosphere, the major uncertainty lies in the competition between its OH reaction and its condensation on aerosol particles, followed by further oxidation in aerosol or aqueous phase.

4.2.5. Reactions of CH_3SO_2H and Formation of CH_3SO_3H

CH_3SO_2H is assumed to have similar H-atom abstractions as those of CH_3SOH, although reaction rate for CH_3SO_2H may be slower due to its stronger $CH_3S(O)O$–H bond. Sensitivity analysis of the mechanism with smog chamber experimental data indicates that reactions of CH_3SO_2H with OH and CH_3SO_3 are predominant, and the contribution from HO_2 and CH_3O_2 is small. Contrary to the reactions of

CH_3SOH, reactions of CH_3SO_2H with OH and CH_3SO_3 have a noticeable, but not overwhelming, effect on the reactivity of the mechanism since only a small portion of CH_3SCH_3 is converted to CH_3SO_2H. Also due to its increase in molecular weight, CH_3SO_2H may condense on aerosol particles or the chamber surface.

The chemical pathways for CH_3SO_3H formation in CH_3SCH_3 photooxidation are basically the same as those in CH_3SSCH_3 photooxidation except that here the relative contribution of H-atom donors to CH_3SO_3 abstraction is changed. Different from photooxidation of CH_3SSCH_3 where a large amount of reactive H-donor, CH_3SOH, is produced, the major H-donors in CH_3SCH_3 photooxidation are HCHO, CH_3SO_2H and CH_3SCH_3, and their contribution is increased relative to CH_3SOH. Similar to $CH_3SCH_3+NO_3$ reaction, the reaction pathway of CH_3SO_3 with CH_3SCH_3 is addition followed by intramolecular H-atom abstraction through a six-member ring.

5. Product Yield Distribution of CH_3SCH_3 and CH_3SSCH_3 Photooxidation

Summaries of the experimental conditions and the product yields of SO_2, H_2SO_4 and CH_3SO_3H from all available literature data are listed in Tables 7 and 8. An examination of the experimental data in Tables 7 and 8 reveals that two ranges of product yields have been reported: (1) low SO_2 and high CH_3SO_3H yields observed by Hatakeyama and his colleagues [Hatakeyama et al., 1982; Hatakeyama and Akimoto, 1983; Hatakeyama et al., 1985], Niki et al. [1983], and MacLeod et al. [1986]; and (2) high SO_2 and low CH_3SO_3H yields measured by several other investigators [Grosjean and Lewis, 1982; Grosjean, 1984; Barnes et al., 1988] and this work. Correspondingly, the experimental conditions used in these two sets of product studies are: (1) high concentrations, extra radical source, artificial light

source, and small reactors, and (2) low concentrations, sunlight, large reactor and long irradiation time. We will show that the differences in the observed yields can be explained, at least qualitatively, on the basis of the differences in the experimental conditions. The following discussion is focused on the effects of concentration, temperature and light intensity on the product yield distribution.

5.1. Effect of Reactant Concentration

Organosulfur compounds must undergo two basic steps prior to the formation of SO_2 and CH_3SO_3H: (1) oxidation through CH_3SO_x or some other intermediates; (2) competition between unimolecular decomposition of CH_3SO_2 and its further oxidation to CH_3SO_3 radical. The effects of high NO_x concentrations on the product yield distribution through step (2) have been discussed in detail in Section 7 of Part I, and it was concluded there that increasing NO concentrations will lead to a decrease in SO_2 yield and an increase in CH_3SO_3H yield. The discussion below will show that a low SO_2 yield and a high CH_3SO_3H yield can also result from high concentrations of NO_x and RSR′ by affecting the oxidation of CH_3SO_x radicals.

The major atmospheric reactions for CH_3SO_x radicals are believed to be oxidation by O_2, NO_2, O_3 and peroxy radicals. However, under the conditions of high initial concentrations used in product-oriented studies [Hatakeyama et al., 1982; Hatakeyama and Akimoto, 1983; Niki et al. [1983]; MacLeod et al., 1986], certain species with high concentrations (such as NO, RSR′, and RONO for OH source) may react with CH_3SO_x radicals (or other intermediates) and terminate their further oxidation to SO_2 or CH_3SO_3H. The following examples illustrate the effects of high concentrations on product yield distribution:

(1). At high NO (> 1 ppm), and $[NO]/[NO_2] > 2$, the $CH_3S + NO$ reaction will compete with CH_3S oxidation by NO_2 to form CH_3SNO. At low light intensity,

reactions of CH_3SO_x with CH_3SNO could compete with CH_3SNO photolysis and produce high molecular weight species, $CH_3SO_xSCH_3$.

(2). High concentrations of NO_x could intercept CH_3SO_x and $CH_3S(O)_xOO$ radicals to produce nitrate or PAN-like high molecular weight compounds.

(3). At high RSR′ concentrations, reaction of CH_3SO_3 with RSR′ could be comparable with its H-atom abstraction, for example:

$$CH_3SO_3 + CH_3SOH \longrightarrow CH_3SO_3H + CH_3SO \quad (1)$$

$$+ CH_3SSCH_3 \longrightarrow CH_3SO_3SCH_3 + CH_3S \quad (2)$$

$$+ CH_3SSCH_3 \xrightarrow{M} \text{Adduct} \quad (3)$$

to form again high molecular weight compound.

The above reactions will definitely reduce the SO_2 product yield, but not necessarily lead to a low CH_3SO_3H yield. The reason is that, in Hatakeyama's experiments, the aerosol products were collected by washing the reactor vessel after 30 min irradiation and 3 hour aerosol sedimentation [Hatakeyama and Akimoto, 1983]. The high molecular weight species (at least those containing a CH_3SO_3 group) could then either react heterogeneously on the reactor surface to form CH_3SO_3H or decompose to produce CH_3SO_3H during later treatment of the aerosol samples. Thus, these possible high molecular weight species may contribute partially to the observed high CH_3SO_3H yield, although the high initial concentrations (CH_3SCH_3: 10–830 ppm, NO: 400–1200 ppm, CH_3ONO: 40 ppm; no concentrations were specified for aerosol product studies conducted in 1983) might be the major factor responsible for the high CH_3SO_3H yield. The very low yields of H_2SO_4 (< 2%) observed by them may be related to their extremely low concentration of H_2O (about 1 ppm). Notice also that high NO concentration alone in the system does not necessarily lead to a low SO_2 concentration since a SO_2 yield of about 50% was observed by

Barnes et al. [1987] when NO was increased from zero to as high as 10 ppm during the experiments. The major reason is probabily that the ratio of [NO]/[NO_2] was always < 1 during the experiments, and the NO_2 concentration was very high (about 10–20 ppm).

It should be emphasized that although the concentrations of CH_3SCH_3 (1.3 ppm) and NO (0.75 ppm) were not very high for the system CH_3SCH_3–NO–air–$h\nu$ studied by Hatakeyama et al. [1985], the zero initial NO_2 concentration, and thus high ratio of NO to NO_2 during the early stage of the experiment where large amounts of CH_3SCH_3 were consumed may have a significant effect on the observed low SO_2 yield (about 30%) since NO was specially treated to remove any NO_2 before their experiments. Also despite the fact that the measured SO_2 yields were still low compared with those observed here, they were significantly higher than those measured from similar systems [Hatakeyama et al., 1982] where higher concentrations of NO and CH_3SCH_3 were used.

5.2. Effect of Temperature and Light Intensity

In addition to the effects resulting from high concentrations, variation of temperature and irradiation light intensity may have some significant effects on the SO_2 production. A change in temperature from 298 K to 308 K, corresponding to the temperature often used in the indoor reactor and the *average* temperature usually encounted in the outdoor smog chamber in summer, will increase the rate constant of CH_3SO_2 decomposition by a factor of 2.5 assuming the activation energy is same as the CH_3–SO_2 bond dissociation energy, 17.2 kcal/mole [Benson, 1978]. The enhancement factor could in fact be higher because the *maximum* temperature could reach 318 K in an outdoor smog chamber. The effect of temperature on the unimolecular decomposition of CH_3SO_3 may also be important. Additionally, the

significant temperature effect on the branching ratio of addition vs. abstraction for CH_3SCH_3 photooxidation can also affect the product yield distribution.

The strong absorption of the CH_3SO_2 radical in the 300–600 nm region with maxima at ca. 350 nm [Chatgilialogou et al., 1987] suggests that the decomposition rate of CH_3SO_2 may be faster in an outdoor smog chamber than that in indoor reactors since the intensity of solar irradition is usually higher than that of artifical light sources. Thus the production of SO_2 may be enhanced under sunlight irradiation.

In summary, a high yield of SO_2 will be observed under low concentrations of NO and organosulfur compounds, relatively high concentrations of oxidants such as NO_2, O_3, or O_2, strong light intensity and high temperature.

6. Implications for Atmospheric Chemistry

The ultimate goal for both kinetic and mechanistic studies of the atmospheric organosulfur photooxidation is to elucidate the chemical pathways of conversion of organosulfur compounds to SO_2 and sulfur-containing aerosols, and to determine the product yield distribution. Three major respects of the chemistry of organosulfur compounds in the clean atmosphere will be briefly addressed in the present section: the major chemical pathways of converting CH_3SCH_3 to SO_2 and sulfur-containing aerosols in the atmosphere, the possible product yield distribution and the important factors affecting the product yield distribution.

The major chemical processes for removing CH_3SCH_3 in the atmosphere are likely to be dominated by OH abstraction in the daytime and NO_3 addition at nighttime. The importance of possible IO + CH_3SCH_3 reaction needs to be further addressed experimentally. CH_3S radical, as the major intermediate generated from CH_3SCH_3, will play an important role in the atmospheric photooxida-

tion of CH_3SCH_3. Under the assumption that the intramolecular conversion from CH_3SOO to CH_3SO_2 is negligible, the major reactions pathways for CH_3SO_x radicals will be oxidation by NO_2 and O_3, competing with the addition of O_2 followed by reduction:

$$CH_3S \xrightleftharpoons{O_2} CH_3SOO \xrightarrow[NO_2]{NO} CH_3SO \qquad (1)$$

$$CH_3S \xrightarrow[NO]{NO_2} CH_3SO \qquad (2)$$

The large concentration ratio of O_2 to NO_2 (about 10^9–10^{11}) does not play a very important role here because of the reverse reaction of O_2 addition. It should be pointed out that the atmospheric importance of the $CH_3SO_x + O_3$ reaction has not been determined, which may be the most important reaction for CH_3SO_x in the atmosphere.

It could be concluded that the major product for organosulfur photooxidation under clean atmospheric conditions is SO_2 although its actual yield may vary with the atmospheric conditions since the concentrations of both RSR' and NO are very low, and more importantly the concentration ratio of oxidizers (including O_3, NO_2 and peroxy radicals) to RSR' is larger than one. This conclusion is consistent with a recent modeling study on organosulfur photooxidation in marine atmosphere [Toon et al., 1987]. However the temperature variation in the atmosphere may have an important effect on the product yield distribution since both the branching ratio of addition vs. abstraction for $OH+CH_3SCH_3$ and the decomposition rate of the CH_3SO_2 radical to produce SO_2 are influenced by temperature. As the temperature decreases from 310 K to 270 K, the branching ratio of the ad-

dition pathway for $OH+CH_3SCH_3$ is increased from 0.13 to 0.68 as estimated by Hynes et al. [1986], and the yields of $CH_3S(O)CH_3$ and $CH_3S(O)_2CH_3$ may be increased. Also for the same variation of the temperature the decomposition rate constant of the CH_3SO_2 radical will be reduced by a factor of about 40 and the yield of CH_3SO_3H may be increased to some extent.

7. Conclusion

The organosulfur photooxidation mechanisms developed in Part I have been evaluated with the data from a series of outdoor smog chamber experiments on the systems CH_3SCH_3–NO_x–air–$h\nu$ and CH_3SSCH_3–NO_x–air–$h\nu$. The product yields, including SO_2, H_2SO_4, CH_3SO_3H, and HCHO, have been measured. The differences of measured product yields between the available product studies have been elucidated in terms of the significant variations of experimental conditions. Through a sensitivity analysis of the mechanism, critical uncertainties related to reaction rate constants and pathways have been identified. Although the simulations of the experimental data evaluate the major assumptions proposed in developing the mechanism in Part I, further experimental work is needed to verify the mechanisms as well as to study them *directly*, including the fates of adducts formed from initial reactions, the major reactions for CH_3SOH, $CH_3S(O)CH_3$ and $CH_3S(O)_2CH_3$ (both measurement of rate constants and identification of products), the importance of intramolecular conversion of CH_3SOO to CH_3SO_2, the further reactions of CH_3SO_x radicals, especially with O_3, and the identification of the missing products. The mechanistic implications for the atmospheric chemistry of organosulfur compounds has been discussed, and SO_2 is concluded to be the major product of organosulfur photooxidation in the clean atmosphere.

ACKNOWLEDGMENT

This work was supported by National Science Foundation grant ATM–8503103. We thank Dr. Wine for communicating their results to us prior to publication.

Table 1 Summary of Measured Parameters and Analytical Methods

Analytical Method	Measured Parameter
Chemical Measurements	
Ultra-violet Photometry	Ozone
Chemiluminescence	Oxides of Nitrogen
Pulsed Fluorescence	Sulfur Dioxide
Gas Chromatography	Organosulfur Compounds
HPLC/DNPH Cartridge	Formaldehyde
Ion Chromatography/Filters	Sulfate, Nitrate and Methanesulfonic Acid
Physical Measurements	
Thermistor	Temperature
Hygrometer	Humidity
Radiometer	Total Solar Radiation Intensity
UV Radiometer	UV Radiation Intensity
Aerosol Measurements	
Electrical Mobility Spectrometer	Aerosol Size Distribution (3–150 nm)
Differential Mobility Analyzer/CNC	Aerosol Size Distribution (10–200 nm)
Electrical Aerosol Analyzer	Aerosol Size Distribution (20–300 nm)
Optical Particle Counter	Aerosol Size Distribution (200–5000 nm)
Condensation Nuclei Counter	Total Nuclei Concentration

Table 2 Initial Conditions for CH_3SSCH_3–Air– $h\nu$

EXPERIMENT	DDS1A	DDS1B	DDS2A	DDS2B
Irrad. Time (min)	184	194	235	245
Ave. Temp. (K)	302	302	311	311
Humidity (%)	28	27	43	43
Initial Conc. (ppm)				
NO	0.000	0.000	0.000	0.000
NO_2	0.000	0.000	0.000	0.000
CH_3SSCH_3	0.793	0.793	0.580	0.580

EXPERIMENT	DDS3A	DDS3B	DDS4A	DDS4B
Irrad. Time (min)	249	259	250	260
Ave. Temp. (K)	307	307	301	302
Humidity (%)	45	45	48	48
Initial Conc. (ppm)				
NO	0.000	0.000	0.000	0.000
NO_2	0.000	0.000	0.000	0.000
CH_3SSCH_3	0.524	0.627	0.339	0.814

Table 3 Initial Conditions for CH_3SSCH_3–NO_x–Air–$h\nu$

EXPERIMENT	DDS5A	DDS5B	DDS6A	DDS6B
Irrad. Time (min)	274	284	328	318
Ave. Temp. (K)	305	306	301	301
Humidity (%)	43	43	49	49
Initial Conc. (ppm)				
NO	0.081	0.611	0.115	0.007
NO_2	0.218	0.050	0.004	0.135
CH_3SSCH_3	0.672	0.636	0.306	0.387

EXPERIMENT	DDS7A	DDS7B	DDS8
Irrad. Time (min)	260	270	158
Ave. Temp. (K)	304	304	296
Humidity (%)	47	48	39
Initial Conc. (ppm)			
NO	0.149	0.158	0.039
NO_2	0.055	0.063	0.002
CH_3SSCH_3	0.526	0.352	0.364

EXPERIMENT	DDS9	DDS10	DDS11	DDS12
Irrad. Time (min)	278	320	252	206
Ave. Temp. (K)	296	299	295	295
Humidity (%)	41	44	45	45
Initial Conc. (ppm)				
NO	0.040	0.040	0.039	0.037
NO_2	0.009	0.005	0.015	0.009
CH_3SSCH_3	0.293	0.688	0.375	0.125
Seed (No. cm^{-3})	2000	20000	30000	25000

Table 4 Initial Conditions for CH_3SCH_3–NO_x–Air–$h\nu$

EXPERIMENT	DMS1A	DMS1B	DMS2A	DMS2B
Irrad. Time (min)	240	250	269	259
Ave. Temp. (K)	306	306	310	310
Humidity (%)	49	49	47	47
Initial Conc. (ppm)				
NO	0.162	0.226	0.114	0.310
NO_2	0.032	0.087	0.047	0.138
CH_3SCH_3	0.656	0.502	0.510	0.566

EXPERIMENT	DMS3	DMS4A	DMS4B	DMS5A	DMS5B
Irrad. Time (min)	260	148	158	216	226
Ave. Temp. (K)	307	306	306	300	300
Humidity (%)	51	53	54	53	53
Initial Conc. (ppm)					
NO	0.186	0.280	0.121	0.003	0.003
NO_2	0.045	0.023	0.020	0.241	0.241
CH_3SCH_3	0.700	0.480	0.478	0.535	0.308
O_3				0.144	0.144

Note: Experiments DMS5A and DMS5B were conducted in the dark.

Table 5 Summary of Measured Loss Rates in Outdoor Teflon Chambers

Species	k $\times 10^4$ $(min^{-1})^a$		k $\times 10^4$ $(min^{-1})^b$	
	Dark	Sun	Dark	Sun
CH_3SCH_3	0.92	—	—	—
CH_3SSCH_3	0.082–0.97	—	—	—
SO_2	—	1.8	1.3	—
NO_2	1.7	1.6	0–2.0 1.6–3.6[c]	1.8–7.9 —
NO_x	0.75	4.7	0.7 1.1–3.5[c]	2.6 —
O_3	2.7	4.5	1.3–3.4	5.1-6.7

Note:

a. The loss rates were measured in this studies in pure air with humidity ranging from 30% to 50%.

b. The loss rates were measured by Grosjean [1985] in dry air (dew point = −20 to −16 °C at T = 18–26 °C).

c. Humid air (RH = 82–86%) was also used to measure the loss rates of species NO_2 and NO_x by Grosjean [1985].

Table 6 Summary of Measured Product Yields

EXPERIMENT	SO_2 (%)	Time (min)	CH_3SO_3H (%)	H_2SO_4 (%)	HCHO (%)
CH_3SSCH_3–air–hν System					
DDS1A	88.7	end	0.03	0.23	27.3
DDS1B	88.5	end	0.00	0.22	14.7
DDS2A	90.1	end	0.02	0.07	14.0
DDS2B	91.2	end	0.00	0.14	18.8
DDS3A	92.8	end	0.01	0.11	10.8
DDS3B	88.2	end	0.00	0.32	9.0
DDS4A	99.0	end	0.45	0.22	27.4
DDS4B	68.7	end	0.24	0.08	12.1
CH_3SSCH_3–NO_x–air–hν System					
DDS5A	72.0	34	5.5	7.1	0.6
DDS5B	56.2	144	6.9	6.8	1.5
DDS6A	57.8	48	1.6	5.5	2.4
DDS6B	62.2	38	2.4	10.8	0.9
DDS7A	59.0	40	2.6	4.7	1.8
DDS7B	61.0	end	2.8	5.9	1.4
DDS8	70.0	85	—	—	—
DDS9	72.6	58	—	—	—
DDS10	70.0	179	—	—	—
DDS11	70.1	72	—	—	—
DDS12	80.7	46	—	—	—
CH_3SCH_3–NO_x–air–hν System					
DM1A	60.8	end	1.9	2.6	4.2
DM1B	71.1	end	2.3	3.4	7.2
DM2A	66.9	end	3.7	1.2	2.2
DM2B	64.1	159	7.3	3.2	1.4
DM3	62.1	end	2.6	3.0	4.1
DM4A	62.5	end	1.9	4.7	24.6
DM4B	64.0	end	1.2	3.3	16.9
CH_3SCH_3–NO_2–O_3–air–dark System					
DM5A	55.0	end	0.0	1.3	68.7
DM5B	68.1	end	0.5	1.9	70.0

Note:

1. The SO_2 yield was the maximum yield measured at time t. In the cases where maximum yield was not reached at the end of the experiments, "end" would be used instead of a value.
2. For the products of CH_3SO_3H, H_2SO_4 and HCHO, only the average yields were measured, and should be considered to be the lower limit of the yields since the wall loss was not accounted for in the data.
3. For SO_2 measured continuously, the product yield at time t is defined as

$$\text{Yield } (t) = \frac{[SO_2]_t - [SO_2]_o}{\sigma([RSR']_o - [RSR']_t)}$$

For the products analyzed off-line, the product yield at the end of the experiment is given as

$$\text{Average Yield} = \frac{\text{Average Conc. at the End}}{\sigma([RSR']_o - [RSR']_t)}$$

where the average concentration is calculated from the total sample collected divided by the total sampling volume. The σ factor is introduced to account for the number of molecules of product that can be theoretically produced per molecule of RSR', i.e., that two SO_2 molecules could be produced from one CH_3SSCH_3, and that one CH_3SSCH_3 or one CH_3SCH_3 could generate two HCHO molecules.

Table 7 Summary of Experimental Conditions and SO_2 Yield

$[RSR']_o$ (ppm)	$[NO]_o$ (ppm)	$[NO_2]_o$ (ppm)	$[X]_o$ (ppm)	Exp. Time (min)	Volume (l)	SO_2 Yield (%)	Ref.
CH_3SSCH_3 Photooxidation in Air							
0.34–0.81	0.000	0.000	0.000	~ 300	2.5×10^4 T	~ 90	(1)
—	—	—	—	—	11 Q	90	(2)
0.13–0.69	~ 0.040	~ 0.005	0.000	158–320	2.5×10^4 T	70–80	(1)
0.31–0.67	0.01–0.61	0.01–0.22	0.000	~ 300	2.5×10^4 T	56–72	(1)
21	0.0	25	0.0	7	420 G	49	(8)
24	15	0.2	C_2H_5ONO: 9	18	11 Q	22	(2)
CH_3SCH_3 Photooxidation in Air							
24	0.0	0.0	H_2O_2: 24	32	420 G	66	(7)
0.48–0.70	0.12–0.31	0.02–0.14	0.000	150–270	2.5×10^4 T	61–71	(1)
1.0–1.5	0.28–0.36	0.13–0.24	0.0	240	8.0×10^4 T	40–74	(5)
0.33–0.68	0.24–0.36	0.0–0.02	0.0	360	$4–80\times10^3$ T	35–51	(6)
1.3	0.75	0.0	0.0	240	6×10^3 P	24–33	(4)
20	14	0.3	0.0	40	11 Q	31	(3)
20	10	0.0	C_2H_5ONO: 10	2	—	22	(9)
20	18	0.0	C_2D_5ONO: 35	5	11 Q	21	(2)
CH_3SCH_3 Oxidation in Dark in Air							
0.31–0.54	0.003	0.24	O_3: 0.144	~ 220	2.5×10^4 T	55–68	(1)
23.0	0.0	0.5	N_2O_5: 50	—	5.8×10^3 T	30–35	(10)

Note:

1. Due to the space limitation, the other experimental conditions employed in the available product studies, including temperature, humidity, light intensity and wavelength, are not listed although some of them were significantly different.
2. For the system CH_3SSCH_3–air–$h\nu$ studied by Hatakeyama and Akimoto [1983], the concentration of CH_3SSCH_3 was not specified. Also the yield of CH_3SO_3H was observed to increase when $[CH_3SSCH_3]_o$ increased.
3. The SO_2 yields measured by Grosjean [1984] ranged from 35% to 94% although only two runs [Figures 1 and 2] were listed.
4. For the surface material of the reactor, G: glass; Q: quartz; T: Teflon; P: PFA.

Reference:

1. This work.
2. Hatakeyama and Akimoto [1983]: Figures 10 and 12.

3. Hatakeyama et al. [1982]: Figure 1.
4. Hatakeyama et al. [1985]: Figure 1.
5. Grosjean and Lewis [1982].
6. Grosjean [1984]: Figures 1 and 2.
7. Barnes et al. [1988]: Figure 4.
8. Barnes et al. [1987]: Figure 3B.
9. Niki et al. [1983].
10. MacLeod et al. [1986].

Table 8 Summary of Experimental Conditions and Measured CH_3SO_3H and H_2SO_4 Yields

$[RSR']_o$ (ppm)	$[NO]_o$ (ppm)	$[NO_2]_o$ (ppm)	$[X]_o$ (ppm)	Volume (l)	CH_3SO_3H (%)	H_2SO_4 (%)	Ref.
CH_3SSCH_3 Photooxidation in Air							
0.34–0.81	0.000	0.000	0.000	2.5×10^4 T	< 1	< 1	(1)
—	—	—	—	11 Q	10	—	(2)
0.31–0.67	0.01–0.61	0.01–0.22	0.000	2.5×10^4 T	1.6–6.9	4.7–10.8	(1)
—	—	—	—	1–11 G	60	< 2	(2)
CH_3SCH_3 Photooxidation in Air							
24	0.0	0.0	H_2O_2: 24	420 G	~ 0	—	(7)
0.48–0.70	0.12–0.31	0.02–0.14	0.000	2.5×10^4 T	1.2–7.3	1.2–4.7	(1)
0.33–0.68	0.24–0.36	0.0–0.02	0.0	$4–80\times10^3$ T	0.6–13.4	1.0–16.9	(6)
~ 10	—	—	CH_3ONO: 40	3 G	> 50	—	(4)
830	400-1210	0—	0.0	1 G	> 50	< 2	(3)
—	—	—	—	1–11 G	> 50	—	(2)
CH_3SCH_3 Oxidation in Dark in Air							
0.31–0.54	0.003	0.24	O_3: 0.144	2.5×10^4 T	< 1	1.3–1.9	(1)

Note:

1. Due space limitation, temperature, humidity, light intensity, and time length are not listed although some of them were significantly different among studies.
2. For the products of CH_3SO_3H and H_2SO_4 , only the average yields were measured by Grosjean [1984] and in this work, and should be considered to be the lower limit of the yields since the wall loss was not corrected for the data.
3. The CH_3SO_3H and H_2SO_4 yields measured by Grosjean [1984] ranged from 0.6% to 13.4% and 1.0 to 16.9, respectively.
4. For the systems studied by Hatakeyama and Akimoto in 1983, the initial concentrations of reactants were not specified.
5. For the system CH_3SCH_3–H_2O_2–air–$h\nu$ the yield of $CH_3S(O)_2CH_3$ was measured to be about 20% by Barnes et al. [1988].
6. For the surface material of the reactor, G: glass; Q: quartz; T: Teflon; P: PFA.

Reference:

1. This work.
2. Hatakeyama and Akimoto [1983].
3. Hatakeyama et al. [1982].

4. Hatakeyama et al. [1985].
5. Grosjean and Lewis [1982].
6. Grosjean [1984].
7. Barnes et al. [1988].

REFERENCES

Balla, R. J., H. H. Nelson, and J. R. McDonald, Kinetics of the reaction of CH_3S with NO, NO_2 and O_2, *Chem. Phys., 109,* 101–107, 1986.

Barnes, I., V. Bastian, K. H. Becker, and H. Niki, FTIR spectroscopic studies of the $CH_3S + NO_2$ reaction under atmospheric conditions, *Chem. Phys. Lett., 140,* 451–457, 1987.

Barnes, I., V. Bastian, and K. H. Becker, Kinetics and mechanisms of the reaction of OH radicals with dimethyl sulfide, *Int. J. Chem. Kinet., 20,* 415-431, 1988.

Benson, S. W., Thermochemistry and kinetics of sulfur-containing molecules and radicals, *Chem. Rev., 78,* 23–35, 1978.

Calvert, J. G., and J. N. Pitts, Jr., *Photochemistry,* John Wiley & Sons, Inc., 1966.

Chatgilialoglu, C., D. Griller, and M. Guerra, Experimental and theoretical approaches to the optical absorption spectra of sulfonyl radicals, *J. Phys. Chem., 91,* 3747–3750, 1987.

Daykin, E. P., and P. H. Wine, A study of the reactions of NO_3 radicals with organic sulfides: Reactivity trend at 298 K, *Submitted to Int. J. Chem. Kinet.,* 1990.

Demerjian, K. L., K. L. Schere, and J. T. Peterson, Theoretical estimates of actinic (spherically integrated) flux and photolytic rate constants of atmospheric species in the lower troposphere, *Adv. Environ. Sci. Technol., 10,* 369–459, 1980.

Grosjean, D., and R. Lewis, Atmospheric photooxidation of methyl sulfide, *Geophys Res. Lett., 9,* 1203–1206, 1982.

Grosjean, D., Photooxidation of methyl sulfide, ethyl sulfide, and methanethiol, *Environ. Sci. Technol., 18,* 460–468, 1984.

Grosjean, D., Wall loss of gaseous pollutants in outdoor teflon Chambers, *Environ.*

Sci. Technol., 19, 1059–1065, 1985.

Hatakeyama, S., M. Okuda, and H. Akimoto, Formation of sulfur dioxide and methanesulfonic acid in the photooxidation of dimethyl sulfide in the air, *Geophys. Res. Lett., 9,* 583–586, 1982.

Hatakeyama, S., and H. Akimoto, Reactions of OH radicals with methanethiol, dimethyl sulfide, and dimethyl disulfide in air, *J. Phys. Chem., 87,* 2387–2395, 1983.

Hatakeyama, S., K. Izumi, and H. Akimoto, Yield of SO_2 and formation of aerosol in the photo-oxidation of DMS under atmospheric conditions, Atmos. Environ., 19, 135–141, 1985.

Hynes, A. J., P. H. Wine, and D. H. Semmes, Kinetic and mechanism of OH reactions wiht organic sulfides, *J. Phys. Chem., 90,* 4148–4156, 1986.

Leone, J. A., R. C. Flagan, D. Grosjean, and J. H. Seinfeld, An outdoor smog chamber and modeling study of toluene–NO_x Photooxidation, *Int. J. Chem. Kinet., 17,* 177–216, 1985.

MacLeod, H., S. M. Aschmann, R. Atkinson, E. C. Tuazon, J. A. Sweetman, A. M. Winer, and J. N. Pitts, Jr., Kinetics and mechanisms of the gas phase reactions of the NO_3 radical with a series of raduced sulfur compounds, *J. Geophys. Res., 91,* 5338–5346, 1986.

Niki, H., P. D. Maker, C. M. Savage, and L. P. Breitenbach, An FTIR study of the mechanism for the reaction HO + CH_3SCH_3, *Int. J. Chem. Kinet., 15,* 647–654, 1983.

Stern, J. E., R. C. Flagan, D. Grosjean, and J. H. Seinfeld, Aerosol formation and growth in atmospheric aromatic hydrocarbon, *Environ. Sci. Technol., 21,* 1224–1231, 1987.

Toon, O. B., J. F. Kasting, R. P. Turco, and M. S. Liu, The sulfur cycle in the

marine atmosphere, *J. Geophys. Res., 92,* 943–963, 1987.

Tyndall, G. S., and A. R. Ravishankara, Kinetics and mechanisms of the reactions of CH_3S with O_2 and NO_2 at 298 K, *J. Phys. Chem.,* 1988 (in press).

Yin, F., D. Grosjean, and J. H. Seinfeld, Mechanism of atmospheric photooxidation of organosulfur compounds, I. Mechanism Development, *J. Atmos. Chem.,this issue,* 1989.

Figure Caption

Figure 1. Schematic diagram of the outdoor smog chamber facility.

Figure 2. Observed and predicted concentration-time profiles for CH_3SSCH_3–air experiment DDS3A.

Figure 3. Observed and predicted concentration-time profiles for CH_3SSCH_3–NO_x–air experiment DDS8.

Figure 4. Observed and predicted concentration-time profiles for CH_3SSCH_3–NO_x–air experiment DDS7A.

Figure 5. Observed and predicted concentration-time profiles for CH_3SSCH_3–NO_x–air experiment DDS8. Competition between $CH_3SOH + CH_3SO_3$ (2) and CH_3SOHHO_2 (3), $CH_3SOH + CH_3O_2$ (4). Ratios of k_3/k_2 and k_4/k_2: (a) 0.25, 0.25 and (b) 2.5, 2.5.

Figure 6. Observed and predicted concentration-time profiles for CH_3SSCH_3–NO_x–air experiment DDS8. Effects of varing $k_{CH_3S+O_3}$ and $k_{CH_3SO+O_3}$: (a) 6.0, 2.0 and (b) 1.5, 0.5 (k is multiplied by 10^{12}).

Figure 7. Observed and predicted concentration-time profiles for CH_3SSCH_3–NO_x–air experiment DDS7A. Competition between addition of CH_3SO to O_2 (1) and oxidation by NO_2 (2) and O_3 (3). Ratios of $k_1/(k_2 + k_3)$: (a) 1.5 and (b) 0.15 (ratios are multiplied by 10^6).

Figure 8. Observed and predicted concentration-time profiles for CH_3SSCH_3–NO_x–air experiment DDS8. Competition between CH_3SO_2 decomposition (1) and

O_2 addition (4). Ratios of $k_1/k_4[O_2]$: (a) 0.84 and (b) 0.42.

Figure 9. Observed and predicted concentration-time profiles for CH_3SCH_3–NO_x–air experiment DMS2A.

Figure 10. Observed and predicted concentration-time profiles for CH_3SCH_3–NO_x–air experiment DMS3.

Figure 11. Observed and predicted concentration-time profiles for CH_3SCH_3–NO_x–air experiment DMS3. Competition between addition (1) and abstraction (2) for $CH_3SCH_3 + OH$ reaction. Ratios of $k_2/(k_1 + k_2)$: (a) 0.72, (b) 0.90 and (c) 0.10.

Figure 12. Observed and predicted concentration-time profiles for CH_3SCH_3–NO_x–air experiment DMS3. The fate of $CH_3S(ONO_2)CH_3$: (a) $CH_3SCH_2 + HNO_3$, (b) $CH_3SONO_2 + CH_3$ and (c) $CH_3S(O)CH_3 + NO_2$.

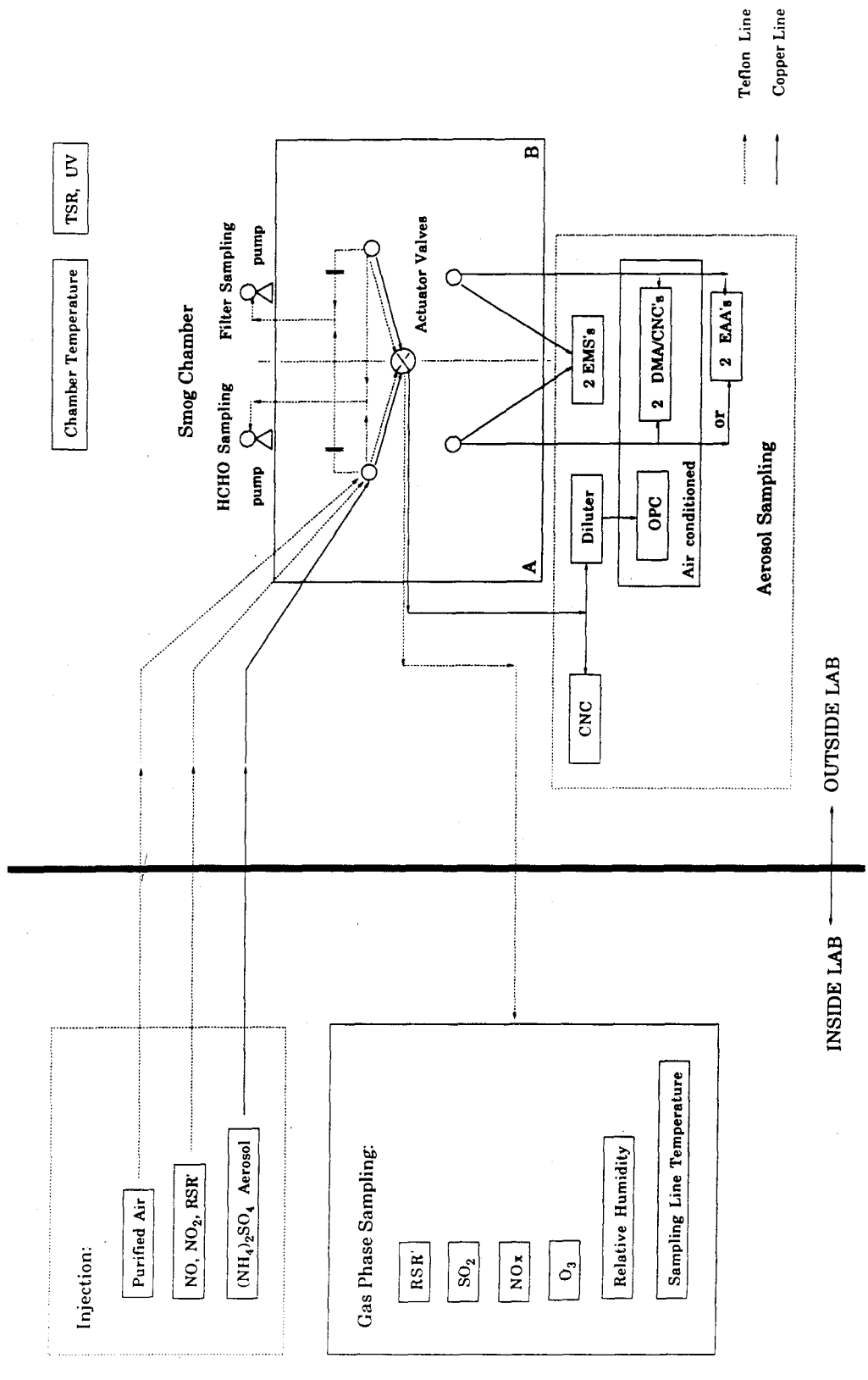
Chamber Temperature
TSR, UV
Smog Chamber
HCHO Sampling pump
Filter Sampling pump
Actuator Valves
B
A
2 EMS's
2 DMA/CNC's
2 EAA's
or
Diluter
OPC
Air conditioned
Aerosol Sampling
CNC
Teflon Line
Copper Line
Injection:
Purified Air
NO, NO_2, RSR'
$(NH_4)_2SO_4$ Aerosol
Gas Phase Sampling:
RSR'
SO_2
NOx
O_3
Relative Humidity
Sampling Line Temperature
INSIDE LAB
OUTSIDE LAB

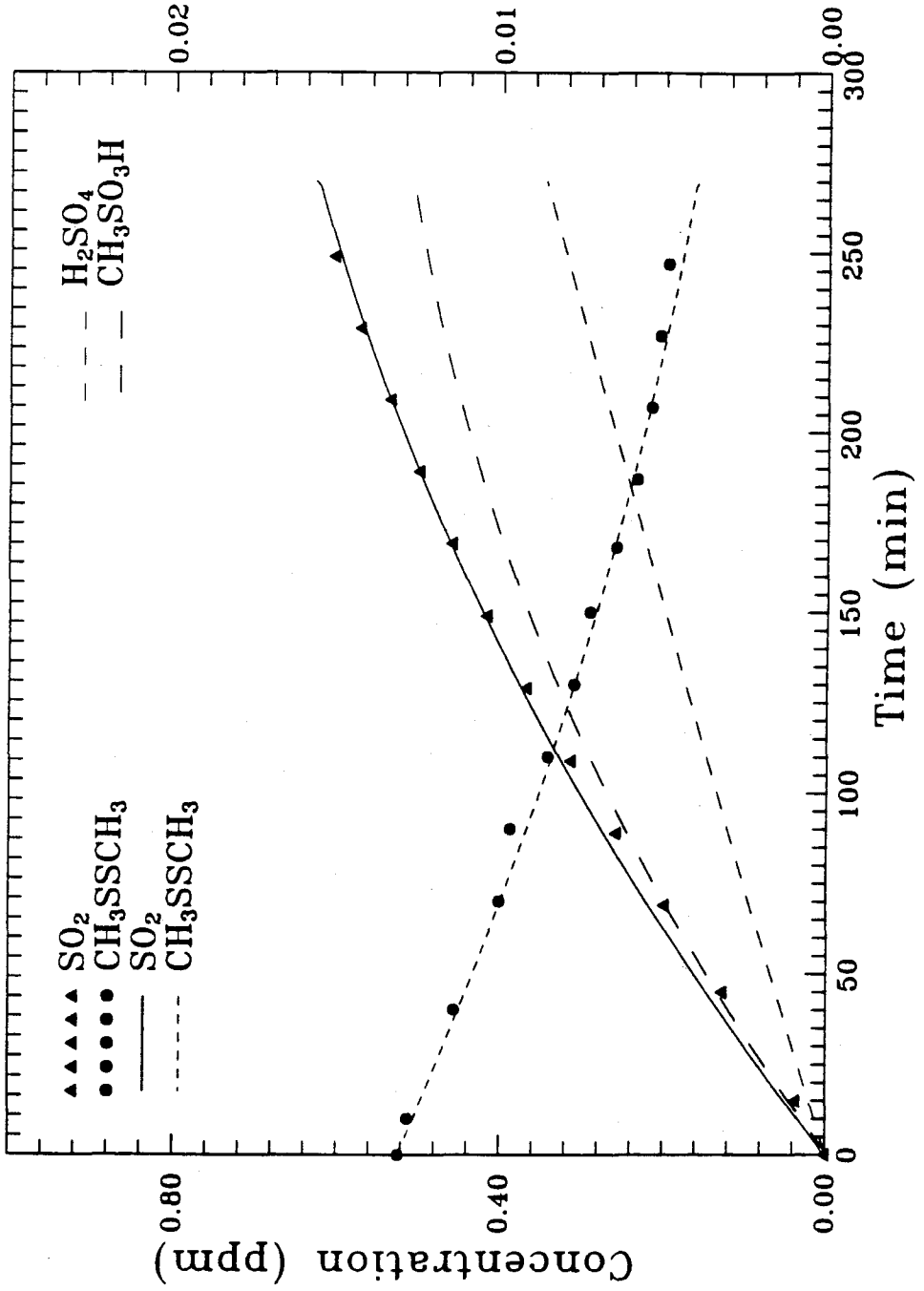

Figure 2
(DDS3A)

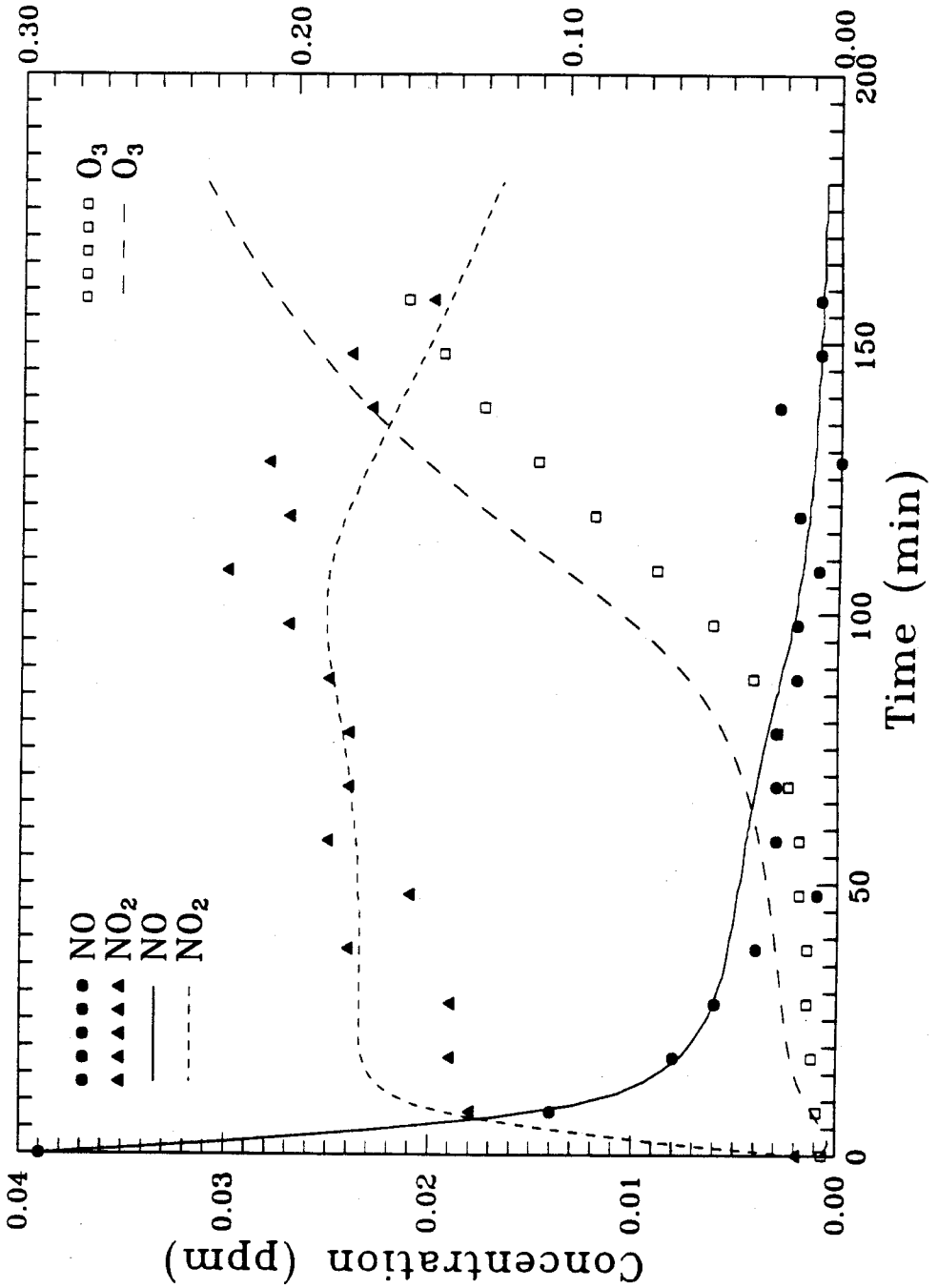

Figure 3
(DDS8)

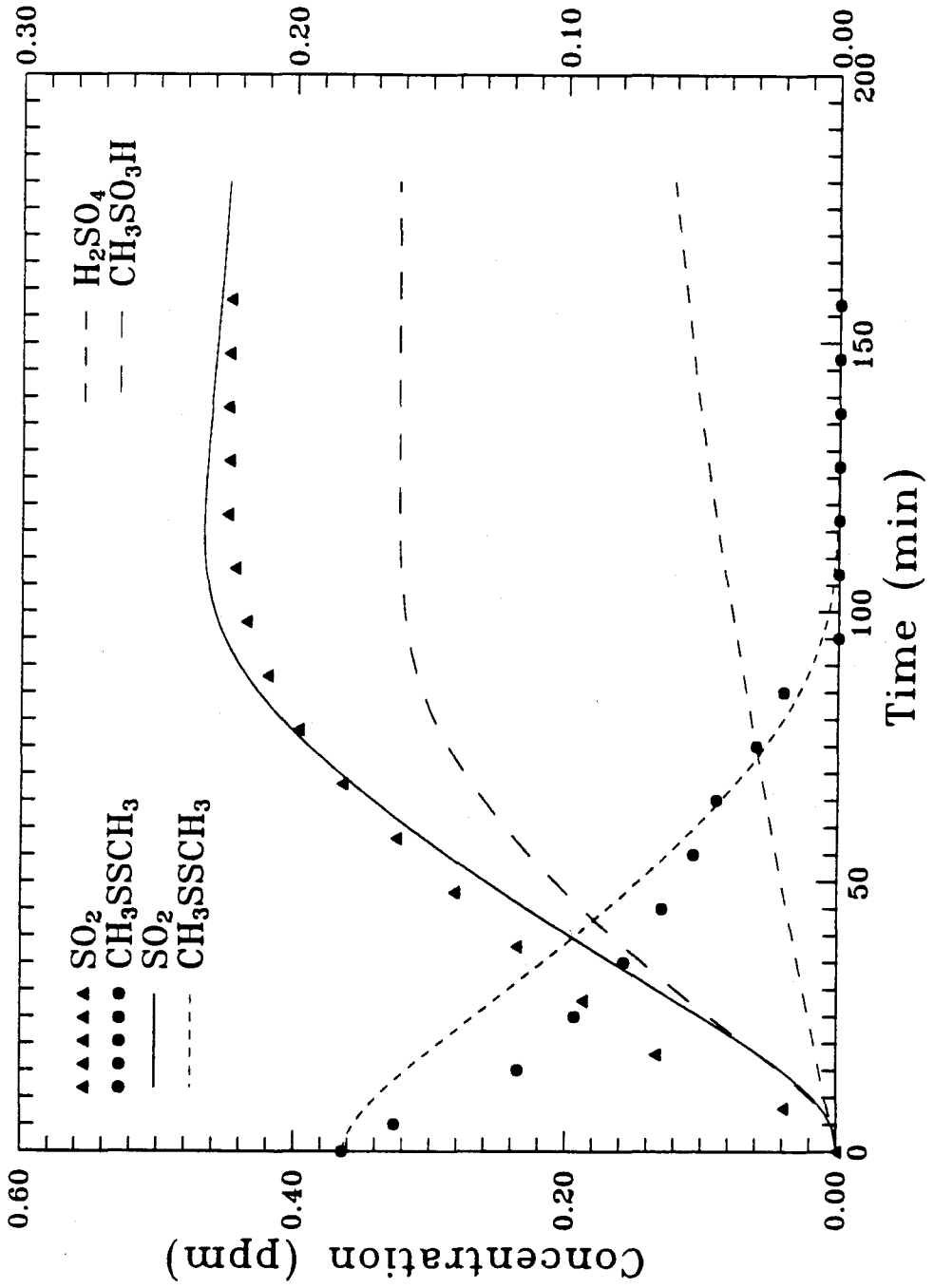

Figure 3
(DDS8)

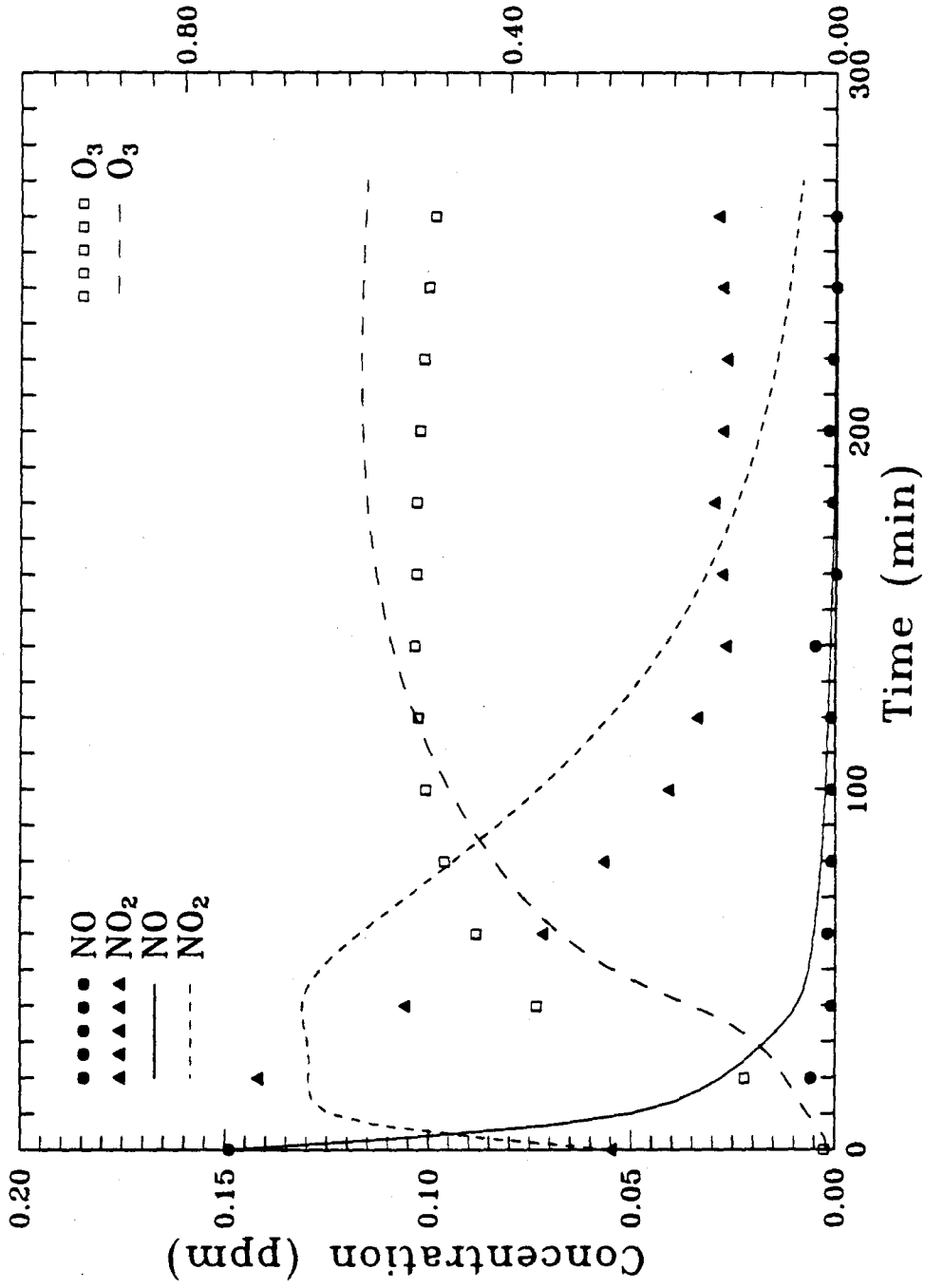

Figure 4
(DDS7A)

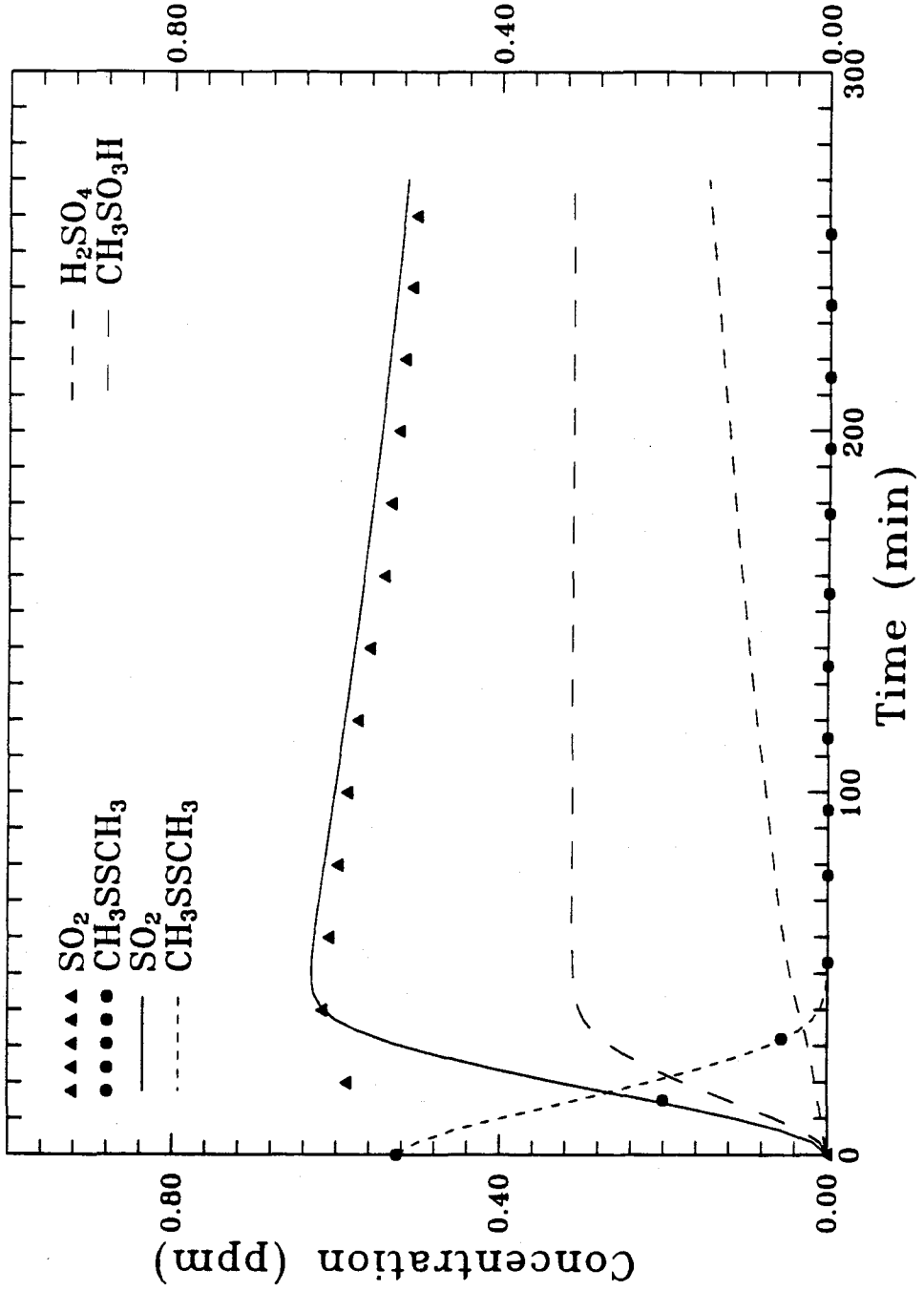

Figure 4
(DDS7A)

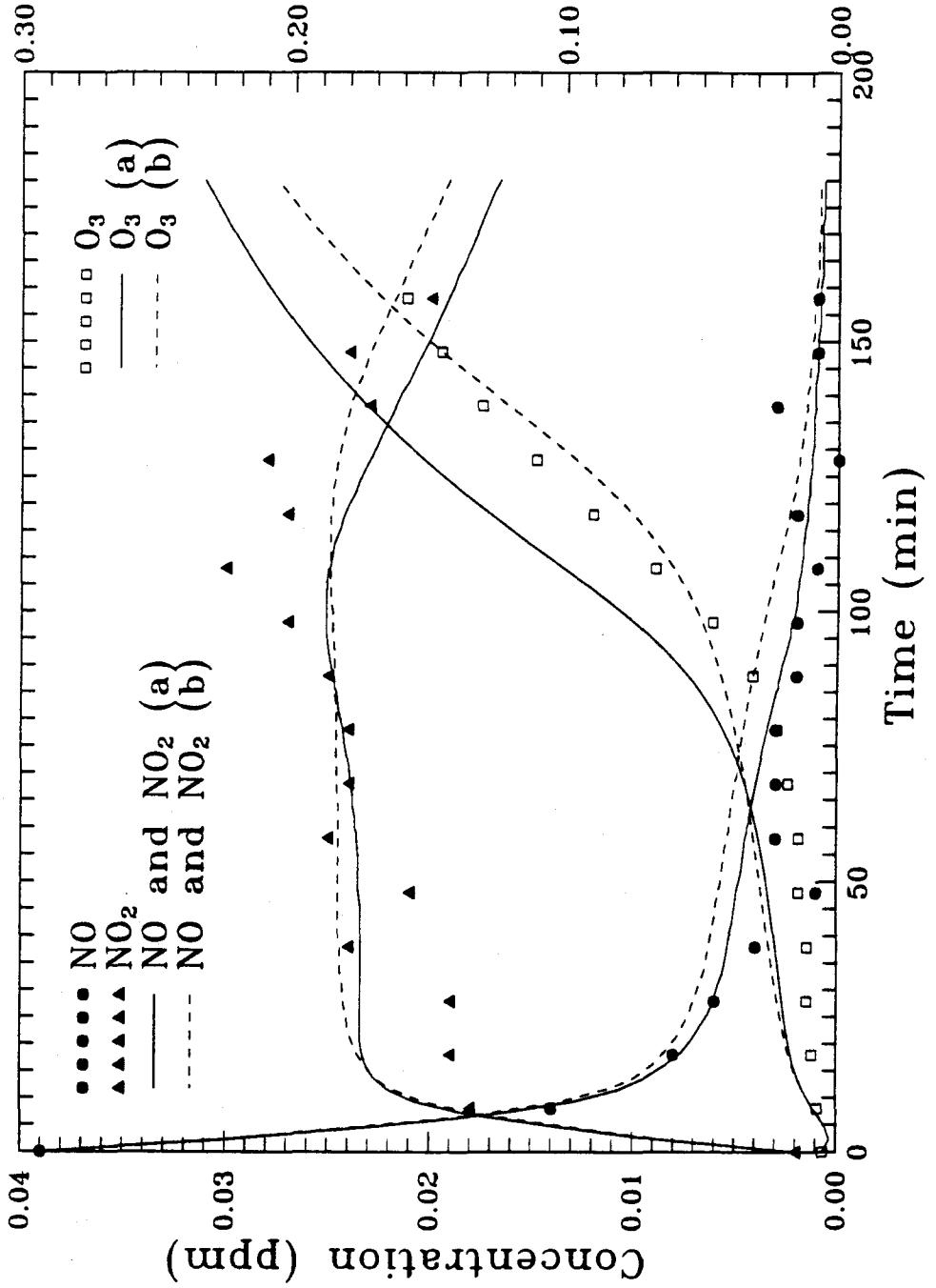

Figure 5
(DDS8)

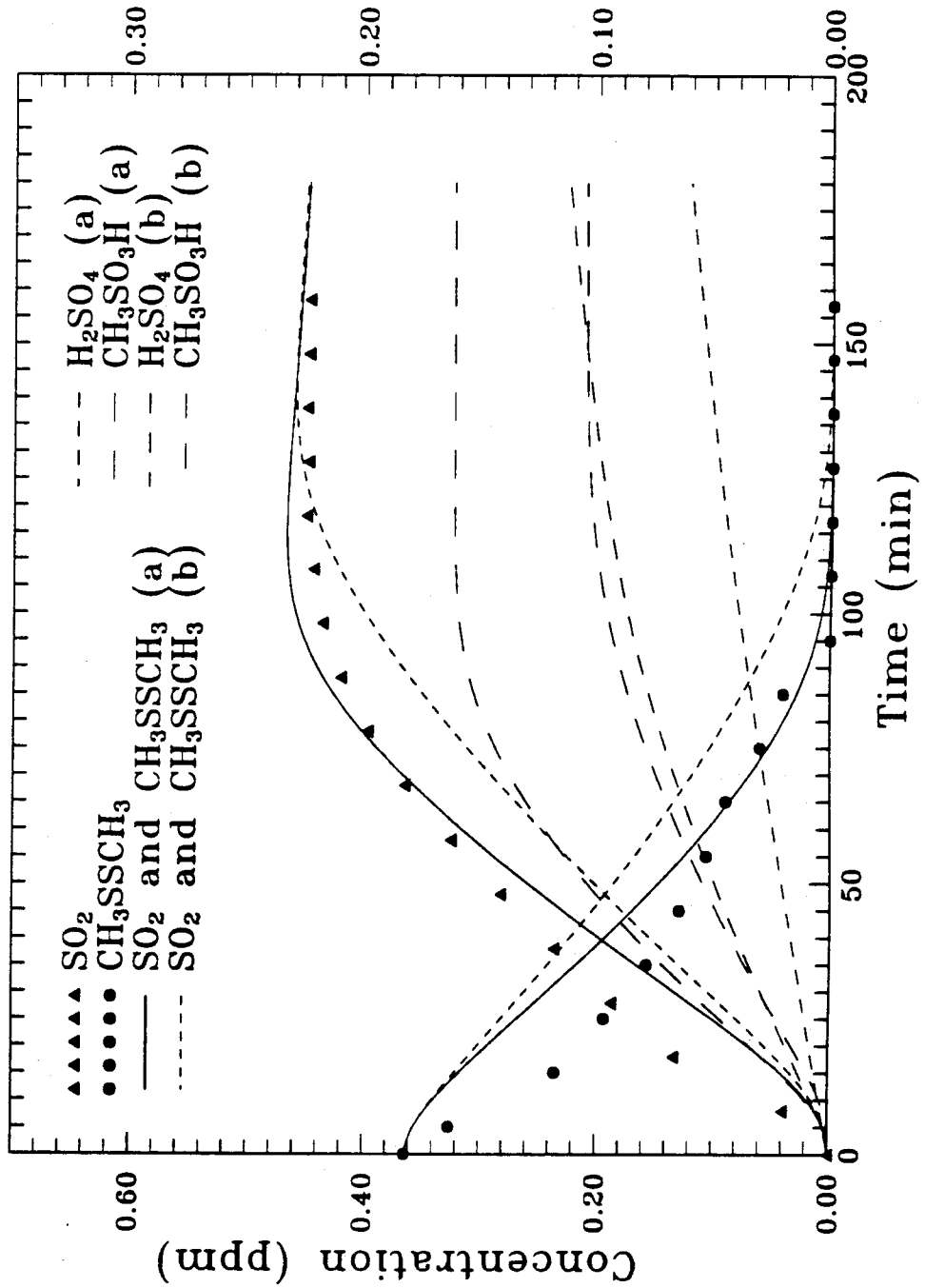

Figure 5
(DDS8)

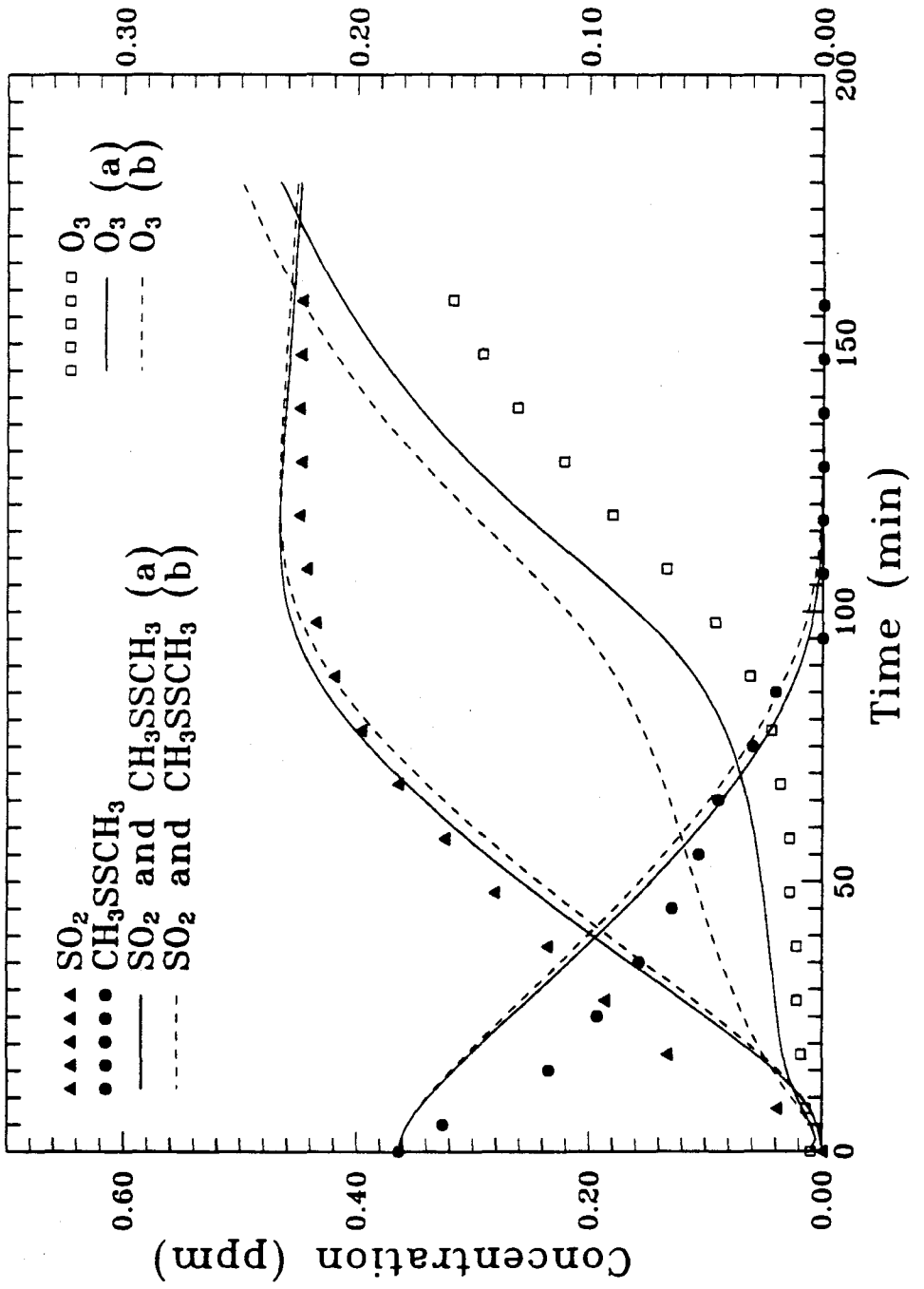

Figure 6
(DDS8)

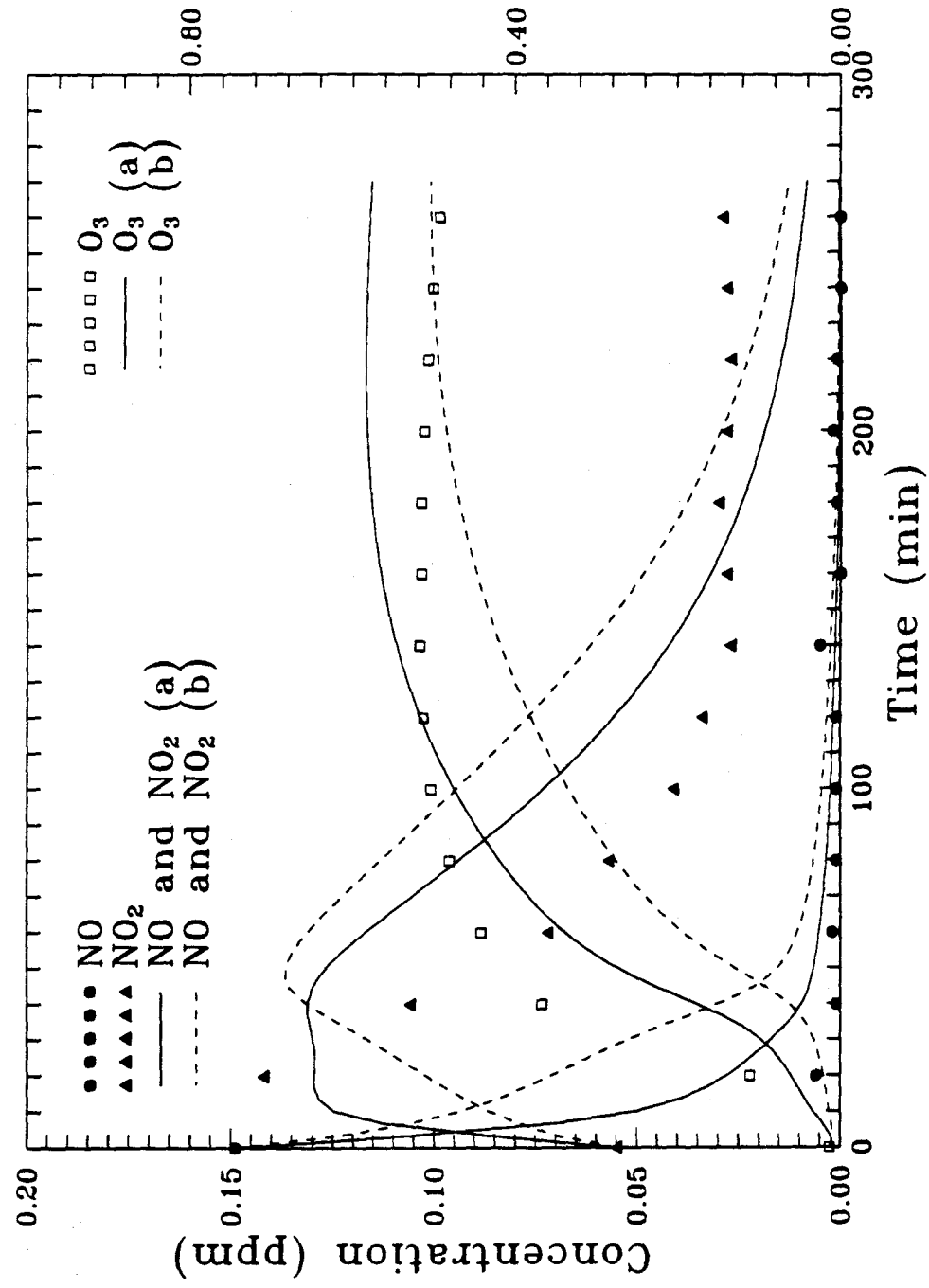

Figure 7
(DDS7A)

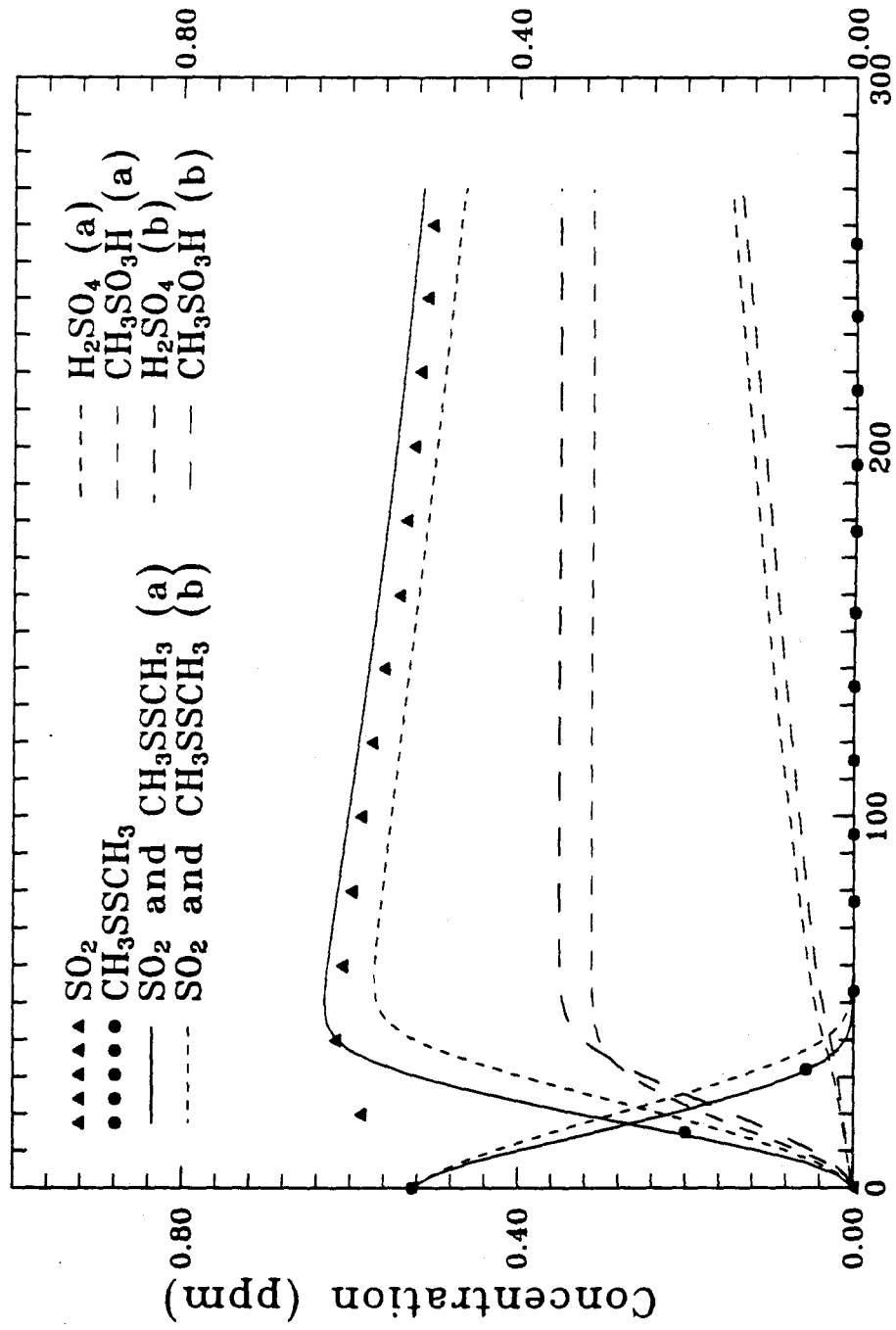

Figure 7
(DDS7A)

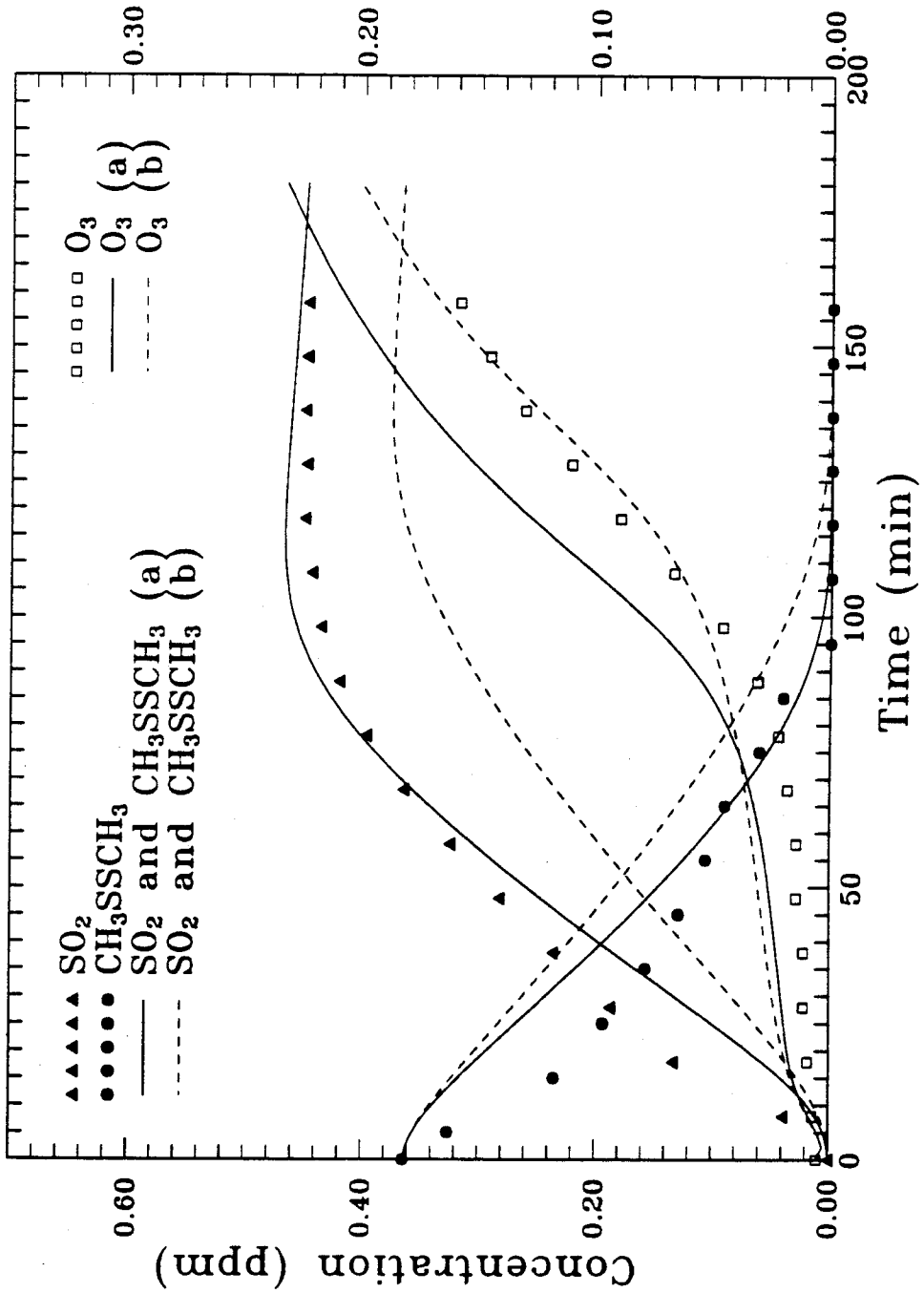

Figure 8
(DDS8)

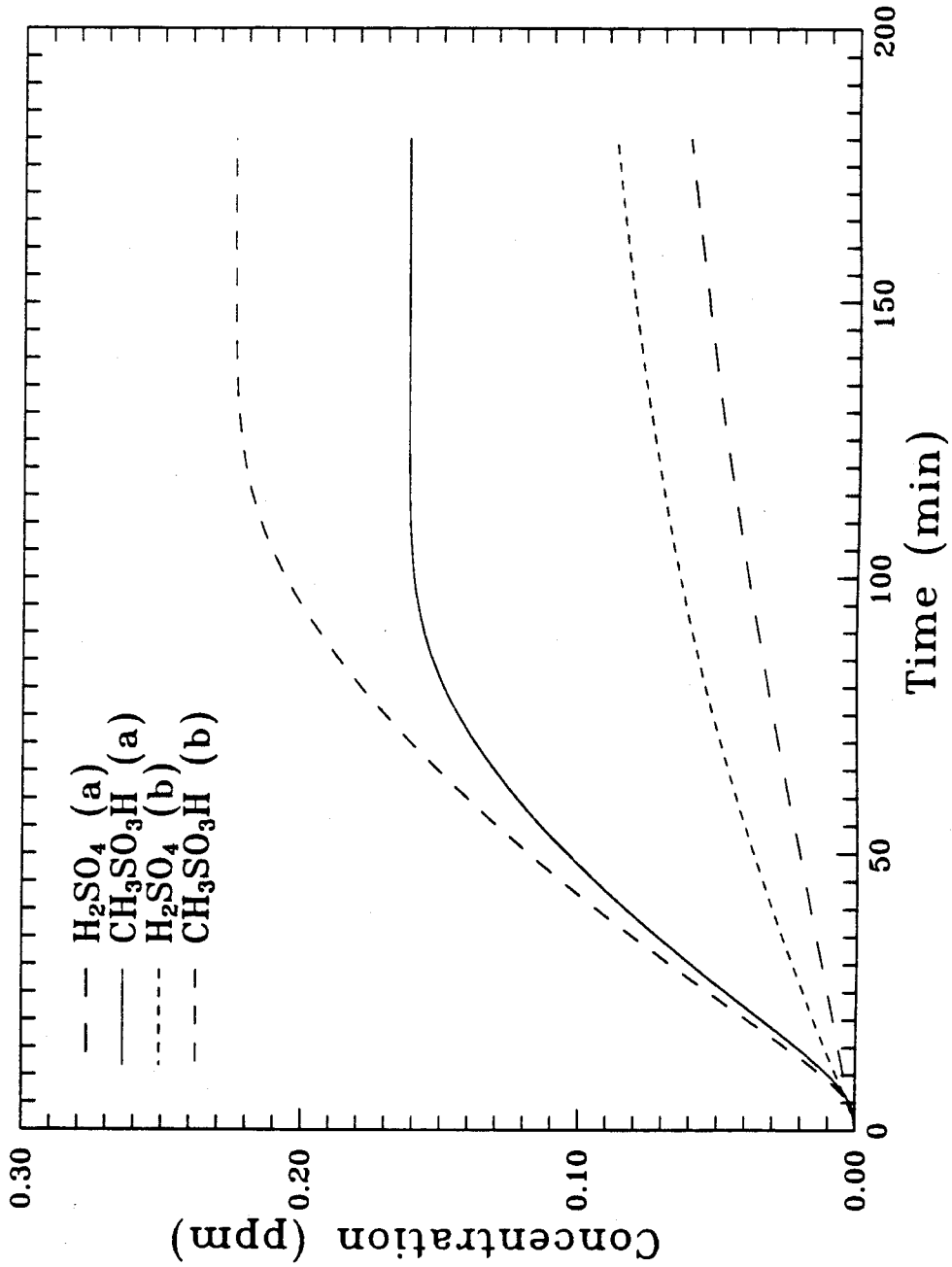

Figure 8
(DDS8)

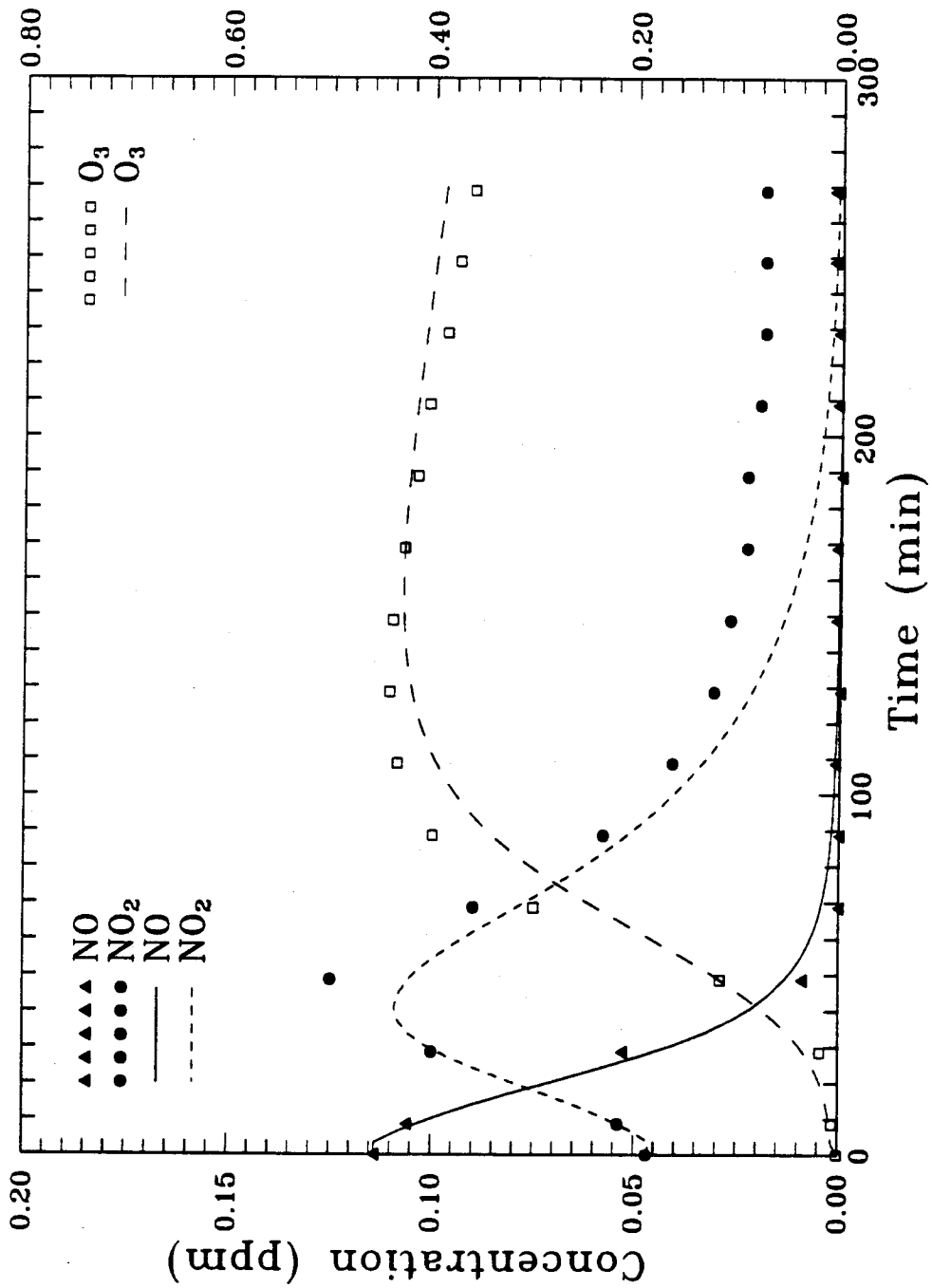

Figure 9
(DMS2A)

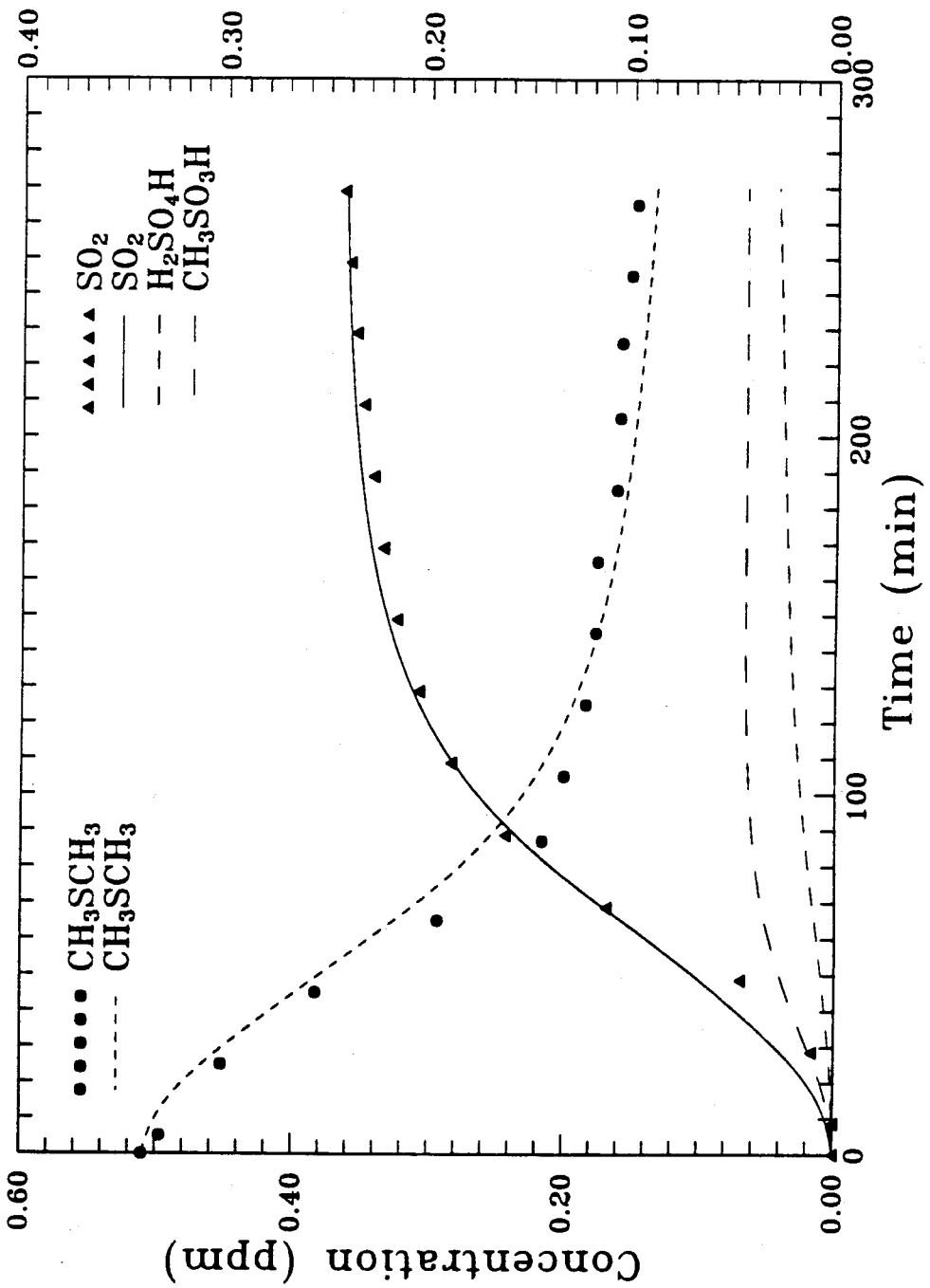

Figure 9
(DMS2A)

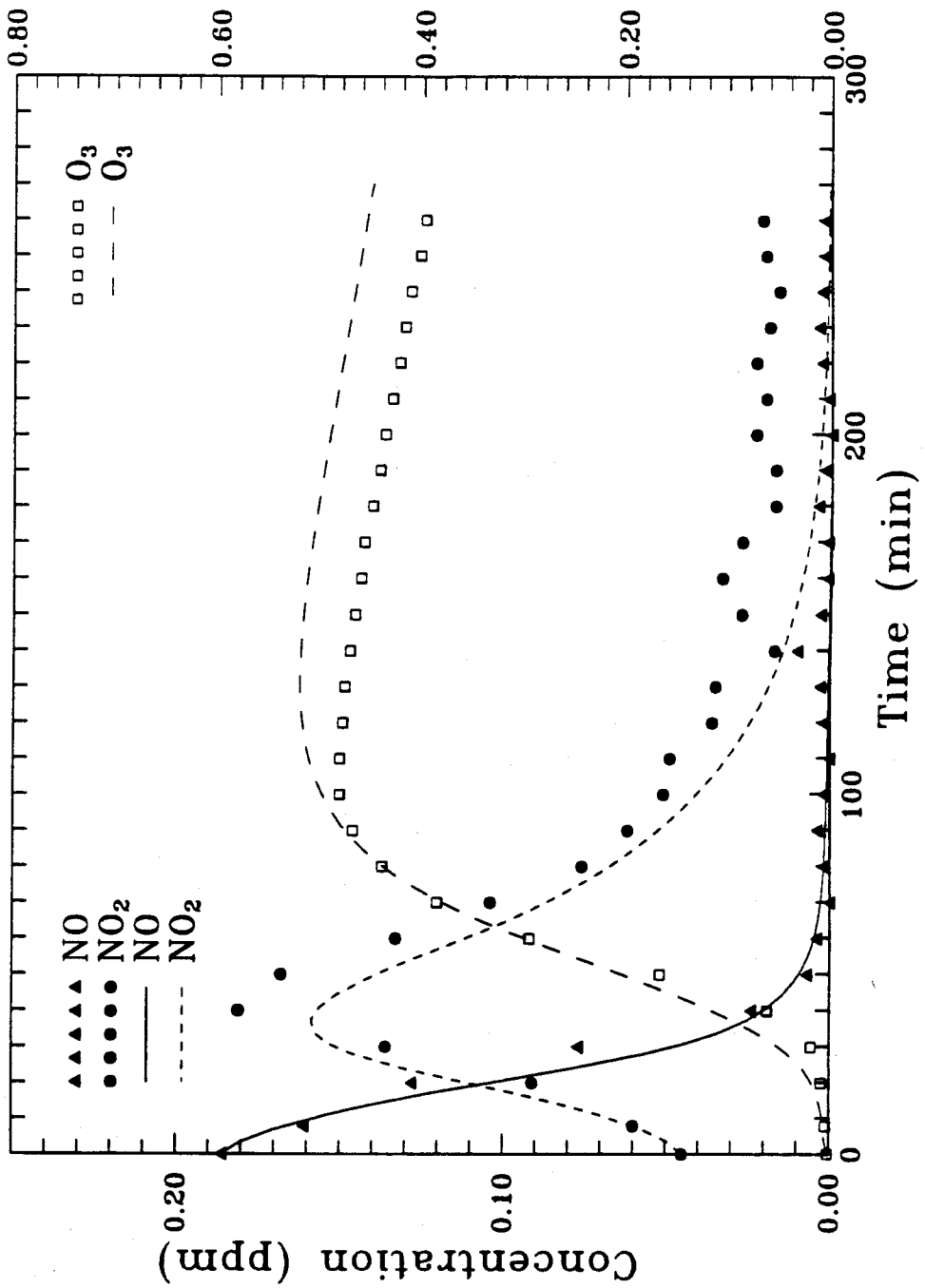

Figure 10
(DMS3)

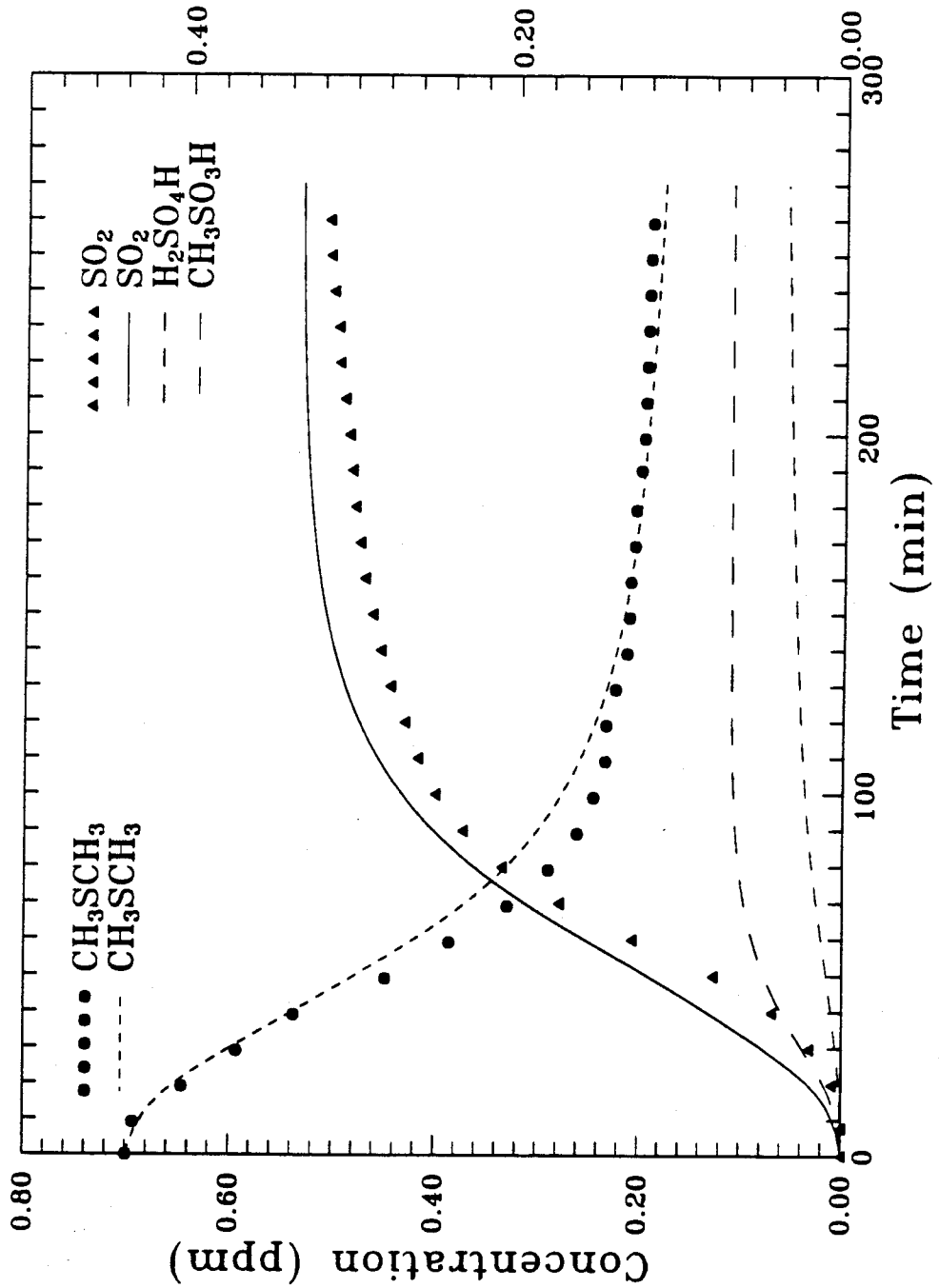

Figure 10
(DMS3)

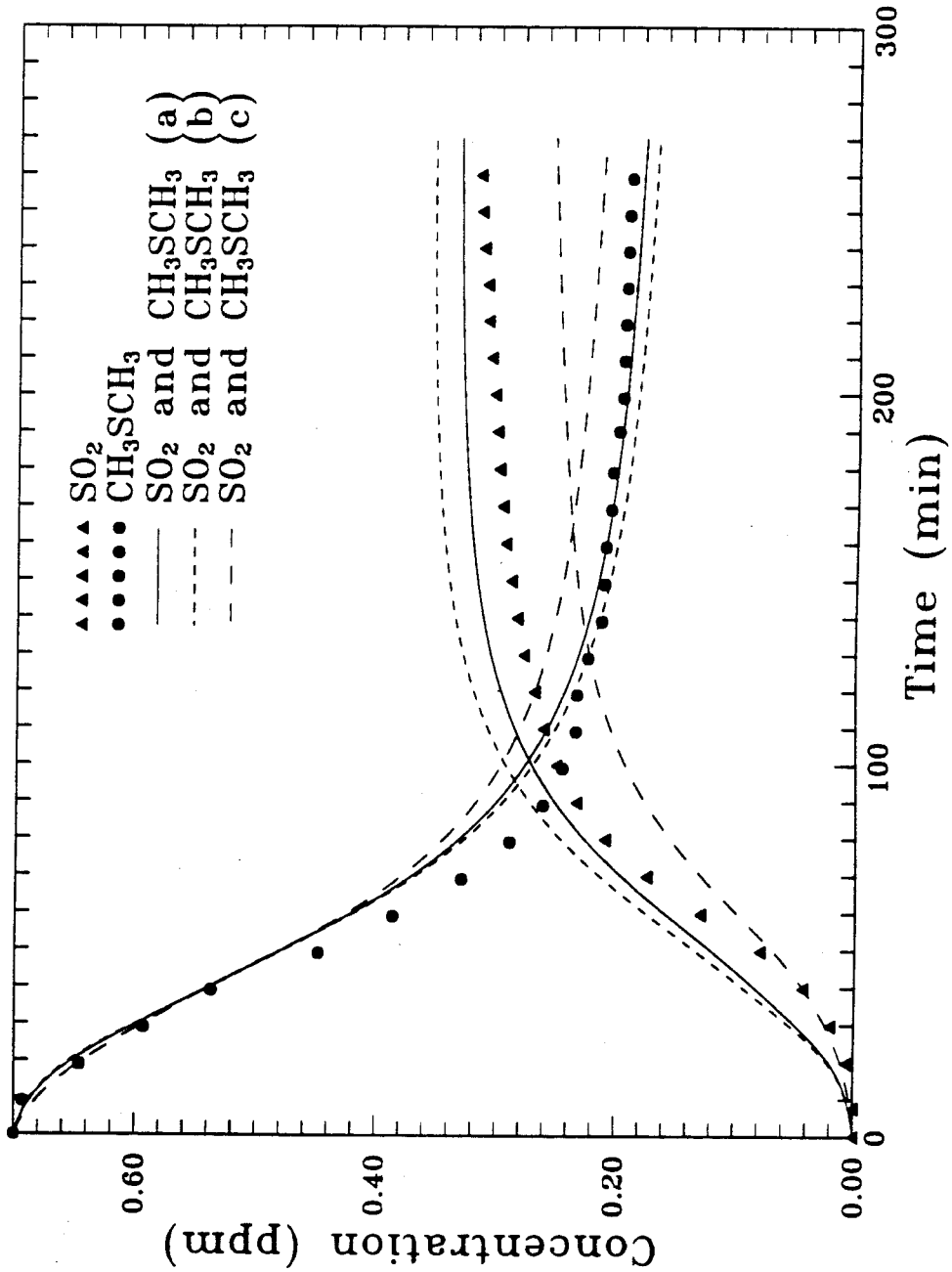

Figure 11
(DMS3)

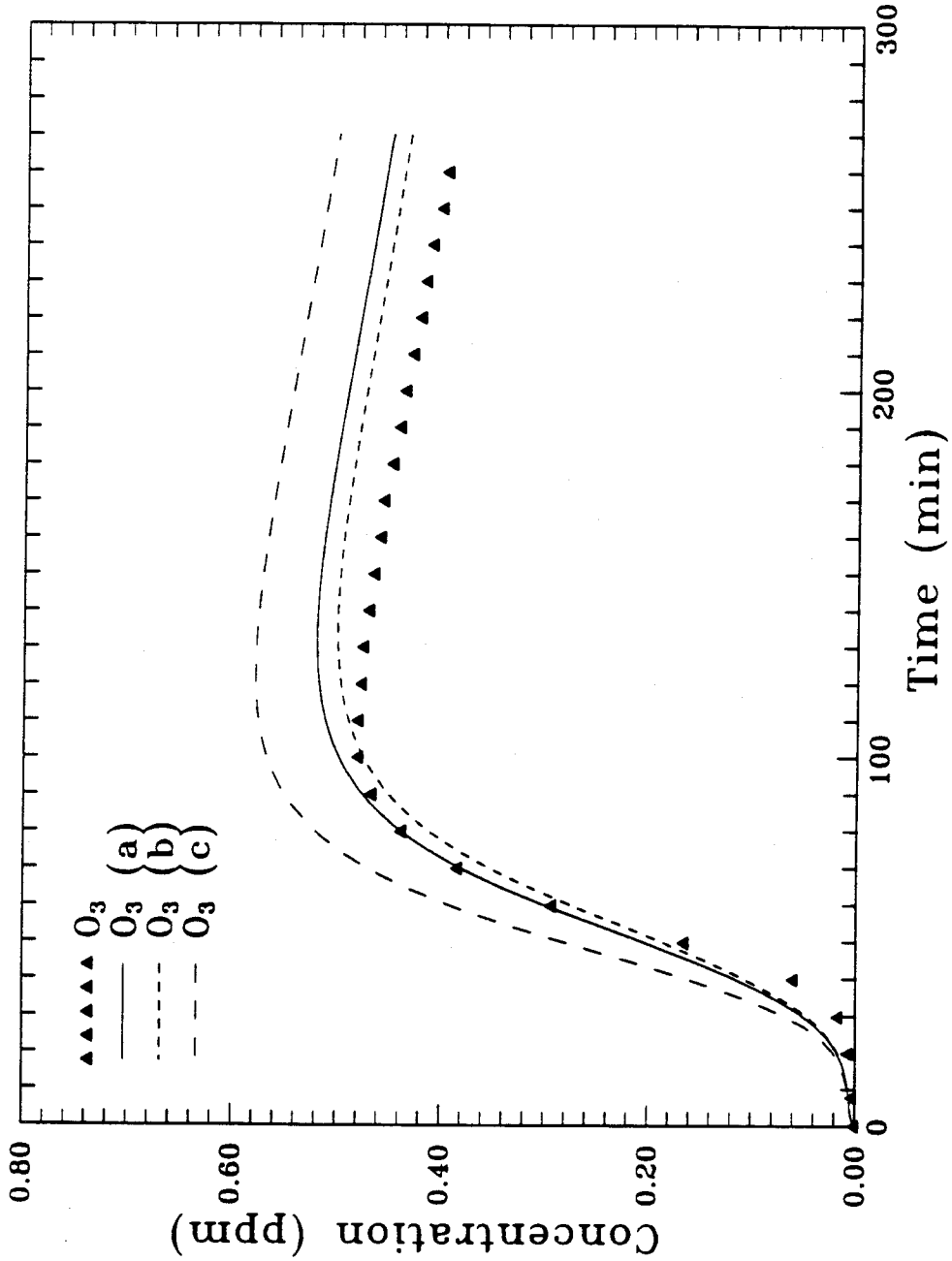

Figure 11
(DMS3)

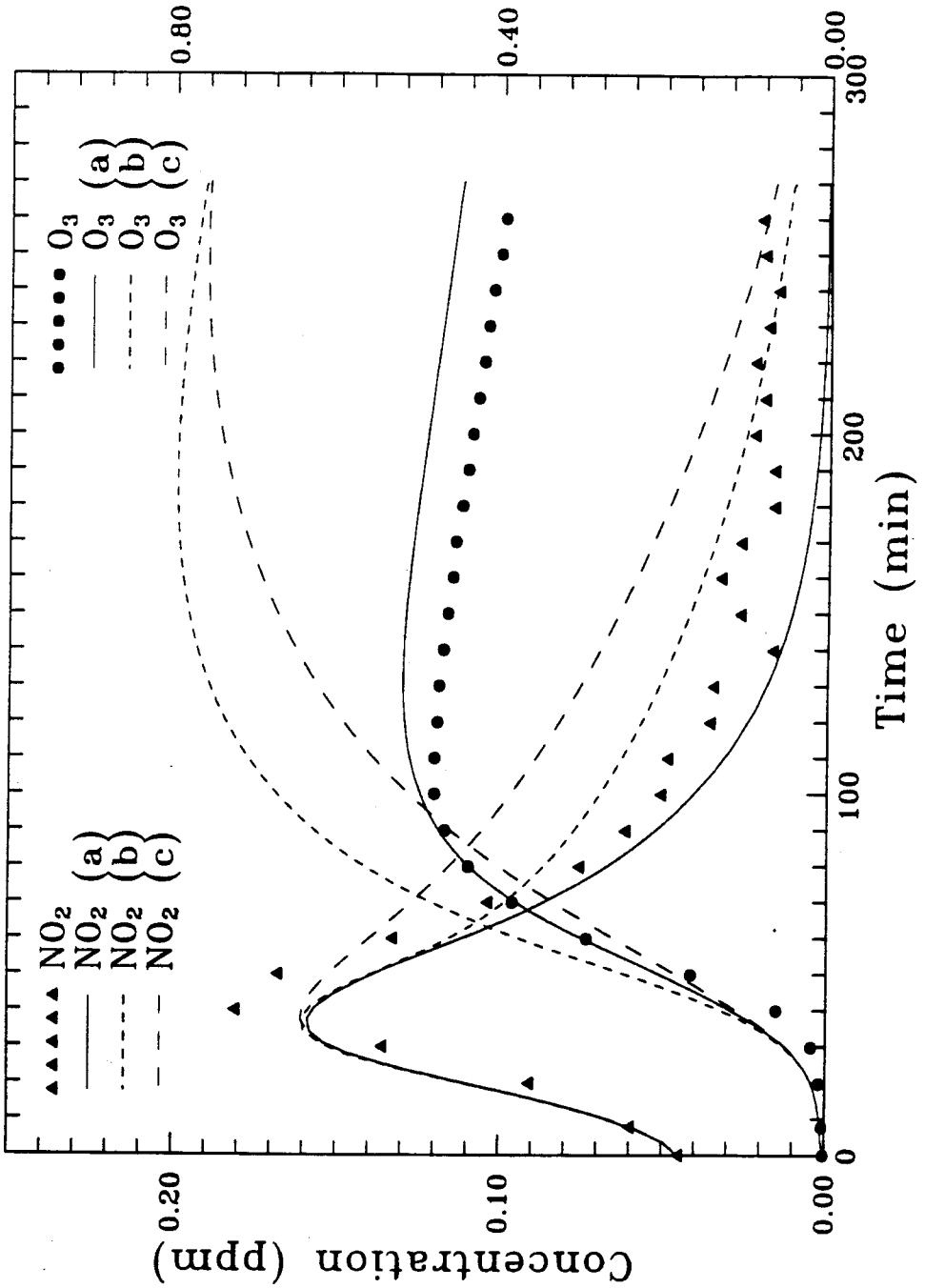

Figure 12
(DMS3)

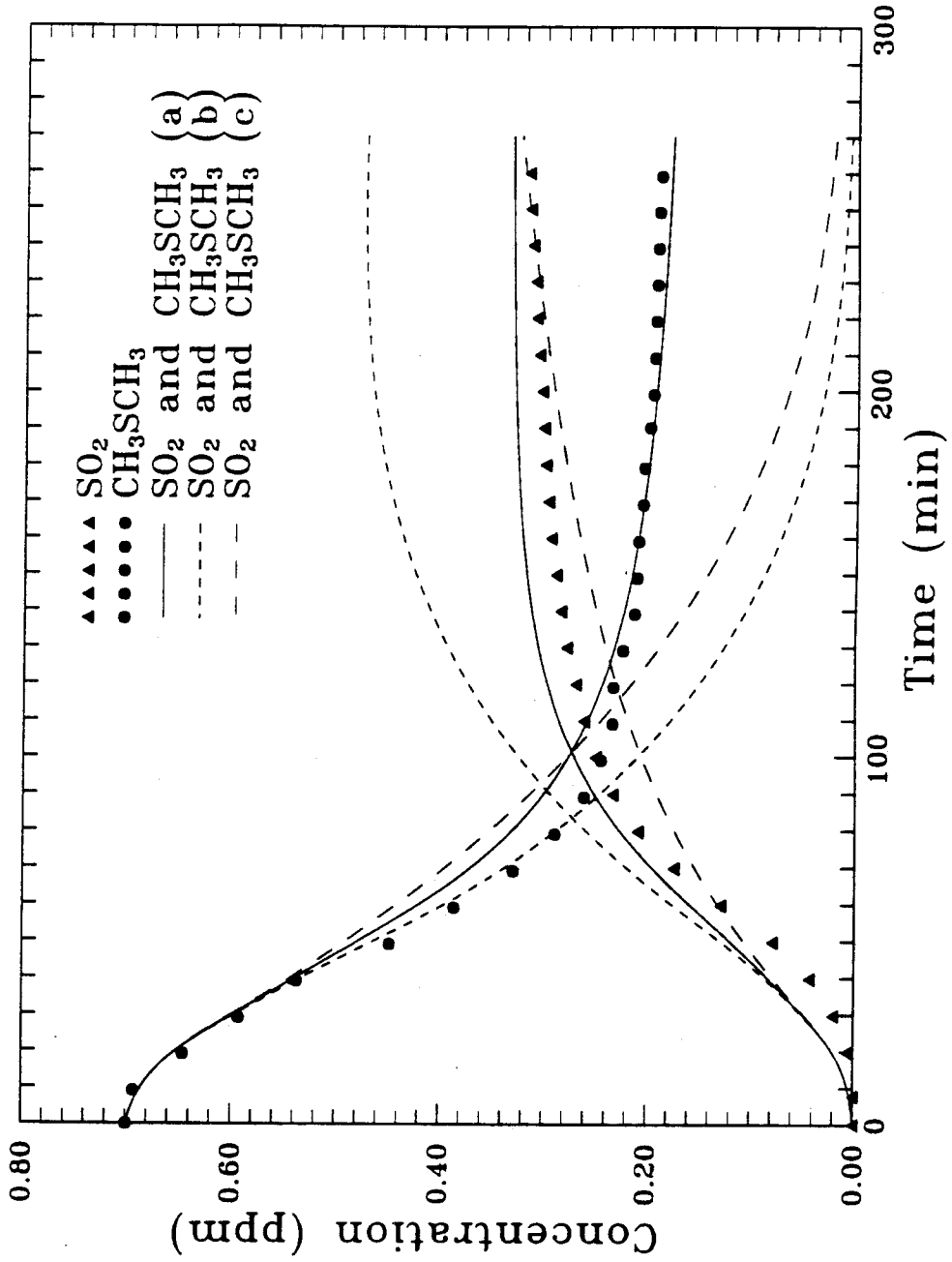

Figure 12
(DMS3)

CHAPTER V

RECOMMENDATIONS FOR FUTURE RESEARCH

1. Introduction

A thorough understanding of chemical kinetics of any reaction system requires the knowledge of three distinct levels: (1) A qualitative description in which the following question will be answered: *what* products are obtained from *what* reagents under *what* conditions? (2) A quantitative thermochemical description in which elementary reactions and transient intermediates in reaction mechanisms will be identified and thermochemical parameters in the Arrhenius equation will be evaluated, i.e., the questions of *how* the reactions proceed, and *how fast* for each of them will be answered. (3) A molecular reaction dynamics level in which elementary reactions are studied between molecules in preselected energy states (not between molecules among a whole collection of states in a thermal distribution) to ascertain *how* each of the energy states leads to a different rate constant or a different product. An accumulation of the above knowledge for different chemical species and reaction systems will improve our ability to predict the possible reaction mechanisms and to estimate rate parameters for other reaction systems, and enable us to understand the chemical reactivity of various species, leading to an understanding of underlying principles and rationale of reactions, i.e., *why*.

Much of the current understanding of atmospheric chemistry has arisen from several decades of intensive investigation of urban air pollution, clean troposphere, and stratosphere through both field and laboratory studies. Due to the complex nature of the atmosphere, a unique experimental method, the environmental chamber, has been developed to generate kinetic and mechanistic data on various atmospheric reaction systems. Based on the experimental data from environmental chambers, computer simulation can be carried out to evaluate the various chemical reaction mechanism. In this chapter, the limitations and possible improvements on envi-

ronmental chambers, and on the evaluation of mechanisms developed by computer modeling will be briefly discussed, and further experimental work will be recommended.

2. Wall Effects

The most significant difference between the real atmosphere and the environmental chamber is by necessity the presence of surfaces in the form of the chamber walls. Although much experimental evidence has suggested that trace contaminants from chamber surface have significant effects on the reactivity of the system studied, the detailed physics and chemistry involved in the wall effects are still poorly understood. One good example is the constant appearance of the *mysterious wall effect* reactions in the various chemical reaction mechanisms developed to evaluate chamber data. In addition, the wall effects always tend to be used as the convenient reason responsible for disagreement between predicted and observed data, and can be adjusted somewhat without much experimental justification.

The environmental chamber wall is characterized by two parameters: surface material and surface-to-volume ratio. In general, chemically inert materials and small surface-to-volume ratio are chosen to minimize wall effects. Until now, two major types of surface materials, glass (Pyrex, borosilicate glass, quartz) and various Teflons, have been used for constructing reactors in atmospheric chemistry studies (sometimes other kinds of materials are used in various parts inside a chamber, including aluminum, stainless steel, gold, invar, and etc.). The surface-to-volume ratio employed ranges from about 40 m^{-1} to 1.4 m^{-1}. Note that the lower limit of the estimated surface-to-volume ratio of the troposphere is about 10^{-4} m^{-1} ($R_{earth} = 6,371km$, and $H_{troposphere} = 10 \sim 15km$), and the actual S/V ratio may be much larger when the various surfaces present in the atmosphere are considered,

including surfaces of buildings, plants, clouds, and particles.

Wall effects mainly result from two important processes on the chamber surface, i.e., possible heterogeneous reactions and adsorption/desorption processes. Heterogeneous reactions have been suggested to occur on chamber surfaces, including decomposition of O_3 to O_2, and conversion of NO_2 to HONO. However, none has been confirmed experimentally at present. Different from heterogeneous reactions, adsorption/desorption processes of many species have been experimentally measured, including O_3, organics, nitrogen- and sulfur-containing compounds, and aerosol particles. In addition to the effects on the mass balances of elements, the major effect due to the chamber surface is the introduction of radicals and various reactive species into the system, many of them serving as the radical sources, e.g., HONO, HCHO, and other organics. The effect of such chamber radical sources is most important on low reactivity systems and on low concentration studies, where they can have significant effects on the reactivity, or even on the reproducibility of the experiments.

The common experimental approach to heterogeneous reactions and release of reactive species due to chamber surface is to characterize the chamber surfaces by injecting a mixture of reactants and measuring the concentration profiles of reactants and products in dark or under light irradiation. The experimental observations which cannot be explained solely on the basis of *known* homogeneous gas-phase reactions (sometime with computer simulation) are considered to result from heterogeneous reactions on the chamber surface or from emissions of some reactive species. A simplified phenomenological description is thus developed to characterize the surface effects. The results obtained from such studies are, however, much more speculative rather than direct experimental evidences because:

1. no clear distinction between homogeneous and heterogeneous reactions (or ef-

fects) can be made from such studies;

2. the knowledge on the *known* homogeneous gas-phase reactions is limited, and highly uncertain in many systems studied;
3. the chamber surfaces are not well-defined, and the reproducibility of the surface is highly uncertain, thus leading to chamber-dependent or history-dependent wall effects, despite that pre-conditioning of chamber surfaces is employed;
4. due to the instrumentation limits, not many porducts, and no reaction intermediates have been identified experimentally;
5. the variation of light intensity, temperature, humidity, surface material, surface-to-volume ratio, and aging of the chamber surface complicates the interpretation of the chamber data on wall effect studies.

More importantly, such simplified phenomenological characteriztation cannot lead to a fundamental understanding of the physical and chemical processes on the chamber surfaces, and may result in erroneous predictions for modeling since the actual surface effects might depend on the co-existence of light irradiation and other species, or have quite different effects under different conditions. Thus, further detailed experimental studies are warrented in order to understand the physics and chemistry of the various heterogeneous processes on the chamber surfaces and to develop better techniques to characterize as well as to minimize the wall effects. The knowledge from these studies will not only enable us to extrapolate the information obtained from environmental chamber studies to the real atmosphere, but will also be directly applicable to various surface processes in real atmosphere.

In addition to the wall effects, heterogeneous reactions on aerosol particles, both inside environmental chambers and in the atmosphere, may be of significant importance because of their much more reactive surfaces and uniform mixing in the air, although the effects of these heterogeneous reactions have still been ignored un-

til now on interpreting smog chamber data. One good example on their importance is that heterogeneous reactions are now believed to play a central role in the chemistry of ozone depletion in the Antarctic stratosphere. The fundamental studies on heterogeneous reactions occurring on aerosol particles are important both on interpreting gas-to-particle conversion studies in smog chamber and on understanding the atmospheric chemistry.

3. Determination of Product Yield Distribution

One of the major objectives for performing smog chamber studies on atmospheric photooxidation of various chemical compounds is to measure the product yield distribution under *actual* atmospheric conditions. However, due to the limitations of the available instruments, the reactant concentrations simulated in smog chamber studies are usually higher than those found in the real atmosphere, thus leading to an uncertainty when the results obtained from smog chamber studies are applied to real atmospheric modeling.

The direct solution to this problem is to develop new techniques with higher sensitivity or to improve the existing instruments by increasing detection limits for both inorganic and organic species measurements. Currently, FTIR is one of the most widely used techniques for product identification as well as for yield determination, and its sensitivity can be improved by increasing resolution and pathlength. However, even in the case that all the necessary instruments with high sensitivity are available, the measured product yields under real atmospheric conditions probably still cannot be directly used for atmospheric modeling because the wall effects are usually very important for systems at very low concentrations, must be understood and characterized clearly. Due to the great difficulties associated with instrumentation development and the complex nature of wall effects, it is apparent that product

yield measurement for many atmospheric compounds at real atmospheric conditions will continue to be a major challenge in the near future.

The alternative approach is to study the effects of reactant concentrations on product yield distribution both experimentally and theoretically (combined with computer simulation) in order to extrapolate the actual product yield distribution to the real atmosphere. This is the area that usually been neglected so far, and but can be improved significantly through careful studies. A common method now used to study the atmospheric fate of various organic compounds is to carry out smog chamber experiments and to measure product yield distribution at lowest concentrations limited by analytical techniques, which are usually still higher than those in real atmosphere. The product yield distribution determined under such concentrations is then extrapolated to the atmosphere with little or no experimental justification. However, significant effects of concentrations on product yields could be expected since organic compounds undergo atmospheric photooxidations through complex competitive reactions of various intermediate species with NO, NO_2, O_3, O_2 and other species. The high concentrations employed in smog chamber studies directly increase the concentration ratio of $[X]/[O_2]$ where X = NO, NO_2, O_3, organic species and radicals. It is the variation of this ratio that influences the competition between reactions of intermediates with O_2 and other species, and may result in a significant effect on product yield distribution. Notice that (1) reactions with O_2 are usually an important, and often the dominant reaction pathway for intermediates in the atmosphere, especially in clean atmosphere, and (2) reactions of intermediates with NO, NO_2, O_3 and organic species are generally fast, thus increasing the ratio of $[X]/[O_2]$ in smog chamber experiments can alter the reaction pathways of intermediates substantially. Therefore, a thorough understanding of the concentration effects on product yield distribution is essential for atmospheric

modeling. This requires smog chamber experiments not only to be conducted at reactant concentrations closest to real atmosphere, but also to span a concentration range as broad as possible. Also, computer simulation for data from such a series of experiments will provide a much deeper and more complete understanding on concentration effects on product yield distribution, *and* on competition reactions of intermediates with NO, NO_2, O_3, organic species and O_2.

4. Evaluation of Reaction Mechanisms

Environmental chamber (or smog chamber) experiments have been widely used in atmospheric chemistry to evaluate the various chemical reaction mechanisms of atmospheric importance. However, the limitation of such evaluation needs to be examined carefully in order to provide more confidence on information obtained from computer simulation of the developed reaction mechanisms.

A detailed examination of the entire process from smog chamber experiments to computer simulation reveals the following common uncertainties in the mechanism evaluation process:

(1) concentration profiles are not available for every important species, and many of the formed products have not been identified;

(2) no major intermediates (radicals) have been directly detected and measured in smog chamber studies, although this information is extremely valuable to evaluation of mechanisms;

(3) mass balance is usually incomplete for carbon, nitrogen and sulfur elements;

(4) the reaction mechanism is developed from very limited information, and many key reaction pathways are often unknown;

(5) many important reaction rate constants have to be estimated either empirically or by some semi-empirical methods, the uncertainty of such estimation can

easily span several orders of magnitudes;

(6) computer simulation of the smog chamber data is carried out based on many important assumptions, and such assumptions are usually difficult to be examined or confirmed experimentally (expecially by smog chamber experiments).

Obviously, the uncertainties of (1)–(3) can be resolved only through development of new analytical techniques and improvement of existing instrumentation. The uncertainties of (4)–(6) are, however, often ignored and have not raised much attention yet. In fact, to develop a *qualitatively correct* reaction mechanism, being consistent with all available experimental information and fundamental chemistry, is the most important and difficult step in the processes of mechanism development and evaluation. In the case that an important reaction pathway is missing or incorrect, any subsequent computer simulation of the reaction mechanism will provide incomplete knowledge or even lead to some wrong conclusions. Moreover, such mistakes are very difficult to avoid, especially at the early stage of the mechanism development, and are unlikely to be discovered from computer simulation by comparing the observed and predicted concentration profiles, since an incorrect reaction mechanism can also be adjusted to have a reasonable agreement between prediction and measurement. Thus, in order to perform a meaningful and successful evaluation, it is essential that in the developed mechanism, each reaction pathway must be chemically correct, and all the important pathways must be included. This is a very challenging goal, especially based only on limited information, and can only be achieved through experimental and theoretical studies of fundamental chemistry.

In the atmospheric reaction mechanisms developed for many organic compounds, the reactions of intermediates with O_2 and its competition with NO, NO_2, O_3 and other species is one of the most critical and common uncertainties. Generally, the reactions of intermediates (such as OH+RH adduct) with O_2 have been

assumed to be the dominant reaction pathways in the computer simulation. Such assumptions, however, have been seldom confirmed by kinetic experiments, and the kinetic data on competition of intermediates with O_2 and other species are very limited, and not available in many cases. Thus, smog chamber experiments should be conducted over a broad range of reactant concentrations in order to provide an important data set for elucidating these competitions by computer simulation.

Regarding the techniques of estimating rate constants and evaluating reaction mechanism by simulation of smog chamber experimental data, they are still more in the stage of art rather than of science. One good example is that the current method of adjusting the rate constants is still a trial-and-error process, and no systematic approach has been applied to optimize various rate constants in order to have a best fit between predicted and observed concentration profiles. Also, an assumed dominant pathway is often tested against experimental data based on many other assumptions. They are coupled to each other, and cannot be tested independently. Thus, one should be aware that the conclusions obtained from mechanism simulation are correct only if all the assumptions are confirmed by experiments. In the case that any assumption is proved to be wrong, part or all of the developed mechanism probably has to be re-evaluated. In this sense, evaluation of reaction mechanisms by simulating smog chamber experimental data serves predominantly as a tool to identify the major uncertainties and important reaction pathways, and as a guidance for subsequent kinetic studies. The close interaction or cooperation between kinetic and smog chamber studies is of crucial importance for establishing (not just evaluating) a reaction mechanism applicable to the real atmosphere.

5. Recommendations for Future Research on Organosulfur Chemistry

Detailed theoretical and experimental investigations have been carried out

for atmospheric chemistry of dimethyl sulfide (CH_3SCH_3) and dimethyl disulfide (CH_3SSCH_3). In the present work, comprehensive mechanisms for atmospheric photooxidation of CH_3SCH_3 and CH_3SSCH_3 are developed based on fundamental considerations of all available kinetic and mechanistic information, and are evaluated with the data from a series of outdoor smog chamber experiments on the systems CH_3SCH_3–NO_x–air–hν and CH_3SSCH_3–NO_x–air–hν. Further studies on organosulfur chemistry in the atmosphere are, however, clearly needed in order to achieve a fundamental understanding of chemical transformation processes in the global biogeochemical sulfur cycle, including

(1) product studies on CH_3SCH_3 photooxidation should focus on identifying missing products and achieving good mass balances of carbon, sulfur, and nitrogen elements;

(2) experimental studies on atmospheric fate of $CH_3S(O)CH_3$, $CH_3S(O)_2CH_3$, and CH_3SO_3H should be carried out in both gas-phase and aerosol- or aqueous-phase;

(3) well-defined kinetic experiments should be conducted for key reaction pathways identified in the present work, including the fate of adducts from OH and NO_3 initial reactions, reactions of CH_3SOH, $CH_3S(O)CH_3$ and $CH_3S(O)_2CH_3$, intromolecular conversion of CH_3SOO to CH_3SO_2, reactions of CH_3SO_x with O_3, H-atom abstractions by CH_3SO_3, and decomposition of CH_3SO_2. The effects of temperature on the rate constants as well as on the reaction mechanisms should be studied in detail;

(4) atmospheric reaction mechanisms for H_2S, COS, CS_2 and CH_3SH should be developed, and combined with reaction mechanisms for CH_3SCH_3 and CH_3SSCH_3 to simulate the clean atmosphere and to address the important issues of global atmospheric sulfur budget, formation of sulfur aerosol in marine air, acid pre-

cipitation in remote areas. The importance of the OH, NO_3 and IO radicals should be evaluated.

APPENDICES

COMPARISON BETWEEN MEASURED AND PREDICTED

CONCENTRATION PROFILES

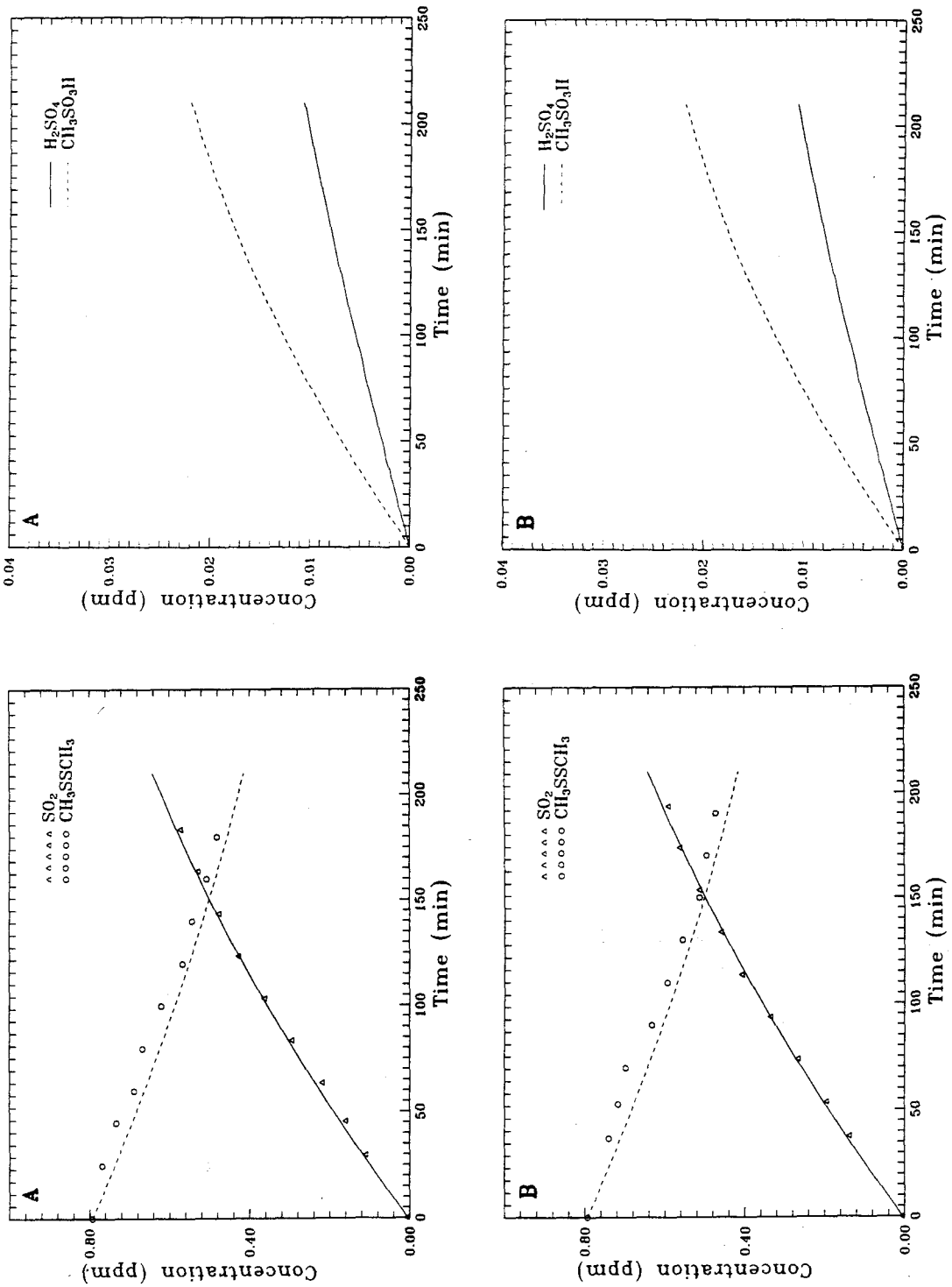

Observed and Predicted Concentration-time Profiles for CH_3SSCH_3-air Experiment DDS1A DDS1B

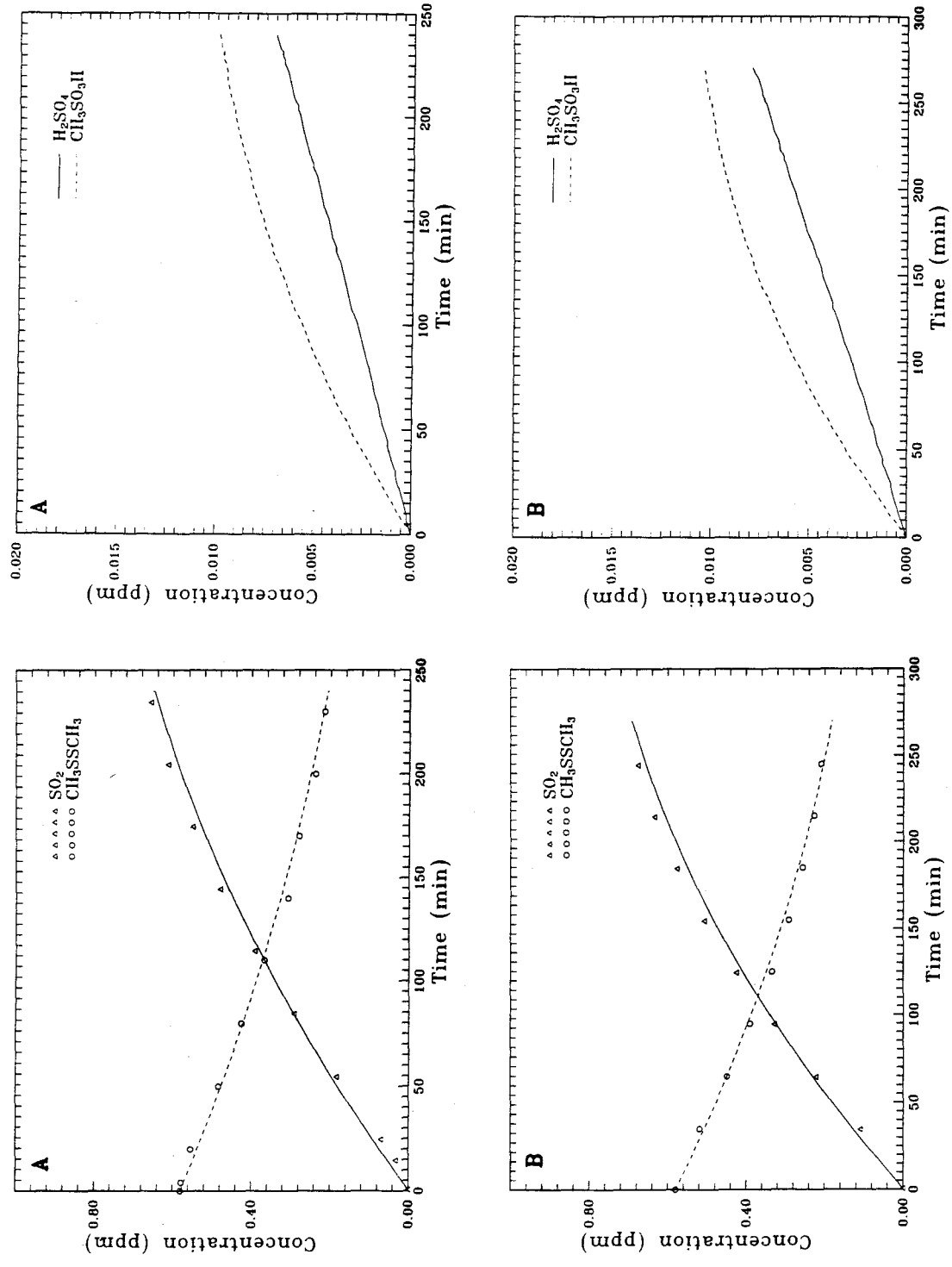

Observed and Predicted Concentration-time Profiles for CH_3SSCH_3-air Experiment DDS2A DDS2B

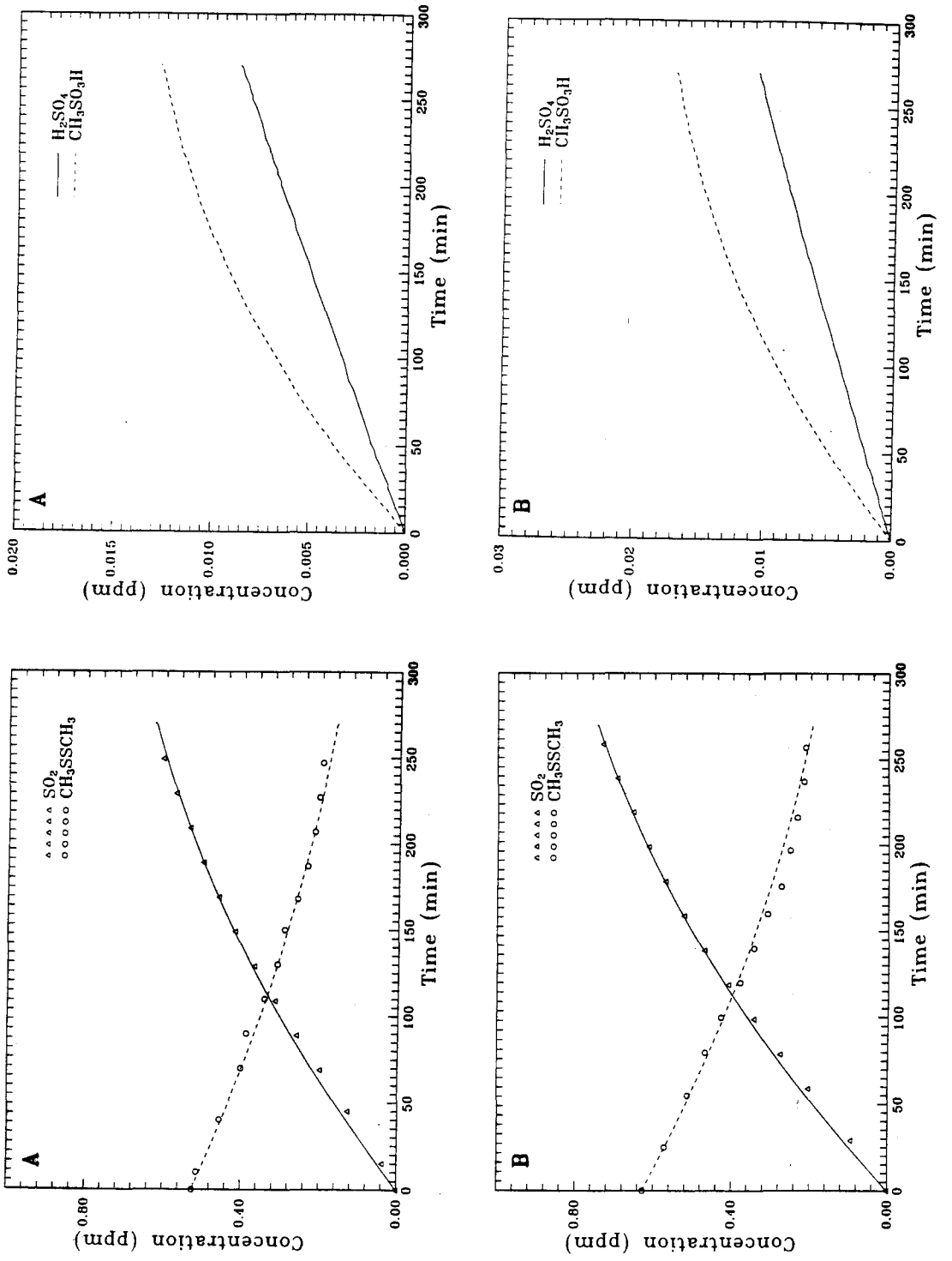

Observed and Predicted Concentration-time Profiles for CH_3SSCH_3-air Experiment DDS3A DDS3B

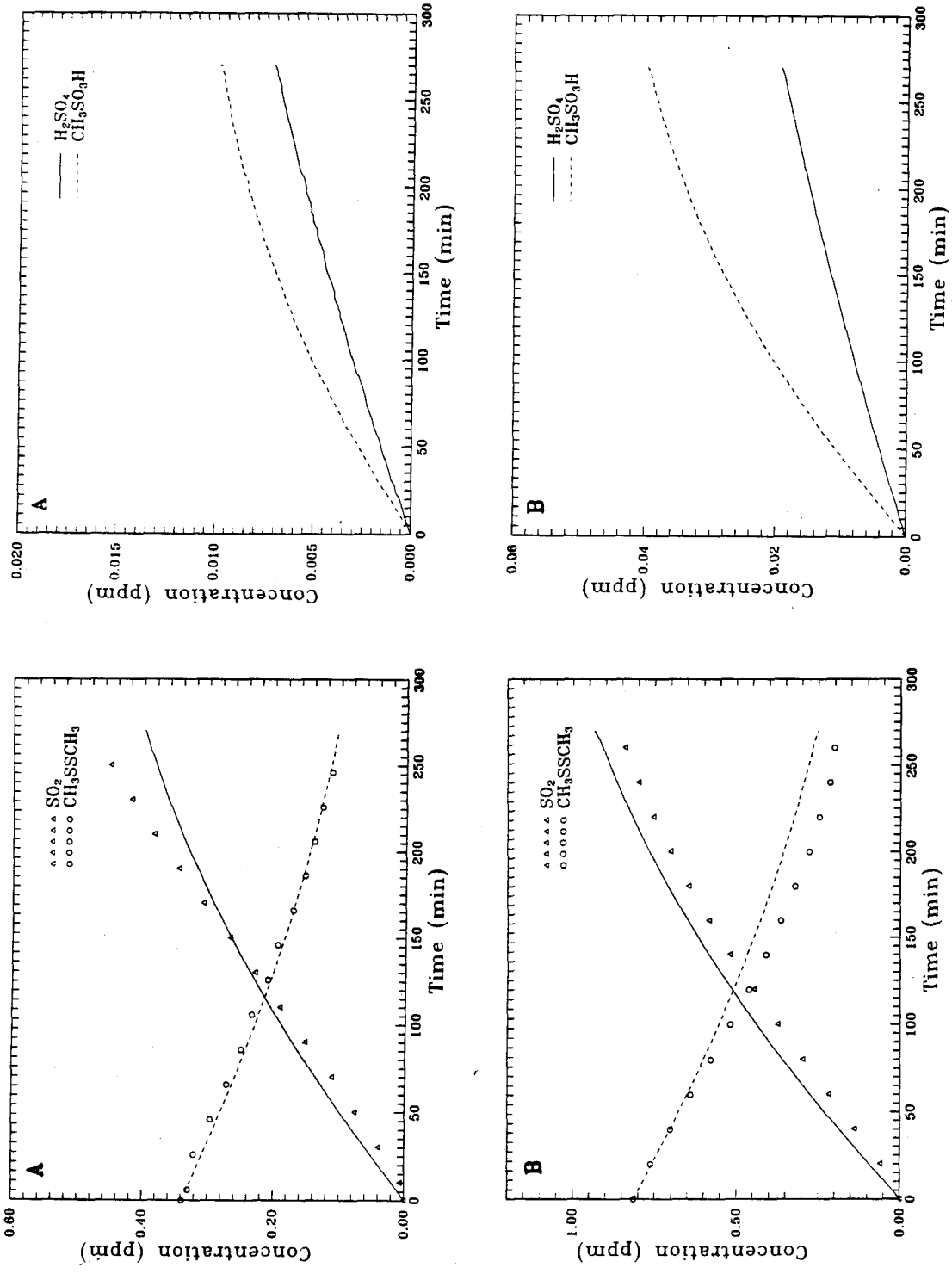

Observed and Predicted Concentration-time Profiles for CH_3SSCH_3-air Experiment DDS4A DDS4B

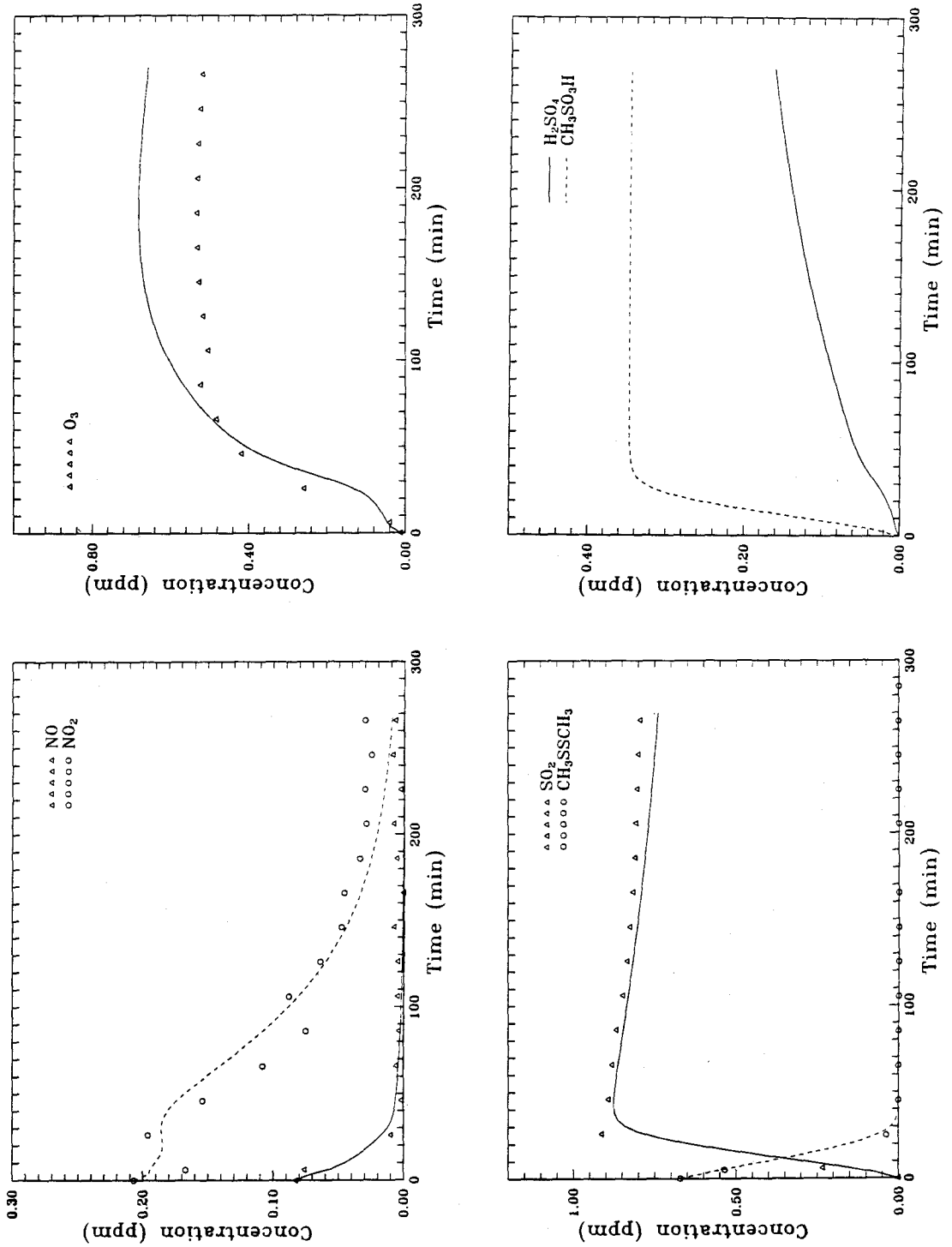

Observed and Predicted Concentration-time Profiles for CH_3SSCH_3-NO_x-air Experiment DDS5A

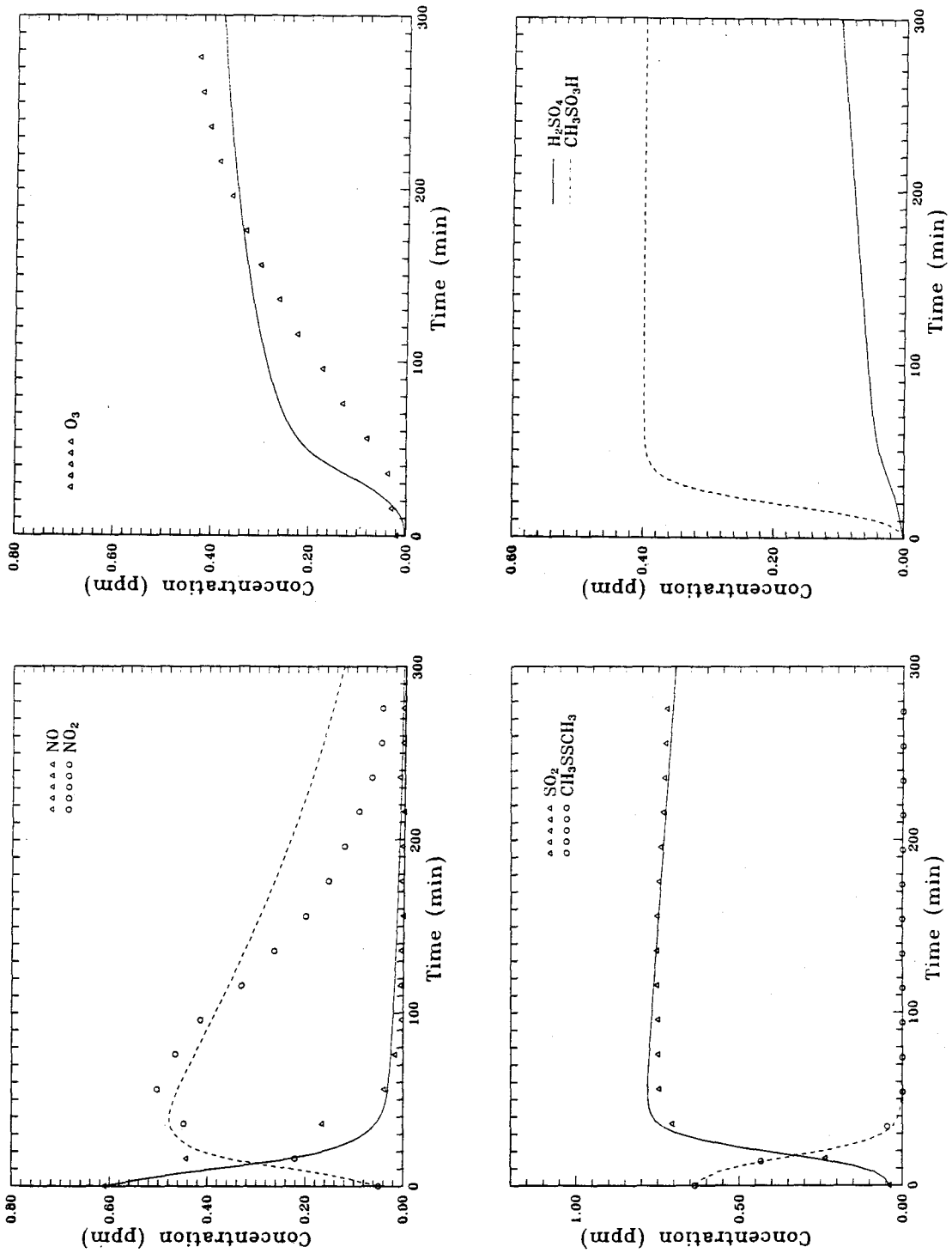

Observed and Predicted Concentration-time Profiles
for CH_3SSCH_3-NO_x-air Experiment DDS5B

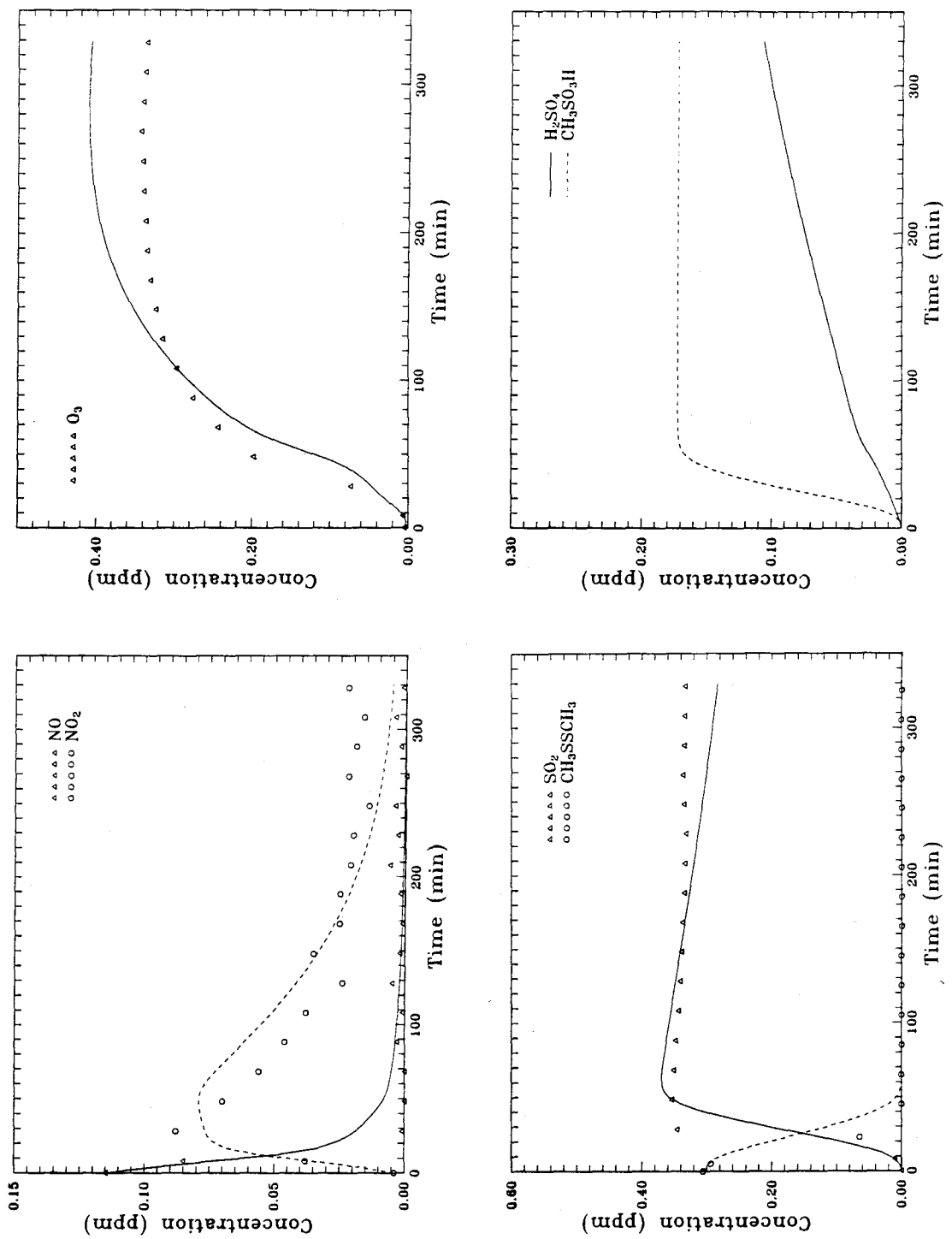

Observed and Predicted Concentration-time Profiles for CH_3SSCH_3-NO_x-air Experiment DDS6A

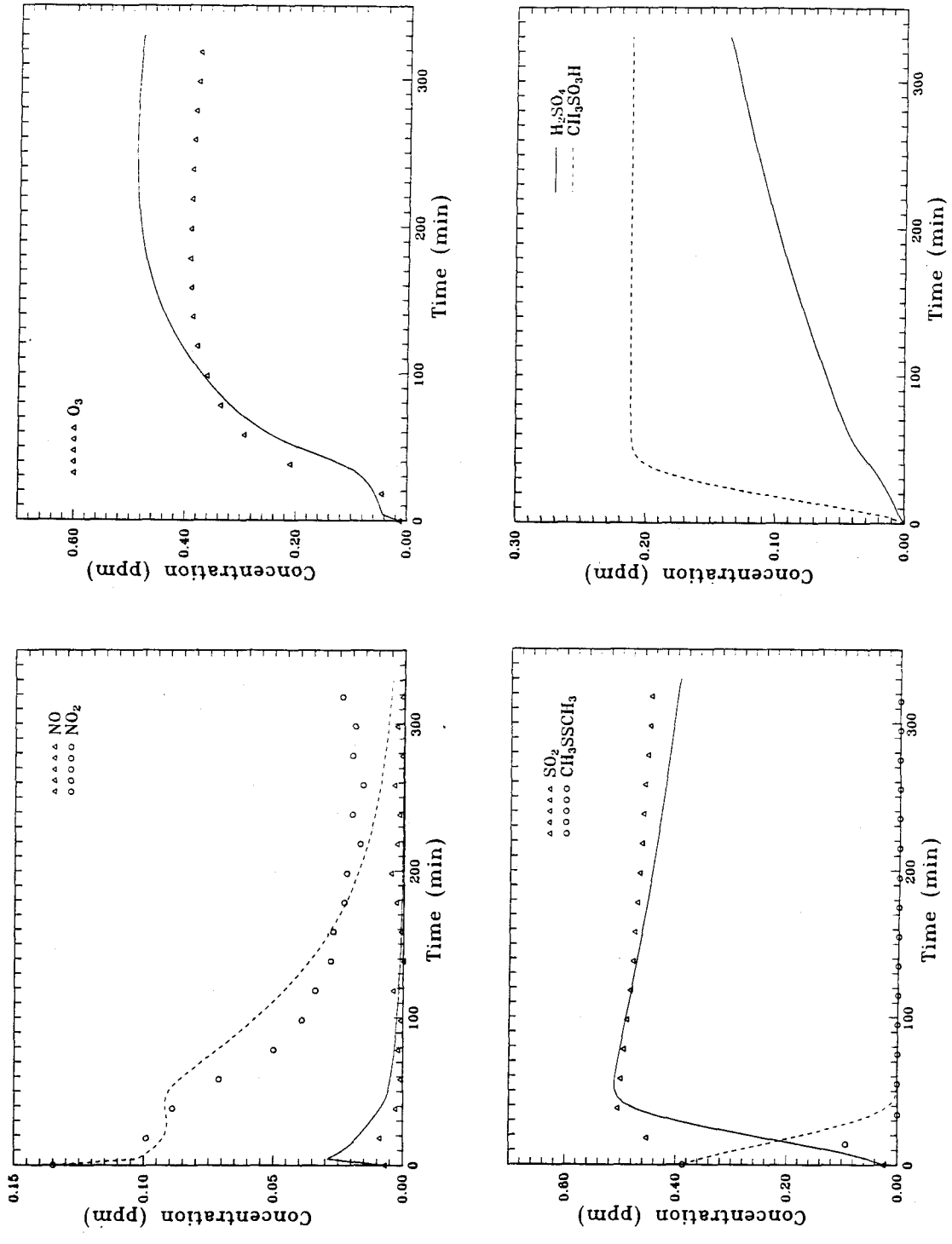

Observed and Predicted Concentration-time Profiles for CH_3SSCH_3-NO_x-air Experiment DDS6B

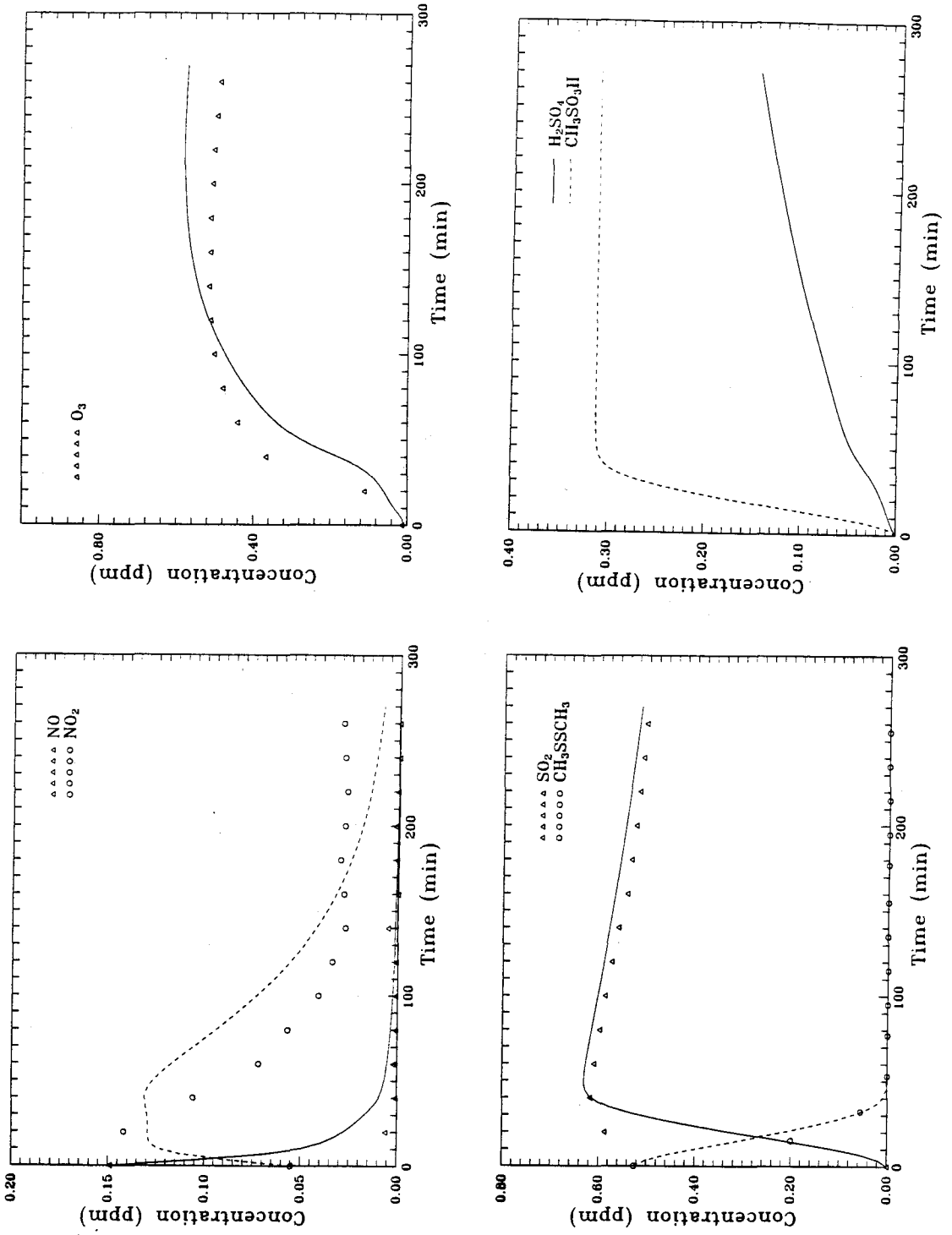

Observed and Predicted Concentration-time Profiles for CH_3SSCH_3-NO_x-air Experiment DDS7A

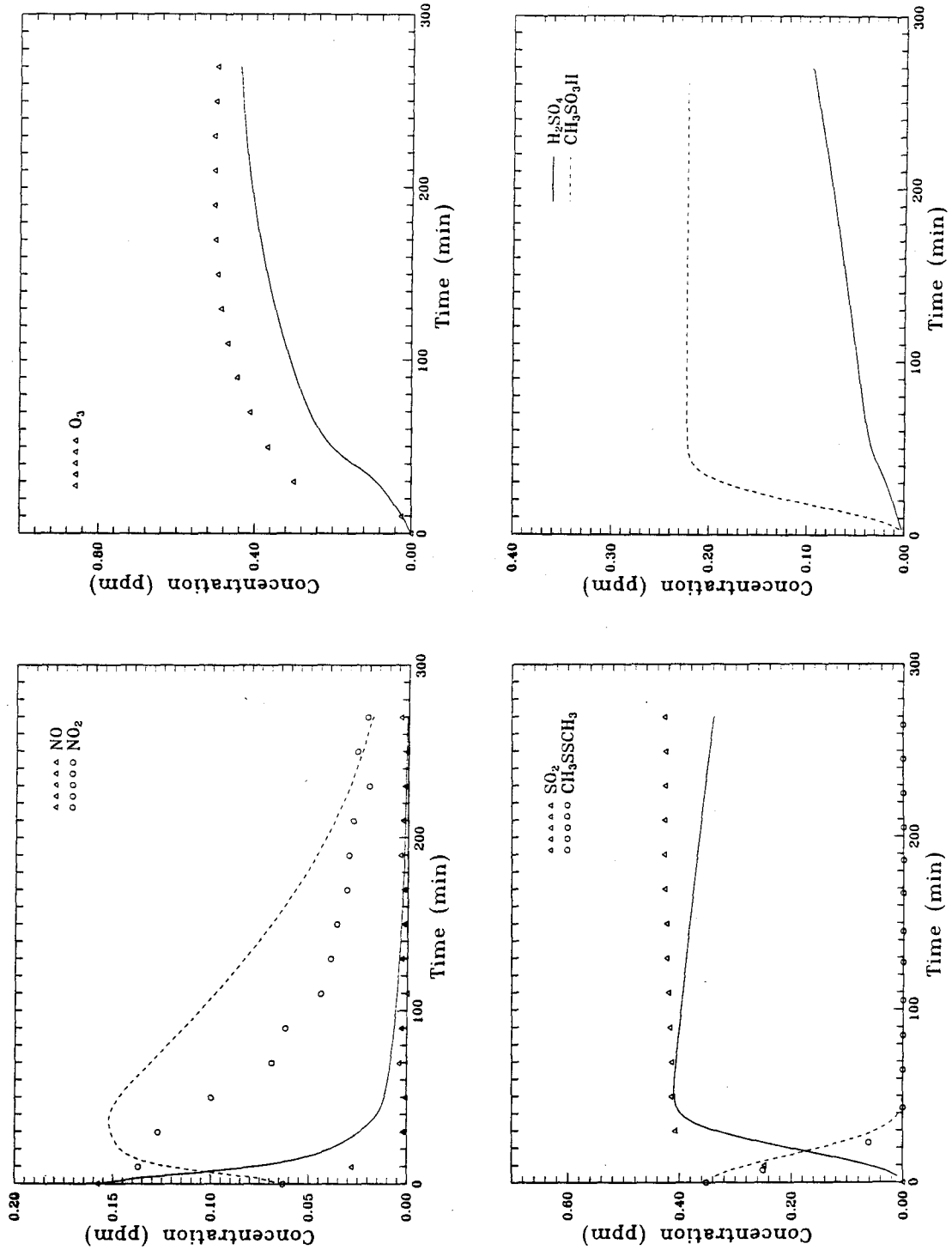

Observed and Predicted Concentration-time Profiles for CH_3SSCH_3-NO_x-air Experiment DDS7B

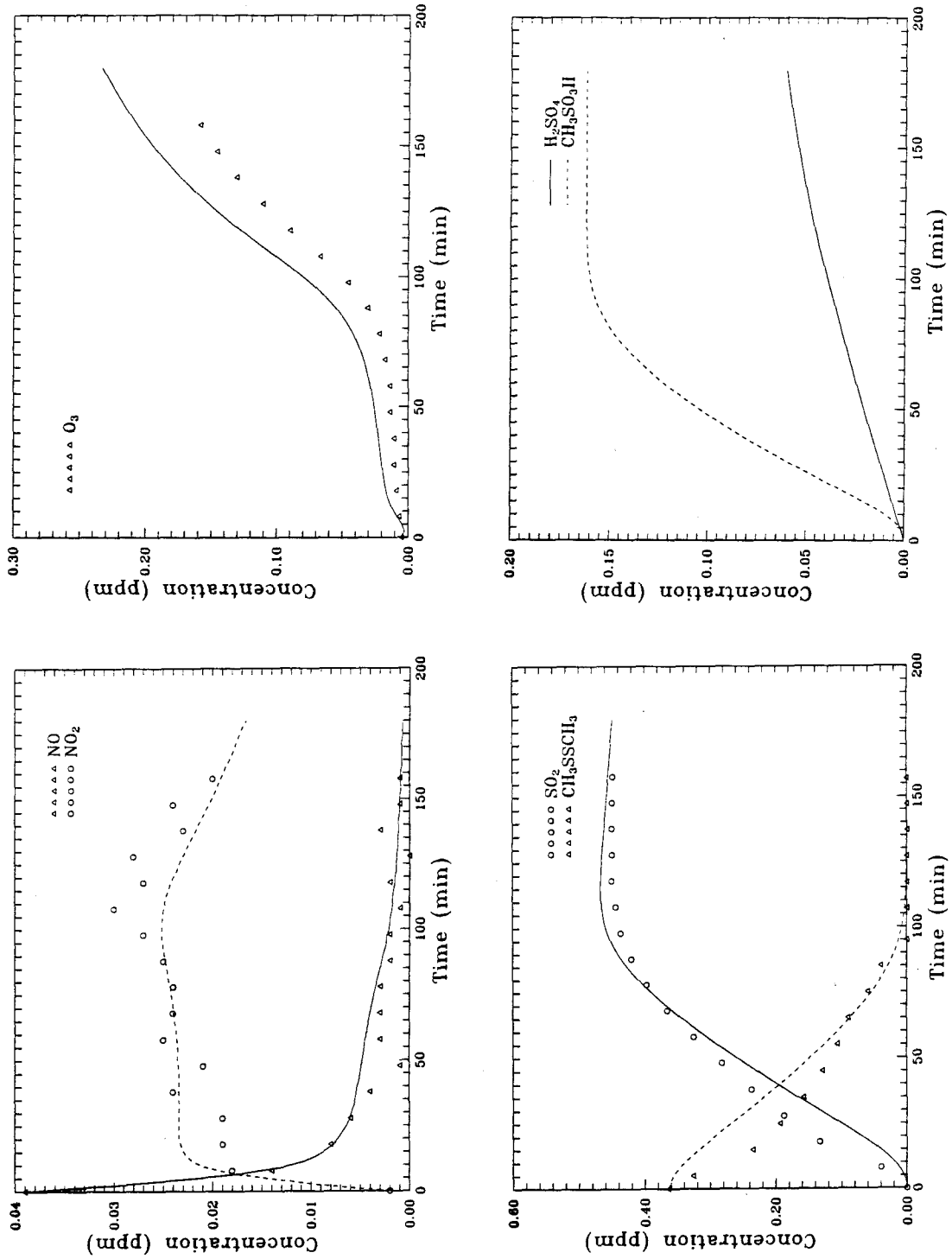

Observed and Predicted Concentration-time Profiles for CH_3SSCH_3-NO_x-air Experiment DDS8

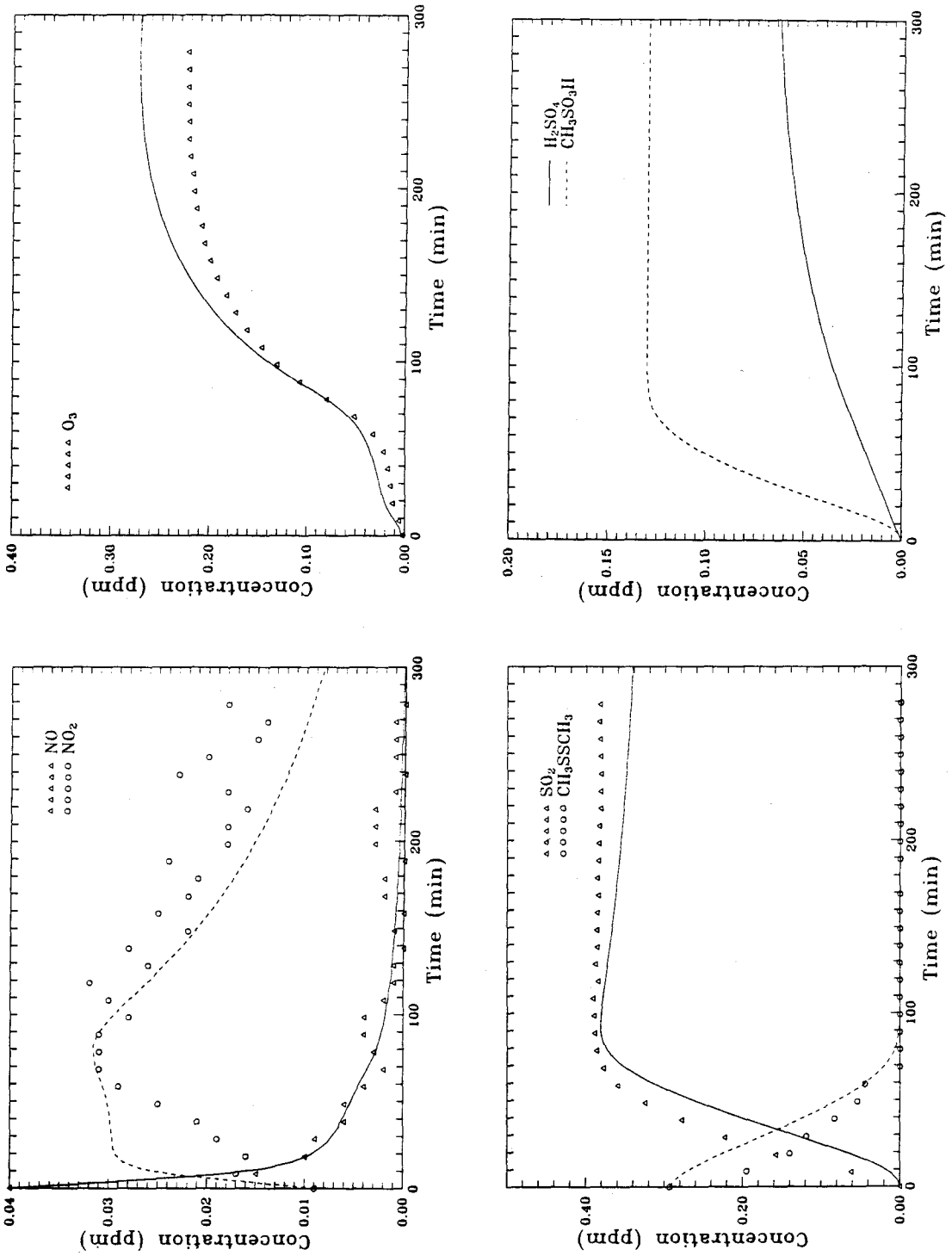

Observed and Predicted Concentration-time Profiles for CH_3SSCH_3-NO_x-air Experiment DDS9

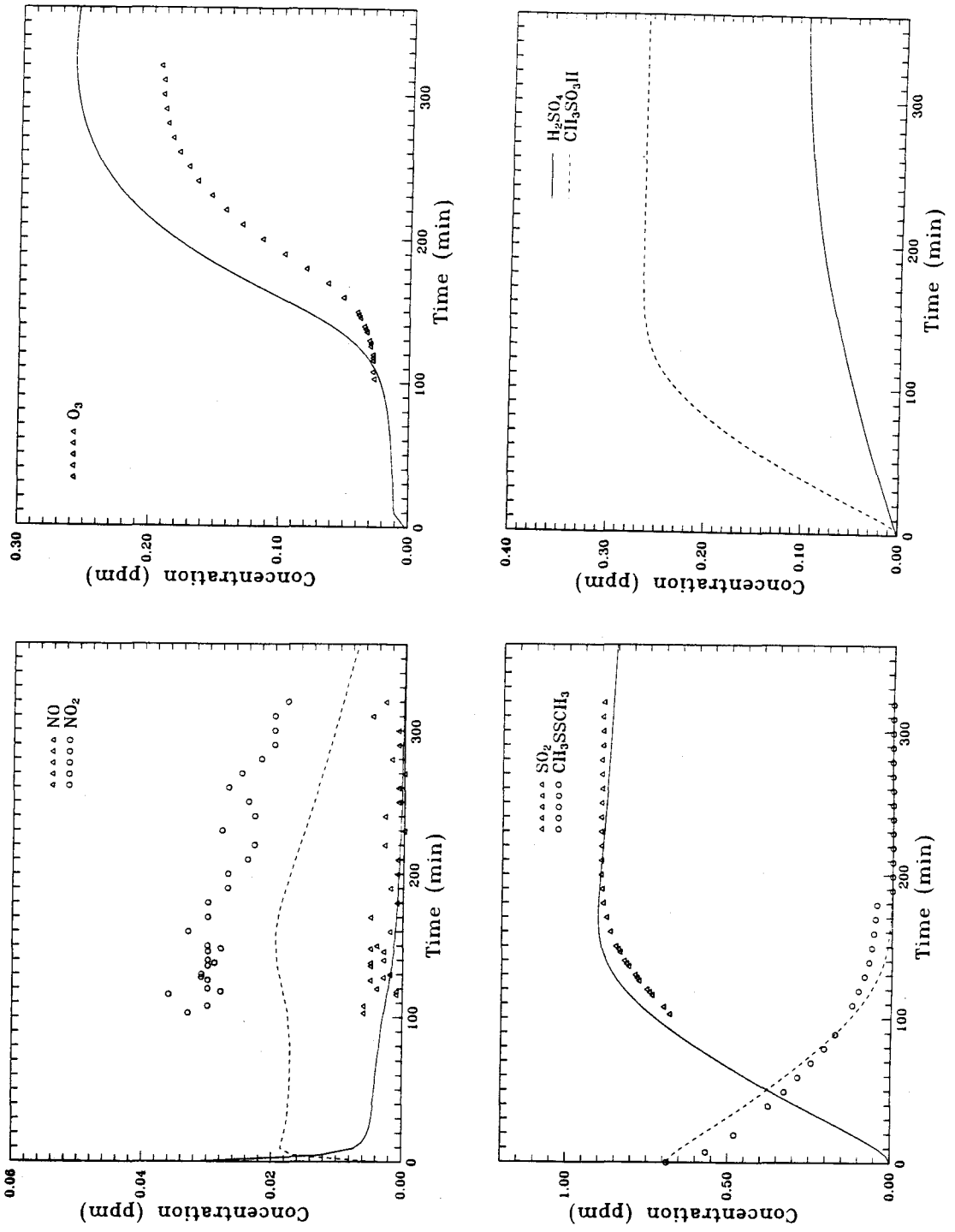

Observed and Predicted Concentration-time Profiles for CH_3SSCH_3-NO_x-air Experiment DDS10

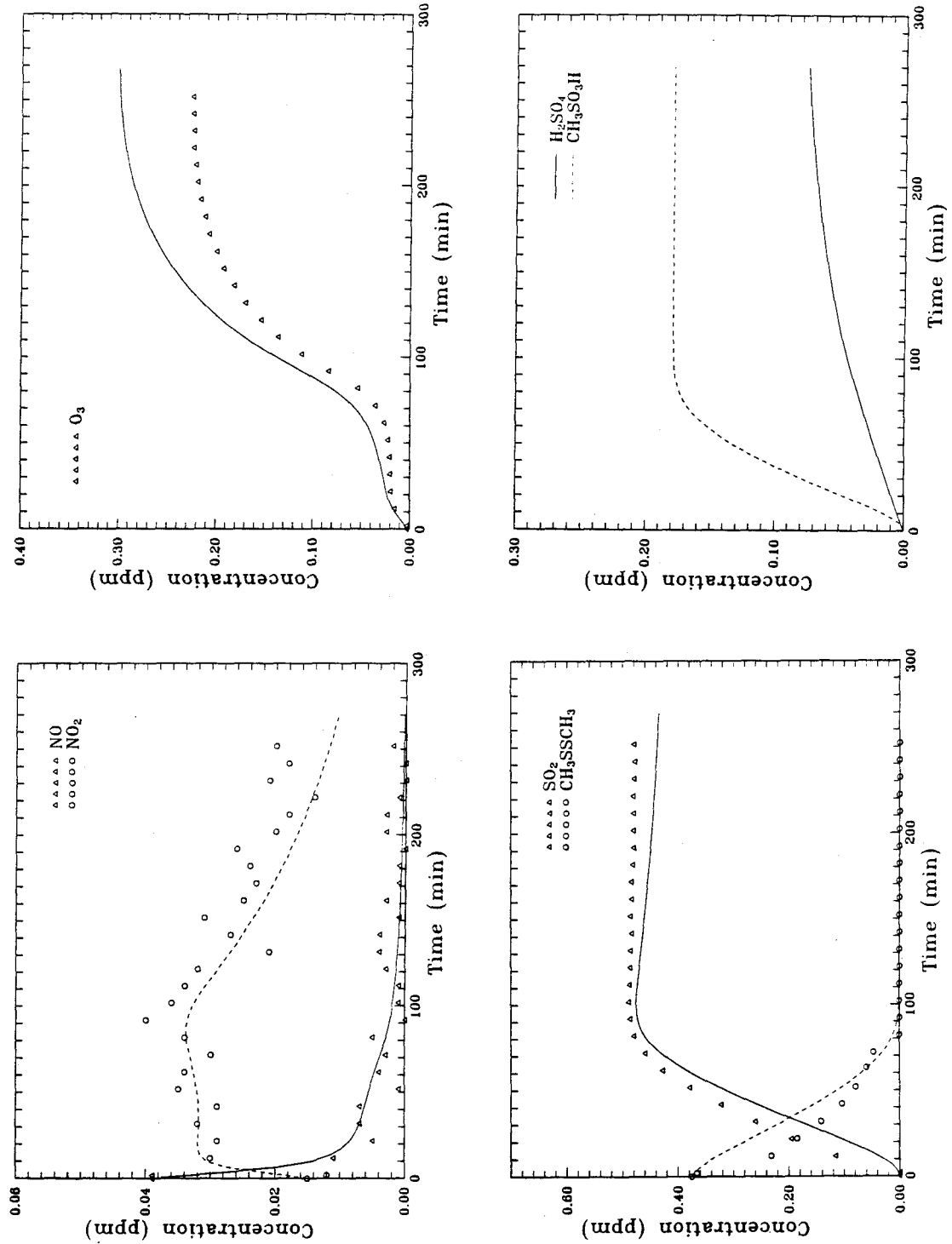

Observed and Predicted Concentration-time Profiles
for CH_3SSCH_3-NO_x-air Experiment DDS11

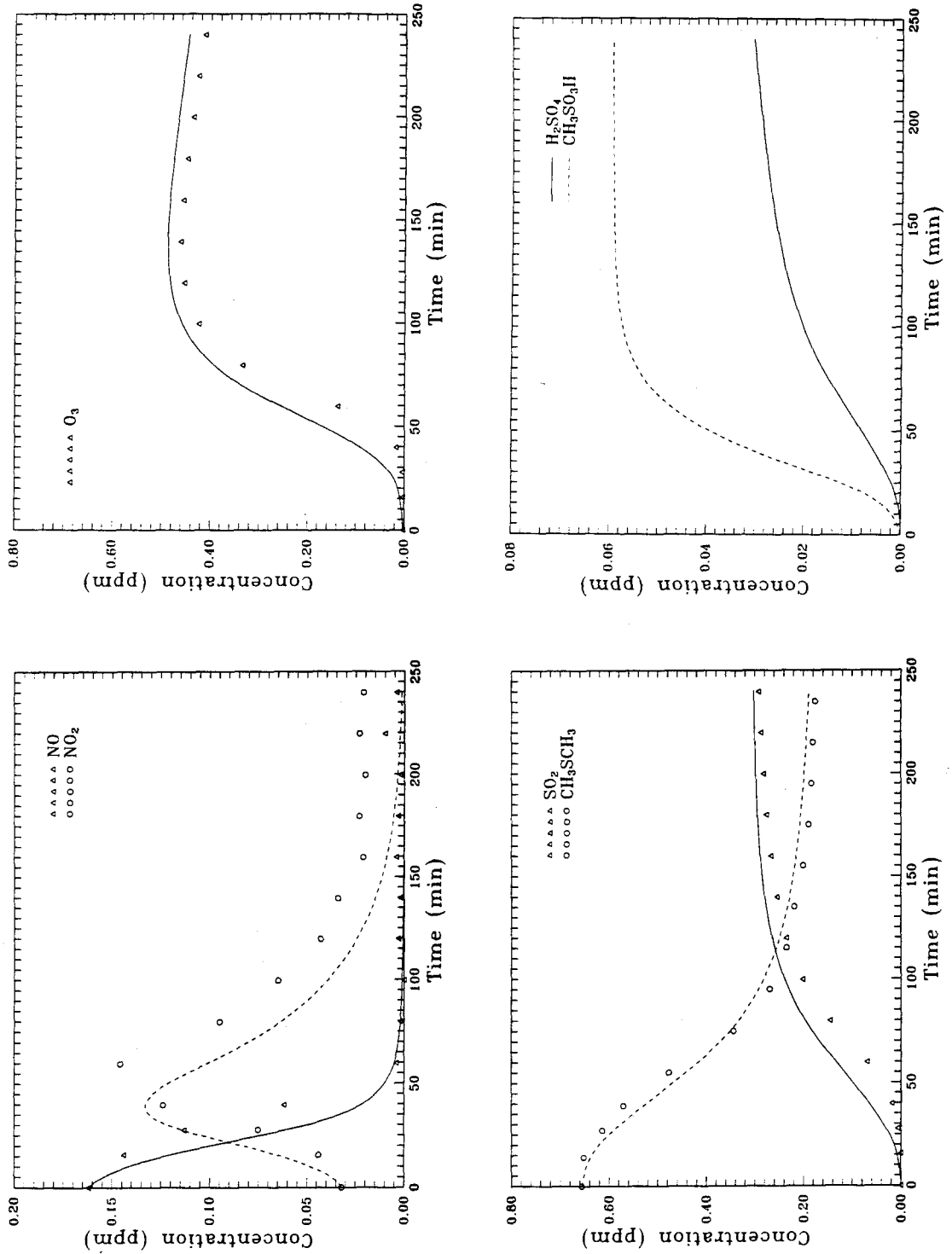

Observed and Predicted Concentration-time Profiles for CH_3SCH_3-NO_x-air Experiment DMS1A

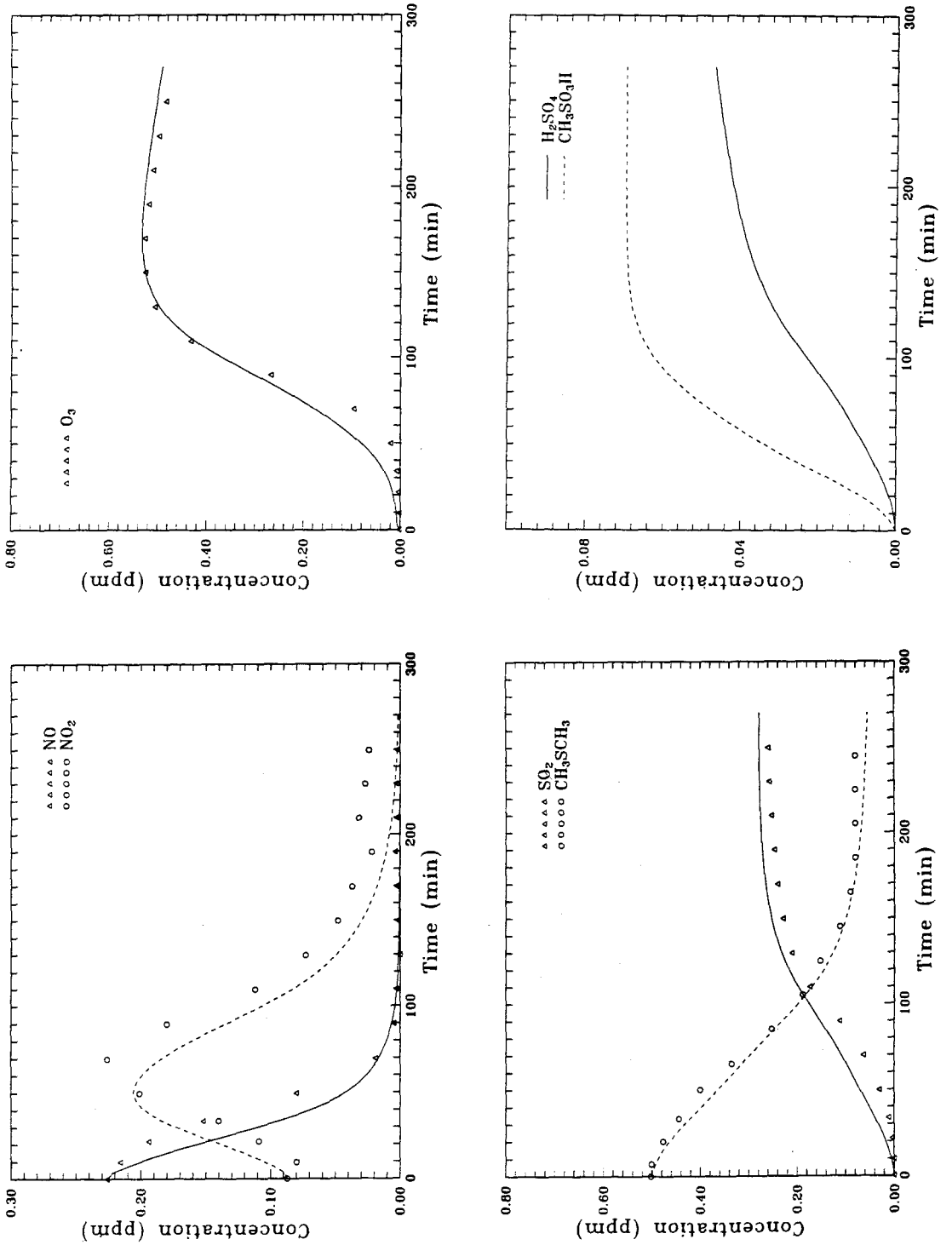

Observed and Predicted Concentration-time Profiles for CH_3SCH_3-NO_x-air Experiment DMS1B

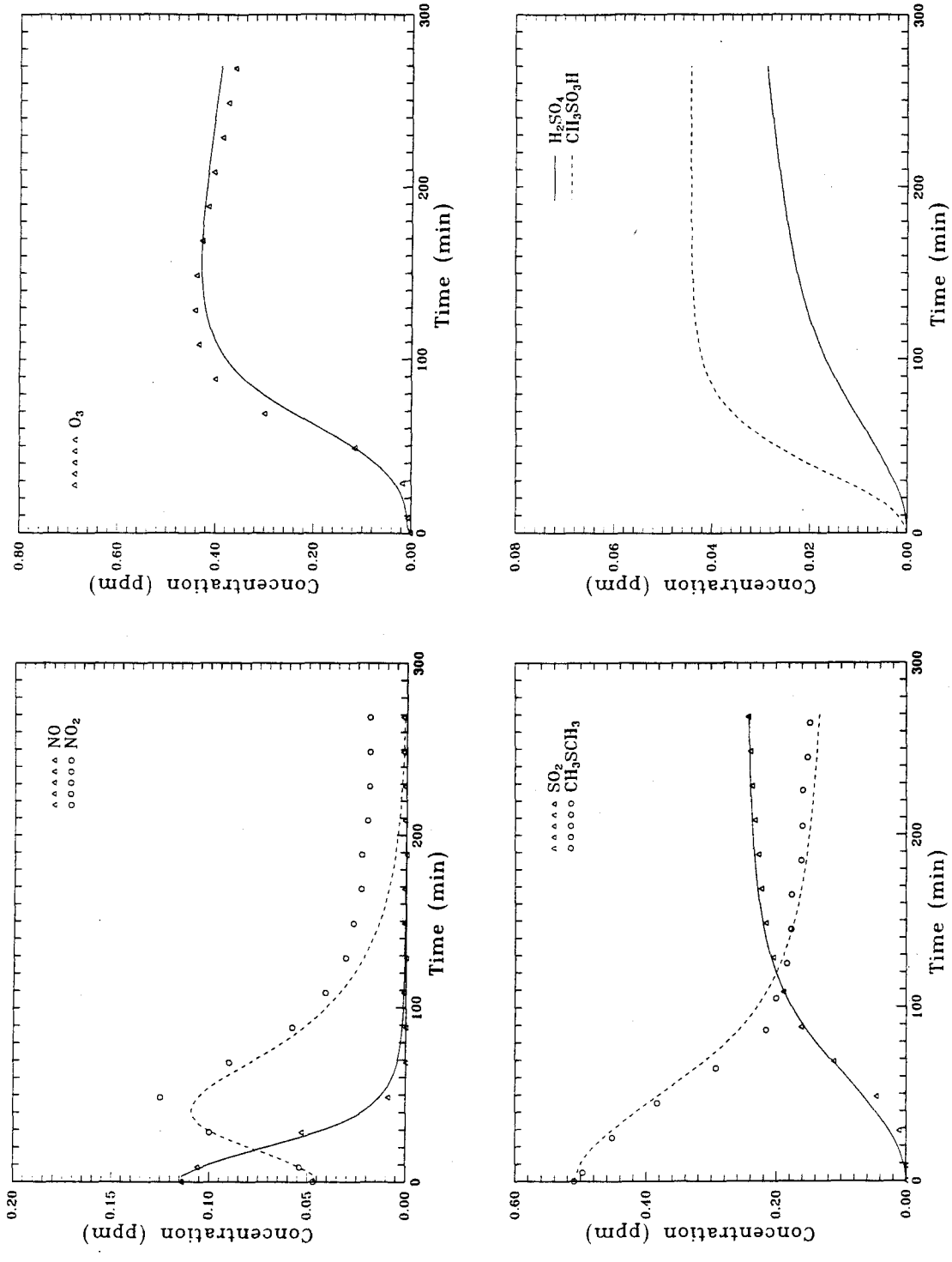

Observed and Predicted Concentration-time Profiles for CH_3SCH_3-NO_x-air Experiment DMS2A

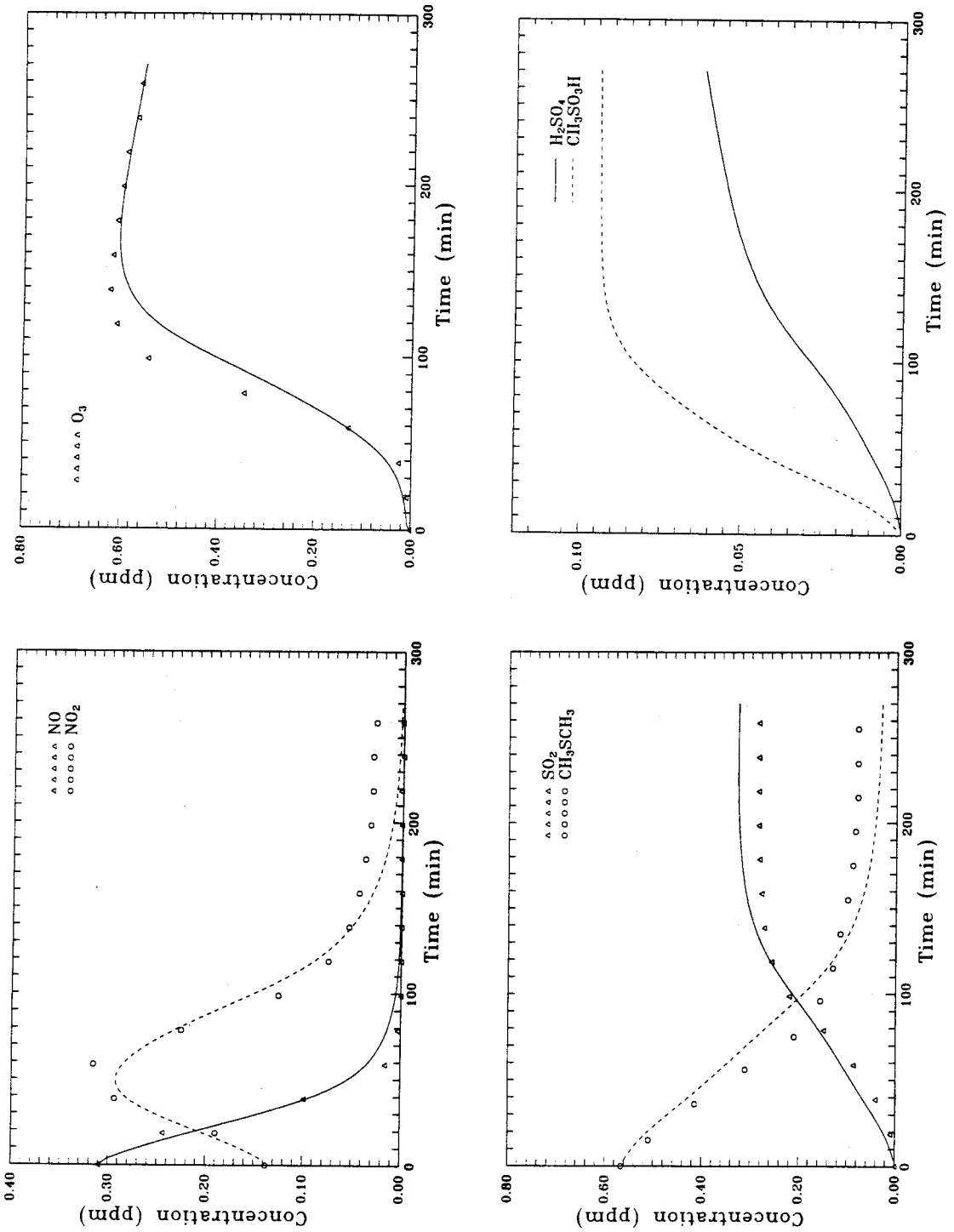

Observed and Predicted Concentration-time Profiles for CH_3SCH_3-NO_x-air Experiment DMS2B

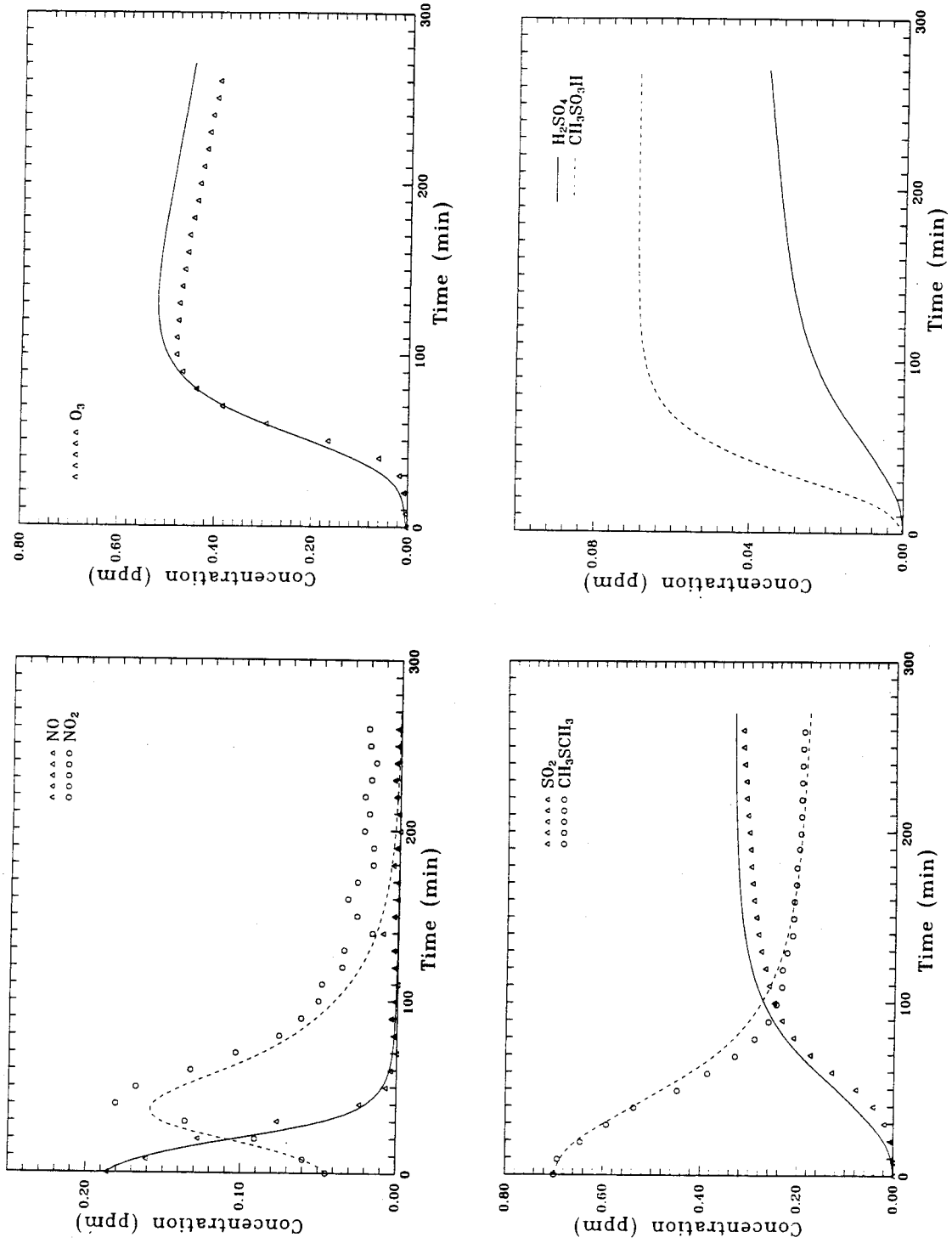

Observed and Predicted Concentration-time Profiles for CH_3SCH_3-NO_x-air Experiment DMS3

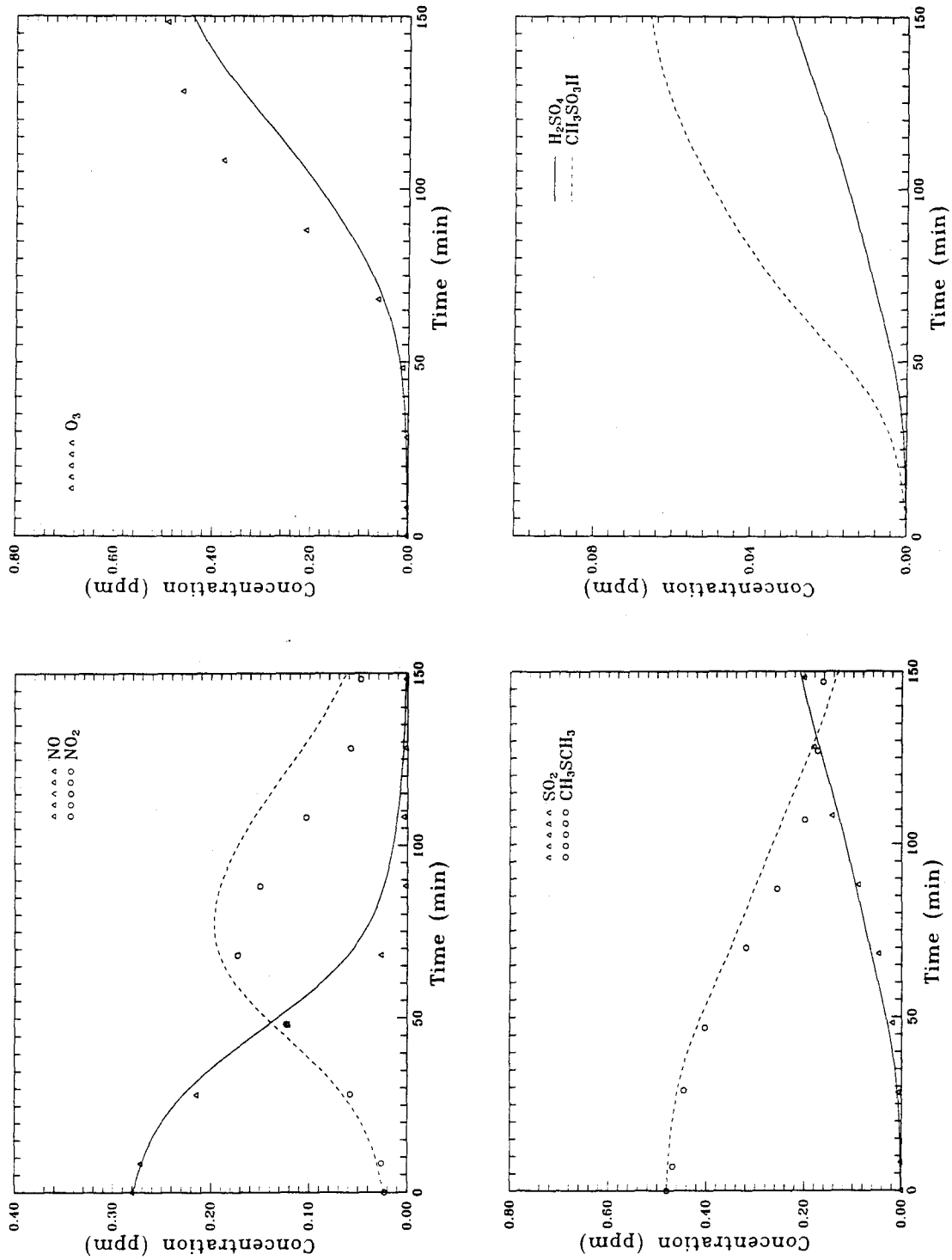

Observed and Predicted Concentration-time Profiles for CH_3SCH_3-NO_x-air Experiment DMS4A

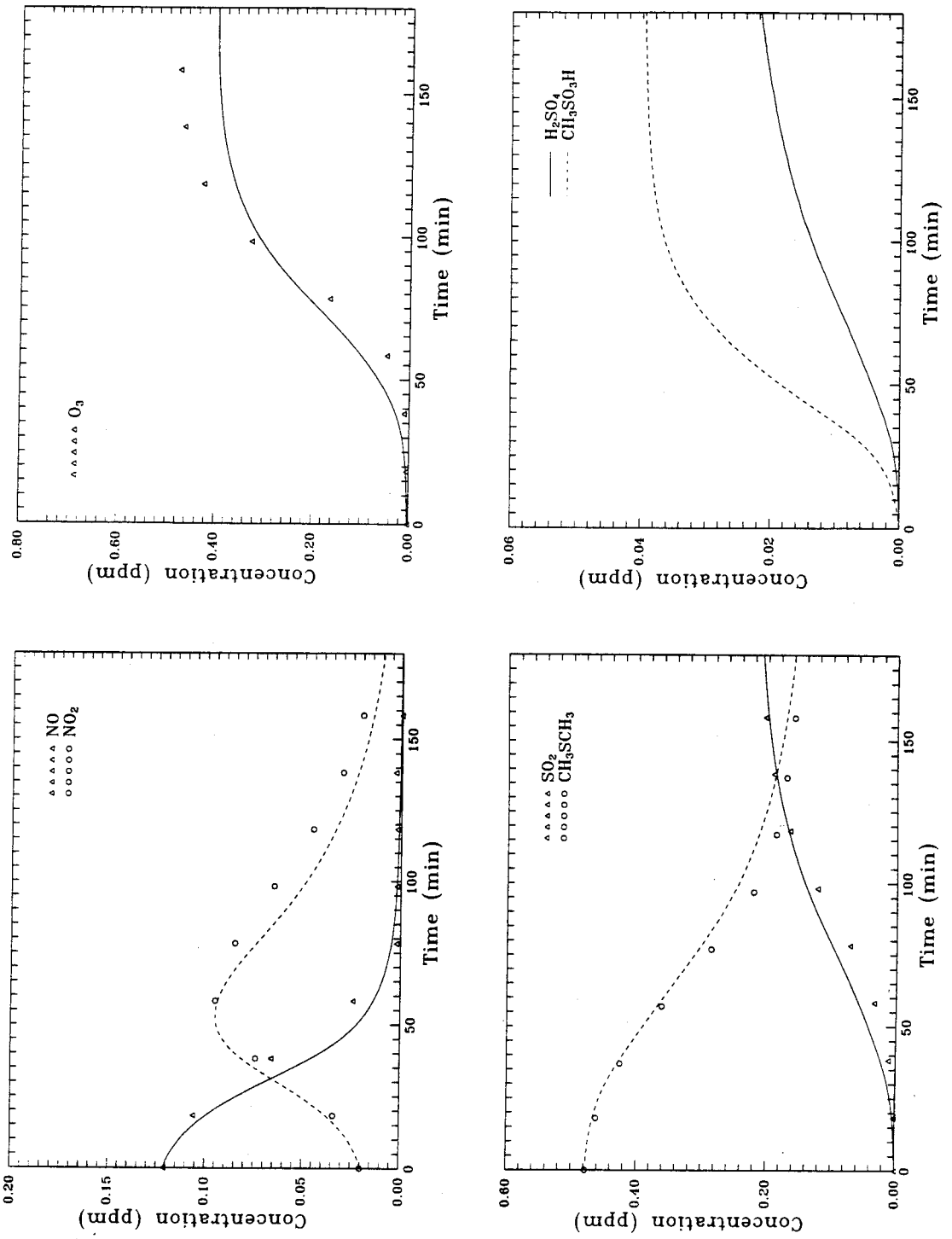

Observed and Predicted Concentration-time Profiles for CH_3SCH_3-NO_x-air Experiment DMS4B